

# Impact of high-end sea level rise scenarios on storm surge barriers in the Netherlands

*Risk analysis of the Maeslant Barrier and the Eastern Scheldt Barrier while incorporating climate change and accelerated sea level rise*



*MSc Thesis*

*M.R. op 't Landt (Mark)*



Rijkswaterstaat  
Ministerie van Verkeer en Waterstaat

 **TU**Delft

## Colophon

### Document: Master Thesis

Title: Impact of high-end sea level rise scenarios on storm surge barriers in the Netherlands  
Subtitle: Risk analysis of the Maeslant Barrier and the Eastern Scheldt Barrier while incorporating climate change and accelerated sea level rise.

Keywords: Sea level rise, Maeslant Barrier, Eastern Scheldt Barrier, climate change, Antarctic contribution, tipping point analysis, Delta Programme.

Location: Delft  
Date: June 16, 2018  
Pages: 215  
Front Page Photo: Eastern Scheldt Barrier & Maeslant Barrier (NL), Beeldbank RWS (2007)

### Graduation Committee

#### **Delft University of Technology**

*Chairman:* Prof.dr.ir. M. Kok (Matthijs)  
Field of expertise: Professor of Flood Risk  
Faculty: TU Delft Engineering and Geosciences; Hydraulic Engineering

*First supervisor:* Prof.dr.ir. M.J.C.M. Hertogh (Marcel)  
Field of expertise: Professor of Integral Design and Management  
Faculty: TU Delft Civil Engineering and Geosciences; Infrastructures and Mobility

*Second supervisor:* ir. R. Jorissen (Richard)  
Field of expertise: Director of the Dutch Flood Protection Programme  
Faculty: TU Delft Civil Engineering and Geosciences; Hydraulic Engineering

#### **Rijkswaterstaat**

*First ext. supervisor:* ir. H. van Waveren (Harold)  
Field of expertise: Principal Expert Flood Protection  
Company: Rijkswaterstaat

*Second ext. supervisor:* ir. R.J.A. Wilmink (Rinse)  
Field of expertise: Adviser Coastal Flood Risk Management  
Company: Rijkswaterstaat

### Author/Student

Name: M.R. op 't Landt (Mark)  
Study number: 4321545  
Faculty: Civil Engineering and Geosciences  
Master: Construction Management & Engineering (CME)  
Institution: Delft University of Technology



Rijkswaterstaat  
Ministerie van Verkeer en Waterstaat

## Preface

This report is the result of my thesis research as part of the master's degree Construction Management and Engineering (CME) at the Delft University of Technology. It provides the latest insights of climate change and sea level rise scenarios and the impact on the remaining lifetime of the Maeslant Barrier and the Eastern Scheldt Barrier. This research investigates the effects of sea level rise to the storm surge barriers and can be used for decision-making about the future of storm surge barriers. Many people have contributed to my research which has been very valuable.

First of all, I would like to express my gratitude to the members of my graduate committee. Finalizing my master thesis would not have been possible without the valuable input of Harold van Waveren and Rinse Wilmink of Rijkswaterstaat and Matthijs Kok, Marcel Hertogh and Richard Jorissen of the Delft University of Technology. Thank you for your input, knowledge and perspectives which have been of great value to this research.

In addition to the committee, I want to mention that Rijkswaterstaat provided frequent qualitative input and feedback. Within the organization, I would like to thank Robert Slomp, Robert Vos, Marc Walraven and Koen Wenker for their input and interest. Without their insights, it was definitely not possible to make such a substantiated risk analysis on the storm surge barriers. Furthermore, I would like to thank Sybren Drijfhout of the KNMI for the interview and feedback on climate change and sea level rise and Marjolijn Haasnoot and Laurens Boucher for the constructive interview about Adaptive Delta Management.

Many others have contributed to this thesis, either by discussions or by giving feedback. Thank you for assisting me through this process.

Mark op 't Landt

Delft, June 2018

## Summary

### **Introduction**

The Netherlands is a low-lying delta and therefore prone to flooding. After the flood in 1953, the Delta Committee was established which commenced the Delta Works to enhance water safety for the society and economy. The Maeslant Barrier and Eastern Scheldt Barrier are the largest and most technologically advanced flood defences which are part of the Delta Works. These storm surge barriers shorten the effective coastline to reduce the risk of flooding within the Rhine-Meuse Delta and the Eastern Scheldt. The climate is changing and the risk of accelerated sea level rise increases. The problem is that the current storm surge barriers are not designed to withstand significant sea level rise. Sea level rise influences the hydraulic loads on the barriers which consequently increase the failure probability of these flood defences.

International research argues that future sea level rise is much more uncertain than previously thought because of the instability of the West-Antarctic ice sheet. Therefore, it is critical to identify the degree of uncertainty of climate change and sea level rise to develop effective strategies for the storm surge barriers. Furthermore, it is important to determine the remaining lifetime of both barriers for various sea level scenarios and to design effective and feasible measures to extend the remaining technical lifetime in case of accelerated sea level rise. These problems lead to the following research questions:

*How can the Dutch storm surge barriers be adapted to extend the remaining lifetime to deal with the risk of accelerated sea level rise due to climate change?*

1. What is the impact of climate change on sea level rise projections for the 21<sup>st</sup> century?
2. What are the hydraulic loads for the Maeslant Barrier and the Eastern Scheldt Barrier and the dykes in the hinterland using the latest sea level rise scenarios?
3. What is the remaining lifetime of the Maeslant Barrier and the Eastern Scheldt Barrier and how many years of extension can be achieved by implementing adjustments?

### **Methodology**

This research consists of two phases in which the research questions will be answered. The first research phase comprehends a literature study about the current policy of flood risk management and climate change. Relevant data about climate change and the latest insights around sea level rise are analyzed to make an updated sea level projection for the Netherlands. Experts in sea level rise and flood risk management are interviewed to substantiate the theory to practical relevance in the Netherlands.

The focus of phase II is on the assessment of the performance of the Maeslant Barrier, Eastern Scheldt Barrier and the inherent water systems based on the latest sea level projections. These two case studies are included to provide explicit solutions to deal with the risk of accelerated sea level rise which shortens the lifetime of both storm surge barriers. First, the hydraulic loads are determined for both storm surge barriers and the dykes that are part of the water system. Assessment program Hydra-NL is used to model the maximum water levels and hydraulic forces on the flood defences for various sea level scenarios. A risk analysis is performed to assess the remaining lifetime of the Maeslant Barrier and Eastern Scheldt Barrier. This analysis includes all risk factors that can affect the technical tipping point and is based on models and expert judgment of specialists.

This analysis helps to substantiate the impact of sea level rise to the storm surge barriers which support developing risk responses that can potentially extend the operating lifetime of both barriers. Subsequently, the advice is given about the most effective strategy and the expected remaining period that the current water system can be preserved.

### **Results & Conclusion**

In 2016, the global average temperature has risen 1.1 °C compared to the pre-industrial period. Moreover, further global warming is expected due to various climate feedback mechanisms. Sea level rise is an inherent consequence of global warming which is probably the most uncertain factor in terms of flood risk management for the Netherlands. According to the Intergovernmental Panel on Climate Change (IPCC), it is almost certain that anthropogenic carbon emissions caused the temperature rise over the last century. Earlier studies argued that

the “business as usual” emission scenario RCP8.5 is likely to be expected by proceeding the current global emission trend, but recent technological innovations and the reduced dependency on fossil energy indicate that a slightly lower emission scenario between RCP4.5 and RCP8.5 is more likely to occur.

Recent global warming resulted in an accelerated rate of global sea level rise and currently increases to  $3.3 \pm 0.2$  mm per year with an extra acceleration of 0.08 mm every year. The accelerated trend is not yet observed in the Netherlands. The regional sea level rise in the Netherlands is currently 1.9 mm per year due to significant variations in wind patterns in the North Sea and gravitational effects of the Greenland ice sheet, which have a reducing effect to regional sea level rise.

DeConto & Pollard (2016) argue that future sea level rise is much more uncertain than previously thought because of the instability of the West-Antarctic ice sheet. Several dynamic processes such as hydrofracturing, grounding line retreat and ice-cliff failure could increase the Antarctic contribution to global sea level rise to a large extent. It is expected that the large contribution begins around the year 2050 when the floating ice shelves could be predominantly disappeared.

The sea level projections for the Netherlands which are based on the latest insights around sea level rise are shown in Table I. In the long-term, sea level rise in the Netherlands could be even more than the global average due to the gravitational effect of ice sheets. The Antarctic ice sheet might become the dominant contributor to sea level rise and has more impact on regions that are relatively far away. The results indicate that both the mean (P50) and the high-end estimate (P95) are significantly increased compared to the IPCC and KNMI’14 scenarios. It is impossible to predict the future emission scenario because of the unknown future climate policies. However, it is presumed that the average between RCP4.5 and RCP8.5 is most likely to occur during this century based on the trend of the carbon intensity. Therefore, the expected median sea level rise is 1.04 m in 2100.

Table I: Projected absolute sea level rise in the Netherlands by the year 2100 compared to 2000.

Percentiles [%]	RCP4.5 [cm]	RCP8.5 [cm]	Average RCP4.5 & RCP8.5
P5	31	63	47
P17	52	87	70
P50	81	128	104
P83	114	175	144
P95	140	214	177
P99	168	258	213

The essential conclusion is that sea level projections are more uncertain than previously thought and 2 m sea level rise or more in 2100 cannot be ruled out. Uncertainty in ice sheet dynamics dominates the high-end percentiles of sea level projections. This research advises to include the full bandwidth of the distribution function of sea level rise projections into the other sea level statistics. This method enables more accurate sea level projections by combining probabilistic sea level rise scenarios. Extra attention should be paid to the potential high-end sea level rise which poses an increased risk for the storm surge barriers.

The storm surge barriers are of main importance because these are the first line of defence to protect the dykes in the hinterland against aggregated hydraulic loads. Therefore, the storm surge barriers will be assessed on the same heaviest safety standard, which will be applied to a dyke within the water system. After the regulation change in 2017, the required safety standards that will be applied to flood defences depend on the chance of failure and the risk of flooding. The applicable safety standard for the Maeslant Barrier is a maximum failure probability of 1/30,000 per year. The new safety standard for the Eastern Scheldt Barrier is 1/10,000 per year.

The intended lifespan for the Maeslant Barrier is 100 years and the Eastern Scheldt Barrier is designed for an operating lifetime of 200 years. The hydraulic loads for the storm surge barriers are mainly influenced by sea level projections. Uncertainty around sea level rise should be incorporated in the risk analysis.

The technical tipping point of the Maeslant Barrier is 0.30 m sea level rise which is expected to occur around 2055. It should be noted that a high-water event in combination with a modest river supply results in a crucial situation for the construction of the Maeslant Barrier. This implies that the large water level difference between

the sea level and the water level within the delta have the potential to exceed the maximum acceptable load on the ball joint of the barrier. Furthermore, the current closing procedure induces a risk of temporarily exceeding critical water levels in Rotterdam due to the relatively late closure. The following adjustments are proposed to extend the remaining lifetime of the barrier:

- maximize the water level difference to 4 m during a closure. The floodgates can be raised temporarily by maximal 2 m to reduce the horizontal force on the construction (2018-2020);
- always perform a turnaround closure to maximize the storage capacity of the Rhine-Meuse Delta and to limit the tidal wave in the harbour (2018-2020);
- optimize the closing process by minimizing the delay to close (2018-2025);
- reduce the failure rate to 1/200 per closure (2025-2035).

The implementation of the above-mentioned measures can be seen as feasible and affordable options to reduce the risk of flooding. It is expected that these measures will extend the operating lifetime of the Maeslant Barrier until approximately the year 2077, which corresponds to 61 cm sea level rise. This expectation lies within the timeframe of the preferred strategy of the Delta Programme to replace the MLK around 2070-2100.

On the other hand, the robustness of the Eastern Scheldt Barrier and the implemented surcharges in the design makes this barrier resistant to a larger extent of sea level rise than previously thought. The technical tipping point is 0.90 m sea level rise which is expected to occur around 2093. The Eastern Scheldt Barrier should remain operational for as long as possible according to the preferred strategy of the Delta Programme. Therefore, it is proposed to implement the following measures within the prescribed timeframe to extend the lifetime of the Eastern Scheldt Barrier:

- reduce the leak opening to 600 m<sup>2</sup> (2030-2040);
- adjust the closing regime (2030-2040).

Both measures will significantly extend the technical tipping point and are feasible within the strategy of the Delta Programme. After implementing the adjustments, the technical tipping point will be reached at 1.30 m sea level rise which will probably extend the lifetime to beyond the end of this century.

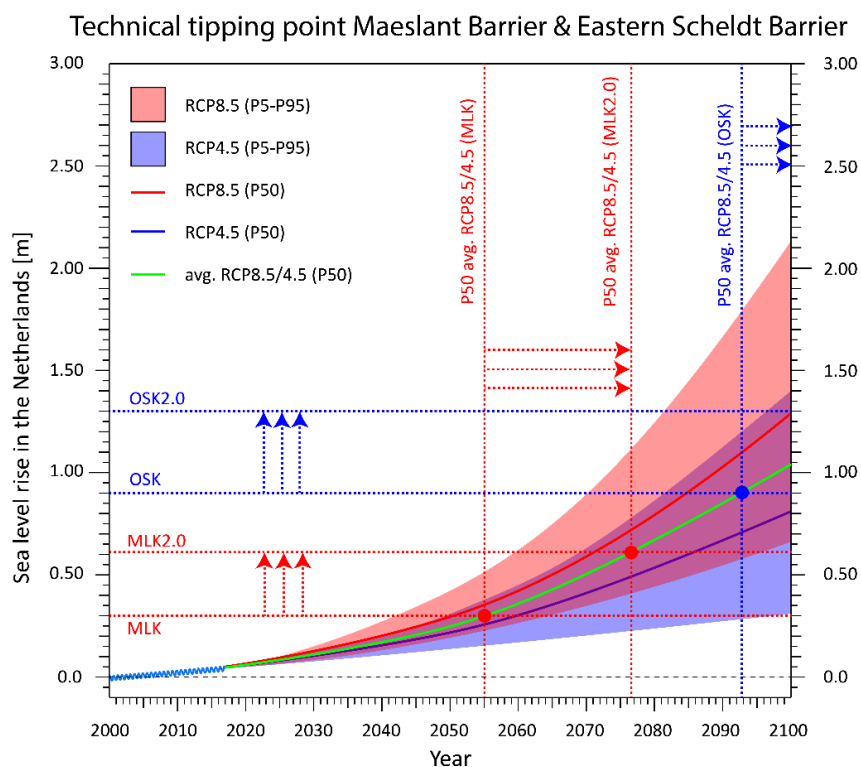


Figure I: Technical tipping point of the Maeslant Barrier (red) and Eastern Scheldt Barrier (blue) combined with sea level rise before and after adjustments (2.0). Tipping points are determined for  $T=30,000$  (MLK) and  $T=10,000$  (OSK). The green line represents the expected sea level rise trend between 2000 and 2100.

# Table of content

Preface.....	I
Summary.....	II
List of Abbreviations.....	VII
1. Introduction.....	1
1.1 Research relevance.....	2
1.2 Problem analysis.....	3
1.3 Research objective.....	5
1.4 Scope.....	6
1.5 Research questions.....	7
2. Research Design.....	8
2.1 Research framework.....	8
2.2 Research Design.....	8
2.3 Research Methodology & Approach.....	9
2.4 Data Gathering and Analysis.....	10
2.5 Report structure.....	11
3. Flood protection.....	12
3.1 History of flood protection in the Netherlands.....	12
3.2 Flood protection in the Netherlands.....	15
4. Climate change.....	25
4.1 Climate background.....	25
4.2 Climate scenarios.....	31
5. Sea level rise.....	36
5.1 Past sea level change.....	36
5.2 Global sea level rise.....	38
5.3 Sea level rise scenarios.....	40
5.4 New insights into the contribution of the Antarctic ice sheet to sea level rise.....	46
5.5 Impact of the increased Antarctic contribution to global sea level rise scenarios.....	49
5.6 New global sea level rise scenario.....	53
5.7 Regional sea level rise in the Netherlands.....	57
6. Hydraulic requirements.....	61
6.1 Statutory Assessment instruments.....	61
6.2 Hydraulic load factors.....	64
6.3 Probabilistic model and test locations.....	65
6.4 Hydraulic loads.....	67
7. Risk analysis.....	77
7.1 Risk analysis of the storm surge barriers.....	79

7.2	Tipping point analysis .....	115
7.3	Strategies .....	130
8.	Conclusions, Discussion and Recommendations .....	133
8.1	Conclusions .....	133
8.2	Discussion .....	137
8.3	Recommendations .....	140
	List of references .....	142
	Appendix .....	150
	Appendix A: Global sea level rise components .....	150
	Appendix B: Local sea level rise components .....	153
	Appendix C: Millennial sea-level commitment .....	159
	Appendix D: Sea level Projections .....	160
	Appendix E: Ice sheet contribution to sea level rise .....	163
	Appendix F: Future Antarctic contribution to sea level rise .....	166
	Appendix G: An overview of levee systems in the Netherlands (2017) .....	169
	Appendix H: Storm surge barriers .....	171
	Appendix I: Hydra-NL .....	181
	Appendix J: Storm surge, tides and waves .....	185
	Appendix K: Test locations and safety standards .....	187
	Appendix L: Storage capacity and storm duration .....	192
	Appendix M: Wave overtopping and water overrun .....	195
	Appendix N: Flow through the leak opening of the Eastern Scheldt Barrier .....	198
	Appendix O: Forces on the floodgates and ball-shaped joint of the Maeslant Barrier .....	199
	Appendix P: Calculation flow velocity and stone grading of the Maeslant Barrier .....	201
	Appendix Q: Analysis of historical storms .....	204
	Appendix R: Failure rate Eastern Scheldt Barrier .....	214

## List of Abbreviations

Abbreviation	English	Dutch
AIS	Antarctic ice sheet	Antarctische ijskappen
BOS	Decisions Supporting System	Beslis en Ondersteunend Systeem
DFFP	Dutch Flood Protection Programme	Hoogwaterbeschermingsprogramma
DP16	DeConto & Pollard (2016)	-
FTA	Fault Tree Analysis	Foutenboom analyse
GDP	Gross Domestic Product	Bruto Nationaal Product
GHG	Greenhouse gases	Broeikasgassen
GIA	Glacial isostatic adjustment	-
GMSL	Global Mean Sea Level	Gemiddeld wereldwijd zeeniveau
GrIS	Greenland ice sheet	Groenlandse ijskappen
HK	Hartel Barrier	Hartelkering
IPCC AR5	Intergovernmental Panel on Climate Change, the Fifth Assessment Report	-
KNMI	The Royal Netherlands Meteorological Institute	Koninklijk Nederlands Meteorologisch Instituut
LIG	Last Interglacial	-
MHW	Critical water level	Maatgevend hoogwater
MLK	Maeslant Barrier	Maeslantkering
NAP	Amsterdam Accordance Datum	Normaal Amsterdams Peil
NOAA	National Oceanic and Atmospheric Administration	-
NWW	Rotterdam Waterway	Nieuwe Waterweg
OS	Eastern Scheldt estuary	Oosterschelde
OSK	Eastern Scheldt Barrier	Oosterscheldekering
P	Percentile of the probability density function	Percentiel in de kansdichtheid functie
PDF	Probability density function	Kansdichtheid functie
RCP	Representative Concentration Pathways	CO <sub>2</sub> emissie scenarios
RMD	Rhine-Meuse Delta	Rijn-Maas (rivieren) Delta
SLR	Sea level rise	Zeespiegelstijging
SMB	Surface Mass Balance	Massa balans van een ijskap
T	Average return period [year] derived from the maximum exceedance frequency per year of the flood safety standard	Gemiddelde herhalingstijd [jaar] afgeleid uit de veiligheidsnorm voor waterkeringen
UN	United Nations	Verenigde Naties
WAIS	West Antarctic Ice Sheet	Westelijke ijskap van Antarctica
WBI	Legal Assessment Instruments	Wettelijk Beoordings Instrumentarium

# 1. Introduction

International research reveals that global sea level rise can accelerate at a much faster rate than predicted earlier. The Dutch delta is vulnerable to substantial sea level changes and it is unknown what the long-term consequences of accelerated sea level rise are for the Dutch storm surge barriers and for the associated areas behind. This study will investigate the impact of accelerated sea level rise on the Dutch storm surge barriers that protect coastal regions against flooding. The focus of this study is predominately on the effects of accelerated sea level rise on the Maeslant Barrier (Dutch: “Maeslantkering”) and the Eastern Scheldt Barrier (Dutch: “Oosterscheldekering”). It is essential to understand the aspects of sea level rise and how the strategies of the Delta Programme should be adapted to deal effectively with accelerated sea level rise in the future.

This chapter starts by presenting the research topic followed by the problem analysis to describe the need for this research. The scope of the research and its relevance are also discussed in this chapter. The central research question, as well as the sub-questions, are formulated in Section 1.5. These questions form the basis for the methodology which is presented in Chapter 2. Chapter 3 is about flood protection in the Netherlands and the characteristics of the Maeslant Barrier and the Eastern Scheldt Barrier will be explained. Chapter 4 is about climate change and the human involvement in global warming. Chapter 5 discusses the global sea level rise scenarios and regional sea level rise scenarios for the Netherlands. Chapter 6 analyses the hydraulic loads of the storm surge barriers and several dykes of the inherent water system. The risk analysis including the calculation of the tipping points will be performed in Chapter 7. The conclusions and answers to the research questions are presented at the end of the report in Chapter 8.

## Introduction to the topic

Sea level rise (SLR) may accelerate at a much faster rate than predicted earlier (DeConto & Pollard, 2016). One of the consequences could be that flood defences need to be reinforced much earlier (in time) than expected and planned. Especially the large hydraulic structures such as the Maeslant Barrier (MLK) and the Eastern Scheldt Barrier (OSK), which are designed for a long lifetime, may need to be renewed or strengthened earlier than predicted. This research will investigate the consequences of sea level rise as well as the possible measures and strategies to cope with high-end sea level rise scenarios.

The potential acceleration of SLR is based on recently acquired knowledge about diminishing ice shelves and the stability of the ice-sheet of Antarctica (DeConto & Pollard, 2016). The stability of the Antarctic ice sheet could reduce drastically around 2050, leading to large-scale crumbling and ice-cliff collapse of land ice. These dynamic processes have not been fully incorporated into the prediction models yet. However, these processes can have a significant impact on the rate of sea level rise. Therefore, the sea level could be much higher at the end of this century than described in the current scenarios of Intergovernmental Panel on Climate Change (IPCC), the Royal Netherlands Meteorological Institute (KNMI) and the Dutch Delta Programme. This research will assess the probability and accuracy of the latest high-end climate scenarios and sea level scenarios.

This research takes the new developments in the sea level rise projections, in combination with other contributing factors, into consideration to outline the risks for water safety of the most prominent storm surge barriers in the Netherlands. This research uses the latest sea level rise scenarios in combination with new sea level rise estimations of the Antarctic ice sheet to investigate the robustness of the Maeslant Barrier (MLK) and Eastern Scheldt Barrier (OSK) to accelerated sea level rise. This research could inform policymakers whether these storm surge barriers can provide sufficient protection against the potentially aggravated hydraulic conditions. The goal of this thesis is to project the remaining lifetime of the MLK and OSK based on the latest insights of climate change and sea level rise. If the remaining lifespan is shorter than the planned 100 years for the MLK and 200 years for the OSK, measures will be proposed that could potentially extend this tipping point.

A tipping point is defined as the extent of sea level rise at which the flood protection system of the Maeslant Barrier or the Eastern Scheldt Barrier no longer offers the desired safety against flooding. These storm surge barriers and the effects to the hinterland will be analysed in terms of water safety to get more clarity about the remaining lifetime while incorporating various high-end sea level rise scenarios. All risk factors that might influence the remaining lifetime of both barriers will be assessed by conducting a technical risk analysis. This will result in recommended measures that should be effective and feasible to improve water safety for the society and the economy. The emphasis is on estimating the risk of sea level rise for those barriers and on developing measures to cope with climate change and sea level rise. In the end, the aim is to provide substantiated advice about the required policy to improve flood protection in the Rhine-Meuse Delta (RMD) and the Eastern Scheldt.

## 1.1 Research relevance

This thesis can contribute to the knowledge about the impact of high-end sea level rise for the Dutch storm surge barriers and the water safety of the associated areas. Furthermore, the provided information about sea level rise by DeConto & Pollard (2016) (DP16) is entirely new and there is not a satisfactory answer to the performance of the Dutch storm surge barriers in the event of possible high-end sea level rise yet. The results of this research might contribute to future policy decision-making which can result in improved flood safety and societal benefits. The primary focus of this research project is on accelerated sea level rise and potential impact on the performance and remaining lifetime of the Maeslant Barrier and the Eastern Scheldt Barrier. Another essential element of this research is the assessment of measures that cope effectively with sea level rise and can potentially extend the tipping point of the storm surge barriers.

### 1.1.1 Background information

Background information is provided to explain the need for this research. The main points of attention are:

- Antarctic contribution to sea level rise is not fully incorporated in the sea level rise models;
- sea level rise could be potentially more than 2 m in the year 2100 including a large uncertainty range;
- the Maeslant Barrier and Eastern Scheldt Barrier are designed for only a limited amount of sea level rise and may not reach the end of their expected technical lifetime;
- the preferred strategy of the Delta Programme may not be sufficient to deal with high-end sea level rise.

DeConto & Pollard (2016) expect that ice melt on Antarctica on its own could cause an additional SLR of approximately 1 m in 2100 and more than 15 m in the year 2500 if carbon emissions are not radically reduced (DeConto & Pollard, 2016). The current KNMI'14 climate scenarios describe maximal 1.00 m SLR in 2100 for the highest emission scenario (KNMI, 2014). It should be noted that this projection does not incorporate the latest insights into the rapid ice sheet dynamics in Antarctica. Rijkswaterstaat usually takes into account 0.85-1 m sea level rise (2000-2100) for their dyke reinforcements (KNMI, 2006). Future sea level rise will be more uncertain than initially thought and, therefore, more than 2 m SLR in the year 2100 cannot be ruled out after including the results of DP16. Uncertainty is an inherent part of the future, but this new knowledge might have consequences for water safety and decision-making in the Netherlands.

At the moment, approximately 26% of the Netherlands is situated below mean sea level and another 33% is prone to the risk of flooding (PBL, 2007). Nearly 70% of the population and economy are prone to flooding (Jorissen, Kraaij, & Tromp, 2016). The risk of flooding increases when sea level rise accelerates because the impact (damage) could drastically increase when flooding occurs. Land subsidence in the western part of the Netherlands increases the impact of flooding even further. In addition, the probability of flooding will increase without reinforcing flood defences according to new scenarios.

The Maeslant Barrier (MLK) and Eastern Scheldt Barrier (OSK) provide flood protection for a significant part of the Dutch economy but are not designed for a high-end sea level rise scenario. The MLK is designed for a lifetime of 100 years including 50 cm sea level rise while the OSK is designed to operate 200 years but only if the relative sea level rise does not exceed 40 cm. This study will analyze the maximum extent of sea level rise that both barriers can withstand and which reinforcements should be implemented to extend their lifespan.

Storm surge barriers should protect large valuable areas against flooding during storms and high-water events. The preferred strategy of the Delta Programme for the MLK and OSK is an open closable barrier that can either be opened or closed depending on the water level and local weather (Delta Programme 2015). The MLK should allow an open water passage available for shipping under normal circumstances. The OSK is open to maintain the intertidal zone in the estuary to preserve the ecosystem in the Eastern Scheldt and can be closed during a high-water event. Sea level rise could affect the closing regime of the barriers and the safety of the areas behind.

## 1.2 Problem analysis

With the growing threat of flooding due to sea level rise, it can be assumed that the need for research in risk management and strategies to reduce the probability and impact of floods, will increase. The threat of flooding is a growing global problem due to sea level rise and land subsidence. Currently, sea level rise is relatively stable at 19 cm per century in the Netherlands (1901-2010), but this is expected to rise (KNMI, 2014). The importance to combine knowledge about sea level rise to the consequences for the Netherlands, in both technical and economic perspective, is widely recognized. However, high-end sea level rise can emerge in a much shorter period than previously thought and more than 2 m sea level rise in the year 2100 cannot be ruled out. Such extreme sea level scenarios that may already become a reality within this century are not investigated yet for the Dutch delta. The most critical problems which are relevant to this research are summarized below:

- sea level rise might accelerate much faster than earlier predicted;
- the consequences of extreme sea level rise and response strategies are not fully understood yet;
- new knowledge about the Antarctic contribution to sea level rise increases the total uncertainty range in predicting the rate of sea level rise;
- the western part of the Netherlands is still an attractive place to live despite the growing flood risk problem which will increase the impact of flooding;
- the MLK and OSK are not designed for accelerated sea level rise;
- reinforcing flood defences takes a long period of time. It might take too long to upgrade flood defences and especially the storm surge barriers when accelerated sea level rise will begin.

Along with the problems above the following risks are:

- the preferred strategy of the Delta Programme might not be robust enough when extreme sea level rise occurs;
- the government might react too late to design improvements when sea level rise accelerates.

It is well-known that a part of the Netherlands is prone to flooding. Extensive research is performed about the current safety level of all primary flood defences, in combination with short-term predictions of climate change. However, some researchers are convinced that sea level rise could increase to a much larger magnitude than is projected in the current scenarios and strategies. In particular, the consequences of significantly accelerated sea level rise for the Dutch flood defences and its low-lying mainland in the long-term perspective are not yet fully understood. The problem is that these low-lying areas are a very attractive place to live because of its economic activities. Despite the vulnerability to flooding, quality of life in the Netherlands is satisfying. Therefore, it is required to continue investing in measures to keep the risk of flooding at an acceptable level. This is called the Delta paradox. It is still unclear how long this policy can be maintained if sea level rise accelerates to a great extent (ENW, 2016).

Also, the combination of accelerated sea level rise and land subsidence could result in more severe damage if the flood defences fail to protect the mainland from flooding. Sea level rise and the volume of (peak) precipitation are the main penalties for climate change while the strength of storms shall probably not increase significantly (KNMI, 2014).

Considerable uncertainty exists in estimating sea level rise in the long-term perspective. First, it is uncertain how the rate of global greenhouse gas emissions will change in the future and what the consequences are for sea level rise. In 2006, scientists and engineers thought that sea level rise could be maximal 85 cm in 2100 compared

to the year 2000 in the high-end scenario (KNMI, 2006). In addition, the expected uncertainty range in this sea level scenario was assumed to be relatively small.

However, new research concludes that the dynamic processes on the Antarctica ice-sheet were not fully incorporated in the models. These processes can significantly contribute to sea level rise. Scientists used probabilistic models and concluded that high-end sea level rise is more uncertain than previously thought. Furthermore, some experts argue that also the average sea level rise can increase to a large extent (Le Bars, Drijfhout, & de Vries, 2017). The relative sea level rise is even higher in combination with land subsidence in the western part of the Netherlands.

The knowledge gap is in linking this new research about sea level rise to the storm surge barriers and the consequences for the water safety in the Netherlands. The focus of the government is on Adaptive Delta Management (Section 3.2.6). This implies that sea level rise must be monitored carefully, and policy must be tested against the latest insights and then modified if necessary (Veerman & Stive, 2008). The preferred strategies of the Delta Programme are based on this principle because major climatological changes are still relatively uncertain. Nevertheless, storm surge barriers are relatively fixed constructions made of concrete and steel and are not very adaptive. In contrast to dykes and dunes, storm surge barriers are not easy to reinforce. The question is for how long the open-closed strategy for the MLK and for the OSK can continue during accelerated sea level rise. This research will focus on the remaining lifetime of both storm surge barriers and the current strategy of the water system based on the latest insights of sea level rise and climate uncertainty.

Furthermore, if the projected high-end rate of sea level rise indeed occurs, it is possible that the government responds too late to plan and build reinforcements. Especially rebuilding or reinforcing large structures like the MLK and the OSK in an efficient way takes many years. A considerable possibility is that these structures will be disapproved earlier than their initially planned lifetime of 100 years and 200 years, respectively. It is still unknown when these structures will not be able to fulfil their water-retaining function by incorporating the new sea level projections. It should be reasonable to determine these tipping points in advance to take measures before these structures are disapproved.

Due to the new safety standards which are enforced in 2017, the current objective is that all flood defences apply to the new rules before 2050 (ENW, 2016). Accelerated climate change together with sea level rise can lead to the problem that many flood defences do not meet the updated safety standard for a long time, which enhance uncertainty and flood risk. The goal of the Delta Programme and the Dutch Flood Protection Programme (DFFP) to reinforce all disapproved flood defences before 2050 indicates that it will take a long time to carry out large projects. It can be supposed that reinforcing all flood defences according to the requirements of the new climate projections will be even more challenging (Delta Programme 2016).

## 1.2.1 Problem statement

The main problems with water safety and the current water system including storm surge barriers in the Netherlands are addressed in the previous section. The problem statement will help to formulate the research questions and should give this thesis more focus. After refinement, the problem statement is as follows:

### Problem statement

“It is unknown for how long the preference for open closable storm surge barriers can be continued to provide sufficient water safety if sea level rise accelerates faster than previously predicted”.

The problem statement refers to the preferred strategy of the Delta Programme for the storm surge barriers in the Netherlands. This research examines the impact of climate change on sea level rise and will investigate the robustness of the Maeslant Barrier and the Eastern Scheldt Barrier and the current water system in relation to sea level rise.

## 1.3 Research objective

The research objective is to provide more clarity in the uncertainty of the latest sea level rise scenarios and the potential consequences to the remaining lifetime of the storm surge barriers. In addition, several adjustments will be analyzed which could potentially extend the lifespan of the Maeslant Barrier and Eastern Scheldt Barrier in case of accelerated SLR. Therefore, the goal is to recommend effective measures that can extend the remaining lifetime and improve long-term water safety in case that sea level rise accelerates faster than predicted.

It is expected that these storm surge barriers can withstand the expected rate of SLR and soil subsidence for the coming decades. The purpose of this research is to assess this hypothesis. The primary objective is to provide insight into the risks, triggered by accelerated sea level rise, that can affect the functioning of the water system of the Rhine-Meuse Delta and the Eastern Scheldt which include respectively the Maeslant Barrier and the Eastern Scheldt Barrier. The aim of the risk analysis is to improve the understanding of the effects of SLR on the storm surge barriers which might improve decision-making for long-term strategies.

The relation between climate change and sea level rise will be a major element in this research. Furthermore, it is important to examine the rate of uncertainty in sea level rise scenarios for the different emission pathways. This research will incorporate the new knowledge of climate change and sea level rise into a new sea level scenario applicable to the Netherlands.

The sea level projection will be used to analyze the dominant risks that can affect the technical tipping point of the MLK and OSK. This risk analysis will include a timeframe to give an indication when these storm surge barriers should be improved to meet the new water safety standard. Another objective is to recommend feasible and affordable adjustments that effectively extend the tipping point and therefore increase the remaining lifetime.

It can be expected that the definitive life-end will be reached at the second tipping point, after adjustments. This cannot be determined very accurately because this will depend on the rate of sea level rise which is still profoundly uncertain. Nevertheless, it can be stated that the open closable strategy of the current water system is under pressure if the second tipping point of the storm surge barriers is reached.

The case studies about the Maeslant Barrier and the Eastern Scheldt Barrier provide insight into their limitations to sea level rise in combination with storm events. These studies will be done to evaluate the climate robustness of both storm surge barriers and the strategies of the Delta Programme.

It is not certain that sea level rise will accelerate to such an extent, but it is necessary to prepare ourselves for the case that it occurs. The goal is to inform policymakers about the risks of accelerated sea level rise and the impact on storm surge barriers.

## 1.4 Scope

Accelerated sea level rise has impact on coastal areas all over the world. Therefore, the scope of this thesis should be defined more precisely. In addition to water safety, sea level rise influences many aspects such as spatial development, economy and nature but also drinking water and groundwater. It is essential to explain the content of this research and to zoom in into specific areas. The aspects below explain the scope of this research.

Area: most international research is focussed on global sea level scenarios. However, the focus of this research is particularly on sea level rise for the Dutch coast. The consequences of sea level rise will be investigated for the MLK and OSK only. Both storm surge barriers are part of a complex water system which implies that also the effects of SLR on the dykes in the Rhine-Meuse Delta and Eastern Scheldt will be evaluated. Nevertheless, this research could contribute to the decision-making process of other estuaries which include storm surge barriers.

Conditions: climate change affects the Earth in many aspects. This research only examines the consequences of climate change in relation to sea level rise. Other Metocean (Meteorology and Oceanography) processes such as flow patterns and coastal morphodynamics are excluded. Storm surge, wave heights and river supply to the RMD are included in determining the hydraulic loads but are not investigated in relation to climate change.

Timespan: the rate of future sea level rise is profoundly uncertain, due to the Antarctic contribution and the uncertainty in future carbon emissions. However, extensive research is carried out on both short-term and long-term timeframes and relevant literature will be used. The key timespan of this research is until the year 2100 because of the lack of literature beyond 2100. The problems for the Netherlands after 2100 can be even more critical but are not included in the analysis due to uncertainty.

Scenario: the risk analysis will be done for sea level rise scenarios based on emission scenarios RCP4.5 and RCP8.5 of the IPCC. More information about these climate scenarios can be found in Chapter 4. It is expected that these two scenarios are the most realistic in terms of future carbon emissions. The relation between emission pathways and sea level rise scenarios is an important element of this research. The focus is predominately on high-end sea level scenarios to identify the potential impact on the MLK and OSK in terms of water safety.

Impact: the impact of sea level rise on the performance of the MLK and OSK is widely addressed in this study. Also, the impact of SLR on the hydraulic loads on several dykes in the Rhine-Meuse Delta and Eastern Scheldt will be determined which can be affected by the performance of both storm surge barriers. It should be noted that these dykes will be assessed for failure mechanism wave overtopping. Other failure mechanisms are beyond the scope of this research. Furthermore, the effect of SLR on the relevant strategies in the Delta Programme and decision-making related to these storm surge barriers will be discussed. The impact of sea level rise on the economy and ecology will be discussed briefly. In-depth analysis of these aspects will be recommended for future research.

Technical elaboration: in-depth research will be performed on the main elements of the MLK and the OSK to be able to determine the technical tipping points that indicate the extent of sea level rise at which these structures do not meet the safety standard. Measures will be proposed that can extend the tipping point and the remaining lifetime of the barriers.

The risk analysis investigates the prominent risks, responses and strategies that can influence the remaining lifetime of the storm surge barriers. Entirely technical designs will not be produced and the focus is only on the main elements such as the arc-shaped doors and the foundation of the MLK and the three sections of the OSK. Connecting structures and secondary components are beyond the scope of this research.

The sea level projections are updated by the latest knowledge about ice sheet dynamics in Antarctica. Regionalisation factors will be applied to project the sea level rise scenario for the Netherlands which will be used to determine the technical tipping points of the storm surge barriers and long-term strategies.

It is important to note that the risk analysis is not performed according to the official assessment method and is based on expert judgement. The results of the risk analysis should be used as a practical enhancement to recognize the effects of sea level rise on the storm surge barriers.

## 1.5 Research questions

The next step is to define the main research question based on the defined problems. The research question is a result of the formulated problem statement and research objectives. The research question needs sub-questions to be more specific and to guide towards a solution.

### Research Question

*How can the Dutch storm surge barriers be adapted to extend the remaining lifetime to deal with the risk of accelerated sea level rise due to climate change?*

### 1.5.1 Sub-questions

The sub-questions will be answered in two phases. The design of these phases is explained in Section 2.2.

#### PHASE I

1. What is the impact of climate change on sea level rise projections for the 21<sup>st</sup> century?

#### PHASE II

2. What are the hydraulic loads for the Maeslant Barrier and the Eastern Scheldt Barrier and the dykes in the hinterland using the latest sea level rise scenarios?
3. What is the remaining lifetime of the Maeslant Barrier and the Eastern Scheldt Barrier and how many years of extension can be achieved by implementing adjustments?

Sub-question 1 is required to understand the aspects of climate change which contribute to sea level rise. Subsequently, based on the results of relevant literature, a scenario can be made to project the rate of sea level rise in the Netherlands. This scenario should be used to determine the hydraulic loads on the storm surge barriers and the dykes in the hinterland which are part of the water system. Based on these results, a risk analysis should be made to determine the remaining lifespan of the Maeslant Barrier and the Eastern Scheldt Barrier. If this analysis leads to a shorter lifespan than initially planned, adjustments and response strategies will be developed to extend the remaining lifetime of the storm surge barriers and the current open closable water system.

# 2. Methodology

This chapter explains the research methodology that is used to gather the information to answer the research questions. The methodology provides information about the research process, the process phases, and the used search methods. The following topics will be discussed in this chapter: the research framework, the research design, research methodology & approach, data gathering & analysis and finally the report structure.

## 2.1 Research framework

The theoretical framework of this thesis is visualized in Figure 2.1. After the literature study, information and data will be collected on climate change, sea level rise scenarios and hydraulic loads of the storm surge barriers. The data will be analyzed to come up research findings that support the arguments for the conclusions of the performance of the storm surge barriers and the inherent water system.

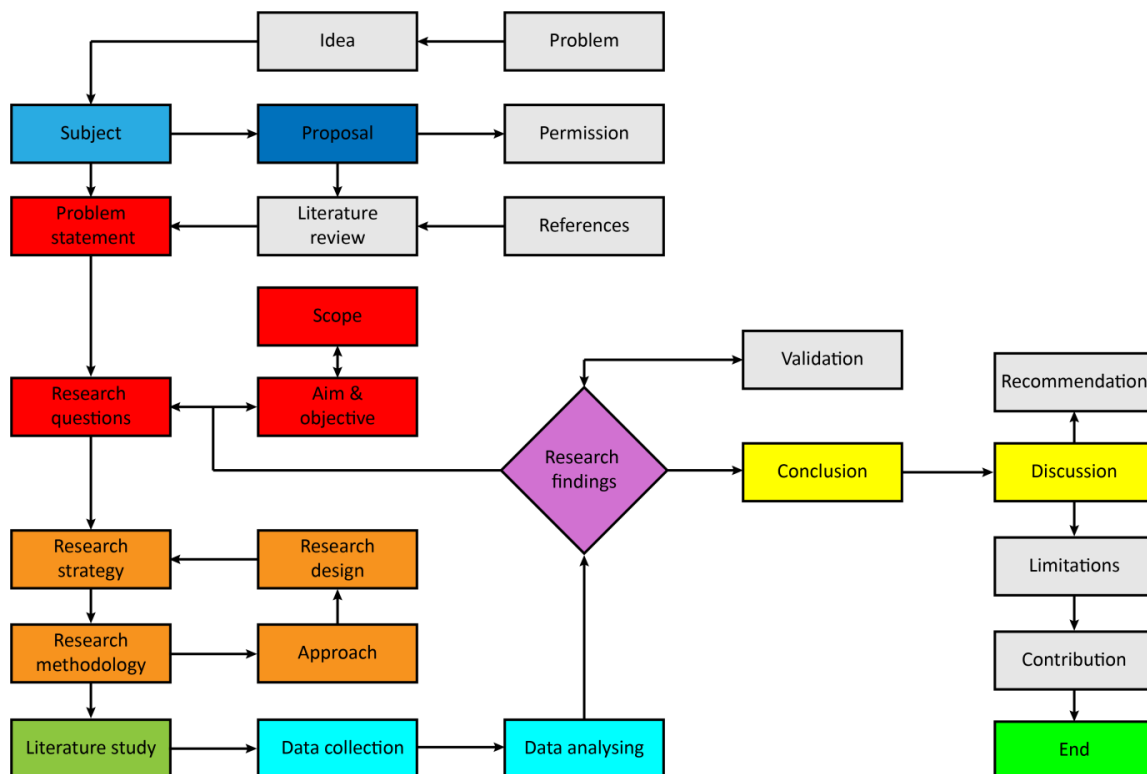


Figure 2.1: Thesis structure.

## 2.2 Research Design

The research will be executed in two phases. Each phase has its own research sub-question(s). The research design of this thesis is shown in Figure 2.2.

Phase I is intended to collect relevant data on climate change and sea level rise which could be useful in phase II. Global warming causes sea level rise and that is why these topics are included in this research. Data will be analysed in order to make a sea level projection for the Netherlands based on the latest insights around sea level rise. Furthermore, this phase helps to understand the magnitude of the effects of sea level rise on the Dutch storm surge barriers.

The focus of phase II is on flood risk management of the Maeslant Barrier and the Eastern Scheldt Barrier and the performance of the inherent water system. First, the hydraulic loads will be calculated for the storm surge

barriers and the dykes in the hinterland using the sea level scenario of Phase I. Then, a risk analysis of both storm surge barriers will be made to fully understand all relevant risks around sea level rise which should help to steer towards appropriate responses to extend the remaining lifetime in the case that high-end sea level rise will occur. Finally, a conclusion and recommendations for future research will be formed.

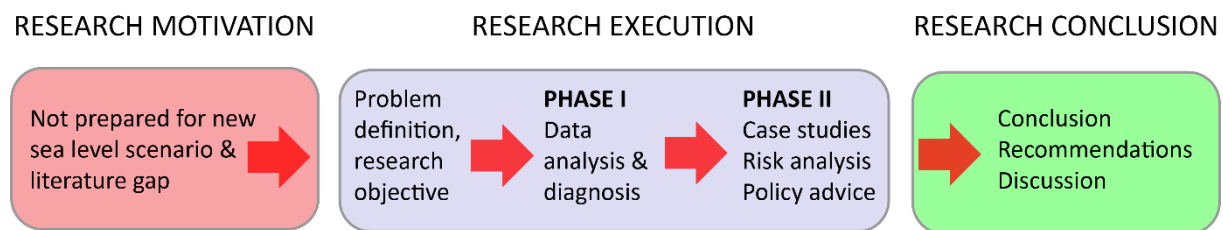


Figure 2.2: Research Design.

## 2.3 Research Methodology & Approach

A research framework will be designed to answer the research questions. The thesis structure also gives an impression of the framework of this research and addresses the functionality of this study. The body of the report is mainly based on knowledge application within the defined scope and is based on a literature study, interviews, and model results. All used literature will be documented to make this thesis reproducible. Interviews, models, and case studies will be performed to substantiate a clear answer to the research questions. This section also describes the used method of the tipping point analysis to assess the resilience of the storm surge barriers to sea level rise.

### 2.3.1 Research function and perspective

An abundance of background information will be used to define the proposed solutions to the research questions. This research will evaluate and compare literature. It is essential to critically analyze the information and data to be able to propose well-grounded recommendations. The primary research perspective that will be used in the beginning is the *problem-analyzing research* (Verschuren & Doorewaard, 2010). This implies that the problem will be critically analyzed in order to come up with substantiated recommendations.

#### **Case Studies**

Two case studies will be included to be able to draw more in-depth conclusions. *“The case study is a research strategy in which the researcher tries to gain a profound and full insight into one or several objects or processes that are confined in time and space”* (Verschuren & Doorewaard, 2010). In this situation, the case studies are about the risk and impact analysis of sea level rise to the most important flood defences in the Netherlands which are the Maeslant Barrier and the Eastern Scheldt Barrier. In-depth research is required in the form of a risk analysis to answer the main research question specifically. The case studies should provide explicit solutions for the sea level rise problem for both storm surge barriers and the inherent water system behind. The main reason why case studies will be performed is to create more specific answers to evaluate the preferred strategy of the Delta Programme and robustness of the storm surge barriers.

#### **Modelling**

Models are useful to deliver important research findings and they can be useful for statistical validation. A combination of literature study and modelling create more objective and reproducible research. This research will use the probabilistic model Hydra-NL to calculate the hydraulic loads for the case studies. This will be done by using the statutory assessment tool (WBI) of Rijkswaterstaat. However, Hydra-NL cannot be used to determine the remaining lifetime of the storm surge barriers and to find adjustments that effectively extend the technical tipping point. This requires a risk analysis based on models and expert judgment of all contributing risk factors.

#### **Interviews**

Experts will be interviewed to compare theoretical information with more practical knowledge. More substantiated conclusions can be made if both types of research match with each other. These interviews can be helpful during all specific phases of this research. Several interviews will be held at Rijkswaterstaat (including members of the operation team of the MLK), Deltares and the KNMI.

### 2.3.2. Method of the tipping point analysis

The focus of the tipping point analysis will be on the Maeslant Barrier and Eastern Scheldt Barrier and their resilience to sea level rise. The technical tipping point of the storm surge barriers can be defined as the following:

*“The extent of sea level rise at which the storm surge barrier can no longer protect the water system at the agreed water level, resulting in substantially increased hydraulic loads on landward dyke trajectories.”*

In order to estimate the remaining life of the storm surge barriers, the following steps in the tipping point analysis are required:

1. define the scope;
2. determine the uncertainty of climate change and the rate of sea level rise;
3. set threshold values and maximum acceptable increased hydraulic loads for the water system;
4. determine the technical tipping points of the storm surge barriers in relation to sea level rise;
5. combine sea level rise and the tipping point to outline the remaining lifetime;
6. develop response strategies and measures to extend the tipping point;
7. determine the extended technical tipping point after implementing adjustments;
8. give a recommendation for required policy in the future.

The technical tipping point is the point when sea level rises to such an extent that the storm surge barrier can no longer protect the hinterland at the agreed water level. By combining the tipping point with climate scenarios, it is possible to derive the moment in the time when the tipping point will be exceeded. Therefore, the effects of climate change on the sea level rise projections should be determined (Chapter 4 & 5). Then, the hydraulic loads will be determined which affect the storm surge barriers and the inherent water system for various plausible sea level scenarios (Chapter 6).

The risk analysis of this study should determine what extent of sea level rise is tolerable for the storm surge barriers by assessment of various risk factors such as the water storage capacity of the water system or the strength of the construction of the storm surge barrier (Section 7.1). The lowest tipping point, measured in sea level rise, is expected to be decisive for the barrier. This tipping point will be combined with the sea level rise scenarios to determine the expected remaining lifetime of the Maeslant Barrier and the Eastern Scheldt Barrier (Section 7.2).

If the remaining lifetime is less than anticipated, several measures and response strategies will be proposed in order to extend the technical lifetime of the storm surge barriers. These measures can consist of various adjustments to the construction, closing procedures or strategies. The extended technical tipping point can be considered as the point that the current water system is not suitable any longer due to climate change (Section 7.2 & 7.3).

## 2.4 Data Gathering and Analysis

Data can be gathered both quantitatively and qualitatively by conducting extensive literature research. The search for relevant literature will start by using appropriate keywords which can be found by using synonyms of essential words which are stated in the general topic, problem statement, research question and sub-questions.

Keywords should be used to find more specific literature on the internet and form the basis of the literature search. The primary search machines will be Google (Scholar), TU Delft library which will increase the chance to find relevant publications from journals and institutions. If relevant literature is found which can contribute to this research, it could be meaningful to search for more publications made by these authors. Furthermore, it is useful to look at the references of an article to explore more relevant studies. All literature will be stored in different maps to keep a clear overview.

Another way to find relevant data is to use the database of Rijkswaterstaat. This digital knowledge platform will be used to find specific technical information about the storm surge barriers and the assessment methods. Hydra-NL is a program to calculate hydraulic loads on various locations for all possible safety standards. The

assessment tool is part of the WBI-2017 and will be used in the risk analysis of the storm surge barriers and the dykes in the hinterland.

A third way to acquire relevant data and information is to carry out several interviews with specialists representing various organizations that investigate climate change and flood risk management.

When the information and data are found, it is important to analyze it critically. Data analysis starts by comparing acquired information with other literature. Data can be evaluated on relevance and reliability by investigating the source, publishing date, authors, and peer reviews. Furthermore, some of the used data will be critically assessed by experts from Rijkswaterstaat and other organisations (KNMI for example).

## 2.5 Report structure

The first chapter is an introduction to the topic and the relevance will be discussed. A general problem description will be explained and transformed into a problem statement. Thereafter, the problem statement will be converted into a research question combined with several sub-questions.

The body of this research will start in Chapter 3 in which the current policy and history of flood risk management in the Netherlands is addressed. Chapter 4 is intended to analyse the latest knowledge about climate change. Current sea level rise and future projections are explained in Chapter 5. This chapter also addresses the potential increasing contribution of the Antarctic ice sheet which intensifies sea level uncertainty to a large extent.

In Phase II, the updated sea level scenarios will be used to determine the hydraulic loads of the Maeslant Barrier, the Eastern Scheldt barrier and several dykes which are part of the Rhine-Meuse Delta and the Eastern Scheldt in Chapter 6.

Chapter 7 will discuss the various risks that might influence the remaining lifetime of the storm surge barriers and therefore the technical tipping point. This chapter discusses the effects of increased hydraulic loads to various risk factors such as the risk of exceeding the storage capacity of the water system, the strength of the construction and the closing procedure. This tipping point analysis helps to substantiate the impact of sea level rise to the storm surge barriers which support developing risk responses that can potentially increase the operating lifetime of both barriers.

Next, advice is given about the most effective strategy and the expected remaining period that the current water system can be maintained. Ultimately, conclusions and recommendations are formed, the results will be discussed and recommendations for future research will be addressed.

# 3. Flood protection

For many years, the Netherlands has a developed policy in flood risk management. For centuries, measures have been taken to ensure safety through flood management. Each flood that caused severe damage has resulted in actions to prevent future floods. Later on, a proactive approach based on statistical analysis was carried out to reach a certain threshold safety level for primary flood defences in the Netherlands. Developments in statistics, (climate) models and projections have led to improved flood defences and reduced uncertainty. These strategies were effective during relatively small changes in environment and climate but may be insufficient for more massive changes such as accelerated sea level rise. Storm surge barriers are expensive constructions that should have a long operating lifetime to be economically viable. Climate change and sea level rise are deeply uncertain on the long-term perspective and are therefore a risk for storm surge barriers.

This chapter will explain historical flood risk management in the Netherlands combined with current policy and adaptive strategies. More focus is addressed to the Maeslant Barrier and the Eastern Scheldt Barrier which are of primary importance in this research. Future climate change together with sea level rise is explained in Chapter 4 and 5 to understand future risk of flooding in more detail.

## 3.1 History of flood protection in the Netherlands

The Netherlands is a low-lying delta and the society protected themselves against flooding by the sea for hundreds of years. Many people in the country have been killed by floods in the past and the 1953 flood disaster is the last major flood catastrophe. The current geology of the Netherlands is formed by the influence of the sea, rivers and by human-induced activities and processes which are explained in this section.

The first inhabitants sought higher grounds to be safe against flooding. The first flood defences were built roughly 2,500 years ago (Iron Age) to inhabit the low-lying areas in the Netherlands. These constructions consisted of dwelling mounds, also called “terps”. These constructed hills were built in coastal areas in Friesland and Groningen to protect people and properties. Ever since, inhabitants of other low-lying regions also began to construct low earthen dykes made of clay to protect small villages and fields (ENW, 2016).

The first dykes were built in the seventh century to protect inhabitants against the sea. Around the year 1000, people successfully managed to control the course of the rivers in the Netherlands. From the twelfth century, dykes were connected to each other, which was the beginning of a levee system. Individuals and small communities were no longer capable of building and maintaining the levees, so water authorities were established in the Late Middle Ages. Nonetheless, floods still occurred regularly (ENW, 2016). Between the 9<sup>th</sup> and 13<sup>th</sup> century, humans started to influence the dynamic behaviour of the river and the geology which was an important period in history for the geology of the Netherlands. From the thirteenth century onwards, human influences further increase when the local inhabitants built small dykes to keep areas permanently dry (Gerritsen, 2005).

Later, this was followed by large-scale land reclamation by damming and draining to create “polders”. Polders are low-lying areas, often below sea level, which are dry-pumped from rising groundwater and are protected by surrounding dykes (Gerritsen, 2005). The main reason to create extra land was to expand agricultural facilities.

In the 16<sup>th</sup> century, many peatlands were dredged and exploited by making use of the dredger bracket. This type of soil can be used as fuel to heat up houses. Lakes were formed by the exploitation of the peatlands and levees were needed to provide water safety for the residents nearby.

In the 18<sup>th</sup> century, water authorities launched projects to redirect some rivers in the Netherlands with dykes to make the areas around the rivers less dynamic and to control water level to create defensive barriers during times of war (SHC, 2007). The first redirection measure was the digging of the Pannerden Canal which was

realized between 1701 and 1709. Many more rivers were adapted and the influence of the rivers on geology was reduced by these measures.

Floods still occurred in the rivers area, so various measures were taken in the nineteenth century. Several spillways were constructed, and rivers were straightened and redesigned to increase the rate of discharge. Furthermore, the Meuse and Waal were separated combined with a heightening of the levees. These measures considerably reduced the numbers of flooding in the region (ENW, 2016).

The “Zuidersea project” was initiated after the flooding in 1916. Many levees failed all over the country and nineteen people died. The areas around the Zuidersea were prone to flooding for centuries and the 1916 flood led to the execution of this ambitious project. The most important project was the enclosure of the Zuidersea by the Afsluitdijk. The main intention was to create more farmland and to protect the hinterland against flooding. The construction of the Afsluitdijk was completed in 1932 and this dyke transformed the Zuidersea into the IJsselmeer. This measure shortened the coastline to a large extent, which reduced the risk of flooding (ENW, 2016). In 1926, when the discharge of the Meuse was too high, major flooding occurred which damaged 3000 houses. At the same time, the peak of the water discharge at Lobith was 12,850 m<sup>3</sup>/s, the highest discharge ever measured (ENW, 2016).

On 1 February 1953, a disaster occurred that changed the flood protection policy. A strong north-west storm in combination with spring-tide water level caused a massive storm surge. The sea level reached a record-breaking height of 4.55 m (Vlissingen). Around 150 dyke breaches were recorded in the primary sea defences followed by more breaches inland. Approximately 750.000 people lived in the affected areas at that time and roughly 100.000 people were evacuated. The flood took the lives of 1836 people and the damage to buildings, dykes and other infrastructure was enormous (Gerritsen, 2005). The breaches and the inundated areas during the 1953 flood are shown in Figure 3.1.

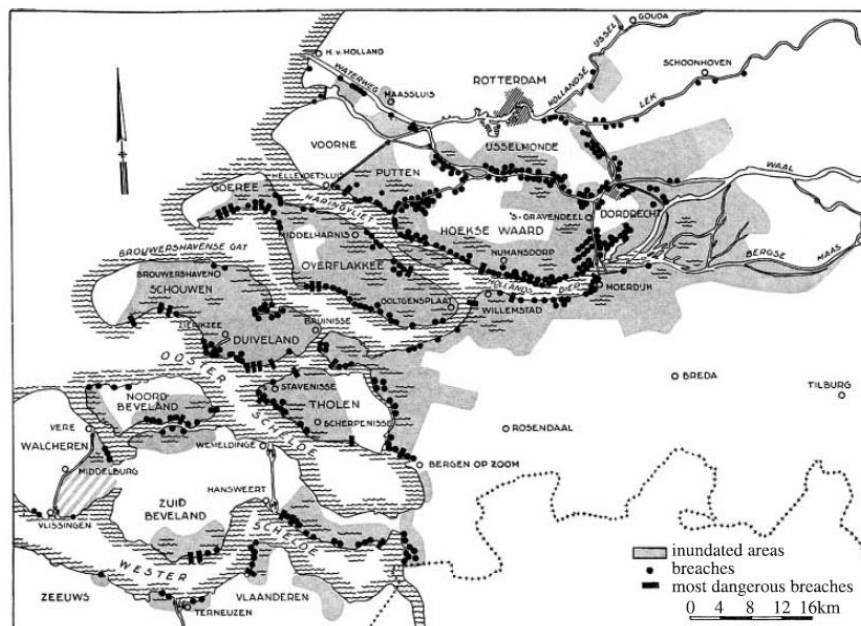


Figure 3.1: Extent of inundations during the 1953 storm (KNMI R. a., 1961).

The disaster initiated the formation of the *Delta Committee*, which is an administrative body, resulting in an essential change in the Dutch flood risk policy. Policymakers learned that the deterministic approach was inadequate. The objective of the Delta Committee was to protect the country against flooding by investigating the possibilities of a new flood risk safety approach. Flood risk should be calculated in a probabilistic method instead of heightening dykes based on the highest known water level. After the flood, the beginning of the Delta Act and the work on the Delta Project (*Delta Works*) was commenced. The decision was made to shorten the Dutch coastline by approximately 700 kilometers by constructing dams. Closed dams and dams that allow water passage during regular days were constructed between the South Holland and the Islands of Zeeland. In this way, the coastal flood defences offer more protection for the dykes inland. The Delta Works are a cluster of flood

protection measures to protect the land within the Dutch delta. The measures consist of storm surge barriers, dams, sluices, locks, and dykes. The Delta Works, and in particular the Maeslant Barrier and Eastern Scheldt Barrier, are known worldwide for their technological development in the protection against floods. The Delta Works create a unique compromise between safety, economy, recreation and nature (ENW, 2016).



Figure 3.2: Flood of 1953 (RWS, 1953).

### 3.1.1 Pro-active flood risk approach (1953 – 2017)

After the 1953 floods, the Delta Committee proposed peak water levels that levees must be able to defend against. This was a simplified way of specifying safety requirements in terms of the probability of flooding which only took water levels into account. A flood defence structure should be able to defend the hinterland against a certain peak water level. From the perspective that such catastrophe should never happen again, the Delta Committee stated that the probability of occurrence of such an event should be very small. In the past, levees were heightened based on the highest known local water level in the past. The method changed, dykes are strengthened based on the probability that a particular design water level will be exceeded. *“It was no longer a matter of responding to flooding, but of taking a proactive approach based on statistical analysis”* (ENW, 2016).

Another change was that the reduction in flood risk is balanced by the costs of reinforcements in the form of a cost-benefit analysis (CBA). This method calculates the required safety standard combined with an economic optimization. Economic optimization can be found by a financial assessment of the expected losses through damage to a flood and the required investments in improving relating flood defences (Boardman, Greenberg, & Vining, 2012).

The highest standards were set in the western part of the Netherlands because the impact would be the highest in terms of damage. Performing a Cost Benefit Analysis (CBA) can point out if it is economically efficient to strengthen dykes to reduce the risk of flood damage. Flood defences in valuable areas would have to withstand water levels with an annual exceedance probability of 1/10,000. At locations where the impact of flooding is relatively small, lower standards were proposed. The Netherlands was divided into levee systems, which are adjacent rings of flood defences and higher ground, which all should comply with their own safety standard. This standard is based on the exceedance probabilities of the design peak water level (ENW, 2016).

The designers took future sea level rise into account due to the proposed lifetime of 100 years of the large defence structures made in the south-west delta during the Delta Works. A relative sea level rise based on extrapolation of measurements was included in the design. Climate change and accelerated sea level rise were not considered at that time (Haasnoot & Middelkoop, 2012).

In 2007, the second Delta Committee was established to identify actions to prevent future disasters, due to climate change and sea level rise (Veerman & Stive, 2008). This committee considered a high-end sea level rise scenario for 2100 and 2200 to evaluate the robustness of the water system. The estimated range was 0.65 m-1.3 m (2100) and 2-4 m (2200). These approximations were based on expert judgement. Policymakers noticed that the current water system should be adapted to overcome sea level rise and climate change (Haasnoot & Middelkoop, 2012). This resulted in the Delta Act and the Delta Programme. The content of the Delta Programme is explained in Section 3.2.5. An overview of the primary levee systems in the Netherlands is shown in Appendix G.

## 3.2 Flood protection in the Netherlands

The history of flood protection forms the basis for current and future flood protection policy in the Netherlands. The definition of flood risk including the relevant factors is explained to address the need for an improved water safety standard. This new standard will provide a minimum safety level for each civilian in the Netherlands in terms of flooding. The new approach in water safety assessment is part of the Water Act, enforced on 1 January 2017, and has its implications on the current water system, the Delta Programme, and the Dutch Flood Protection Programme.

### 3.2.1 General water system

The Netherlands has 17,691 km of levees and other flood defences to protect its inhabitants and infrastructure (HSK, 2015). Most flood defences are constructed such as dykes, dams, locks, and storm surge barriers but some defences are natural barriers such as dunes and high grounds (Rijkswaterstaat, 2015a). Without flood defences, almost 60% of the area in the Netherlands is vulnerable to flooding because 26% of the Netherlands is situated below sea level and another 33% is prone to flood risk originating from sea or rivers (PBL, 2007).

Primary flood defences provide protection against flooding from the sea, major rivers and large lakes. All primary flood defences, 3449 km in total, should have a specified safety level with an annual exceedance probability. This exceedance probability is set because floods cannot be completely ruled out. Rijkswaterstaat manages 249 km of the largest dykes, dams and dunes, five storm surge barriers and many locks. The water boards manage the other 90% of primary flood defences in their own regions (IHW, 2017).

The Netherlands also has regional defences along canals and smaller lakes. A characteristic of a regional dyke is that it offers protection against the inland waterway floods and these types of barriers do not have national and legal status. A failure in regional defences will generally have a smaller impact than a breach in the primary defences but can still have considerable consequences. The safety standards for regional defences are set by the provincial authorities. Finally, the country also has many flood defences with no specific status, for which no safety standards have been specified in national or provincial legislation (ENW, 2016).

### 3.2.2 Storm surge barriers

A storm surge barrier is a closable barrier located in river estuaries and waterways. Storm surge barriers are designed to protect the area and water system behind the barrier for extreme water levels caused by storm surge in combination with springtide. Storm surge barriers can close temporarily during extreme high-water levels to protect a large valuable area against flooding. During normal daily weather, these constructions usually provide an open connection with the sea. Storm surge at the North Sea is a risk to water safety because of the temporarily high sea water levels which are caused by the combination of high wind speeds and the relatively low water depth of the North Sea. Rijkswaterstaat manages and maintains all five storm surge barriers in the Netherlands (Rijkswaterstaat, 2015a). Four of the five storm surge barriers were built as part of the Delta Works that was initiated after the 1953 North Sea flood. The Maeslant Barrier and Eastern Scheldt Barrier are the well-known storm surge barriers in the Netherlands and have unique characteristics. More information about these barriers is described below.

#### 3.2.2.1 Maeslant Storm Surge Barrier

The Maeslant Barrier (MLK) is constructed between 1991 and 1997 and is located in the Rotterdam Waterway (Dutch: "Nieuwe Waterweg"). This watercourse is the vital shipping route towards the port of Rotterdam. The unique design of the closable storm surge barrier is the result of the requirement that the barrier should not impede shipping. Therefore, the storm surge barrier should only close in exceptional cases to prevent flooding. The Maeslant Barrier provides flood protection to more than one million people in South Holland by reducing the hydraulic loads for the dykes in the Rhine-Meuse Delta.

Initially, it was thought that the Delta Works were completed by building the OSK in 1986. However, dyke improvements in Rotterdam and along the "Nieuwe Waterweg" would not provide sufficient protection for the areas behind. The storm surge barrier appeared to be an attractive solution in terms of safety, environmental impact and costs. Also, this solution could be realized significantly faster than the planned dyke reinforcements.

Especially, dyke reinforcements in the urban area could create major challenges with considerable risks. In 1987, the Dutch government decided that the MLK should be built (Deltawerken, 2004).

The MLK is designed for a lifetime of 100 years including 50 cm sea level rise. The MLK is the only storm surge barrier in the world with such large movable elements. The length of the water-retaining doors is 216 meters each and are designed to withstand a water level of +5 m NAP. Under normal circumstances, the doors are completely open and stored in a dock along the river, making the port of Rotterdam accessible to ships. The floodgates are closed in case of a storm surge and once per year during the test procedure. The first closure of the MLK was a fact during a storm on 8 November 2007. The total closing procedure takes several hours because it takes almost two hours to fill the hollow doors with water, allowing them to sink to the bottom of the river. The total height of the doors is 22 m. As soon as the high-water event is over, the doors are drained. The floodgates will float and can return to their dock. It is crucial to open the barrier as quickly as possible because the river continues to discharge water which increases the water level behind the closed barrier.

The closing computer system (BOS) works fully automatically to minimize the chance of human error. During a closure, specialists should always be on site to intervene if something goes wrong. A careful consideration will be made whether the MLK should be closed. This is a trade-off between damage control in the vulnerable low-lying areas outside the dykes and the accessibility of the port of Rotterdam. A precondition is that the barrier must be closed in time at a predicted water level of +3.00 m NAP in Rotterdam or +2.90 m NAP in Dordrecht. The BOS system calculates the expected water levels on the basis of predicted high water levels, current water levels and river discharges of the Rhine and Meuse.

The MLK is a category-B flood defence barrier. This means that the MLK offers protection to the primary flood defences (category A) behind the barrier by lowering the maximum water level originating from the sea. The flood defences behind the MLK should, therefore, meet the required safety standard. The hydraulic requirements for the category A flood defences are lower because of the presence of the MLK.

To prevent flooding of the Europoort area during an extreme storm, the construction of an additional storm surge barrier in the “Hartelkanaal” was required. The Hartel Barrier is another storm surge barrier that operates in line with the MLK. The Hartel Barrier and the Maeslant Barrier form together the Europoort Barrier which protects Rotterdam against flooding. In addition, this Europoort barrier consists of several dyke improvements in the area between Dordrecht and Hoek van Holland.

Another primary aspect of the barrier is the reliability of the closure operations. In 2001, research showed that the closure operation was not reliable with a failure probability of approximately 10% per closure. Since then, Rijkswaterstaat has significantly improved the operation processes and maintenance of the barrier, increasing the current reliability to 99% (Rijkswaterstaat, 2017a). More information about the Maeslant Barrier is described in Appendix H.



Figure 3.3: The Maeslant Barrier (Rondvaart Europoort, 2016).

### 3.2.2.2 Eastern Scheldt Barrier

The Eastern Scheldt Barrier (OSK) has been built between 1976 and 1986 and is located between Schouwen-Duiveland and Noord-Beveland. It is the largest storm surge barrier in the world with a total length of 8.5km of which 3km is lockable. It concerns a half-open defence structure that can be shut off by floodgates in the event of a high-water. The construction consists of 65 pillars and 62 movable steel doors. The floodgates are about 42 m wide and weigh 260-480 metric tons each.

The OSK was built to guarantee water safety in Zeeland for the next 200 years. The barrier has been designed for a maximum sea level of +5.2 m NAP, corresponding to a high-water situation that occurs statistically once in the 4,000 years (Rijkswaterstaat, 2007). The height of the barrier is +5.8 m NAP at location Roompot and Schaar and +5.6 m NAP at Hammen providing space for 40 cm relative sea level rise (SLR + vertical land decline). Latest calculations show peak levels of +5.09 m NAP to +5.14 m NAP for T=4,000. After the regulation change in 2017, the failure probability of the OSK should be maximal 1/10,000 per year (Deltares, 2017a). More information about the regulation change is provided in Section 3.2.4.

When sea level exceeds +2.75 m NAP, the operation team discusses if a closure is needed. This meeting takes place in the control building located on the barrier. If the expected sea level on the North Sea exceeds +3.00 m NAP, the team is obligated to close the gates. The total closing time takes 82 minutes, so it is essential to investigate the forecasted sea level in the last hours before a high-water event. An emergency locking system is operational if all other operations fail. When this happens, the doors close automatically when sea level rises above +3.00 m NAP.

This OSK closes on average once per year. The aim is to achieve a water level of +1 m NAP on the Eastern Scheldt. This water level will be maintained for approximately 10 hours, as the barrier cannot be reopened until the next low tide. If it is predicted that the next high water will also be higher than +3 m NAP, the aim is to limit the water level on the Eastern Scheldt to +2 m NAP after the second closure of the barrier.

Initially, it was planned to close the Eastern Scheldt estuary completely. The unique saltwater environment in the Eastern Scheldt estuary would be lost due to the closed water reservoir. After considerable resistance, the plan was changed in 1976 to build a barrier, which only has to be closed during extreme water levels. The unique saltwater environment, the mussel and oyster cultivation and the tidal activity will be maintained by this change. The barrier is designed to maintain 75% of the tide activity in the Eastern Scheldt, with open floodgates. The construction costs of the barrier were estimated at approximately 2.5 billion euros which was much more than for the original plan (Deltawerken, 2004). More information about the OSK is described in Appendix H.



Figure 3.4: The Eastern Scheldt Barrier (Ingenieur, 2016).

### 3.2.3 Flood Risk

The history of the Netherlands by means of flood protection and flood disasters show that managing flood risk is extremely important. Flood risk concerns the possible impact of flooding and the probability that it will occur. It specifies the consequences and the probability of these consequences. The risk is expressed as the following: *probability times economic damage*.

Flood risk can be expressed more qualitatively in economic risk, societal risk, and individual risk. This approach is included in the Dutch law in 2017. Understanding flood risk and the relative impact on society and economy is of key importance to be able to develop measures that can reduce this vulnerability and may support decision-making on flood risk management (ENW, 2016).

#### **Economic risk**

Economic risk refers to the (annual) costs of the risk expressed in euros per year. Economic risk is often equal to the expected annual value of the damage, the product of the probability and the damage. Economic risk is an essential element in the cost-benefit analyses. The idea is that the government can efficiently spread the costs of potential damage among all the inhabitants of the Netherlands (ENW, 2016). Otherwise, everyone pays the costs of the damage for themselves, which could be too high to bear.

#### **Societal risk**

Societal risk describes the likelihood of a large number of casualties. This is important because disasters that take many lives lead to great unrest and make people feel unsafe (ENW, 2016). This is a mental issue because large accidents have a more significant impact on society than many small accidents. In 2016, 629 people died in traffic in the Netherlands (SWOV, 2017). The 1953 flood, for example; caused 1836 fatal casualties which was worldwide news and still in our memory and resulted in large-scale measures. Important to note is that more people lost their lives in traffic over the last 4 years than during the 1953 flood. It is clear that small probability, but high impact accidents are assumed to be more important than numerous individual accidents.

#### **Individual risk**

Economic risk, societal risk and cost-benefit analyses relate to risks for a large population of people. Individuals, however, can face a more substantial risk which is not addressed in the risk factors above. "The local individual risk (LIR) is a measure of risk which expresses the probability that a person permanently located at a particular place will die as a result of flooding" (ENW, 2016). Setting a limit for local individual risk provides everyone in the Netherlands a basic level of protection in regions protected by dykes.

#### **3.2.3.1 Uncertainty in flood risk management**

Quantification and classification of uncertainties in flood risk management are very important but also extremely difficult. In determining both the likelihood and the consequences, we are dealing with uncertainty. For example; it is uncertain when a storm occurs that is able to cause a flood. Furthermore, it is uncertain what the impact is of a flood if it does occur. For decision-making, it is essential to know what uncertainties exist, how significant they are and whether they can be reduced in practical terms (ENW, 2016).

Uncertainties are caused by natural variability and it is impossible to predict and the exact reality. Furthermore, knowledge uncertainties of physical phenomena such as water movement and soil subsidence cannot be modelled precisely. The following uncertainties are important for the calculation of flood risk:

- uncertainty of future climate change;
- uncertainty about extreme weather;
- uncertainty about the strength of flood defences;
- model uncertainty;
- uncertainty about the consequences of flooding.

All uncertainties above will be discussed in this research, but the primary focus will be on the MLK and OSK, which are the most prominent storm surge barriers in the Netherlands. Therefore, a correlation exists between

uncertainty in climate change, extreme weather statistics and model uncertainty. It is essential that these links are understood and included in the analysis of calculating flood risk.

Climate change is potentially the most uncertain factor in determining flood risk. It is unknown how climate change evolves over time and if the global policies will lead to a successful energy transition that may slow down climate change. Chapter 5 will explain climate change and the different scenarios in more detail. One of the main effects of climate change is sea level rise. Future sea level rise is profoundly uncertain and it is proposed to incorporate *mean sea level rise* and *high-end scenarios* into flood risk management. Scientists address the uncertainty of the rate of future sea level rise in a probability distribution function (PDF). High-end sea level rise scenarios refer to the upper part (95<sup>th</sup> percentile) of the PDF. High-end events are unlikely to occur ( $\leq 5\%$ ) but cannot be ruled out due to the potentially high impact on society and economics. The probability that high-end sea level rise occurs is relatively small, but the impact on water safety could be significant. Therefore, it is required to assess whether the storm surge barriers provide sufficient protection to the hinterland for the projected rate of sea level rise and in case that high-end (small probability, high impact) sea level rise scenarios occur.

It is impossible to predict extreme weather at a specific time and place. In the context of coastal flood risk, extreme weather refers to storm surge and waves in front of flood defence structures. However, it is possible to indicate the chance that a particular water level will be reached or exceeded. This probability can be determined by statistical analysis of time series of water levels and waves over the last century. These time series are limited compared to projections for events with a yearly probability of 1/10.000. It is required to extrapolate the time series to indicate very small probability events that could have a large impact. This is shown in Figure 3.5.

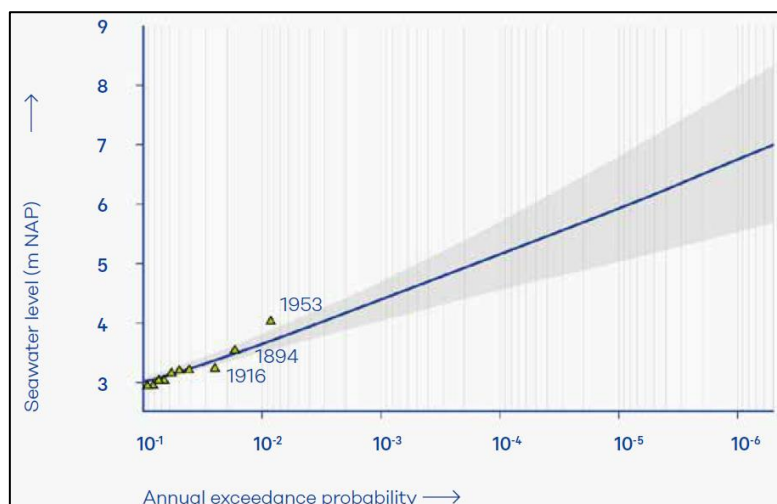


Figure 3.5: Annual probability of exceedance a certain peak water level based on extrapolation (ENW, 2016).

The actual strength of storm surge barriers is relatively uncertain. The constructions are designed with formulas with large safety margins because sophisticated models were not available at that time. The MLK is designed with the use of relatively simple models to calculate the forces on the barrier and the stability of the subsoil, but several properties of the structure have a relatively large uncertainty bandwidth. The soil parameters cannot be quantified at each specific place and have to be simplified. Understanding the strength of the subsurface is essential to quantify the stability of hydraulic structures and other flood defences. Therefore, it is important to understand the subsurface and soil parameters as detailed as possible.

Models are always a simplification of a complex reality. Every input parameter has an uncertainty. Models are based on past observations and partly on subjectivity are therefore always surrounded by uncertainty. Nevertheless, models are needed to calculate water safety and flood risk of flood defences, but it is important to understand the limitations of models. This study uses the probabilistic model Hydra-NL to calculate the hydraulic loads on both storm surge barriers and relevant dykes. This model also uses various simplifications which are described in Appendix I.

The consequences of flooding depend on many uncertain factors, such as the location and development of dyke breaches, flow velocity through the affected area and the vulnerability of the people, buildings and infrastructure in those areas (ENW, 2016). Also, It is uncertain how many victims can be caused by a flood. In this regard, it is essential that proper evacuation- and response plan will be made. Within this research, the consequence of a failed storm surge barrier to the hydraulic loads of the water system and dykes will be assessed.

### **3.2.3.2 Risk measures and reinforcements**

If flood risk surpasses the acceptable risk, measures should be taken to reduce the probability and/or impact of flooding. The choice of a risk measure depends on the factors that determine how dangerous an imminent event is perceived to be. Strategies are required to improve water safety in an efficient and viable way. These strategies are set out in the Delta Programme. Specific projects that are needed to comply with safety requirements are specified in the Dutch Flood Protection Programme (DFPP). Both the Delta Programme and the DFPP are explained in more detail in Section 3.2.5 and 3.2.7. The recommended strategies and risk measures for the Maeslant Barrier and Eastern Scheldt Barrier will be described in Section 7.3.

### **3.2.4 Next level flood safety policy and assessment (2017)**

Dutch experts identified several weaknesses in the previous flood risk policy. The Dutch government acknowledged these weaknesses and was aware of the need for improvement. With the National Water Plan, the need for a revision of the protection standards approach was announced (Tsimopoulou, 2015).

In the old safety standard, flood defences should have the height and strength to withstand a peak water level that statically occurs once in the thousand(s) of years ( $T=1,250$  until  $T=10,000$ ). The standard was set for a dyke ring and gave requirements for the required dyke height.

In 2017, a new water safety methodology combined with new safety requirements was set into law in the Dutch Water Act. Everyone in the Netherlands should receive the same level of protection against floods. The required safety standard that will be applied to a specific dyke section depends on the risk of flooding and the consequences of flooding.

The new flood safety policy was needed because the economic value in various areas and therefore the potential damage of flooding is significantly increased over last decades. Furthermore, experts have gathered more knowledge about the failure mechanisms and consequences of flood defences by using more sophisticated models. With computer simulations, the risks for each area can be mapped out to enable more targeted investments in flood defence measures.

The Water Act has made the transition from standards for dyke rings to standards for dyke sections (trajectories). The consequences of flooding of a dyke ring depend on the location where the water passes through or over the dyke. A dyke trajectory is part of the flood defence, where the consequences of a breach at any location within the trajectory lead to similar consequences. The switch to standards for dyke sections provides a more accurate overview of the consequences and impact of potential flooding at different locations. In 2017, all flood defences in the Netherlands will be assessed according to this new principle. This methodology is laid down in the statutory assessment tools (WBI-2017).

Based on the new standards, flood defences have a chance of failure (between  $1/300$  and  $1/30,000$  per year) instead of a predefined high-water level. This is the probability of loss of the water-retaining capacity of a dyke section, so the area protected by the dyke section is flooded in such a way that it leads to fatalities and/or substantial economic damage. That is why the new safety standard is generally increased because dykes can fail in several ways which could previously not be determined very accurately. The flood defences can fail due to other failure mechanisms which are not only caused by a maximal water level such as macro-stability and piping. Still, the height of a flood defence structure is one of the three most essential aspects. Water levels and the actual and required height of the flood defences will be referred to the Amsterdam Accordance Datum (NAP).

The new standard is set for every dyke trajectory in the Netherlands. Each dyke trajectory will be assessed in terms of potential flooding area, casualties and impact on damage, nature of the threat and the length of the dyke trajectories.

The new standards for dyke trajectories are derived because of the following new safety policy:

- everyone in the Netherlands receive at least a protection level of  $10^{-5}$  per year (fatality rate due to flooding is below 1/100,000 per year);
- more protection is provided in areas where might be:
  - a large group of victims;
  - significant economic damage;
  - severe damage caused by the loss of vital and vulnerable infrastructure of national importance. (Flood Protection Programme, 2017)

This change was necessary because the country is fundamentally changed in recent decades. The population and economic activity are considerably increased in many areas. Also, the knowledge about the strengths of the dykes and flood defences is increased to a large extent. Models are used to simulate potential flood areas and can also consider the effects of climate change. This development has increased the understanding in quantifying both the strength of flood defences as well as the impact in case of flooding (Flood Protection Programme, 2017).

The standard is now explicitly based on the possible consequences of flooding behind flood defences. The unit has changed to the probability of flooding, which applies to dyke and dune trajectories and flood defences. Rijkswaterstaat and water authorities have been working together to strengthen the dykes and dunes. The possible consequences have been identified more efficiently than in the past, with a greater focus on fatalities and victims. For the first time, the loss-of-life risk has played an essential role in the revision of standards for flood defences. The government has decided that the probability of a life loss due to flooding may not exceed 1/100,000 per year in all protected areas of the Netherlands (ENW, 2016). In the new system, primary defences have been divided into one or more levee segments, each of which has its own safety standard. An overview of the levee segments is shown in Appendix G.

The new flood safety policy is based on three key aspects. First, new safety standards and standards are established for the primary flood defences. These changes generally lead to slightly more stringent requirements for the flood defences, which will be reinforced to be able to meet the new safety regulations. Cities and other valuable areas should, therefore, provide additional flood protection due to the potential of many victims and significant economic damage. Vital and vulnerable infrastructure, such as public utilities, power plants and hospitals, receive extra attention. Flood defences that already meet the new requirements will be maintained carefully. Second, the spatial layout of the area behind the dykes is better examined. The goals can possibly also be achieved by measures behind the dykes. Specific spatial development measures behind the flood defences may also reduce the number of victims and economic damage. Third, evacuation plans are set up for all regions. In addition, everyone is informed about the flood risks and contingency opportunities. Victims can be prevented if people are well prepared and know what to do in case of a disaster.

The policy goal is that all flood defences meet the new standards before the year 2050. The new water safety standards are part of the new water safety policy, derived from the Delta-decision water safety (Rijkswaterstaat, 2017b). The new system provides more continuous insight into the state of the flood defences and warns early to carry out the necessary reinforcements (Section 3.2.7 Dutch Flood Protection Programme).

### 3.2.4.1 Safety standard

In the Water Act, the primary flood defences are divided into sections that have been standardized separately. Both storm surge barriers are the first line of defence (Dutch: “voorliggende waterkeringen”). Storm surge barriers have the function to protect dykes on the landward side by reducing the hydraulic loads during a storm event. In the Water Act, the definition of the minimum safety standard for the MLK and OSK is the following:

*The probability of loss of the water-retaining capacity of a specific flood defence trajectory, resulting in a substantially increased hydraulic load on a backward dyke trajectory (Water Act Art. 1.1.1).*

For most trajectories, the law prescribes two safety standards: a signalling value and one minimal safety value. The signalling value is stricter than the required minimum safety (limit value) and is meant to warn the administrator that the flood defence structure probably will no longer meet the minimum required protection level in the foreseeable future. This signalling value gives the operator time to prepare the reinforcement tasks. The signalling value is usually three times stricter than the lower limit value. According to the Water Act, the updated maximum yearly probability of flooding for the MLK is 1/30.000 and 1/10.000 for the OSK (Rijksoverheid, 2016). The new safety standards for all relevant dyke sections are shown in Appendix K.

The process for reinforcement projects is the following:

- administrators assess the dyke trajectory according to the statutory assessment methodology and inform the Minister of Infrastructure and Water Management if a dyke section does not satisfy the signalling value;
- reinforcements projects are prioritized in the High-Water Protection Programme based on urgency and ranked based on the actual risk of flooding;
- the designs of the reinforcement tasks are (usually) formed on the basis of the lower limit requirement, given the conditions at the end of the service life.

Storm surge barriers such as the MLK and OSK have movable elements to close the barriers only during high-water events. In addition to a probability of failure per year, it is necessary to set a separate standard for the reliability of the closure. This chance of a non-closure is taken into account when the hydraulic loads for dyke sections behind the storm surge barriers will be determined. This additional standard is not defined in the Water Act due to the complexity. The chance of a non-closure is included in the derivation of the hydraulic load for the dyke trajectories (Witteveen+Bos, 2017).

## 3.2.5 Delta Programme

The Delta Programme is initiated in 2010 and is aimed to provide water safety to the Netherlands for today and in the future. The Delta Programme works on effective, integrated solutions for water safety and freshwater tasks which are of national importance. The Delta Programme is under the direction of the Delta Commissioner and will be executed by collaboration between state, provinces, water boards and municipalities. Together they proposed joint solutions and preferred strategies to improve water safety. This means that there is a shared understanding of the national approach to enhance water safety and availability of fresh water in the Netherlands in the future until at least 2050. The Delta Programme will be developed every year to show the progress of the projects and to propose decision-making and strategies based on the latest information. The preferred strategies of the Delta Programme are different for multiple areas in the Netherlands. All preferred strategies originate from the following universal principles:

- Delta Decisions are used as a framework;
- anticipate in advance instead of reacting to disasters;
- Adaptive Delta Management: make cost-effective measures and be aware of developments;
- link strategy with other spatial ambitions for an integral approach (Delta Programme 2015).

Strategies are established for many different aspects. However, the scope of this research is only on the Maeslant Barrier, Eastern Scheldt Barrier, and the water safety of both backward water systems. Therefore, the strategies of the MLK and OSK are the most important in this study, but some other strategies can also be relevant to the storm surge barriers. The preferred strategies that are relevant to this research are:

- *Maeslant Barrier*: protect the Rhine-Meuse Delta with an open closable storm surge barrier in the “Nieuwe Waterweg”. The same strategy is proposed after replacement of MLK (2050-2100). Locks might replace the MLK in the case of highly accelerated sea level rise (Delta Programme 2018);
- *Eastern Scheldt Barrier*: a future-proof approach to flood risk management and to the erosion problem in the intertidal zone. Adjusted management regime for the OSK to decrease sand erosion. Preserve the estuary environment (tidal activity) by maintaining an open water passage to be able to close the storm surge barrier during extreme storm surge;
- *Flood prevention*: dyke reinforcements and room for the rivers;
- *New safety standards*: all flood defences should meet new water safety standards before the year 2050.

Dykes will be strengthened or renewed according to predictions models at that time for a lifetime of 50 years. The MLK is designed for a lifetime of 100 years including 50 cm sea level rise while the OSK is designed to operate 200 years but for 40 cm relative sea level rise.

The strategies above are intended to be applicable till at least 2050 and still preferred in 2100. The focus of the Delta Programme is particularly until the year 2050 because climate change is still profoundly uncertain after this timeframe. The long-term perspective until the year 2100 should be defined later depending on the developments in social-economic and climate perspective (Delta Programme 2016).

However, new insight into climate change and SLR could have a substantial impact on the strategies described above. Therefore, it might be possible that these strategies should be modified earlier than predicted. This research will investigate the technical tipping points of the preferred strategies for the Maeslant Barrier and Eastern Scheldt Barrier to indicate the timeframe when the current barriers strategies become inappropriate.

### 3.2.6 Adaptive Delta Management

Adaptive Delta Management is an implementation strategy of the Delta Programme. Adaptive Delta Management deals with uncertainties to support decision-making regarding water policy, planning and infrastructural investments.

The preferred strategies of the Delta Programme are adaptive. The concept of adaptive delta management is to work on the implementation of measures and to be flexible to respond to developments and uncertainties in climate and society. Climate change and socio-economic developments are deeply uncertain in the long-term which requires an adaptive approach. This implies that sea level rise must be monitored carefully, and policy must be tested against the latest insights and modified if necessary (Veerman & Stive, 2008). Also, it is key to monitor developments in climate and society in both the past and future to be able to react in the correct way when measures are required (Delta Programme 2016). Adaptive Delta Management is mainly about the assessment of the impact of climate change, to be able to develop adaptation measures and to determine the effectiveness, robustness and flexibility of the adaptation strategy. Adaptive Delta management helps to design water management plans and consists of six steps:

1. problem analysis: analyse vulnerabilities and opportunities for different scenarios;
2. identification of measures: identify solutions and quantify effects;
3. design multiple adaptation pathways (scenarios): based on step 2;
4. design of an adaptive plan: identify critical values;
5. implementation of the plan: execution and implementation of measures to keep options open that might be needed in future;
6. monitoring system: monitor trends allowing adjustment of adaptation strategy and scenarios when needed (Deltares, 2014; Haasnoot M. J., 2013).

### 3.2.7 Dutch Flood Protection Programme

The Dutch Flood Protection Program (DFFP) is the primary implementation program of the Delta Programme. “The DFFP is a long-term alliance of the Dutch Water Authorities and the Ministry of Infrastructure and Water Management, but also a methodology in which the Ministry, regional water authorities, scientific institutes, consultancy and construction companies participate” (Jorissen et al., 2016).

The DFFP is a continuous program of the (reinforcement) projects of flood defences that will be executed in the next six years. This implies that this program does not have a predetermined end, but it is updated annually. All reinforcements are planned and funded by the DFFP. Flood defence structures are tested in assessment rounds. Disapproved flood defences will be reinforced based on urgency as defined in the DFFP. The procedure of the DFFP is about prioritization and programming based on urgency. The projects are ranked on the basis of the actual risk of flooding, probability times the expected damages, fitted within budget (Jorissen et al., 2016).

In 2017, all flood defences will be tested if they are in compliance with the new statutory water safety standards. The new assessment methodology and changed standards can change the rank of projects within the programme. The planned projects are prioritized based on the distance between actual safety and the required safety. It is evident that the most urgent projects will be executed first to minimize the risk of flooding.

The primary objective is to reinforce flood defences, both climate-proof and robust, to the new safety standards before the year 2050 (Delta Programme 2016). Additional goals of the DFFP are to improve performance in project management, to enhance the quality of more integrated solutions and to expand the cooperation between all authorities involved (Jorissen et al., 2016).

# 4. Climate change

Climate change is the most uncertain factor in terms of flood risk management in the Netherlands. One of the main effects of climate change is future sea level rise. The future rate of sea level rise is uncertain and it is essential to incorporate both the expected scenarios and high-end climate scenarios (small probability, high impact) into flood risk management. In 2013, the IPCC concluded that it is very likely that human influence was dominant in causing the temperature rise over the last century (IPCC, 2013).

A climate scenario is a plausible and coherent presentation of the future climate, prepared to investigate the consequence of human-induced climate change (IPCC, 2013). A climate change scenario projects the future climate change conditioned on either a certain amount of temperature rise or a greenhouse gas emission scenario. Climate scenarios are very relevant for flood protection in the Netherlands because these should be used to assess the robustness of the Maeslant Barrier and Eastern Scheldt Barrier to climate change.

Climate change may also influence river discharge which could have an impact on the flood defences around rivers. Despite, this study focusses on the effects of climate change on sea level rise.

## 4.1 Climate background

“Climate background” explains the concepts of climate and climate change in order to understand the basics of climate processes and climate scenarios. This section addresses the main drivers and feedbacks behind climate change and the reasons why the Earth is warming. This background provides the basis to understand the climate factors that trigger global sea level rise which may be a risk for the Dutch storm surge barriers.

### 4.1.1 Weather and Climate

An important distinction should be made between weather and climate. Weather is the atmospheric condition at a specific place at a specific point in time. Meteorological elements such as temperature, air pressure, humidity and wind define the current weather (Cubasch et al., 2013). Weather is generally described in short time frames between several minutes to maximal 2 weeks. Climate is about the average weather over a period of 30 years. Climate is often defined as more than just the average weather and includes the variability. Climate is measured in terms of statistics of conditions in the atmosphere, hydrosphere, geosphere and biosphere. An exact description of climate is: “Climate is usually defined as the average weather, in terms of the mean and variability of relevant quantities over a period of time ranging from months to millions of years” (Cubasch et al., 2013). Climate variability refers to the change in scatter and extremes which are possible in both directions. Changes in climate affect not only average temperatures but also extreme temperatures, which might increase the likelihood of weather-related natural disasters (Earth Observatory, 2001). Climate change refers to a significant shift in the statistical climate distribution with time (Schär, 2004). An example is shown in Figure 4.1.

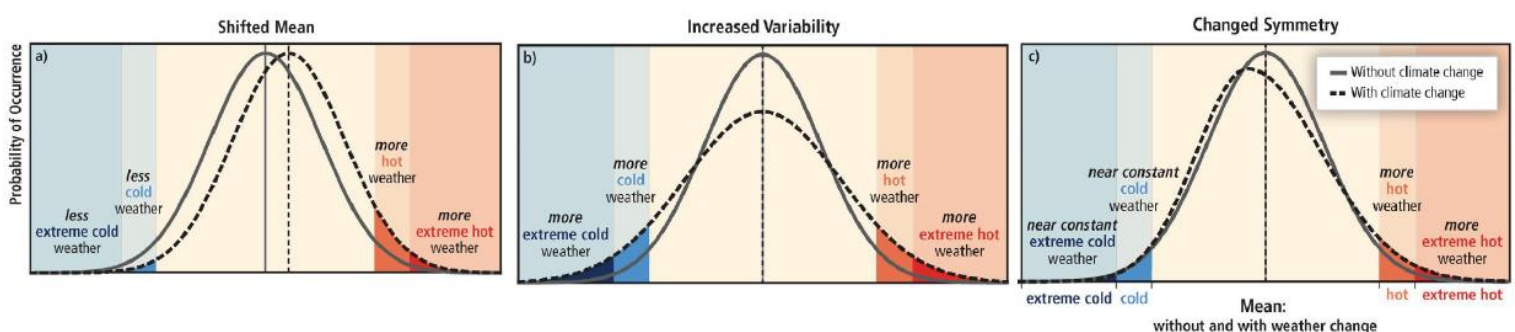


Figure 4.1: Example of statistical shift in climate distribution, change in Variability and a changed symmetry (White et al., 2013).

### 4.1.2. Earth's energy budget

The Earth's climate system is driven by solar radiation. Incoming shortwave solar radiation warms the Earth. In response, the Earth emits thermal longwave radiation (LWR), which is infrared radiation, back to space to maintain radiative balance and a relatively stable temperature. The current global average energy budget is shown in Figure 4.2. The global average incoming solar shortwave radiation is  $340 \text{ W/m}^2$  whereof approximately 50% is absorbed by the surface of the Earth. Approximately  $100 \text{ W/m}^2$  of solar radiation is directly reflected to space by gases, aerosols, clouds and by the Earth's surface (albedo). Circa  $79 \text{ W/m}^2$  is absorbed by the atmosphere.

The infrared radiation (thermal energy) emitted from the Earth's surface is primarily absorbed by atmospheric gases such as water vapour, carbon dioxide ( $\text{CO}_2$ ), methane ( $\text{CH}_4$ ), nitrous oxide ( $\text{N}_2\text{O}$ ) and other greenhouse gases. These greenhouse gases send a large part of this infrared energy back to the Earth's surface which increases the surface temperature. Furthermore, clouds absorb thermal energy and emit LWR in all directions. The downward directed component of this LWR adds heat to the lower layers of the atmosphere and to the Earth's surface. Both processes are called the greenhouse effect (Cubasch et al., 2013).

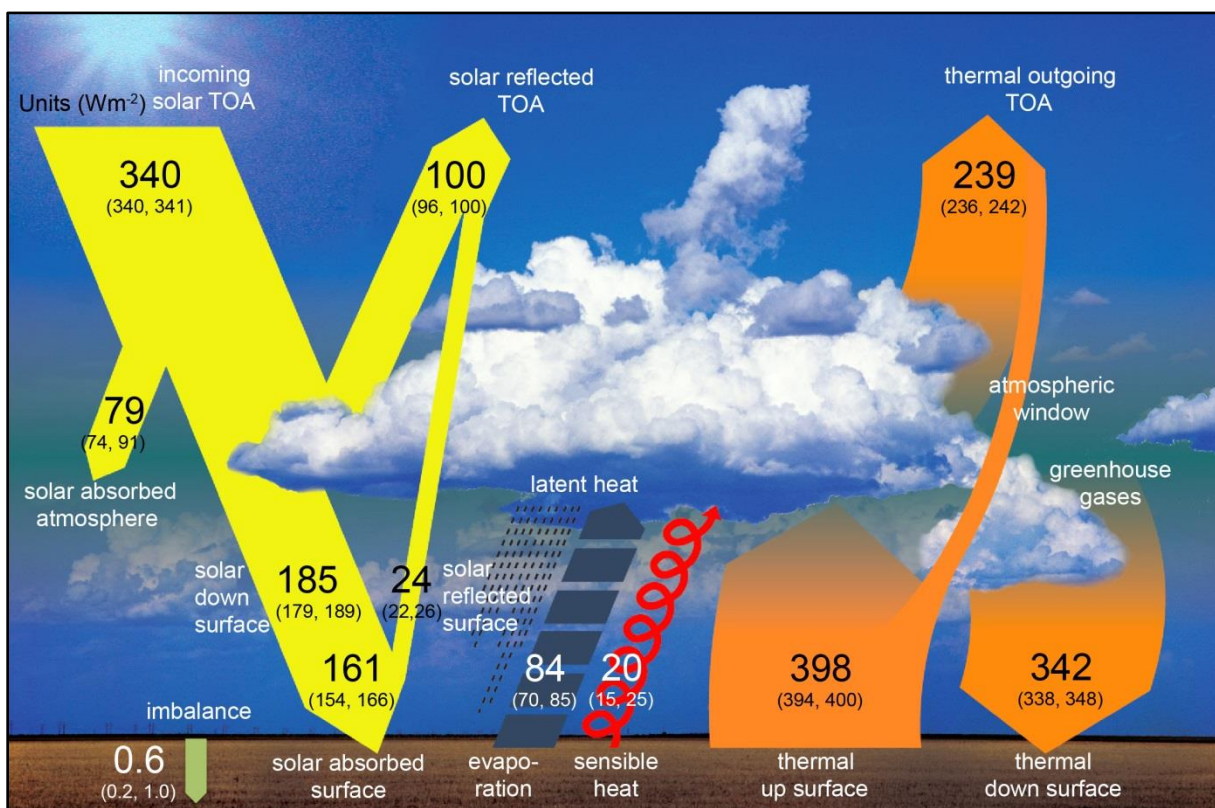


Figure 4.2: Global mean energy budget under present-day climate conditions. Numbers refer to the individual energy fluxes in  $\text{W/m}^2$  (Hartmann et al., 2013).

### 4.1.3. Climate change

Climate change is caused by changes in the global energy budget. This could be caused either by a change in incoming shortwave radiation or outgoing longwave radiation. The main drivers of climate change are shown in Figure 4.3. An increase in greenhouse gases is an important driver of climate change because it increases the amount of longwave radiation (LWR). A substantial part of the LWR will be reflected back to the Earth which can disturb the earth's radiative balance. Other drivers that can enhance climate change are visualized in Figure 4.3. At the moment, the Earth is warming and not in radiative balance. Hartmann et al. (2013) estimate an observed imbalance in the average global heat storage of  $0.6 \text{ W/m}^2$ , measured between 2005 and 2010. However, significant uncertainty exists in the calibration of the measurements because these energy fluxes cannot be directly measured by satellite sensors. Furthermore, surface measurements are not always locally or globally

representative. These uncertainties might add  $2 \text{ W/m}^2$  of radiative imbalance (Hartmann et al., 2013). The current effective radiative forcing is showed in Section 4.2.1.

Changes in the atmosphere, land, ocean, biosphere and cryosphere, both natural and anthropogenic, can perturb the Earth's energy budget, producing a radiative forcing that affects climate (Cubasch et al., 2013). The Earth is susceptible and dynamic and small changes can have severe consequences for the climate system. Some dynamical changes and feedbacks of the system are explained in Section 4.1.4.

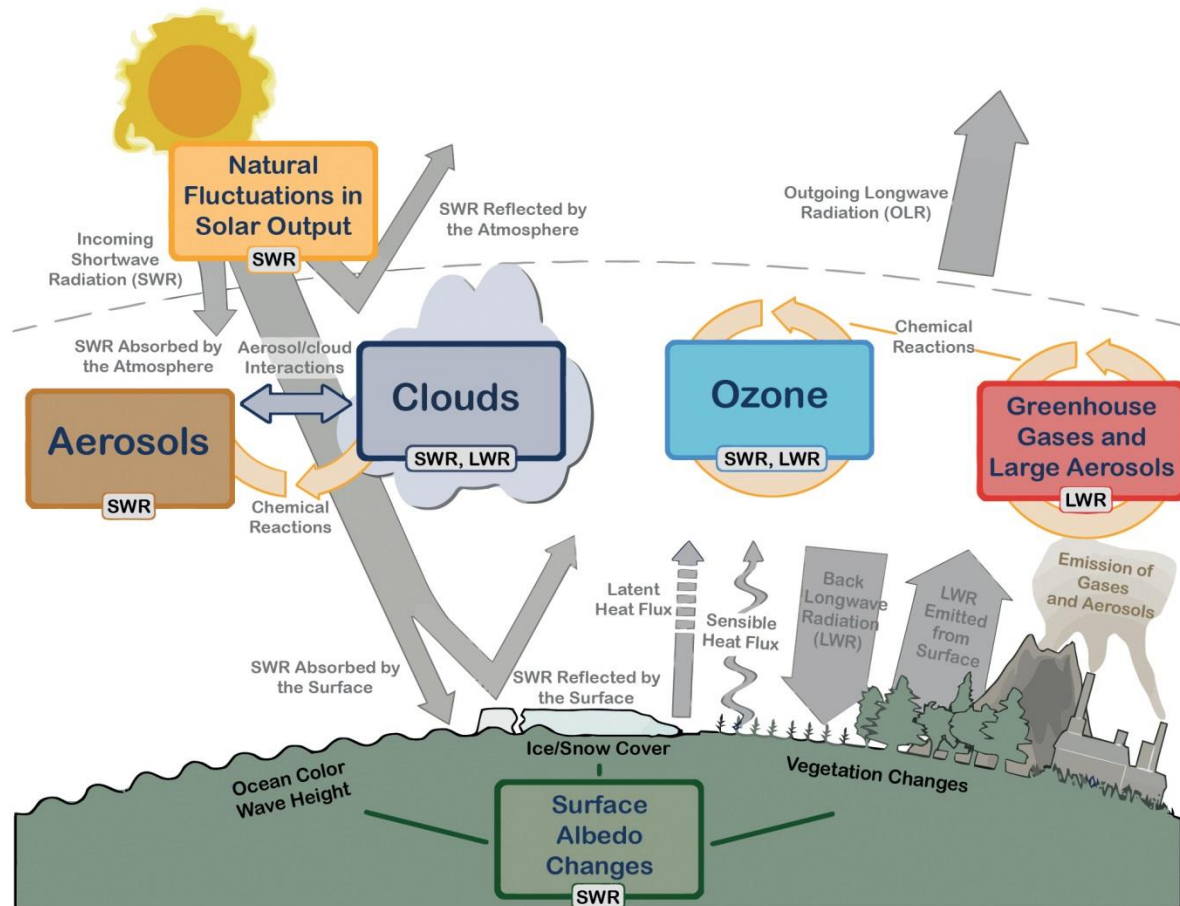


Figure 4.3: Climate drivers in the Earth climate system (Cubasch et al., 2013).

#### 4.1.4. Climate dynamics and feedbacks

Earth's climate system will change as a response to changing conditions and forcings (Figure 4.3). This response can be reduced or enhanced due to climate feedback mechanisms. Climate feedbacks can be either positive or negative, which implies that they increase or reduce the effect of the initial climate forcing. The response of the Earth to climate forcings is slowed by the inertia of the oceans and the ice sheets on Greenland and Antarctica. It could take centuries or millennia before ice sheets respond to a climate forcing. The problem is that the human-made climate forcing increases rapidly while the climate system responds slowly, that we only observe a partial response (Hansen, Sato, Russel, & Kharecha, 2013). The Earth is not in balance and is warming, so we are committed to much more climate change.

Albedo ("whiteness") is a measure of reflectivity of sunlight of the surface and atmosphere and is a crucial factor that controls temperature on Earth. The average albedo of the Earth at the top of the atmosphere, its *planetary albedo*, is roughly 30%. This albedo varies widely over the surface because of the different geological and environmental features (Bortman, Brimblecombe, Freedman, & Cunningham, 2003). Clouds and snow are highly reflective and play an essential role in controlling Earth's temperature. Changing the planetary albedo from 30%

to 29% increases the absorption of solar radiation in the climate system by  $3.4 \text{ W/m}^2$  (Wild, 2016). This shows that the climate system is very sensitive to changing forcings.

An example of a positive feedback is the ice-albedo feedback. Sea ice covered with snow is very reflective with an albedo of 0.5-0.9 [-] (NSIDC, 2017). When the air temperature increases due to an increase of greenhouse gases, sea ice could disappear which reduces the local albedo drastically to roughly 0.06 [-] for the ocean surface (NSIDC, 2017). This change leads to more energy absorbing area which further increases the average local temperature.

Water vapour is a passive climate feedback. Observations and models show that the relative humidity is approximately constant, so the total amount of water vapour is governed by temperature. An increase in surface temperature increases the amount of water vapour in the atmosphere. Water vapour is a powerful greenhouse gas which enhances the greenhouse effect, and more water vapour in the air leads to further surface warming (Cubasch et al., 2013).

The dominant negative feedback is the increased emission of energy through longwave radiation as surface temperature increases. This can be called the blackbody radiation feedback (Cubasch et al., 2013).

It is important to recognise the timescale of a feedback mechanism in order to determine their impact on the climate system. Feedbacks of clouds and water vapour operate in several hours or days, while the feedbacks relating to oceans can take centuries. The most relevant feedbacks are visualized in Figure 4.4.

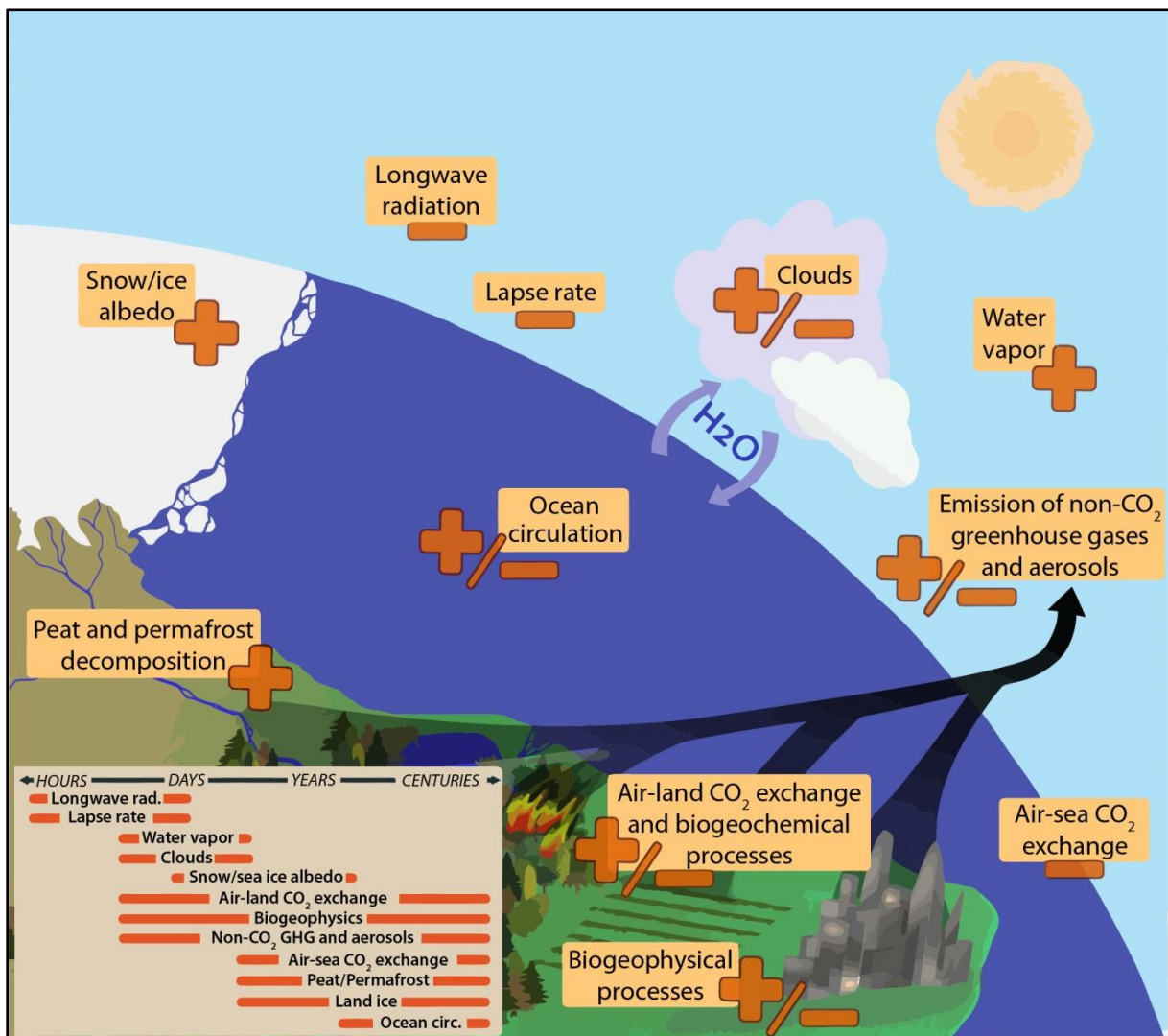


Figure 4.4: Climate feedbacks and their timescales (Cubasch et al., 2013).

### 4.1.5. CO<sub>2</sub> and Milankovitch cycles

CO<sub>2</sub> is the principal anthropogenic greenhouse gas that affects the Earth's radiative balance. Arrhenius was the first scientist that quantified the contribution of CO<sub>2</sub> to the well-known greenhouse effect (Arrhenius, 1896). CO<sub>2</sub> is a naturally occurring gas but is heavily increased in the last centuries due to burning fossil fuels, such as gas, oil and coal. Furthermore, CO<sub>2</sub> is the by-product of burning biomass, land use changes and industrial processes. Water vapour (H<sub>2</sub>O), nitrous oxide (N<sub>2</sub>O), methane (CH<sub>4</sub>) and ozone (O<sub>3</sub>) are the other primary greenhouse gases in the Earth's atmosphere, but CO<sub>2</sub> is the most critical reference gas for global warming (Planton, 2013). Also, water vapour is a powerful greenhouse gas but the lifetime in the atmosphere is very short in contrast to CO<sub>2</sub>.

Anthropogenic global CO<sub>2</sub> emissions are started around the year 1750, but the dominant increase in carbon emissions began around 1950 (Figure 4.5). About 40% of these anthropogenic CO<sub>2</sub> emissions have remained in the atmosphere since 1750. The other 60% was removed from the atmosphere by sinks, and stored in natural carbon cycle reservoirs (IPCC, 2014). Especially, the relatively long time to remove CO<sub>2</sub> from the atmosphere results in climate change.

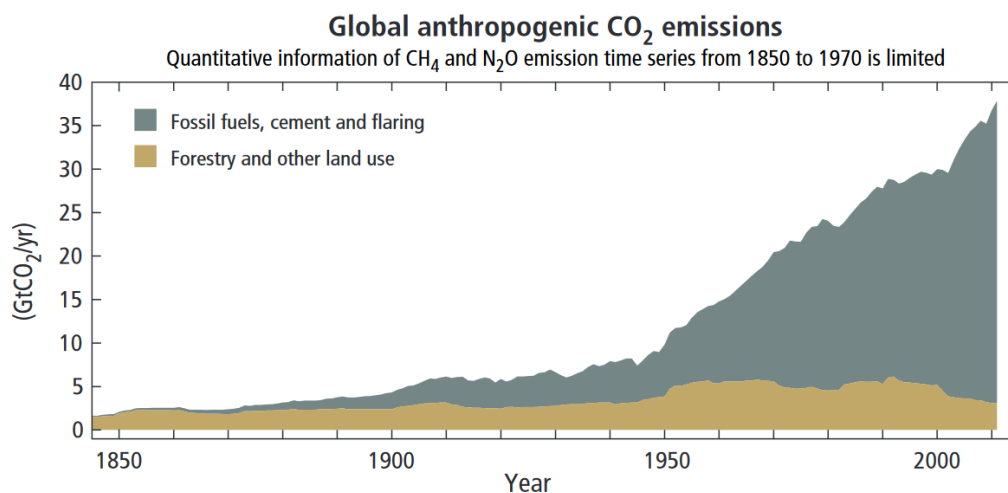


Figure 4.5: Global anthropogenic emissions (IPCC, 2014).

A prominent example of natural climate variability over long time periods is the Ice Age cycle. Analysis has been made with the use of ice cores and ocean sediments to estimate the CO<sub>2</sub> concentration and temperature of the last 800,000 years. In this long timeframe, the Earth has gone through various periods with multiple ice ages (Figure 4.7). Interglacials and ice ages come along approximately every 100,000 years (Figure 4.6). These are called the Milankovitch cycles and are caused by three main changes to the earth's orbit. The shape of the Earth's orbit around the sun (eccentricity) varies between an ellipse in a circular shape. The distance from Earth to the sun varies what lead to changes in the global temperature over time. In addition, eccentricity has two cycles of 100,000 years and 413,000 years. The tilt of the earth's axis relative to the sun is roughly 23°. This tilt oscillates between 22.5° and 24.5° (obliquity) in cycles of 41,000 years. In addition to the fact that the earth spins around its own axis, the orientation of the rotating Earth's axis also circles (Skeptical Science, 2016). This cycle, called precession, takes roughly 23,000-26,000 years.

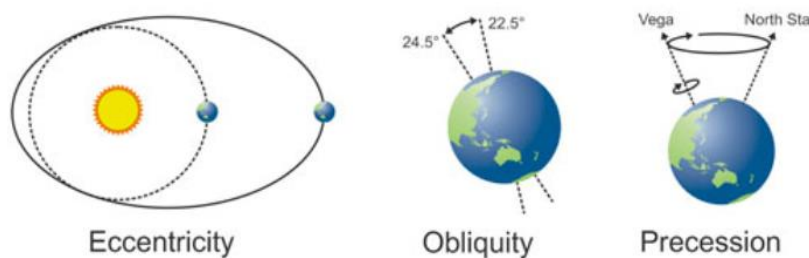


Figure 4.6: The three orbital variations of the Earth (Milankovitch cycles). Eccentricity: changing the shape of the Earth's orbit. Obliquity: changes in the tilt of the Earth's rotational axis. Precession: change in the orientation of the rotational axis of Earth (Skeptical Science, 2016).

The collective effect of these orbital cycles causes long-term changes in the amount of sunlight hitting the earth at different seasons, particularly at high latitudes (Skeptical Science, 2016). This will change the atmospheric temperature distribution worldwide. Small changes in the incoming solar energy affect the cryosphere (Earth's ice cover) and biosphere (ecosystems) to a large extent (Council, National Research, 2012). Still, there are some missing links and problems to understand the role of Milankovitch cycle that cause ice ages.

Temperature rise and the atmospheric CO<sub>2</sub> concentration have a close correlation (Figure 4.7). The interesting thing to note is that past temperature rise actually leads CO<sub>2</sub> by roughly 1000 years. Martin et al. (2005) argue that warming oceans caused by orbital changes decrease the solubility of CO<sub>2</sub> in the water. As a result, the deep oceans give up more CO<sub>2</sub>, emitting it into the atmosphere (Martin, Archer, & Lea, 2005), (Toggweiler, 1991). A new equilibrium will appear with a higher CO<sub>2</sub> concentration of roughly 280 ppm in the Interglacial periods. The outgassing of CO<sub>2</sub> from the deep ocean intensified the original atmospheric warming and combined with the relatively weak forcing from Milankovitch cycles deglaciation may occur.

Global warming in the past was leading to the increase in CO<sub>2</sub> levels, but today we observe the opposite reaction. Increasing carbon emissions amplify global warming and oceans take up CO<sub>2</sub> with various natural processes (carbon pumps). The biological pump and the solubility pump are two carbon pumps that contribute to a higher concentration of CO<sub>2</sub> in the deep ocean. These processes reduce the atmospheric CO<sub>2</sub> concentration. These processes can help to restore equilibrium in the carbon cycle (Marinov & Sarmiento, 2004).

The anthropogenic contribution of the last centuries to the concentration of CO<sub>2</sub> is undoubtedly visible in Figure 4.5. The CO<sub>2</sub> concentration is risen from 280 ppm in the year 1750 to roughly 409 ppm in May 2017. As an indication, the CO<sub>2</sub> concentration in 1960 was 317 ppm, 370 ppm in 2000 and 400 ppm in 2015 (NOAA, 2017). These values are measured at places without local air pollution and are representative worldwide and increase continuously. The main characteristic of CO<sub>2</sub> is that it is distributed uniformly in the atmosphere. The last time when such concentrations occurred was 3 million years ago in the Pliocene period. Reconstructions showed that the sea level was probably 10-30 m higher in that period compared with today (Deconto & Pollard, 2016). This shows that sea level could be susceptible to changes in CO<sub>2</sub> concentrations.

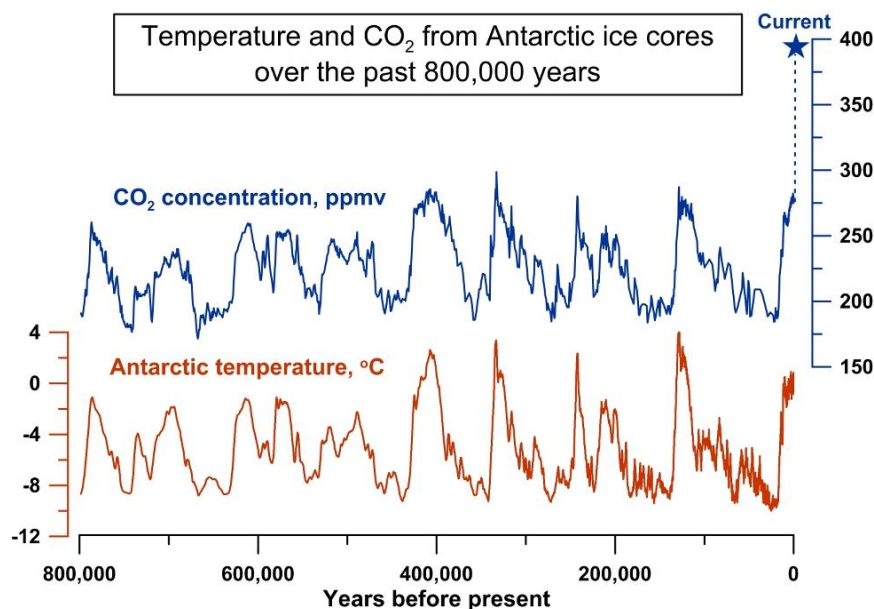


Figure 4.7: Antarctic temperature and CO<sub>2</sub> over the past 800,000 years (Curtis, 2015).

## 4.2 Climate scenarios

Climate scenarios are constructed from climate models to give an indication of the uncertainty in forcing and response (Arnell, Brown, & Gosling, 2016). This research takes different climate scenarios into consideration to recognize the primary drivers of sea level rise. In 1988, the first computer models appeared to project climate change due to anthropogenic warming. In 1990, the International Panel on Climate Change published the First Assessment Report on climate change including four climate scenarios (IPCC, 1990). These scenarios are developed in every assessment. The IPCC scenarios are known worldwide and extensively used to predict future sea level rise. In Chapter 5, the sea level rise projections of the IPCC predictions are compared to other scenarios.

This research uses the climate scenarios of the Fifth Assessment Report (AR5) of the IPCC. An important conclusion of the IPCC AR5 is the following expectation: “Human activities are continuing to affect the Earth’s energy budget by increasing the atmospheric concentration of important greenhouse gases and aerosols and by changing land surface properties” (Cubasch et al., 2013).

### 4.2.1 Radiative forcing

The focus of this chapter is the current radiative imbalance and the projections of future radiative forcing. The radiative balance and Earth’s climate system is explained in Section 4.1.2. Radiative forcing quantifies the change in energy fluxes caused by changes in climate forcers (drivers). Positive radiative forcing refers to surface warming while a negative forcing leads to cooling.

Radiative forcing is the net change in the energy balance of the Earth system due to imposed perturbation. “Radiative forcing is expressed in watts per square meter averaged over a particular period of time and quantifies the energy imbalance that occurs when the imposed change takes place” (Myhre et al., 2013). Radiative forcing is about the radiative change between two periods. The effective radiative imbalance can be estimated from changes in ocean heat content, complemented by radiation measurements from space by satellite records (von Schuckmann et al., 2016). The time evolution between the pre-industrial (1750 A.D.) period, present day, and the expected value in the year 2100 is often used (Myhre et al., 2013).

The effective radiative forcing of the Earth is reconstructed and measured from 1750 until 2011 (Figure 4.9 and 4.10). The effective radiative forcing was roughly zero in 1750 because anthropogenic emissions started after that period. It is expected that the human influence on climate started at the end of the 18<sup>th</sup> century. The steam engine, invented in 1769 by James Watt, was the first machine that produces anthropogenic greenhouse gases (Hawkins et al., 2017). It is evident that the effective forcing is increased every year due to the growing emissions of various greenhouse gases. In 2011, anthropogenic emissions resulted in a net positive radiative forcing of 2.3 W/m<sup>2</sup> (mean value). It is hard to measure this forcing, and therefore a large spread of 1.13-3.33 W/m<sup>2</sup> (5-95% confidence) is included in the estimations (Figure 4.9). Nevertheless, this value is much higher than in the past. The estimated net radiative forcing in 1950 was 0.57 W/m<sup>2</sup> and roughly 1.25 W/m<sup>2</sup> in 1980 (IPCC, 2013).

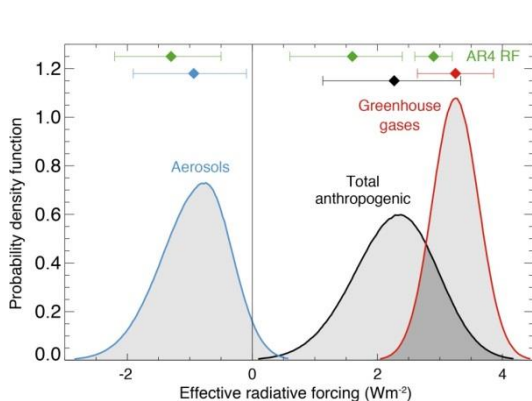


Figure 4.8: PDF of radiative forcing of GHG, aerosols and total anthropogenic forcing (1750-2011) (Myhre et al., 2013).

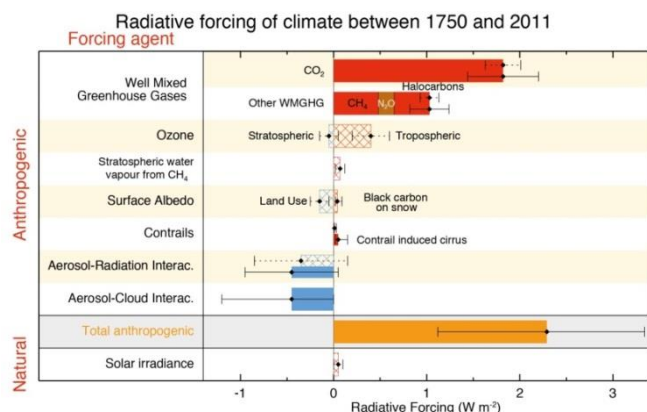


Figure 4.9: Radiative Forcing and each individual contribution (1750-2011) (Myhre et al., 2013).

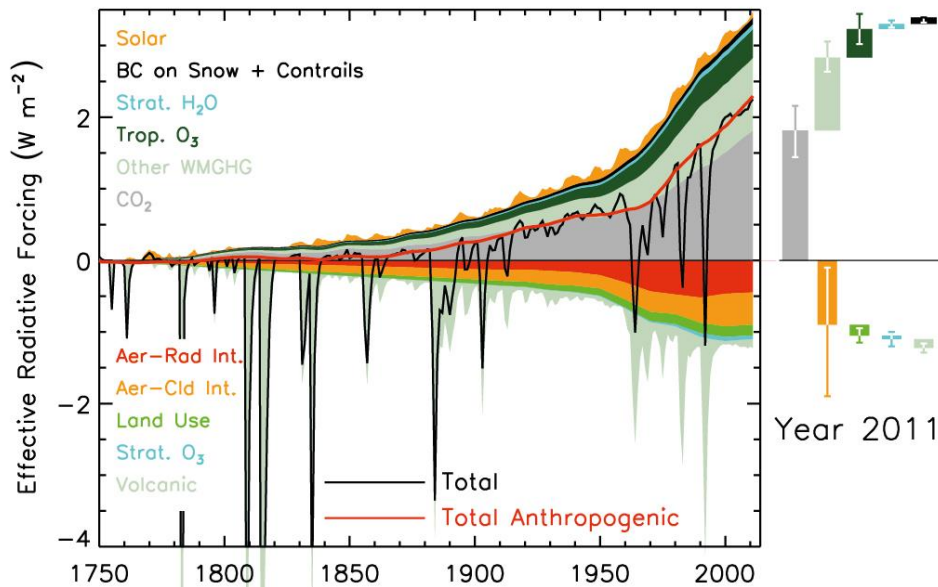


Figure 4.10: Effective radiative forcing between 1750 and 2011 (Myhre et al., 2013).

CO<sub>2</sub> is the primary forcing agent with an estimated forcing of 1.8 W/m<sup>2</sup> while all other greenhouse gases combined contribute roughly 1.2 W/m<sup>2</sup>. Changes in the ozone also have a positive contribution to radiative forcing. The total positive contribution of greenhouse gases to radiative forcing is approximately 3.0 W/m<sup>2</sup>. Important to note is that these forcings are incremental values between the year 1750 and 2011 (IPCC, 2013).

Aerosols are often assumed as less important while these particles can cool the earth considerably. Aerosols are airborne suspensions or particles that reside in the atmosphere for at least several hours. Typical examples of aerosols are dust, fog and smoke. Aerosols can have either a natural or anthropogenic origin. Aerosols may influence climate in several ways (IPCC, 2013):

- aerosol-radiation: directly through scattering and absorbing (solar) radiation;
- aerosol-cloud: indirectly by modifying the optical properties and lifetime of clouds.

Volcanic eruptions cause a dramatic increase of aerosols in the atmosphere which results in large negative spikes in Earth's radiative balance. Aerosols reflect sunlight before it reaches the Earth's surface and these particles affect clouds. Clouds can form more easily in combination with aerosols. The effect of clouds on climate is complex because clouds can either warm and cool the Earth.

The negative radiative forcing by aerosols is estimated at 1 W/m<sup>2</sup> with a considerable uncertainty range due to complexity. The change in radiative forcing is caused by a large anthropogenic contribution which is much larger than the natural contribution. Solar irradiance is a vital natural forcer which leads to past glacial and interglacial periods. Nevertheless, this forcing agent contributes to only 0.05 W/m<sup>2</sup> in the timeframe between 1750 and 2011 (Myhre et al., 2013).

## 4.2.2 Global warming

Global warming is the observed rise in global average temperature of the Earth's climate system. Global warming is a synonym for climate change. In 2013, the IPCC concluded that it is very likely that the human influence was dominant in causing the temperature rise over the last century (IPCC, 2013). Global average temperature increase is the result of the radiative imbalance because the amount of incoming solar radiation is slightly higher than the leaving radiation.

The pre-industrial period is not defined precisely. For temperature calculations, various institutions, including the IPCC, use period 1850-1899 or 1880-1899. However, the year 1750 is used as the pre-industrial period for calculations of the radiative forcing. It is advised to consistently use the reference period which is defined as "pre-industrial". Hawkins et al. (2017) suggest that the period 1720-1799 should be used as pre-industrial (Hawkins et al., 2017).

In 2016, the global average temperature has risen by 1.1 degrees compared to the year 1850-1899 (World Meteorological Organization, 2017). The expected warming between 1720-1799 and 1850-1899 is a global temperature increase of 0.05 °C. The global warming compared to the pre-industrial (1720-1799) is therefore 1.15°C. In 2015, global warming exceeded 1 °C compared to pre-industrial (Hawkins et al., 2017) (Climate Analytics, 2016).

Even when the current global CO<sub>2</sub> concentration does not increase further, and that human emissions are immediately ceased, the atmosphere probably contains enough CO<sub>2</sub> to increase global warming to 1.3 °C. This means that the Earth is probably committed to 1.3 °C global warming to restore a climate equilibrium (Aton, 2017). Furthermore, it can be expected that global warming increase even further due to the decrease in the number of aerosols. Aerosols have a cooling effect on Earth's atmosphere because of their reflectivity of sunlight. Combustion engines and other machinery emit aerosols in addition to greenhouse gases. Policies to reduce carbon emissions also reduce aerosols, because these particles have the ability to disappear out of the atmosphere quickly. On the other hand, greenhouse gases (GHG) remain in the atmosphere for decades. Therefore, it could be the case that "green policies" increase global warming. However, without global intervention, global warming increases further. To conclude, it could be the case that we are nowadays committed to more than 1.5 degrees of global warming without increasing the CO<sub>2</sub> concentration.

### 4.2.3 IPCC projections

The IPCC was established in 1988 by the World Meteorological Organization and the United Nations Environment Programme to provide governments comprehensive knowledge about climate change, potential impacts and options for adaptation and mitigation. The latest IPCC report is the Fifth Assessment Report (AR5) which is published in 2013 (Cubasch et al., 2013). The sixth Assessment Report (AR6) is in progress and will be published between 2018 and 2022.

One of the main conclusions of the IPCC is that the human influence on the global climate system is clearly visible (Church et al., 2013). The IPCC identified four different emission pathway scenarios for the long-term perspective. These scenarios are based on their radiative forcing in the year 2100.

High-end scenario RCP8.5 refers to a positive net radiative forcing of 8.5 W/m<sup>2</sup> at the end of this century. Scientists expect that this scenario could occur without worldwide policy intervention. Human population will rise combined with economic growth. In that case, GHG emissions continue to rise on an annual basis until at least 2100. The atmospheric CO<sub>2</sub> concentration could be more than 1000 ppm in 2100 including an average surface temperature rise of more than 4°C compared to 1986-2005 (IPCC, 2014). The expected temperature range for this emission pathway is a 3.5-4.8 °C rise relative to pre-industrial (IPCC, 2014). However, even higher temperatures cannot be excluded (IPCC, 2013). This emission pathway (RCP8.5) will be used as high-end emission scenario throughout this report.

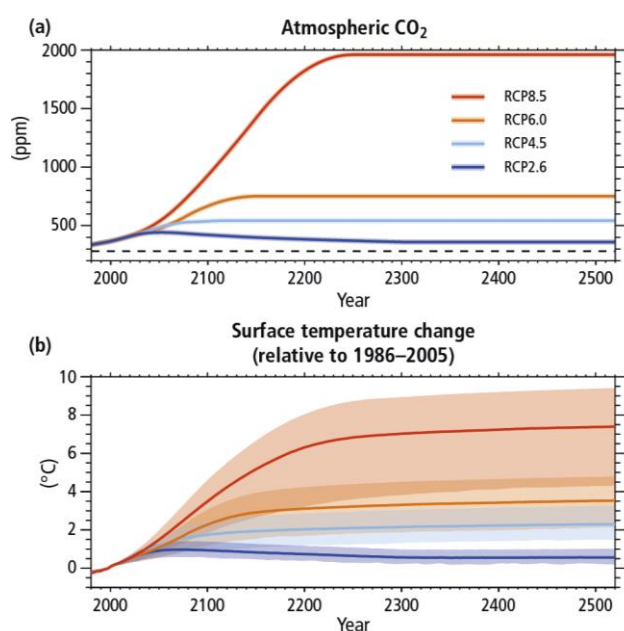


Figure 4.11: Relating carbon emissions with scenarios and global temperature rise (2000-2100) (IPCC, 2014).

RCP4.5 is the modest climate scenario of the IPCC. This pathway would require a substantial reduction of GHG emissions over the next few decades. By the end of the century, the GHG emissions should be reduced by almost 50% compared with today. Emissions are projected to rise slightly until 2040 to a maximum of 55 Gt CO<sub>2</sub> annually with an estimated CO<sub>2</sub> concentration of 550 ppm (Figure 4.11). Global emissions should decrease significantly after 2040 to meet RCP4.5, which is a very challenging task. The estimated temperature rise is 2-3.5 °C relative to pre-industrial.

Many countries are developing and economic growth leads to more pollution. This should change and large-scale emission reductions have large technological, economic, social, and institutional challenges (IPCC, 2014).

RCP2.6 is the only climate scenario that projects limited warming of approximately 2 °C relative to pre-industrial CO<sub>2</sub> levels. It is important that the CO<sub>2</sub> concentration does not exceed 450 ppm and that the net emissions rapidly decrease to zero around the year 2085 (Figure 4.12). After 2085 the effective emission pathway should be below zero, which is a very ambitious target. The main target of the Climate Agreement of Paris was maximal 2 degrees global warming compared to the pre-industrial levels with the intention to limit global warming to 1.5 °C. Sanderson et al. (2016) expect that even scenario RCP2.6 is not enough to reach the target of the Agreement of Paris and that more negative emissions are required to reach this agreement (Sanderson, O’Neill, & Tebaldi, 2016). The current net radiative forcing is approximately 2.3 W/m<sup>2</sup> with a large uncertainty bandwidth of 1.13 W/m<sup>2</sup> (P5) and 3.33 W/m<sup>2</sup> (P95).

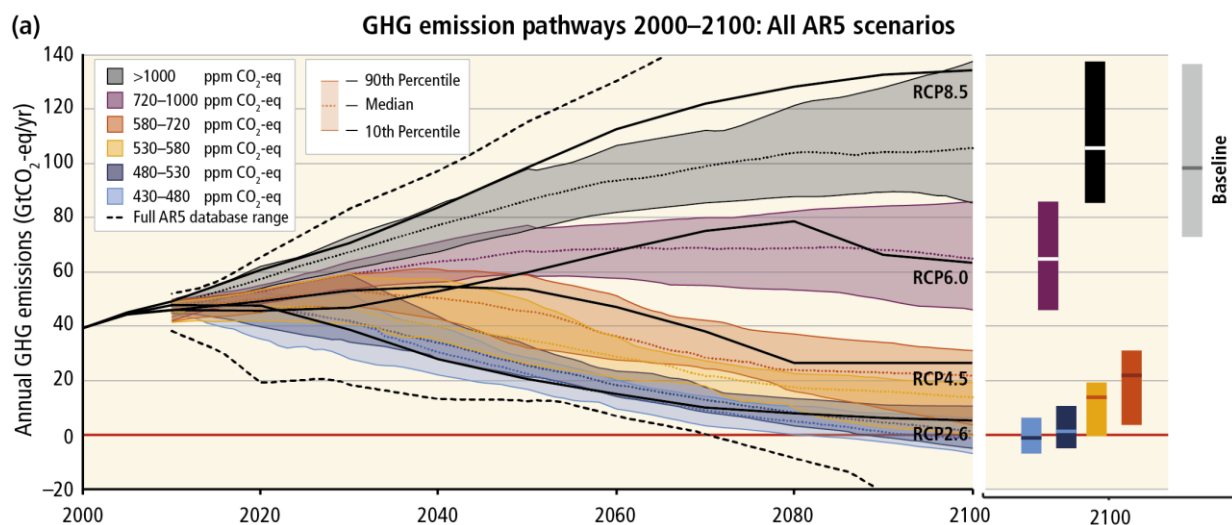


Figure 4.12: Annual carbon emission pathways (IPCC, 2014).

#### 4.2.4 Expected climate scenario

In 2013, the IPCC gave four scenarios for probable ranges of global temperature increase. The IPCC did not provide any likelihood for the scenarios which depend on socio-economic developments. Furthermore, these IPCC scenarios are not based on a fully statistical approach (Raftery, Zimmer, Frierson, Startz, & Liu, 2017). A recent study, however, estimates the expected likely scenario range based on statistics instead of expert judgement.

Raftery et al. (2017) are the first that made a statistical model that calculates the probabilistic range of future global carbon emissions until the year 2100. Other projections were based on a combination of statistical modelling and expert judgement. The model is based on probabilistic CO<sub>2</sub> and temperature forecasts, carbon intensity, Gross Domestic Product (GDP) per Capita developments and the rate of population growth. Furthermore, these results are compared with the four RCP scenarios (IPCC). The United Nations (UN) has updated their population growth projections (United Nations, Department of Economic and Social Affairs, 2015). This improvement is made with the use of a probabilistic Bayesian model. The median of the UN population projection increases from the current 7.2 billion to 11.2 billion in 2100. The primary increase is expected in Africa whose population could increase from its current 1 billion to 3.9 billion people (United Nations, 2015).

Raftery et al. (2017) argue that emission scenarios are less dependent on population growth than thought before. Another interesting conclusion is that the carbon intensity (CO<sub>2</sub> emissions per unit of GDP) is declining in most countries over the last years (Raftery et al., 2017). This implies that carbon emissions are not required to obtain economic growth. This may show that the dependence on fossil fuels declines over the last years. Raftery et al. (2017) suggest that future policies should target carbon intensity to reduce future global emissions.

Raftery et al. (2017) expect that the average global temperature rises by 3.2 °C with only a 5% chance to limit the temperature increase within 2 °C in the year 2100. It is expected that limiting global warming to 1.5 °C is almost impossible (<1%). These results are obtained by combining the projected distribution of carbon emissions (relating GDP, population and carbon intensity projections) with the relationship between cumulative CO<sub>2</sub> emissions and global warming described by the IPCC. The large spread considers the uncertainty in future population growth, economic growth, carbon intensity and climate sensitivity (Raftery et al., 2017). The results are shown in Figure 4.13 and 4.14.

The results show that only a 5-10% chance exists that RCP8.5 will be the reality based on the current projections of the IPCC and the UN. This study suggests that RCP8.5 might be not such a likely scenario to occur, which was thought to be “business as usual” (IPCC, 2013). More probable is the RCP6.0 scenario according to the current pathway in emissions, population, economic development and technology. Another conclusion that can be made is that limiting global warming within the Paris Agreement (1.5-2.0 °C) is almost impossible, without extreme technological development in the energy transition.

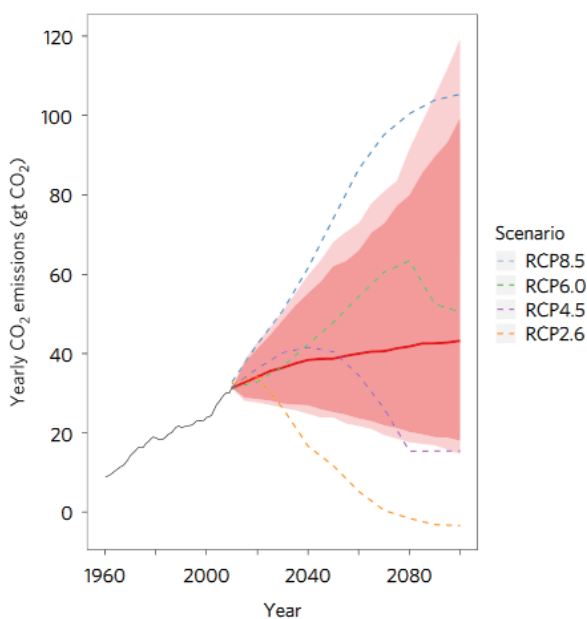


Figure 4.13: Probabilistic forecast of yearly CO<sub>2</sub> emissions within the 21<sup>st</sup> century, combined with IPCC RCP scenarios. The solid red line is the predictive median, the heavily shaded region is the likely range (P90 interval), the lightly shaded region is the P95 interval, and the IPCC RCP scenarios are the dashed lines (Raftery et al., 2017).

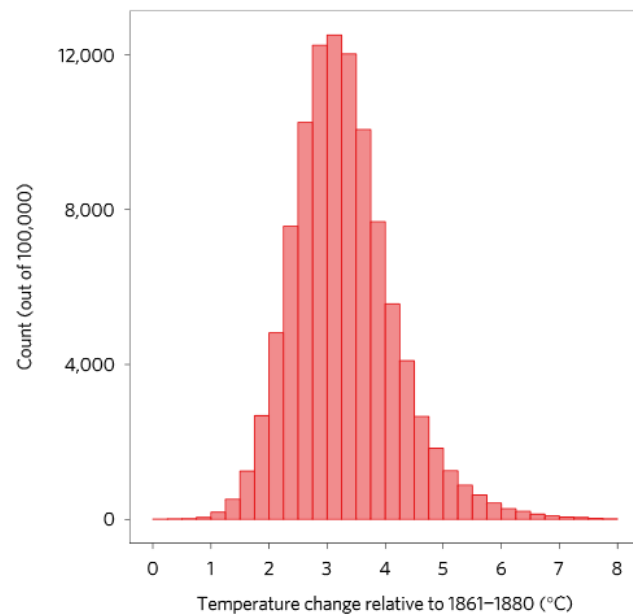


Figure 4.14: Histogram of the predictive distribution of the global mean temperature increase relative to 1861–1880 in degrees according to the statistical model of (Raftery et al., 2017).

Important to note is that the study of (Raftery et al., 2017) does not explicitly incorporate future legislation that can change future emissions beyond of the current projections. “It is based on past emissions, which implicitly account for legislation and regulation changes over the past 30 years since climate change became a global issue” (Raftery et al., 2017). It is evident that the carbon intensity has been reducing steadily over that period and it is assumed that this improvement continues. However, the last economic crisis started in 2008 may have an impact on the reducing carbon intensity. Further research could either confirm or reject this trend of reducing carbon intensity. The study did not consider a substantial shift to renewable energy in the next decades. In the end, more studies should be carried out to project the future emission pathway more precisely. These results are based only on one study and future climate policy is always uncertain. It is interesting to see that RCP8.5 is probably not the most likely emission scenario to occur.

This research will examine the effects of climate change on sea level rise for both RCP4.5 and RCP8.5 in Chapter 5 “Sea level rise”. Unfortunately, substantial research on climate change and sea level rise is limited for RCP6.0. It is expected that the high-end scenario will be RCP8.5 and the low-end seems to be RCP4.5. RCP2.6 is almost out of reach according to the analysis (Raftery et al., 2017).

# 5. Sea level rise

Global warming results in sea level rise by melting ice-sheets, glaciers, steric effects, land water changes superimposed by regional changes in surface winds, ocean currents, temperature, and salinity (Church et al., 2013), (Arnell et al., 2016). Sea level rise (SLR) directly influences the coastal environment and results in higher flood risk. It is critical to quantify the future rate of sea level rise for climate change mitigation and coastal planning efforts (Little, Urban, & Oppenheimer, 2013). Long-term sea level rise driven by global climate change causes considerable risks to coastal countries and the Netherlands in particular. Millions of people in the Netherlands live in areas below current mean sea level and are potentially at risk of coastal flooding. This chapter will discuss many sea level projections all over the world to come up with a probable sea level rise scenario for the Netherlands.

The Netherlands is a low-lying country and future sea level rise can have a large impact on water safety, economy, and policy aspects. Therefore, this chapter investigates past and current sea level rise and compares studies which made sea level rise projections. It is complicated to forecast local sea level rise because it is dependent on many different processes and feedback loops. These processes will be described in Section 5.7.

The average sea level was around +0.03 m NAP in the Netherlands (1981-2010). In the year 2017, the average sea level along the Dutch coast was +0.11 m NAP which was a record (Deltares, 2018). Sea levels around the globe deviate a lot due to many processes such as gravitational pull, ocean currents, salinity gradient and long-sustaining weather conditions. For instance, the La Nina event in 2010 and 2011 in western America caused a temporary decline in global sea level of several millimetres because of the massive terrestrial water storage of rainwater (Yi, Sun, Heki, & Qian, 2015). The average sea level change between 1993 and 2012 is shown in Figure 5.1. It is visible that the average trend shows a net sea level rise. However, this timeframe is too short to extrapolate local values to predict future SLR. Officially, we can speak of climate change when the average sea level statistics change over a period of 30 years. This has not been the case, but sea level is risen so quickly during the last 20 years, that this will definitely change the average sea level by combining the last 20 years and the next 10 years.

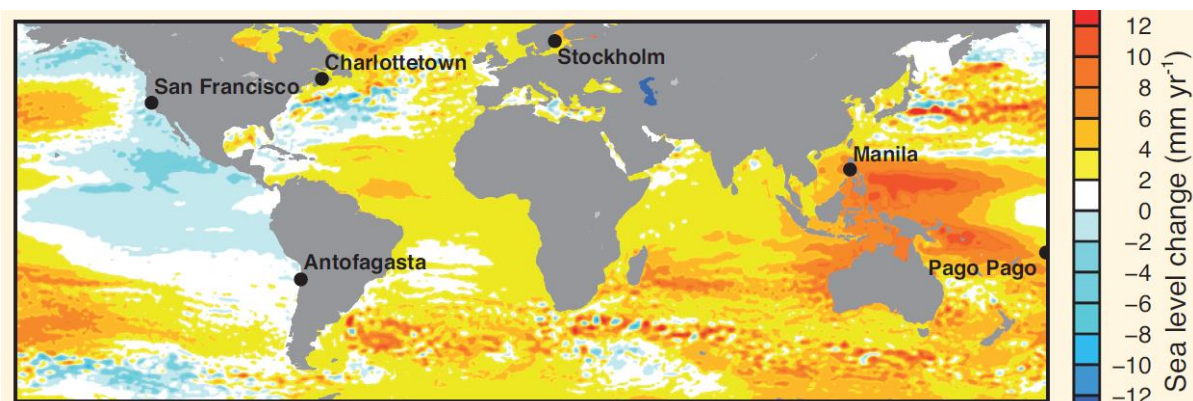


Figure 5.1: Map of rates of change in sea surface height (geocentric sea level) for the period 1993–2012 from satellite altimetry (Church et al., 2013).

## 5.1 Past sea level change

Sea level change of the past millions of years can be reconstructed with oxygen isotope ratios ( $\delta^{18}\text{O}$  relative to  $\delta^{16}\text{O}$ ). These ratios provide insight into the effects of temperature and ice-volume in different periods. Chemical measurements of isotopes are derived from ice cores, sediment cores, rock cores, coral growth rings and tree rings. These measurements give insight into past global changes in gas concentrations which result in changing temperature and sea levels.

Global sea level changes continuously in the past millions of years. Ice volume changes produced relatively rapid sea level changes in the geological history. Tectonic activity can also have a role in controlling global sea level. In the warm Cretaceous period (80-90 million years ago) sea level was 100-170 m higher than today while the oceans were 10-12 °C warmer. This sea level was probably higher than when all current ice-sheets would melt combined with 10-13 m rise due to thermal expansion (Miller K. , 2009). There are significant uncertainties in predicting past sea level change for such long-time scales which is long enough for significant changes in shape and volume of the ocean basins (Hansen et al., 2013).

Sea level estimations of the Pliocene period (1-5 million years ago) are expected to be more accurate, but still, many uncertainties are used in the analysis. The maximum sea level in the Pliocene was expected to be +15-25 m with large fluctuation which is shown in Figure 5.2 (Hansen et al., 2013). An important conclusion is that this period resulted in sea level fluctuations of 20-40 m with only a few degrees global temperature change (Hansen et al., 2013). The IPCC, however, did not expect more than 20 m sea level rise during this period (Church et al., 2013).

Antarctic ice core estimates suggest that the global temperature was 1.5 °C to 2.0 °C warmer than the pre-industrial around 401,000 – 411,000 years ago. Assessment studies resulted in a global mean sea level (GMSL) of 6-15 m higher than current GMSL. There was medium confidence that most of the ice sheets of Greenland and West-Antarctica were lost combined with a reduction in the East-Antarctic ice sheet. Despite the uncertainties, the IPCC confirmed that ice sheets are relatively sensitive to moderate warming (Church et al., 2013).

During the Last Interglacial, which was 123,000 – 119,000 years ago, the sea level was approximately +4-9 m higher compared to today. This is confirmed by the geological evidence of coral reefs (Hansen et al., 2013). Temperatures were at that time similar to today with +1°C relative to pre-industrial (Dutton et al., 2015).

GMSL was approximately 120-130 m lower during the last glacial period around 22,000 years ago. This is also shown in Figure 5.2. Global average temperature is risen by 4 degrees which causes sea level to rise to present-day values. Important to note is that atmospheric temperatures stabilized 11,000 years ago, while the ice sheets shrank for another 8,000 years before they stabilized. This phenomenon resulted in 45 m SLR before reaching (roughly) present-day values 3,000 years ago. This showed that ice sheets respond relatively slow to atmospheric temperature changes (POST, 2017).

Global sea level has risen by 0.19 m between the year 1901 and 2010 in response to thermal expansion and glacier loss due to global warming (Dutton et al., 2015). More information on sea level rise in the last century can be found in Section 5.2 “Global sea level rise”.

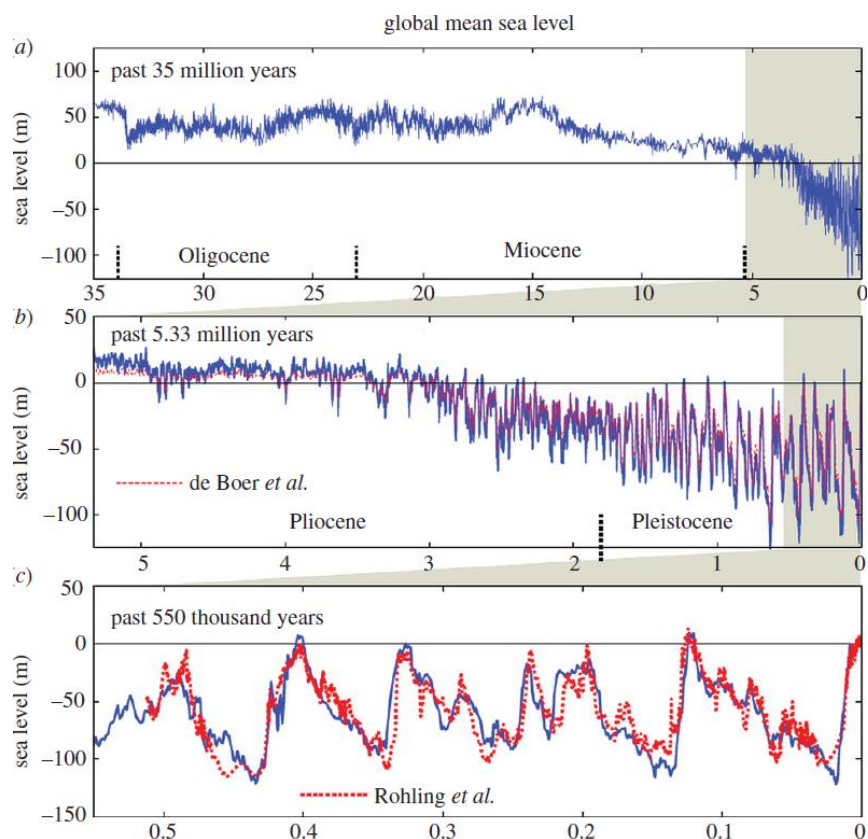


Figure 5.2: Sea level reconstructions from  $\delta^{18}\text{O}$  proxies over the last 35 million years (de Boer, Van de Wal, Lourens, & Tuetter, 2010) (Rohling et al., 2009) (Hansen et al., 2013).

## 5.2 Global sea level rise

Global mean sea level (GMSL) rise is a result of global warming, melting ice originating from ice sheets and glaciers and water exchange between land and sea (Yi et al., 2015). Global sea level rise is the main response to global climate change and environmental changes. First, it was thought that sea level rise was linear with an additional increase in the last few years. Past sea level rise was  $1.2 \pm 0.2$  mm per year between the year 1900 and 1990 (Yi et al., 2015). This rise is accelerated over the last 20 years on a global scale. The average sea level rise between 1993 and 2004 was  $3.40 \pm 0.18$  mm per year while  $3.49 \pm 0.14$  mm per year was measured between 2004 and 2015 (Dieng, Cazenave, Meyssignac, & Ablain, 2017). This acceleration was measured by high-precision satellite altimetry recordings. For validation purposes, scientists also calculated sea level rise with the sea level budget equation. This is a calculation of the mass change of the oceans by several contributors and a calculation of the thermal expansion of the oceans. If both the altimetry records and the sea level budget are in line with each other, there is a considerable certainty in the estimation.

This correlation is missing for the years 1993-1998 because the measured GMSL by altimetry records was lower than estimations made by the sea level budget. Sea level rise was quite linear based on altimetry record between 1993 and 2015, but not for the sea level budget. This is shown in Figure 5.3, where the black curve shows the altimetry records and the red curve represents the sum of all components (sea level budget).

Six processing groups, among which NASA and NOAA, found that the satellite was adrift during the first years after installation (1993-1998) which gave a distorted view of the rate of sea level rise. Altimetry data from tide gauge records were used to estimate the deviation of the satellite measurements. The difficulty was that tide gauges are prone to local vertical land motion which should be corrected. A correction for the drift of the satellite was made and the correction was between  $0.9 \pm 0.5$  mm to  $1.5 \pm 0.5$  mm per year, depending on the vertical land motion (Watson et al., 2015). The corrected altimetry records are shown in Figure 5.3b. This correction made a significant change in the sea level trend and in the consensus that GMSL rise is accelerating.

Both the altimetry data and sea level budget are in line with each other and show a noticeable increase in sea level rise. The results are shown in Table 5.1.

Table 5.1: GMSL change (incl. TOPEX A drift correction) in mm/year (Dieng et al., 2017), (Yi et al., 2015)<sup>1</sup>

GMSL (mm/year)	Jan 1993 to Dec 2004	Jan 2004 to Dec 2015	Jan 2010 to Jul 2014 <sup>1</sup>
Altimetry	$2.67 \pm 0.19$	$3.49 \pm 0.14$	$4.49 \pm 0.62^1$
Sea level budget (all components)	$2.46 \pm 0.31$	$3.27 \pm 0.16$	$4.33 \pm 0.60^1$

An accelerating rise could be observed over the last 20 years after including the adrift correction (Dieng, Cazenave, Meyssignac, & Ablain, 2017). Yi et al. (2015) show a further increase in sea level rise between 2010 and 2014. This is also visible in Figure 5.3. The negative spike in 2011 is caused by long-sustaining La Nina event together with some other abnormal durable weather events (Yi et al., 2015). These events caused a massive water vapour uptake and land water storage which reduced GMSL temporarily. It was observed that sea level rise restored in the year afterwards. The IPCC thought that the rise between 2011 and 2013 was temporarily due to the La Niña event. “The rapid increase in GMSL since 2011 is related to the recovery from the 2011 La Niña event” (Church et al., 2013). This does however not explain the continuing accelerated sea level rise after 2013.

Despite the relatively short timescale of 20 years, it can be concluded that global sea level rise is no longer linear according to the  $1.2 \pm 0.2$  mm per year (1900-1990) trend. The accelerated sea level rise trend is clearly visible, but it is still not certain if this acceleration will increase further. This is probably very dependent on the future emission pathway of greenhouse gases. Roughly 40 cm global sea level rise is to be expected at the end of this century by extrapolating the sea level trend over the last 10 years. However, global sea level rise does not increase linear anymore, so more sea level rise is to be expected. This is confirmed by the latest results of (Nerem et al., 2018). They conclude that global sea level rise is currently 3 mm per year and increases by 0.08 mm for every year. This would result in an annual rate of SLR of 10 mm per year and 60 cm in total by 2100 if this trend continues (Nerem et al., 2018). More information about sea level projections is given in Section 5.3.

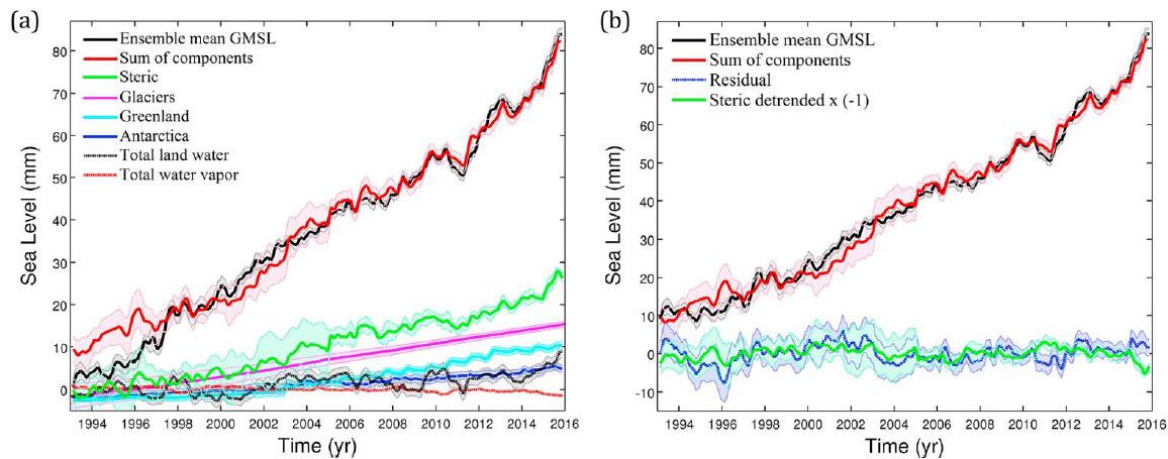


Figure 5.3: Average ensemble GMSL (altimetry) in black compared to the sum of components (sea level budget) in red. (a) GMSL without a drift correction (black). (b) GMSL with a drift correction (black) (Dieng et al., 2017).

Since 1993, the global mean sea level is monitored by satellite altimetry while previous measurements were based on tide gauges. Tide gauges are not very accurate, and mistakes are made easily because of the vertical land movement in the region. However, tide gauge data is important to assess potential errors in the altimeter estimate (Nerem et al., 2018). Satellites can become adrift and can deviate from their orbit. Studying the sea level budget helps to understand all processes individually which provides better projections for future sea level change. It is also a method to estimate the accuracy of altimetry records (Dieng et al., 2017). The impact of all components that contribute to sea level rise is expressed by the sea level budget equation:

$$GMSL(t) = GMSL_{oceanmass}(t) + GMSL_{steric}(t)$$

$GMSL_{oceanmass}$ : change in mass of the oceans;

$GMSL_{steric}$ : contribution of ocean thermal expansion to sea level change.

The mass change of the oceans represents changes in mass of glaciers, ice sheets, land water storage, water vapour, snow, and permafrost. Using this equation makes it possible to compare the observed rate of sea level rise with the sum of contributions (Dieng et al., 2017).

Dieng et al. (2017) estimated the sea level budget over the same period as the latest altimetry records by satellites (1993-2015). All contributions are analyzed individually by using six different datasets. The individual contributions are shown in Table 5.2 and explained in Appendix A. All terms of the sea level budget are also shown in Figure 5.3.

Table 5.2: trends and standard errors estimated for the different terms of the sea level budget (Dieng et al., 2017).

GMSL (mm/year)	Jan 1993 to Dec 2004	Jan 2004 to Dec 2015
Glaciers	0.71±0.10	0.78±0.07
Greenland	0.32±0.04	0.82±0.06
Antarctica	0.29±0.04	0.33±0.06
Land water	0.23±0.10	0.25±0.08
Water vapor	-0.03	-0.05
Sum of mass components	1.52±0.15	2.13±0.14
Ensemble mean steric effects (sea water expansion)	0.94±0.27	1.14±0.09
Sea level budget (all components)	2.46±0.31	3.27±0.16

Ocean temperature and glaciers react on shorter timescales than the ice sheets of Antarctica and Greenland. That is the main reason why steric effects and glacier loss were the dominant contributors to sea level rise in the 20<sup>th</sup> century. The contribution of the ice sheets of Antarctica and Greenland is increased since 1990, partly from increased outflow induced by warming of the oceans (Church et al., 2013). A recent study shows that the Antarctic contribution might be even more than initially thought (Appendix A) (IMBIE Team, 2018). In the end, we can conclude that global sea level rise increases not linear anymore and that an accelerated trend is visible.

Figure 5.4 presents the global sea level change over the last 300 years and the latest projections for the 21st century. The expected sea level rise between the pre-industrial period and the year 2000 is approximately 0.27 m. The first accurate measurements in the Netherlands date from the year 1890 and measurements that represent global sea level change were scarce at that time. Global sea level change from the year 1700 onwards is estimated by tide gauge data and additional information (Rijksoverheid, 2016). Figure 5.4 gives the impression of the impact to flood risk management if the high-end scenario of Le Bars et al. (2017) becomes a reality. More information about this high-end scenario can be found in Section 5.5.1.

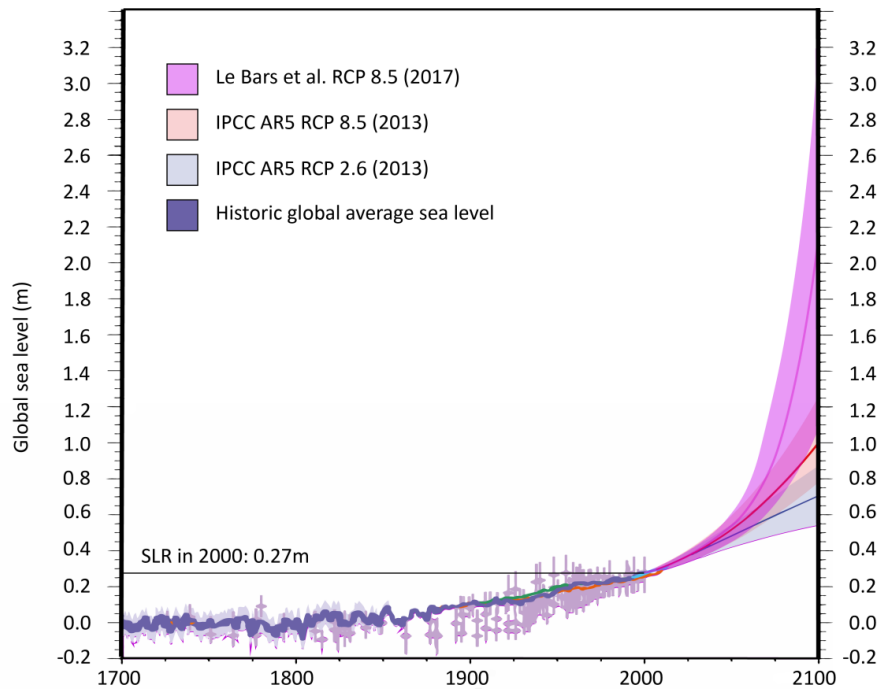


Figure 5.4: Sea level rise between the year 1700 and 2013 and projections for 2100 by the IPCC (Church J. P., 2013) and (Le Bars, Drijfhout, & de Vries, 2017).

## 5.3 Sea level rise scenarios

It is difficult to estimate past sea level rise, and therefore it is even more complicated to project future sea level rise because scenarios are based on historical sea level rise data and ice sheet models. Furthermore, it is difficult to project sea level rise because the heat that enters the ocean should be quantified (Le Bars et al., 2017).

Many models that project future sea level rise use isotope proxies and the size of the ice sheets in the past (Section 5.1). Furthermore, sea level rise depends on the evolution of the oceans, atmosphere, land-ice, and human impacts on land water storage. The evolution of these components is uncertain and difficult to predict, especially at a time when the earth is not in radiative equilibrium (Section 4.2.1). Due to the increase of greenhouse gases in the atmosphere, global warming will be enhanced, and the increase of ocean temperature is of primary importance to predict future sea level rise (Le Bars et al., 2017). At long time scales, projections are possible by assessing how the average climate conditions will change and result in a change of averaged sea level (de Vries, Katsman, & Drijfhout, 2014). Important to note is that the earth is already committed to several meters of sea level rise by currently observed global warming (Levermann et al., 2013). Sea level commitment refers to the amount of expected sea level rise over very long-time scales by keeping current global CO<sub>2</sub> concentration at a constant level. Sea level commitment is explained in more detail in Appendix C. It is evident that the GMSL will rise, but the rate is unknown due to many complex interactions in the climate system. Various scientists expect that the GMSL will continue to rise throughout the 21<sup>st</sup> century and beyond, because of global warming that has already occurred and the expected warming that is yet to occur due to the future carbon emissions (Sweet et al., 2017), (Le Bars et al., 2017).

The four largest organizations that provide sea level rise scenarios will be included in this research. The IPCC consists of one worldwide panel of scientists who reviews the current state of climate science. Three other institutions project sea level rise, especially for their own governments. The KNMI create scenarios for the Netherlands which are presented in section 5.3.2. The NOAA for the United States and the UK government for the United Kingdom also constructed sea level scenarios which are presented in Appendix D. All three organizations collaborate with the IPCC, but they provide local specific knowledge relevant to their own countries.

This research will compare the latest insights of sea level rise and the various scenarios. The organizations also have a lot of information about climate change, but the focus of this chapter will be on sea level rise only. The scenarios are updated every four or five years thus the latest insights are missing. Some researchers publish new articles which could be relevant for the next scenarios in 2018 and 2019. This research will investigate these articles in Section 5.4 and 5.5. These studies could be relevant for water policy in the Netherlands.

### 5.3.1 IPCC

The IPCC reports provide information about Earth’s atmosphere, hydrosphere, geosphere, biosphere and cryosphere. Also, the IPCC report has one specific chapter with the focus on sea level rise projections. The Fifth Assessment Report (AR5) is the latest IPCC report which is published in 2013.

The IPCC made sea level rise scenarios for all four Representative Concentration Pathway (RCP) scenarios which are shown in Table 5.2. The IPCC expects 75 cm SLR for RCP8.5 with a high-end estimate of 0.98 m. The expected sea level trend is shown in Figure 5.5. More information about the emission scenarios can be found in Section 4.2.3. The IPCC suggests that it is very likely that global mean sea level rise will exceed the current observed sea level rise in the 21<sup>st</sup> century. It is noteworthy that the AR5 considers the 5-95<sup>th</sup> percentile of the probability density function as “likely” range. The IPCC states that the likelihood of occurrence of this range is 66-100% (Church et al., 2013). This will give an additional uncertainty and various scientists calculated this uncertainty range (Kopp et al., 2014; Le Bars et al., 2017). More information about the uncertainty range can be found in Section 5.3.3.

Table 5.2: Projected global sea level rise for four emission scenarios (Church et al., 2013).

IPCC Sea level rise projections for 2100	5 <sup>th</sup> percentile	50 <sup>th</sup> percentile	95 <sup>th</sup> percentile
RCP2.6	0.28 m	0.44 m	0.61 m
RCP4.5	0.36 m	0.53 m	0.71 m
RCP6.0	0.38 m	0.55 m	0.73 m
RCP8.5	0.52 m	0.74 m	0.98 m

The projected effect of all contributing factors to sea level rise is presented in Figure 5.6 for the four emission pathways. The contribution of Antarctica is estimated at 0.04 m (P50) to 0.12 m (P95) including Surface Mass Balance (SMB) and ice sheet dynamics (Church et al., 2013). More information about SMB and ice sheet dynamics can be found in Appendix E. In 2013, the IPCC was already aware that high-end sea level rise is uncertain due to the uncertainty of the dynamic effects of the Antarctic ice sheet. The collapse of the marine-based ice sheets of Antarctica (MISI) can lead to a higher rise than the current 95% confidence range. Despite this uncertainty, the IPCC does not expect that a potential collapse of the West-Antarctica ice sheet (WAIS) increases global sea level with more than several tenths of a meter within this century (Church et al., 2013). Several studies published since the IPCC AR5 reports have suggested that MISI may already start in West-Antarctica (Joughin et al., 2014; Favier, 2014). More information is provided in Section 5.4.

To conclude, based on observations and an improved understanding of future climate and sea level change, it is virtually certain that sea level rise will continue for the next centuries (Church et al., 2013). Nevertheless, the rate of future sea level rise is uncertain. The IPCC advice to consider sea level rise, combined with climate variability and extreme events, in a risk management framework for coastal planning in regions that may be affected by sea level rise.

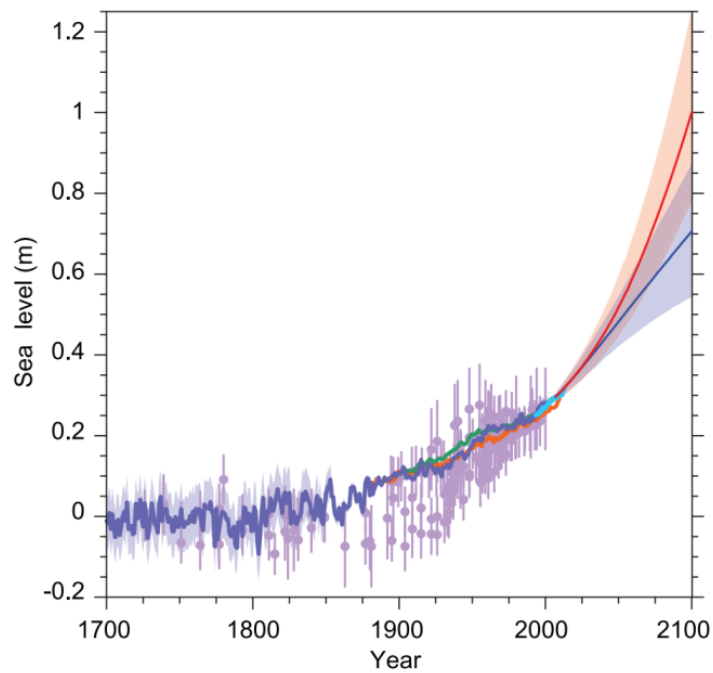


Figure 5.5: Global sea level rise including IPCC projections for 2100. Combination of paleo-sea level data, tide gauge data and altimeter records (Church et al., 2013).

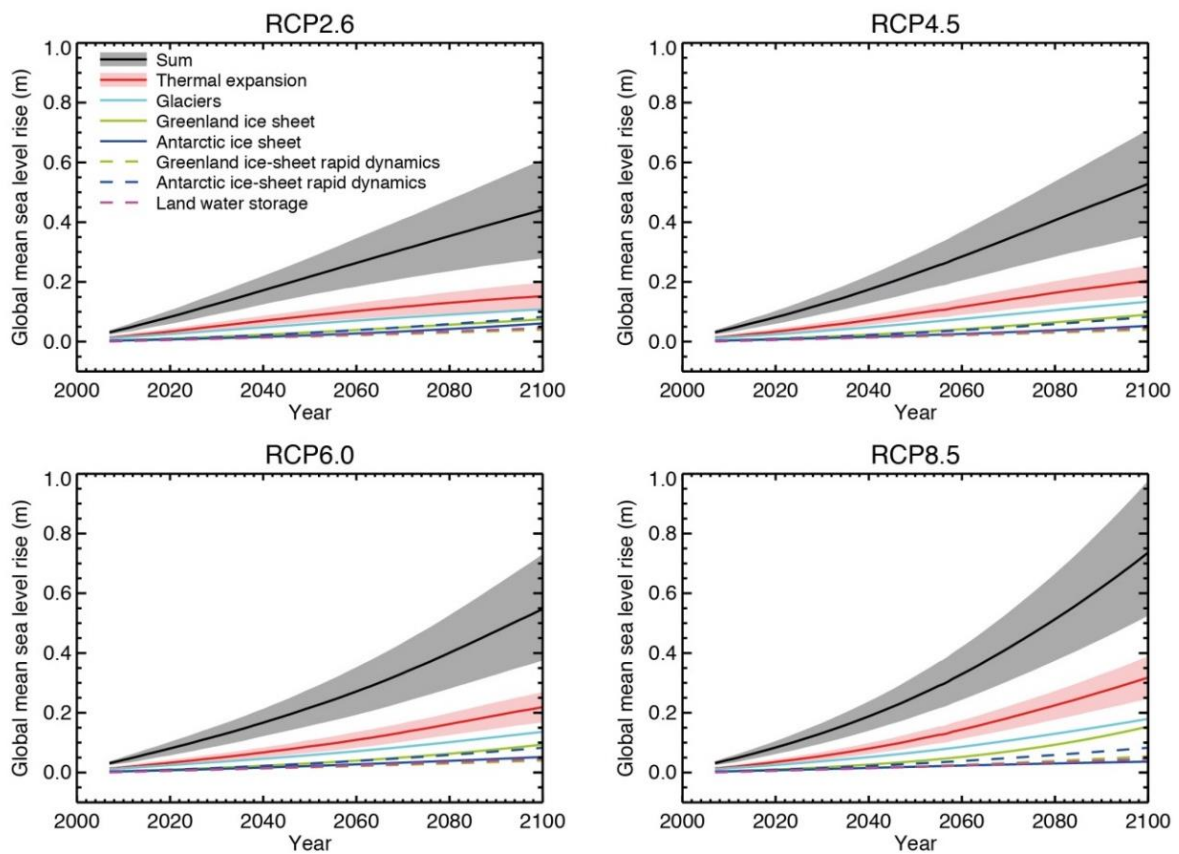


Figure 5.6: Sea level scenarios for RCP2.6, 4.5, 6.0 and 8.5. Including particular contributions (Church et al., 2013).

### 5.3.2 KNMI

In 2014, the KNMI set several climate scenarios which are still applicable to the Netherlands. The KNMI'14 scenarios are intended as an instrument for calculating the effects of climate change or for developing opportunities and adaptation strategies. These scenarios are still widely used for designing dyke reinforcements. The main differences with the KNMI'06 scenarios, which used global average values, is that the KNMI'14 scenario includes local responses and dynamic ocean effects. Furthermore, KNMI'06 used model simulations of Coupled Model Intercomparison Project Phase 5 (CMIP5) while KNMI'14 used model calculations of CMIP3.

In 2014, the expectation was that sea level rise becomes increasingly relevant for the Dutch coast. The KNMI designed two scenarios "W" and "G" that follow the representative temperature pathways of the IPCC. The KNMI'14 scenarios are consistent with IPCC AR5 (Church et al., 2013), but provide an alternative viewpoint, which is more accessible and readable for the policymakers and the general public of the Netherlands.

The W-scenario shows similar results as the RCP8.5 about sea level change estimates. The G-scenario shows overlap with the RCP4.5 and RCP6.0 scenarios. The main conclusions of these sea level scenarios are shown in Table 5.4 and Figure 5.7 & 5.8.

Table 5.3: Steering values of global-mean temperature change and estimated sea level rise which is used in the KNMI'14 scenarios. The values are compared to the 1986-2005 average (de Vries et al., 2014) \* (KNMI, 2014).

Scenario	2050 Temperature	2085 Temperature	2085 sea level rise	2100 Temperature	2100 sea level rise
G-scenario	+1.0 °C	+1.5 °C	25-60 cm	+1.6 °C	30-75 cm*
W-scenario	+2.0 °C	+3.5 °C	45-80 cm	+4.0 °C	50-100 cm*

The 95<sup>th</sup> percentile (P95) of the W-scenario of KNMI'14 shows an estimated sea level rise of 1.00 m. KNMI'06 describes 0.85 m SLR for P90 which is about 0.95 m for the high-end estimate (P95) (KNMI, 2014).

Important to note is the expectation that sea level rise will accelerate for both scenarios. Furthermore, local temperature in the Netherlands rose on average 1.4 °C between 1951 and 2013 which is much more than the global average, because land surface will warm more than the ocean surface (KNMI, 2014).

In 2014, the KNMI expected that the sea level contribution from Antarctica by the year 2100 is roughly 20 cm due to ice sheet dynamics, with the possibility to have a small converse effect on sea level rise due to a positive Surface Mass Balance. The contributing factors and impact to sea level rise are shown in Figure 5.8. Precipitation increase accumulation which may result in a reduced effect on sea level rise. However, the KNMI expected that uncertainty around sea level rise increases due to model uncertainty and rapid dynamic components of the Antarctic ice sheet (de Vries et al., 2014). The impact and timescale of potential Marine Ice Sheet Instability (MISI) are unknown. The KNMI also included a 15 cm additional sea level rise due to this uncertainty, similar to the projections of the IPCC (KNMI, 2014).

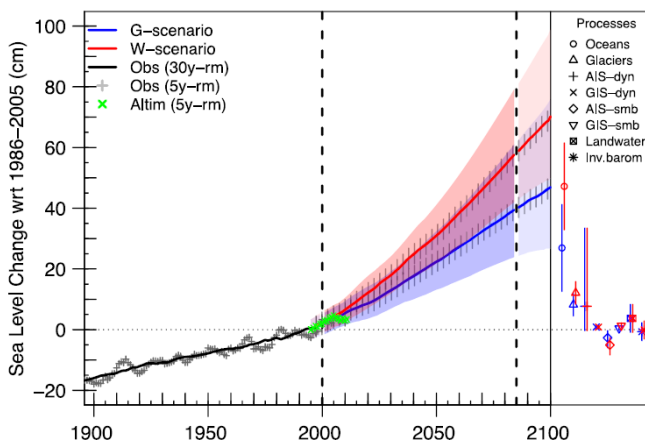


Figure 5.7: Scenarios for sea level rise along the North Sea coast (de Vries et al., 2014).

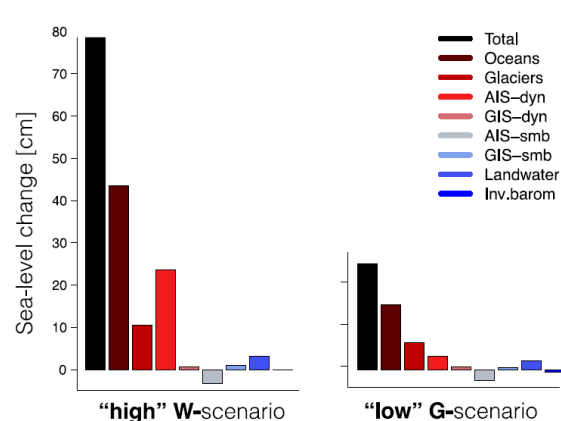


Figure 5.8: Contributions (cm) to the high W-scenario (left) and the low G-scenario (right) in 2085 (de Vries et al., 2014).

### 5.3.3 Other high-end scenarios

The IPCC is the largest organization in projecting future sea level rise. Many other projections were made after the latest IPCC report (AR5) which is published in 2013. Interesting to note is that the latest scenarios predict a higher rate of sea level rise and the end of this century than thought earlier. This knowledge is based on the latest data of the different contributors to SLR. This chapter only describes the results of the sea level projections of various studies which are shown in Table 5.5 and 5.6.

Important to note is that the projections of the IPCC AR5 should be adjusted to obtain the full probabilistic range. This correction is visualized in Figure 5.9. After correcting the IPCC AR5 scenarios, it is possible to compare the results to the other scenarios. The IPCC used a bandwidth of 90% (5%-95%) in their scenarios while they suggest that that bandwidth is a “likely” possibility to occur. The word “likely” in the IPCC report corresponds to a minimum 66% certainty which is not exactly 90% (IPCC, 2013) (Church et al., 2013). The reason for this is that the AR5 did not exclude the possibility of higher sea level rise because of the limitations in ice sheet modelling. Therefore, it is required to modify the standard deviation of the normal distribution to obtain a full probabilistic density function (PDF). This adjustment is the only way to show the full range of plausible outcomes. The properties of the PDF (adjusted) change after incorporating the full probabilistic range (Figure 5.9).

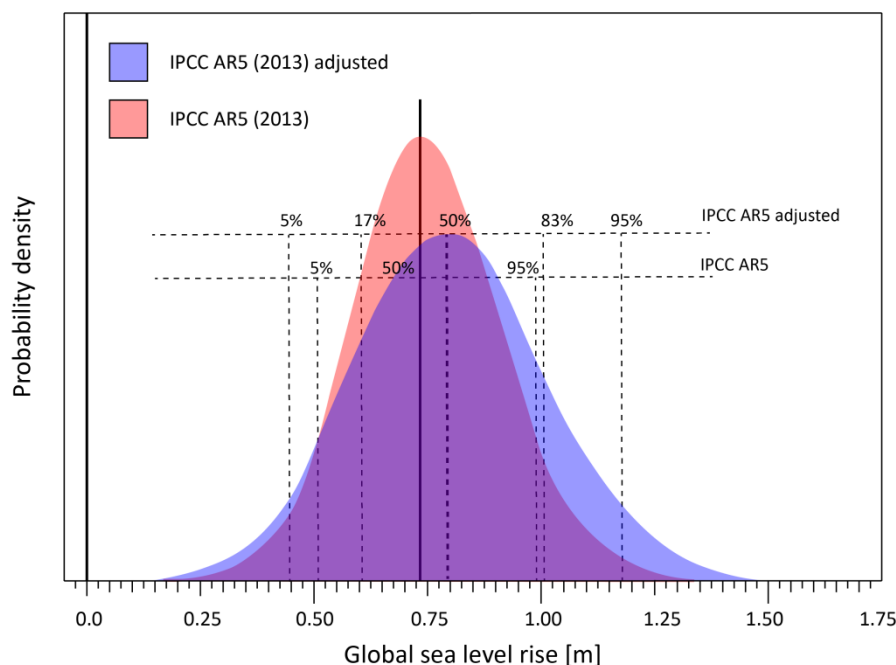


Figure 5.9: Comparison between standard PDF and adjusted PDF of IPCC AR5 scenario RCP8.5. Adjustment factors by (Kopp et al., 2014).

According to (Kopp et al., 2014), (Grindsted, Jevrejeva, Riva, & Dahl-Jensen, 2015), (Jevrejeva, Grindsted, & Moore, 2014) and (Jackson & Jevrejeva, 2016) the range of the IPCC (5%-95%) changes to approximately 17%-83% to represent the full probability range. According to Le Bars et al. (2017), it is important to multiply the standard deviation by 1.64 to change the likelihood of the 5%-95% model range from 90% to 66% which is the minimum likelihood of the AR5. Both scientists computed this value slightly different, because of difference in the type of distribution function and its skewness. The differences between both computations are explained in Section 5.5.3. The projected increase in sea level rise between the year 2000 and 2100 for the IPCC scenario is visualized in Figure 5.10. The 95<sup>th</sup> percentile for sea level rise increases from 98 cm to 118 cm in the year 2100 for the RCP8.5 emission pathway.

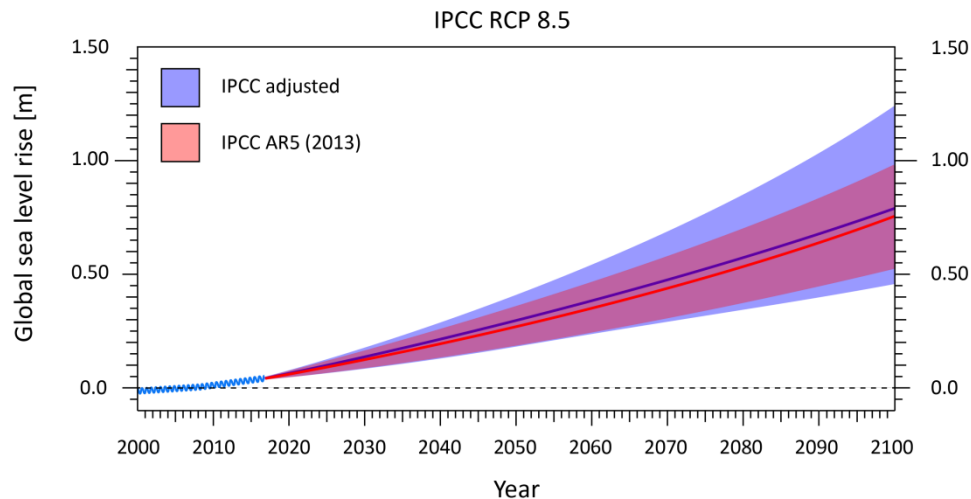


Figure 5.10: Sea level rise pathway for RCP8.5 of both the standard IPCC scenario and the adjusted version by (Kopp et al., 2014).

Many scientists included a higher uncertainty of the Antarctica ice sheet into their high-end projection which increases the high-end tail to a large extent compared to the IPCC AR5 scenarios. For example; according to both Grindsted et al. (2015) and Jackson & Jevrejeva (2016), the 5%-95% range for contribution to sea level rise of only Antarctica is -7 to 94 cm respectively. All recently published scenarios for global sea level rise of both RCP8.5 and RCP4.5 are shown in Table 5.5 and 5.6.

Table 5.5: Sea level rise projections for RCP8.5 in cm (Church et al., 2013) (Johansson et al., 2012) (Horton et al., 2013) (Rohling et al., 2013) (Kopp et al., 2014) (Jevrejeva et al., 2014) (Grindsted et al., 2015) \*: adjustment by (Kopp et al., 2014) & (Jackson & Jevrejeva, 2016).

Sea level projections in cm for RCP8.5	Percentile (P)						
	5%	17%	50%	83%	95%	99%	99.9%
'Adjusted' AR5 (2013) *	37	54	75	98	118	140	
Johansson et al. (2012)	26	41	72	118	155		
Horton et al. (2013)	50	70	≈100	120	150		
Rohling et al. (2013)	≈30		≈70	90 (68%)	190		
Kopp et al. (2014)	52	62	79	100	121	176 (99.5%)	245
Jevrejeva et al. (2014)	47	58	≈75	≈120	180		
Grindsted et al. (2015)	45	58	80	120	183	240	
Jackson & Jevrejeva (2016)	51	63	84	121	167	222	

Table 5.6: Sea level rise projections for RCP4.5 in cm. (Church et al., 2013) (Schaeffer, Hare, Rahmstorf, & Vermeer, 2012) (Bamber & Aspinall, 2013) (Kopp et al., 2014) \*: adjustment by (Kopp et al., 2014) & (Jackson & Jevrejeva, 2016).

Sea level projections in cm for RCP4.5	Percentile (P)						
	5%	17%	50%	83%	95%	99%	99.9%
'Adjusted' AR5 (2013)	22	36	54	72	85	100	
Schaeffer et al. (2012)	64 (10%)				121 (90%)		
Bamber & Aspinall, (2013)	33		61		132		
Kopp et al. (2014)	36	45	59	77	93	147 (99.5%)	215

## 5.4 New insights into the contribution of the Antarctic ice sheet to sea level rise

Thermal expansion of seawater and melting of mountain glaciers have dominated global mean sea level (GMSL) rise over the last century. However, mass loss from the Greenland and Antarctic ice sheets is expected to rise and exceed other contributions due to future global warming (Dutton et al., 2015). Various scientists addressed already a higher uncertainty of the Antarctic ice sheet in their process models than initially thought in the IPCC AR5, but these scenarios were still relatively consistent with the IPCC AR5 results. In 2016, new processes in the Antarctic ice sheet have been modelled by DeConto & Pollard, and the results could be very important for flood protection strategies in many coastal countries. This new knowledge shows that sea level scenarios are relatively uncertain, and that high-end sea level rise is a possibility. This study will cope with the risks and uncertainty of high-end sea level rise by making a response plan for the Dutch storm surge barriers.

### 5.4.1 Antarctic ice sheet contribution

Sea level fluctuations in the past, which are based on oxygen isotope ratios, were probably much larger than in ice sheet models (Hansen et al., 2013). Therefore, it could be the case that some important processes were missing in last ice sheet models. This philosophy is confirmed by Levermann et al. (2013) and DeConto & Pollard (2016) (DP16) who suggest that the Antarctic ice sheet (AIS) might be more sensitive to global warming than calculated be in the ice sheet models. Models improve continuously because of increasing computer capacity and samples in the field. New information about ice sheet dynamics of Antarctica should reduce uncertainty in the projections, but now, the opposite is the reality. Latest insights into the Antarctic contribution increase the projected rate of sea level rise and inherent uncertainty even further.

DeConto & Pollard (2016) are the first that project a significant contribution of the West-Antarctic ice sheet to sea level rise within a relatively short time-scale. The West-Antarctic ice sheet alone has the potential to raise global mean sea level by approximately 4.3 m (Fretwell et al., 2012). DP16 is the first published research that succeeded to model complete new dynamic processes of the Antarctic ice sheet. Their results might be a game changer for current coast policies around the world. DP16 argues that the following dynamic effects can drastically increase ice mass loss of the West-Antarctica ice sheet (WAIS):

- Hydrofracturing: cracking and fracturing of ice shelves by surface meltwater and rain.
- Grounding line retreat: the retreat of ice supported by land, due to oceanic melt.
- Ice-cliff failure: instability of high vertical ice wands leads to failure.

Where previous reports argue that only Marine Ice Sheet Instability (MISI) is a risk for future sea level rise which drives uncertainty, DP16 shows even more severe processes and consequences. The ice sheet dynamics and associated processes are visualized in Figure 5.11. Ice-shelf hydrofracturing can accelerate ice shelf (floating ice) loss which reduces the buttressing effect for the massive Antarctic ice sheet (land ice). Due to the loss of floating ice, tall vertical cliffs remain which could collapse under its own weight. This Marine Ice Cliff Instability (MICI) have the potential to increase Antarctic mass-loss rates to a much larger extent than earlier thought which could have a large impact on global sea level rise.

Atmospheric warming in West-Antarctica could result in rain and meltwater which influence crevassing and calving rates of floating ice shelves (Banwell et al., 2014). This hydrofracturing of ice percolates the ice shelves and reduces its strength.

Grounding line retreat, a process driven by ocean warming which melts ice below sea level, can increase the risk of cliff failure even further. Rignot et al. (2014) confirm that large-scale grounding line retreat is already started and will accelerate in the West Antarctic ice sheet (Rignot, Mouginot, Morlighem, Seroussi, & Scheuchl, 2014). The grounding line separates land ice and floating ice and is below the ocean surface. Nearly half of the AIS is supported by bedrock that is hundreds of meters, or more, below sea level which is essential for the grounding line retreat mechanism (Fretwell et al., 2012). The reverse sloped bed of the supporting rock accelerates grounding line retreat and increases the marine terminating cliff height. High cliffs of roughly 800 m (whereof 90 m above the surface) or more will collapse under their own weight and longitudinal stress (DeConto & Pollard,

2016). Moreover, the flux of ice across the grounding line will increase non-linear as a function of its thickness. Both will cause massive mechanical cliff failures which will continue until the local atmospheric and ocean temperature are cold enough to form new buttressing ice shelves, which could take thousands of years. This faster rate of ice-cliff collapse would yield faster rates of ice-sheet shrinkage (Griggs et al., 2017).

The large-scale retreat due to cliff failure probably starts around 2050, when large parts of the ice shelves, which have a significant buttressing effect, are expected to be lost. This accelerating ice retreat is already underway on the Greenland ice sheet (GIS) and might start soon in Antarctica. Some glaciers on Greenland lose 10-14 km in length every year due to ice-cliff collapse in particular (Joughin et al., 2012).

The new model includes MICI processes and is the first that shows comparable results that match past sea level fluctuations (DeConto & Pollard, 2016). Sea level projections are thus not equivalent to past sea level rise without incorporating hydrofracturing and ice-cliff failure (Griggs et al., 2017). All described dynamic processes and the difference between MISI and MICI is visualized in Figure 5.11 and explained in more detail in Appendix E & F.

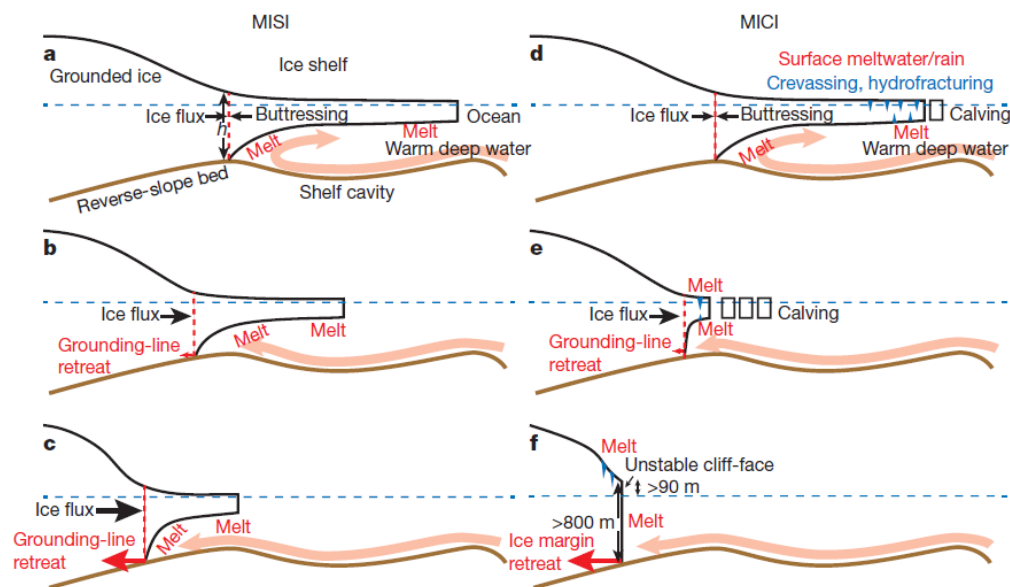


Figure 5.11: (a-c) show MISI and the melting ice shelf. (d-f) show MICI with accelerated ice shelf retreat and cliff collapse. Both processes are triggered by ocean and atmospheric warming (DeConto & Pollard, 2016).

The dynamic model of DP16 included both MISI and MICI. DeConto & Pollard (2016) argue that the Antarctic ice sheet is very sensitive to global warming and project a large difference between the RCP scenario pathways. This model showed that ice sheet melt on Antarctica could potentially contribute 1.14 m to global sea level rise with  $1\sigma$  of 0.36 m in 2100 compared to the year 2000. This is the result of RCP8.5 and counts only for Antarctica. For RCP2.6 and RCP4.5, this contribution is  $0.16 \pm 0.16$  m and  $0.58 \pm 0.28$  m respectively. The high-end contribution (P95) for RCP8.5 and RCP4.5 is 1.73 m and 1.04 m respectively.

Other contributions of Greenland, glaciers, thermal expansion, and land water are not included in DP16. This is in contrast to the IPCC projections which expected that Antarctica is relatively immune to short-term global warming. So, it seems important to regulate global warming in order to limit sea level rise. The projection of DeConto & Pollard (2016) is considerably higher than the old upper bound of the IPCC AR5 which is 30 cm (P95) for combining surface mass balance (SMB) and rapid ice dynamics of the Antarctic ice sheet (Church et al., 2013). This estimation was based on older ice sheet models that were not capable of calculating dynamic processes such as hydrofracturing and cliff failure. Important to note is that AR5 already indicated that the effects of ice sheet dynamics of Antarctica to SLR are uncertain. For that reason, the AR5 assessed the “likely” (66% probability) range of their sea level projections. More information about the AR5 and other scenarios can be found in Section 5.3.3 “Other high-end scenarios”.

The Antarctic ice sheet gains mass through snowfall and loses mass through submarine melting and iceberg calving. Paolo et al. (2015) argue that ice volume losses of floating ice shelves increased 70% in the last decade around the West-Antarctic ice sheet (WAIS) (Paolo, Fricker, & Padman, 2015). DP16 concluded that ice shelves should first disappear to start large-scale ice mass loss of the WAIS. Paolo states that ice shelf loss is already started which may indicate that some dynamic processes described by DP16 are already beginning. An overview of the locations where mass changes occur in Antarctic ice shelves is shown in Appendix F.

Antarctica contributes already to sea level rise by approximately 0.3 mm per year (Dieng et al., 2017). This relatively small contribution is probably caused by grounding line retreat in the WAIS. The significant increase in sea level contribution is expected after 2050 when most ice shelves may be lost. All dynamic processes together might increase the annual contribution to sea level rise to roughly 25 mm per year (RCP8.5) at the end of this century (Deconto & Pollard, 2016).

The Antarctic contribution to the different RCP pathways is shown in Figure 5.12. The high-end projection is even higher ( $1.14 \text{ m} \pm 0.36 \text{ m}$ ) because of the ocean temperature correction in the Amundsen and Bellingshausen seas. More detailed information about the results of DP16 can be found in Appendix F.

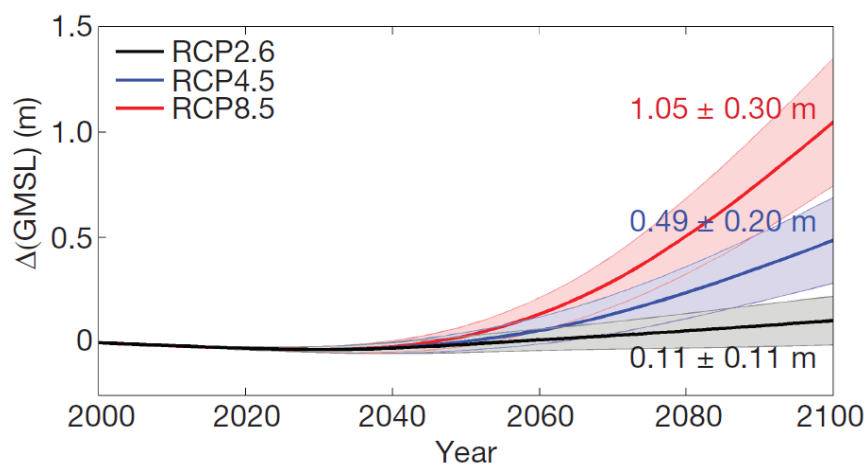


Figure 5.12: Antarctic contribution to sea level rise with  $1\sigma$  standard deviation and without ocean temperature correction (DeConto & Pollard, 2016).

### 5.4.2 Uncertainty in model results

The results of DP16 might have an enormous impact on current sea level scenarios. However, the dynamic ice sheet mass loss is still very uncertain. Including MICI dynamics in an ice-sheet model is difficult because modelling ice fracture mechanics is very complicated. Various interacting processes should be included such as stress regime, water depth, ice thickness, flow speed, bathymetry, the spacing of crevasses, mélange, tides etc. (Griggs et al., 2017). It is only possible to parameterize the representation of cliff failures. It is clear that this will increase uncertainty.

There are some uncertainties and limitations in the simulations of the report of DP16 which can either underestimate or overestimate ice sheet retreat. First, it should be emphasized that the model ensembles are based on a single climate model. Second, there is a lack of observations in the regions of the Antarctic ice sheet about ice properties, ocean temperature and bathymetry (Griggs et al., 2017).

Third, there is uncertainty in past sea level rise (Section 5.1). Ice sheet models are based on proxies of ancient climate change during the Last Interglacial and the Pliocene period. The small difference in the parameters of past sea level rise has sufficient impact on the projections. DP16 provides sea level projections assuming Pliocene sea level rise of 5-15 m and 10-20 m which give different results. Improved ancient sea level estimates are needed to develop the model combined with improved climate studies of the RCP scenarios (DeConto & Pollard, 2016). Fourth, DP16 computed a symmetric probability distribution for the Antarctic contribution. However, the impact of ice sheet dynamics on sea level rise is still very uncertain, indicating that the distribution should be asymmetric with a large high-end tail.

The timing when substantial sea level rise occurs due to Antarctic contribution is still profoundly uncertain, depending on the rate of the loss of buttressing ice shelves. DeConto also notes that it is not possible to completely eliminate high-end sea level rise for low emission scenarios (Griggs et al., 2017).

The results of DP16 do not represent the full space of plausible outcomes, and even more sea level rise cannot be ruled out. The maximum ice-cliff collapse rate used in the model is 1-5km per year, while the current observed rate of ice-cliff failure of a glacier in Greenland is roughly 10-14 km per year for the tallest vertical ice-cliffs (Joughin et al., 2012). DeConto suggests that the Antarctic contribution can increase to 2 m in the year 2100 by changing this input parameter. This will be researched at this moment.

It is not entirely sure that hydrofracturing cause ice shelves to disappear so rapidly. Ice-sheet models poorly represent the melt-water buffering capacity of firn, which is a layer between new snow and ice. Meltwater might be absorbed by this layer, which limits crevasses and hydrofracturing (Kopp et al., 2017). It is not sure of the mélange (floating ice after cliff failure) provide an additional buttressing effect which could reduce accelerating ice-cliff collapse (Fretwell et al., 2012).

The results of the model indicate that atmospheric warming will primarily cause ice sheet instability, but observations show that the warming of seawater will be the dominant cause of hydrofracturing. The model does not seem to be perfectly calibrated on the current situation. Moreover, the rate of retreat of ice shelves will depend on the course of Antarctic warming in response to various factors including ozone hole recovery, tropical dynamics and feedbacks between ice-sheet, earth, ocean, and sea-ice. These processes are not included in DP16 (Griggs et al., 2017). Future assessment of these shortcomings can either increase or decrease uncertainty.

In summary, ice shelves already losing mass over the last decades which reduces the buttressing effect for land-ice (Paolo et al., 2015). This process can influence the stability of the WAIS with significant ice sheet loss at risk. The question is how fast ice shelves disappear that could enhance large scale ice-cliff instability. Ice sheet dynamics are still poorly understood and more scientific research is needed to either confirm or reject the results of DP16.

## 5.5 Impact of the increased Antarctic contribution to global sea level rise scenarios

The results of DP16 have resulted in more uncertainty in projecting sea level rise, and it might be the case that previous scenarios were missing essential elements that should be incorporated. Even though the revelations of the DP16 are relatively new, two studies made global sea level scenarios based on the results of DP16 (DeConto & Pollard, 2016).

Le Bars et al. (2017) and Kopp et al. (2017) created new scenarios which incorporate the results of DP16. These sea level projections are different from the previous scenarios KNMI'14 and IPCC AR5, because of the new evaluation of the contribution of Antarctic ice sheet. These new sea level scenarios have increased uncertainty in the high-end projections to a large extent.

The IPCC AR5 assumed that the contribution of dynamical processes in the Antarctica ice sheet was independent of the RCP scenarios. DeConto & Pollard (2016) argue that it highly depends on future temperature pathways which increase the high-end predictions. They suggest that it is still possible to limit sea level rise by performing an active global climate policy.

There is some criticism of the results in DP16 also explained in Section 5.4.2 "Uncertainty." Kopp et al. (2017) argue that the resulting GMSL projections should not be viewed as probabilistic because the DP16 ensembles were not constructed from probabilistic distributions and taken from a limited set of paleo-sea level reconstructions. However, DP16 can be seen as semi-quantitative information about potential future changes and a degree of deep uncertainty in sea level projections (Kopp et al., 2017). Despite this limitation, Kopp calculated a probabilistic scenario because of the absence of additional studies.

This new uncertainty implies that the high-consequence, low-probability projections are becoming more important, especially for critical long lifetime infrastructure.

### 5.5.1 Projected global sea level rise including extra Antarctic contribution assessed by (Le Bars et al., 2017)

Le Bars et al. (2017) carried out a full probabilistic assessment incorporating the results of the processes modelled by DP16 for 100%. The results of Le bars et al. (2017) are shown in Figure 5.13 and Table 5.7. The outcome of the research revealed an average sea level rise of 1.84 m in 2100 including a large uncertainty bandwidth. The probability density function is normally distributed, and the calculated high-end (P95) GMSL rise is 292 cm in the year 2100 for RCP8.5. This implies that a 5% chance exists that future sea level rise will exceed that value. Even significant sea level rise is expected for scenario RCP4.5 with a high-end (P95) of 177 cm. The complete results including the more modest scenario RCP4.5 are shown in Table 5.8.

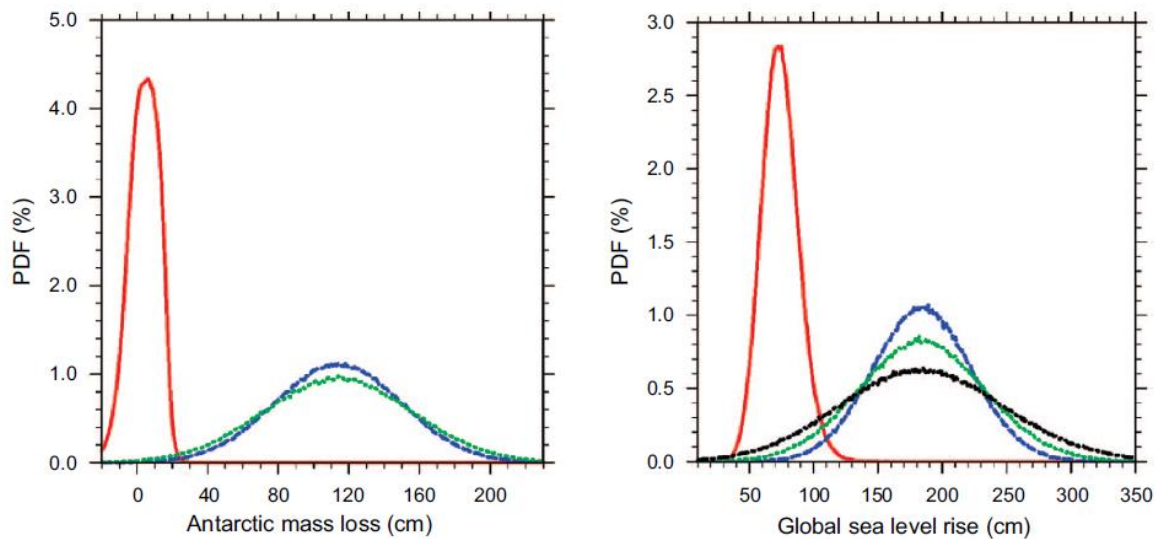


Figure 5.13: Comparison of the probability distribution of Antarctic mass loss (left) and global total sea level rise (right) in 2100 compared to 1985–2005 for scenario RCP8.5. The figure includes IPCC AR5 (red), Antarctic mass loss DP16 (blue), including temperature dependent Antarctic mass loss DP16T (green). The sensitivity of global estimates to the  $\gamma$  parameter representing CMIP5 model ensemble uncertainty is also added: DP16T with  $\gamma = 1.64$  (black) instead of 1 for the other curves (Le Bars et al., 2017).

Table 5.7: Percentiles of the PDFs according to Le Bars (2017) of total global sea level rise in 2100 compared to 1986–2005 for RCP8.5 using three methods: IPCC AR5, Antarctic contribution from DeConto & Pollard (2016) (DP16) and including a temperature dependence in the Antarctic contribution (DP16T) (Le Bars et al., 2017).

SLR [cm] RCP8.5 year 2100	AR5		DP16	DP16T	
Percentiles (P)	$\gamma = 1$	$\gamma = 1.64$	$\gamma = 1$	$\gamma = 1$	$\gamma = 1.64$
1	44	36	96	71	41
5	51	46	121	104	81
10	56	51	135	121	103
20	62	58	152	143	131
50	73	73	184	184	184
80	85	90	216	225	238
90	92	99	233	247	268
95	98	108	247	265	292
99	111	127	273	299	339

Table 5.8: Percentiles of the PDFs according to Le Bars et al. (2017) of total global sea level rise in 2100 compared to 1986–2005 for RCP4.5 using three methods: IPCC AR5, Antarctic contribution from DeConto & Pollard (2016) (DP16) and including a temperature dependence in the Antarctic contribution (DP16T) (Le Bars et al., 2017).

SLR [cm] RCP4.5 year 2100	AR5		DP16	DP16T	
Percentiles (P)	$\gamma = 1$	$\gamma = 1.64$	$\gamma = 1$	$\gamma = 1$	$\gamma = 1.64$
1	30	25	37	25	12
5	36	32	57	48	37
10	39	36	67	61	52
20	43	42	80	76	70
50	52	52	105	105	106
80	62	64	130	134	142
90	66	70	143	150	161
95	70	76	153	162	177
99	78	87	173	186	208

The significant shift in the mean of the probability function is entirely caused by replacing the IPCC AR5 value for Antarctica by the new high-end estimate. The changed higher quantiles originate from two other extensions, which are explained below. These results are obtained by implementing three computations:

1. the full joint probability of IPCC AR5 sea level rise scenario;
2. Antarctic contribution modelled by DP16 (DeConto & Pollard, 2016);
3. temperature dependence with Antarctic ice sheet dynamics (DP16T).

The IPCC AR5 made projections which have, according to their calculations, a likely chance (66%) of occurrence. In short, the IPCC is thus not sure of their own projections and did not include all potential outcomes. The full joint probability distribution is required to obtain more plausible projections of sea level rise which are comparable with other scenarios (Section 5.3.3). Consequently, the tails of probability distribution increase. The high-end outcome of the revised AR5 is 108 cm (P95) according to Le Bars et al. (2017).

This scenario used the projections of the IPCC AR5, but replaces the Antarctic contribution by the projections of DP16. The contribution from Greenland ice sheet and glaciers is not changed because DP16 only assessed the Antarctic ice sheet. After replacing the Antarctic contribution, the new upper bound is 247 cm SLR. Important to note is that the results in Table 5.7 include the highest results of DP16. DeConto and Pollard were also aware of the limitations in their own research, so they also made a scenario based on different paleo climatologic data of the Pliocene period which resulted in slightly reduced values. These can be found in Appendix F.

Le Bars et al. (2017) concluded, based on a symmetric distribution function, that sea level rise is even higher for high percentiles when the contributions are assumed to be correlated. Processes that are (partially) correlated with temperature are ocean thermal expansion, land glaciers, ice caps, surface mass balance (SMB) and ice sheet dynamics. Le Bars et al. (2017) deviate from the IPCC AR5 by considering that the ice sheet dynamics of Antarctica are also reliant on temperature change. The floating ice shelves should first disappear to start large-scale ice cliff failure. Ice shelf loss is caused by melt and hydrofracturing. Hydrofracturing occurs due to atmospheric surface warming. Oceanic warming will accelerate grounding line retreat. These two processes are correlated to global temperature on long time scales (Le Bars et al., 2017).

It makes sense to include temperature correlation because the higher local temperature will enhance hydrofracturing and ice shelf loss. Higher ocean temperature also accelerates grounding line retreat. Both processes will drive ice-cliff collapse which is expected to become the primary contributor of ice sheet loss. The impact of this change is significant which indicates that the degree of correlation is important for the high percentiles of the probability distribution function.

The probability distribution of Le Bars et al. (2017) is symmetric according to the results of DP16. However, high-end sea level rise is uncertain due to the ice sheet dynamics, and the high-end tail should, therefore, be larger than the low-end tail.

### 5.5.2. Projected global sea level rise including extra Antarctic contribution assessed by (Kopp et al., 2017)

Kopp et al. (2017) substituted Antarctic ice sheet ensembles of DP16 into the probability distribution of Kopp et al. (2014). The results of Kopp et al. (2014) are shown in Appendix D. Kopp et al. (2017) argue that the results of DP16 should not be seen as probabilistic because DP16 ensembles were not constructed from probabilistic distributions of key parameters and are based on a limited set of observations. Kopp suggests that these results should be viewed as semi-quantitative information about potential changes. A key conclusion is that the results show that there is considerable uncertainty in sea level projections.

The mean sea level rise (P50) increases from 74 to 146 cm for RCP8.5 and from 55 to 91 cm for RCP4.5 by including DP16 instead of the IPCC estimate (Kopp et al., 2017). The P95 increases to 243 cm for RCP8.5.

Table 5.9: Sea level projections in cm including DP16 (Kopp et al., 2017).

SLR [cm] by year 2100	RCP2.6	RCP4.5	RCP8.5
Percentiles (P)			
1	18	39	80
5	26	50	93
17	37	66	109
50	56	91	146
83	78	125	209
95	98	158	243
99	111	180	267
99.9	122	197	297

### 5.5.3. Differences between high-end sea level scenarios

This section discusses the differences in the results and model parameters between the sea level scenarios of Le Bars et al. (2017) and Kopp et al. (2017). The forecasted trajectory of sea level rise according to both scenarios is shown in Figure 5.14 and 5.15. The IPCC AR5 scenario is included to visualize the substantial differences in the total sea level rise. It is noticed that the accelerated rise is expected to start around the year 2050 because both studies include the results of DP16 for 100% into their analysis. It is not expected that sea level rise deviates significantly from the IPCC AR5 scenarios before the year 2050 because the large-scale Antarctic contribution to sea level rise is expected to begin around that period.

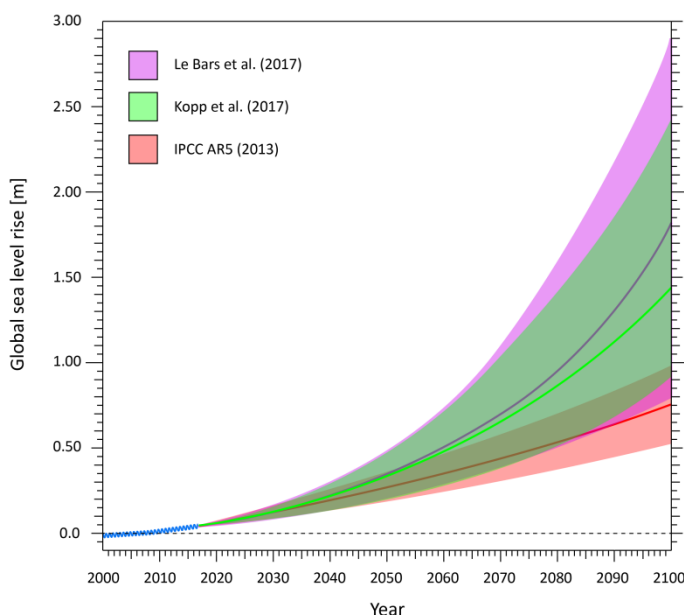


Figure 5.14: Projected sea level rise trajectory for RCP8.5. Bold lines represent mean sea level rise (50%) and shaded area indicate 5-95% probability range.

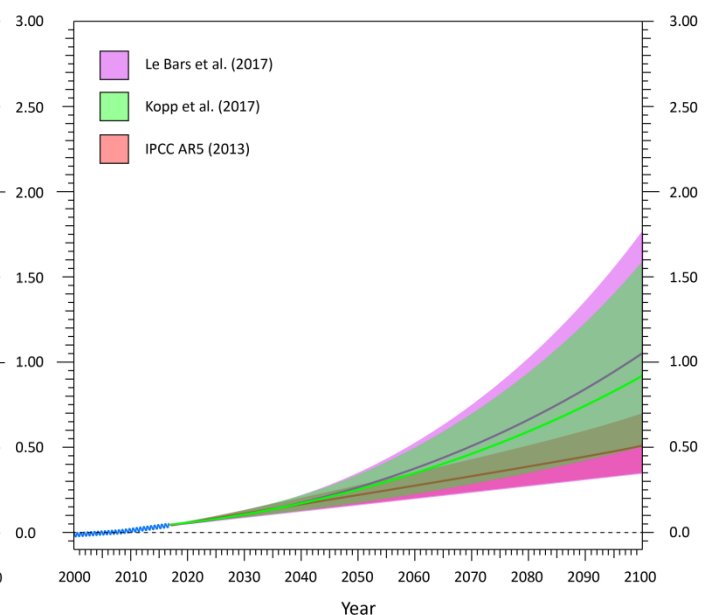


Figure 5.15: Projected sea level rise trajectory for RCP4.5. Bold lines represent mean sea level rise (50%) and shaded area indicate 5-95% probability range.

Kopp et al. (2017) calculated the full joint probability of the AR5 combined with the input of DP16 in a different way compared to the method of Le Bars et al. (2017). First, Kopp et al. (2017) used one lower estimate of DeConto & Pollard (Appendix F) with an average contribution for Antarctica of  $0.64 \pm 49$  cm (RCP8.5) instead of  $1.14 \pm 36$  cm which is used in the calculation of Le Bars et al. (2017). Both studies used different input values of the uncertainty in past sea level rise in the Pliocene period which explains the main difference between the results. Kopp used a past sea level rise reference based on a Pliocene estimate of 5-15 m instead of 10-20 m. Second, the results of Kopp et al. (2017) are obtained by a t-distribution combined with a gamma ( $\gamma$ ) of 1.7 for standard deviation. Le Bars et al. (2017) used a normal distribution with a different gamma of 1.64 for standard deviation. The skewness of the probability density function is imperative for high-end estimates. It can be noted, that the high-end results of Kopp et al. (2017) should be even slightly higher than the results of Le Bars et al. (2017) using the same contribution of Antarctica due to the skewness of the distribution function.

In addition, Le Bars et al. (2017) add a temperature uncertainty to the Antarctic contribution while Kopp et al. (2017) did not include this uncertainty. Furthermore, Le Bars et al. (2017) made ice sheet dynamics depend on temperature, while both Kopp et al. (2017) and the IPCC AR5 assumed independence. In the end, it is difficult to substantiate the correlation between all parameters in both reports, since this information has not been made public. Correlation is very important in determining sea level rise and is partly based on subjective assumptions.

## 5.6 New global sea level rise scenario

Accelerated global sea level rise is confirmed by a trend of 3.3 mm per year (1993-2017) while this was averagely 1.7 mm per year over last century (Lindsey, 2017). Many scientists project further acceleration in sea level rise over the 21<sup>st</sup> century (Church et al., 2013) (Johansson et al. 2012) (Horton et al., 2013) (Rohling et al., 2013) (Kopp et al., 2014) (Jevrejeva et al., 2014) (Grindsted et al., 2015) (Jackson & Jevrejeva, 2016). Further global warming and the inertia effect of the global oceans and atmosphere are the main reasons behind accelerated sea level rise expectations. This section summarizes the relevant conclusions of previous chapters to construct new sea level scenarios which are presented in Section 5.6.2.

### 5.6.1 Background

The Fifth Assessment Report (AR5) shows the latest sea level rise scenarios of the IPCC. The high-end estimate (P95) is 98 cm SLR for RCP8.5 in the year 2100 (Church et al., 2013). The complete results are shown in Table 5.3. Soon after the publication of the AR5 results various scientists argue that the IPCC did not include the full bandwidth of possibilities in their PDF. The high-end estimate (P95) of the IPCC is 118 cm when obtaining a full joint probability (Kopp et al., 2014). The reason for the increased high-end estimate is that the IPCC did not include the total uncertainty about the Antarctic ice sheet contribution in their projections due to ice sheet model limitations to capture dynamic processes (Church et al., 2013). More information about reference studies and the limitations of the IPCC is provided in Section 5.3.3.

Grindsted et al. (2015) suggested that sea level rise is not normally distributed but highly skewed with a long high-end tail. Ice sheet dynamics have a larger uncertainty towards higher sea level change values, which results in an asymmetric probability distribution (de Winter et al., 2017). This implies that the high-end tail of the distribution function is larger than the low-end tails.

The PDF of the new global sea level scenario is given in Figure 5.16. The probability density function shows that future sea level rise is much less certain than expected before in the IPCC AR5. Furthermore, the PDF is not normally distributed and is asymmetric. The results of the IPCC AR5 are transformed into a full joint distribution combined with the additional uncertainty of the Antarctic contribution. The yellow shaded area indicates the bandwidth (P1-P99) of sea level rise in the year 2100, based on the assessment of the results of DP16 (DeConto & Pollard, 2016), (Kopp et al., 2017) and (Le Bars et al., 2017). The confidence interval (P5-P95) of the IPCC AR5 scenario is within the orange shaded area. This projected high-end sea level rise was considerably higher than the projections of the IPCC.

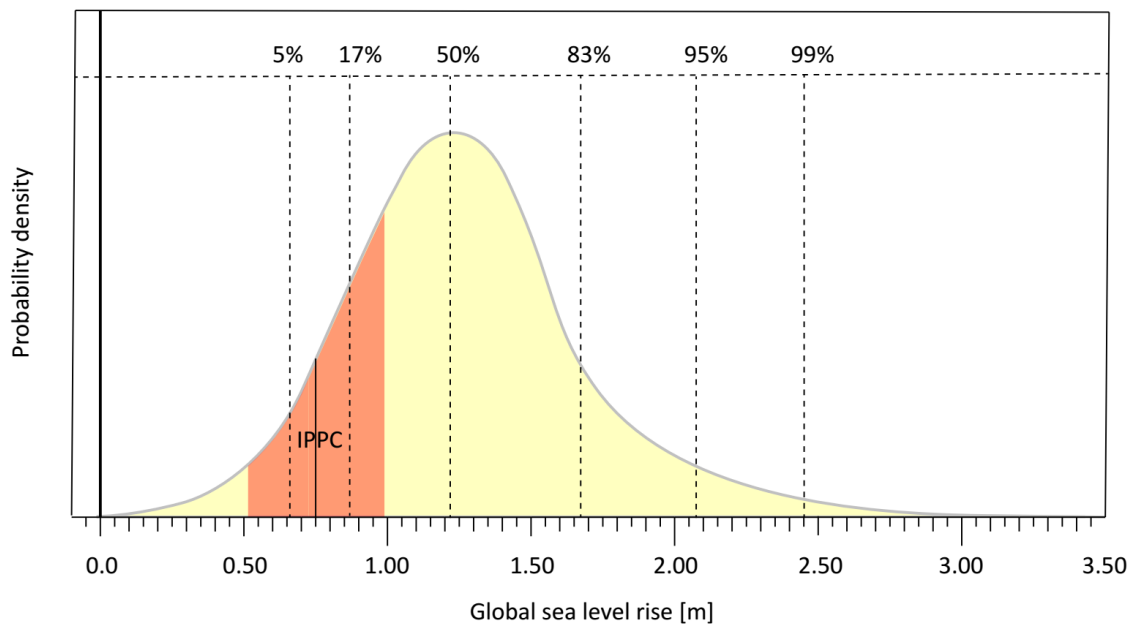


Figure 5.16: Uncertainty in projected global mean sea level rise for RCP8.5 visualized in a PDF. The vertical black line and red shaded range show the median and likely range as projected in IPCC AR5.

The conclusions of DeConto & Pollard (2016) changed the way of thinking of many scientists towards sea level rise. Despite the limitations of DP16 (Section 5.4.2), it showed that future sea level rise is even more uncertain than previously thought. Previous extreme scenarios such as the UK High++ (1.9 m sea level rise in 2100) which was seen as an absolute upper limit, might be not that unexpected at all (Appendix D).

Le Bars et al. (2017) and Kopp et al. (2017) included the results of DeConto & Pollard (2016) into their sea level projections (Section 5.5). These studies replaced the new results for earlier IPCC projections despite all limitations and uncertainties. High-end sea level rise scenarios have a probability of 5% to occur. Nevertheless, high-end estimates cannot be excluded in the development of adaptation strategies to deal with accelerated sea level rise. Le Bars et al. (2017) and Kopp et al. (2017) project respectively 292 cm and 243 cm in the high-end scenario (P95) for RCP8.5. Projected high-end (P95) SLR is 177 cm and 158 cm for the more moderate scenario RCP4.5 according to Le Bars et al. (2017) and Kopp et al. (2017). The degree of correlation between contributing factors such as ice sheet dynamics and temperature change is very important for determining high-end sea level projections. Quantification of correlation is partly based on subjective motivation which can lead to a large spread between the scenarios of the reference studies. This uncertainty is the primary driver of an increased high-end estimate for sea level rise.

## 5.6.2 New global sea level rise projections

This section presents the new global sea level scenario according to this study. Sea level projections for RCP4.5 and RCP8.5 for the year 2100 are given in Table 5.10. It is not possible to project future climate policies, but recent research shows that the trend of increasing carbon emissions is slowing down (Raftery et al., 2017). Therefore, the expected emission scenario is likely to be the average between RCP8.5 and RCP4.5. There is only a very small possibility that RCP2.6 is reachable. More information can be found in Section 4.2.4.

The results are based on a combination of various studies and each of them has a specific weighting factor (Table 5.11). The used factor gives an indication of the accuracy and relevance of the results of the reference study. Le Bars et al. (2017) and Kopp et al. (2017) fully included the results of the increasing Antarctic contribution described in DP16. The results of DP16 sound reasonable but are not supported yet by other climate studies. Furthermore, there are limitations in the results of DP16 that can either underestimate or overestimate the Antarctic contribution. Therefore, this study cannot rely entirely on the results of DP16 and will also use results of previous studies. Further research should provide more clarity about the results of DP16 before they are included in water safety policy. Despite, the results of DP16 will increase the sea level rise projection in this research and especially the uncertainty.

This study used the results of various reference studies in projecting a new global sea level rise scenario which is presented in Table 5.10. The used scenarios including the weighting factors are shown in Table 5.11.

Table 5.10: Global sea level rise projections between 2000 and 2100 based on literature research.

Projected SLR [cm] year 2100	RCP4.5	RCP8.5	Average RCP4.5 & RCP8.5
Percentiles (P)			
5	37	67	52
17	53	87	70
50	78	122	100
83	110	169	139
95	135	207	171
99	159	245	202

Table 5.11: Used reference studies and weighting percentages for RCP4.5 and RCP8.5.

Used reference studies	DP16		IPCC AR5 (adjusted)				
	(Le Bars et al., 2017)	(Kopp et al., 2017)	(Kopp et al., 2014)	(Grindsted et al., 2015)	(Church et al., 2013)	(Jackson & Jevrejeva, 2016)	Bamber & Aspinall, (2013)
RCP4.5	25%	25%	16.67%	-	16.67%	-	16.67%
RCP8.5	25%	25%	12.5%	12.5%	12.5%	12.5%	-

This study shows a global high-end sea level projection of 135 cm (RCP4.5) and 207 cm (RCP8.5) in 2100. The results are obtained by performing extensive literature study and combining new information into a sea level scenario. Changes in the high-end tails (P95-P99) of the probability distribution are much larger than the shift of the mean (P50) because of the increased uncertainty.

Both Kopp et al. (2017) and Le Bars et al. (2017) used the results of DP16 for 100% into their scenarios. As already explained in Section 5.4, DP16 is the first that modelled dynamic processes of the Antarctic ice sheet. The results of DP16 have limitations, but the results of the IPCC did not even include ice sheet dynamic processes. Therefore, sea level projections made by Le Bars et al. (2017) and Kopp et al. (2017) which use the results of DP16 are included for 50% in the new scenarios for RCP4.5 and RCP8.5. This percentage is also based on the statement that the results of DP16 match with past historical rate of sea level rise, which makes the results more plausible. More research is needed that can either increase or reduce this percentage.

The other studies also count for 50% and are based on the IPCC AR5 including a small increase in the uncertainty of ice sheet dynamics. Grindsted et al. (2015) and Jackson & Jevrejeva (2016) include additional uncertainty in the Antarctic contribution which should be the appropriate approach to clarify the total uncertainty. However, these two studies do not contain a sea level projection for RCP4.5. Kopp et al. (2014) computed the full bandwidth of the IPCC AR5 including expert elicitation of Bamber & Aspinall (2013). The results of the sea level rise in IPCC AR5 are made by Church et al. (2013) and are adjusted by various studies (presented in Section 5.3.3). The ratio between the used reference studies is debatable and can significantly change the given scenario. Nevertheless, there is still no clear indication to use a different ratio. However, it is advised to use the latest upcoming new studies to validate the given scenario more specifically.

It is clearly visible that recent studies argue that the Antarctic contribution will be more uncertain than previously thought. Also, no studies which are published recently, estimate that the Antarctic contribution would be less than predicted in the IPCC AR5. Nevertheless, it is evident that the focus of this study is more on high-end sea level scenarios since the risks of extremely accelerated sea level rise are not clear yet for the storm surge barriers in the Netherlands. The used weighting factors lead to a scenario that projects more sea level rise than previous estimations and can be assumed to be realistic due to the increased uncertainty in future sea level rise and Antarctic ice sheet dynamics. Nonetheless, more scientific studies and observations in the field are required to test the validity of the results.

The sea level scenarios of both RCP8.5 and RCP4.5 are shown in a time path in Figure 5.17 and 5.18. The results of the IPCC AR5 are included in shaded red to indicate the differences. The focus of this study is on median sea level rise (P50) and high-end sea level scenarios which indicates the 95<sup>th</sup> percentile (P95) of the probability density function.

There is still a significant spread due to all uncertainties and especially in the dynamic response of the Antarctic ice sheet. The total spread between all scenarios is shown in lightly shaded blue. It is assumed that the results of Le Bars et al. (2017) show the maximum sea level rise according to DP16 (light blue). Section 5.4.2. explains that potential high-end sea level rise can be even higher due to uncertainty in the maximum ice cliff failure rate. It is assumed that the maximum ice cliff failure is not higher than the currently chosen 1-5 km. The motivation for this assumption is that melting processes on Antarctica are far behind of Greenland because of much colder atmospheric temperatures. More extensive research might clarify if the maximum ice cliff failure rate in the model of DP16 should be higher.

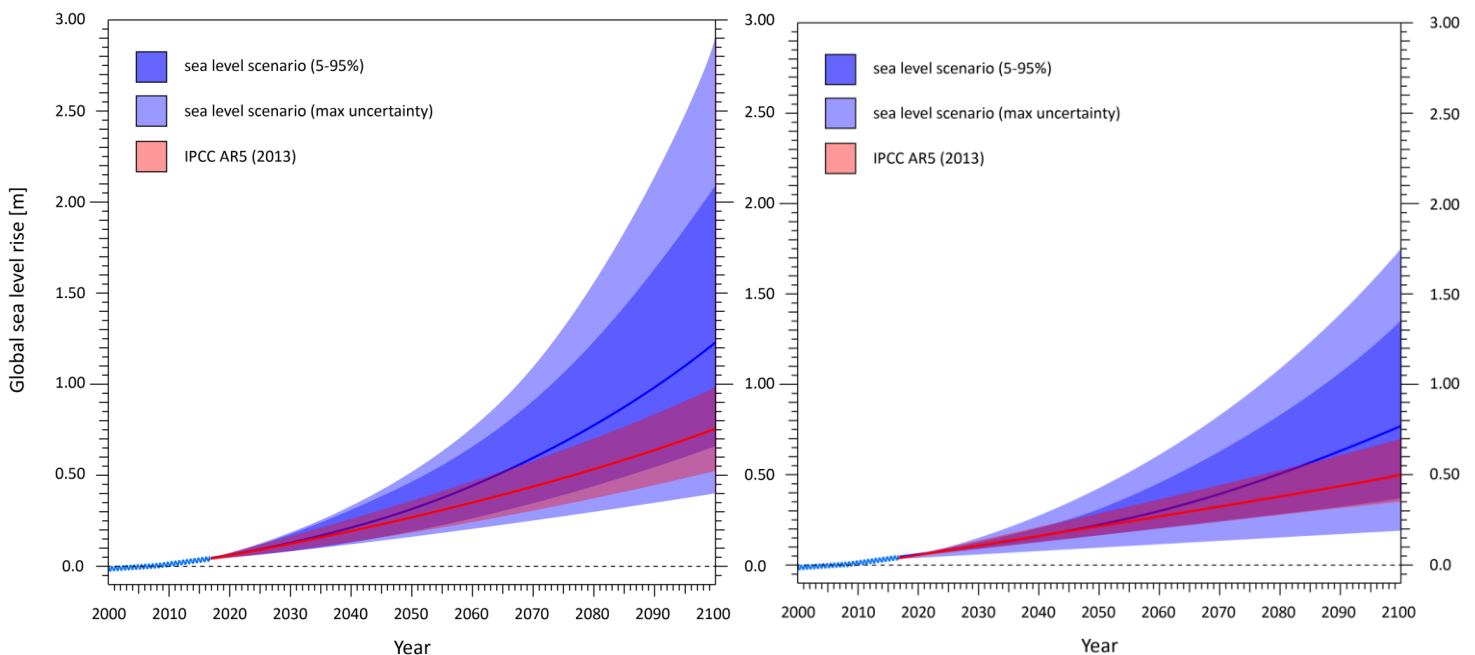


Figure 5.17: (blue) sea level rise scenario for RCP8.5 according to literature research, (red) sea level rise according to IPCC AR5.

Figure 5.18: (blue) sea level rise scenario for RCP4.5 according to literature research, (red) sea level rise according to IPCC AR5.

The blue line represents the expected mean sea level rise for RCP8.5 (Figure 5.17). It is predicted that the mean sea level rise deviates from the IPCC AR5 after the year 2045-2050 when large-scale ice sheet loss on Antarctica might start. High-end sea level rise is approximately 40-45 cm in 2050 compared to the year 2000. Kopp et al. (2017) examined a maximum rate of sea level rise of 18 mm per year in the year 2050 and more than 40 mm per year in the year 2100.

The sea level estimates for RCP4.5 are much lower (Figure 5.18). The high-end estimate is 25 cm sea level rise in the year 2050 with a rate of 8-10 mm per year. In 2100, the maximal rate of sea level rise is expected at 15-20 mm/yr. Kopp et al. (2017) estimated 10 mm per year in 2050 and 20 mm in the year 2100.

To conclude, it is impossible to say that it is 100% certain that future sea level rise will be within a particular threshold value. Nevertheless, it can be concluded that sea level rise projections are more uncertain than previously thought. It will be proposed to include sea level projections probabilistically instead of a fixed value for designing flood defences. More information about including probabilistic sea level rise into other sea level statistics is given in Section 5.7 and Chapter 6 “Hydraulic requirements”.

## 5.7 Regional sea level rise in the Netherlands

Sea level rise is a threat to coastal cities, infrastructure and ecosystems. Sea level rise is not uniform globally but is affected by various regional factors (Grindsted et al., 2015). All relevant regional factors that have an impact on regional sea level in the Netherlands are explained in Appendix B. The distinction should be made between temporary changes and long-term changes. Temporarily changes refer to weather conditions while long-term changes refer to climate change. Local average sea level change is affected by ocean circulation and by geographical variations in the temperature and salinity of the sea. These regional influences might change during global warming (Lowe et al., 2009). Another important distinction that should be made is relative sea level rise and absolute sea level rise. The vertical land motion of the land surface can enhance (or decrease) sea level change relative to the land. Absolute sea level rise does not include land surface changes and is measured with satellites.

### 5.7.1 Regional factors of sea level rise

Global sea level rise always has implications for regional sea level rise, but the extent of this rise can be very different among different areas. The degree of the difference between global and regional sea levels is determined by regional factors. Past and current variations in the distribution of land ice, for instance, affect the gravitational field of the Earth which causes regional fluctuations in the average sea level (Church et al., 2013). All regional factors that affect local sea level rise in the Netherlands are explained in Appendix B.

#### 5.7.1.1 Spatial fingerprint

Each contributor to sea level rise has a distinct spatial fingerprint. All masses on earth, gravitationally attract the oceans around them. Reduced mass due to ice sheet loss reduces this gravitational pull combined with an elastic rebound of the solid earth (Grindsted et al., 2015). Mass distribution does even have an effect on Earth's rotation (Milne & Mitrovica, 1998). Changing distributions of ice and water can shift the Earth's pole (the physical North and South Poles) and rate of rotation, which modifies the main gravitational response (Griggs et al., 2017). The loss of ice mass would have a strong effect on the regional sea level due to the gravitational and solid earth deformation effects (Gomez, 2015). The effects of earth's rotation are partly included in the fingerprint calculation but cannot be thoroughly examined in this research due to its complexity.

Water mass exchange between land and the ocean will be redistributed according to a geographical pattern (de Winter et al., 2017). This is the "*sea level fingerprint*". The sea level fingerprint shows the fraction of the global average SLR at a specific location on earth. The Antarctic fingerprint for the Netherlands is approximately 1.2 [-] which should be interpreted as having 1 m global sea level rise caused by only Antarctic melt will raise regional sea level in the Netherlands with 1.2 m (Hay, Morrow, Kopp, & Mitrovica, 2015). The sea level fingerprint in the Netherlands for the Greenland ice sheet (GrIS) melt is 0.2 [-]. A contribution of 40 cm to global sea level rise caused by the GrIS only will result in approximately 0.08 m sea level rise in the Netherlands.

#### 5.7.1.2 Relative sea level rise

A distinction should be made between absolute and relative sea level rise. GMSL rise is measured from altimetry data (satellites) which measures absolute sea level change. Relative sea level change is measured at a specific location by tide gauges which can be affected by geologic motion. Vertical land decline increases the amount of relative sea level rise. Vertical land movement combined with sea level rise leads to elevated risks of flooding and increases the upward flux of seepage consisting of brackish and nutrient groundwater (Hoogland, van den Akker, & Brus, 2012). Vertical land movement can be caused by both natural and anthropogenic factors. All factors that may contribute to vertical land movement in the Netherlands are explained in Appendix B.

The degree of contribution of the different factors to the vertical land movement differs widely across the country. The observed natural vertical land decline, without human influence, in the Netherlands is 0.2-1.5 mm/yr. The natural geological contributors are glacial isostatic adjustment (GIA), tectonic activity and deep layer auto-compaction (Kooi, Johnston, Lambeck, Smither, & Molendijk, 1998), (Hoogland et al., 2012). This number does not include anthropogenic factors such as gas/oil extraction, salt extraction, groundwater extraction and water drainage. Anthropogenic factors can increase vertical land movement in some areas by more than 1 m within a century, while other locations are not affected. All anthropogenic factors are explained in Appendix B.

The soil under flood defences decreases roughly 0-4 mm per year, depending on the location (STOWA, 2017). Important to note is that some flood defences are located in areas prone to subsidence because of gas/oil extraction.

There are some gas extraction points near the Maeslant Barrier (MLK), but these locations are expected to close in 2018-2020 (Hijma, Kooi, & Erkens, 2017). It is unclear if more gas fields will be explored in this area in the future which makes it impossible to provide accurate long-term projections. Therefore, the contribution of vertical land movement due to gas fields is estimated at  $2\pm 1$  cm at the MLK for the timespan 2000-2100. The total vertical land movement at the MLK is projected at  $6\pm 8$  cm (2000-2100), also including GIA effects ( $3\pm 2$  cm), tectonic activity ( $0\pm 5$  cm) and auto-compaction (1 cm) in that area. The OSK is located in an area with limited vertical land decline and is expected to decline with  $3\pm 6$  cm (2000-2100). This value includes GIA effects ( $2\pm 1$  cm), tectonic activity ( $0\pm 5$  cm) and auto-compaction (1 cm) in that area. Potential residual settlement due to the weight of the construction is not included but is expected to be relatively low. This is because both structures are constructed on reinforced (pre-loaded) subsoil. The effect of vertical land movement on the performance of the storm surge barriers is analyzed in Section 7.2.2.

### 5.7.1.3 Dynamic ocean response

Global warming can change ocean circulation patterns and other dynamic ocean-atmosphere responses. Freshwater fluxes originating from the melting ice sheet of Greenland have been shown to perturb the Atlantic meridional overturning circulation (MOC). As a result, most climate models project a decrease of the MOC between 0 and 50% for the next century (KNMI, 2017). The dynamic ocean response to freshwater forcing is very uncertain. (Church et al., 2013). These effects are not included in current sea level change models (Grindsted et al., 2015). One other prominent aspect of dynamic ocean responses is temperature change. The steric sea level expansion is different over the global ocean basins which are attributed to differential heating and salinity changes of various ocean layers (Yin, Griffies, & Stouffer, 2010). Yin et al. (2010) calculated that the dynamic response of steric effects in the Netherlands is similar to global mean. Climate change may also change wind patterns all over the world which are still very uncertain.

In the end, it is difficult to include all regional factors correctly into a climate-sea level model and project future regional sea level rise for the Netherlands. Several processes cannot be included in the models yet and there is a large uncertainty in the spread between the different factors in the model. Despite some limitations, some scientists computed sea level rise scenarios including regional factors applicable for the Netherlands (5.7.2).

## 5.7.2 Regional sea level rise scenarios for the Netherlands

In the Netherlands, sea level rises on average 1.9 mm per year, and the total sea level increase was 23 cm over the last 125 years (Rijksoverheid, 2016). This figure is obtained from six tide gauge stations. Global sea level rise over the last century (between 1901-2010) was roughly 19 cm (Church et al., 2013). Regional sea level rise in the Netherlands is slightly accelerated over the last decades because 1.2 mm per year is measured between 1951 and 1980 (KNMI, 2014). This was roughly similar to the global mean of  $1.2\pm 0.2$  mm per year between 1900 and 1990 (Yi et al., 2015). There is a broad consensus that climate change and global warming will result in further accelerated sea level rise. This is already measured globally (3.2 mm/yr) over recent years, but not to the same extent for the Netherlands (2 mm/yr) where this increase is still relatively linear (de Ronde, Baart, Katsman, & Vuijk, 2014), (Rijksoverheid, 2016).

Linear sea level rise is probably caused by the fact that the natural variations in the North Sea, associated with wind variations, are much larger than for the world average sea level (KNMI, 2014). Another reason might be that the sea level fingerprint for the Netherlands by ice sheet melt from Greenland (GrIS) is smaller than for the global average (Appendix B). The contribution of the GrIS to sea level rise in the North Sea is therefore relatively low compared to the global average. On the other hand, the sea level fingerprint is larger by melting ice originating from Antarctica, but this ice sheet does not yet melt at the same velocity as the GrIS.

Grindsted et al. (2015) computed (relative) regional sea level rise projections for the Netherlands. Their research included spatial fingerprints of land water and mass distribution. Furthermore, they modelled GIA effects and the dynamic ocean response in combination with the climate scenarios. Grindsted et al. (2015) used the same

data as the Fifth Assessment Report (AR5) of the IPCC for determining global sea level rise but with an increased uncertainty of the Antarctic ice sheet contribution. The P5-P95 range for the sea level contribution of only Antarctica is -7 to 94 cm while the mean is kept in line with the AR5. The results are shown in Table 5.12 for two coastal cities in the Netherlands.

Table 5.12: Sea level projections of Grindsted et al. (2015) for RCP8.5 for the year 2100.

Sea level Projections of (Grindsted et al., 2015) for RCP8.5 in 2100 [cm]	5%	17%	50%	83%	95%	99%
Global	45	58	80	120	183	-
The Hague	44	59	83	120	179	246
Den Helder	45	60	84	121	180	247

The results for regional sea level rise are similar to the global projection for RCP8.5. It is clear that Grindsted et al. (2015) did not use the latest information about the Antarctic contribution to sea level rise. The results of DP16 revealed an increase of Antarctic contribution from 4 cm to 106-114 cm for RCP8.5 in the year 2100 (Church et al., 2013), (DeConto & Pollard, 2016). The increasing contribution of Antarctica has a larger impact on the Netherlands than for the global average due to the sea level fingerprint.

Le Bars et al. (2017) computed (absolute) regional sea level rise for the Netherlands using the regionalisation method of de Vries et al. (2014). In contrast to Grindsted et al. (2015), these results showed absolute sea level rise and did not include GIA effects. The used fingerprint factors for the GrIS and AIS are 0.2 [-] and 1.1-1.2 [-] respectively. One important distinction compared to the results of Grindsted et al. (2015) is that the latter used a correlation according to AR5 (independent rapid ice sheet dynamics). Le Bars et al. computed this differently by making rapid ice sheet dynamics dependent on temperature (Section 5.5.1). The results for regional sea level rise according to Le Bars et al. (2017) are shown in Table 5.13.

Table 5.13: Absolute sea level projections of (Le Bars et al., 2017) for RCP4.5 and 8.5 for the year 2100 [cm].

Sea level Projections of (Le Bars et al., 2017) for year 2100 [cm] (global and regional)		P5	P10	P50	P90	P95
RCP4.5	Global	37	52	106	161	177
	The Netherlands	26	44	108	174	193
RCP8.5	Global	81	103	184	268	292
	The Netherlands	75	101	195	289	317

The results show that regional sea level in the Netherlands could be higher than the global average in the year 2100. This is only the case with the assumption that the Antarctic contribution is much greater than previously thought (DP16). It is also clear that significant sea level rise might be expected for both climate scenarios (RCP8.5 and RCP4.5) in 2100 for the Dutch coastal flood defences.

Table 5.14 (p. 60) shows the regional sea level rise in the Netherlands. These results are obtained by using factors of the regionalization approach which is constructed by de Vries et al. (2014) and Grindsted et al. (2015) combined with the results of Table 5.10. The bandwidth is slightly increased due to increased uncertainty of the regional factors. The Antarctic fingerprint for the Netherlands (1.1-1.2) is the dominant contributor to the increased regional sea level scenarios compared to the global sea level projections. The sea level fingerprint of Greenland is 0.2 [-] which has a reduced effect for regional sea level rise in the Netherlands. Nevertheless, this effect is relatively small. In total, the projections for the 95<sup>th</sup> percentile (P95) are slightly increased compared to the global projections which are provided in Table 5.10.

Several studies suggest that the probability function of sea level rise should be asymmetrically distributed towards higher high-end values (de Winter et al., 2017), (Grindsted et al., 2015), (Bamber & Aspinall, 2013). This implies that the probability distribution is asymmetric with a large high-end tail. In other words, the P95 of the probability distribution is further away from the mean (P50) than the P5. This is statistically viable because higher values are required to incorporate the increasing uncertainty of sea level rise.

Table 5.14: Regional (absolute) sea level rise projections for the Netherlands between the year 2000 and 2100 based on literature research.

Projected regional sea level rise [cm] by the year 2100	RCP4.5	RCP8.5	Average RCP4.5 & RCP8.5
Percentiles (P)			
P5	31	63	47
P17	52	87	70
P50	81	128	104
P83	114	175	144
P95	140	214	177
P99	168	258	213

The contribution of Antarctica to global sea level rise is expected to surpass other contributing factors, leading to a higher rate of regional sea level rise for the Netherlands than for the global average. The regional high-end (P95) sea level estimate is 7 cm higher than the global projection for RCP8.5 due to the considerable uncertainty in the Antarctic ice sheet dynamics. The mean (P50) regional sea level rise increases from 122 to 128 cm for RCP8.5. In total, 104 cm SLR is expected in the North Sea between 2000 and 2100. This projection is constructed for the expected emission scenario which is the average between RCP8.5 and RCP4.5 according to the analysis of Raftery et al. (2017). The projected sea level pathway for the three emission scenarios is shown in Figure 5.19. The observed rate of sea level rise in the Netherlands is currently behind global values, but it is predicted to change after 2050 when large-scale ice mass loss of Antarctica could begin.

It is proposed to include the full bandwidth of the sea level probability distribution to project the future hydraulic loads for flood defences. This implies that it is advised to use sea level rise scenarios probabilistically instead of one fixed high-end value to examine the risk of flooding more precisely. Sea level rise can be included into other sea level statistics with a likelihood of 1. Therefore, the mean (P50) sea level rise should be used in the assessment of the storm surge barriers including the analysis of the effects of high-end SLR (P95) to be sufficiently prepared in case of highly accelerated sea level rise. Currently, coastal flood defences are usually designed with a fixed level of sea level rise between 0.85 m and 1 m according to the high-end estimate of the KNMI'06 or '14 scenario. The proposed sea level rise scenario is higher than currently used in the designs and will result in increased hydraulic loads. The revised hydraulic loads are examined in Chapter 6 in more detail.

Finally, sea level rise will continue for centuries and will accelerate even further. This study focusses on the year 2100, but the effects beyond the year 2100 (2100-2500) would be increasingly important for adaptation plans in the future.

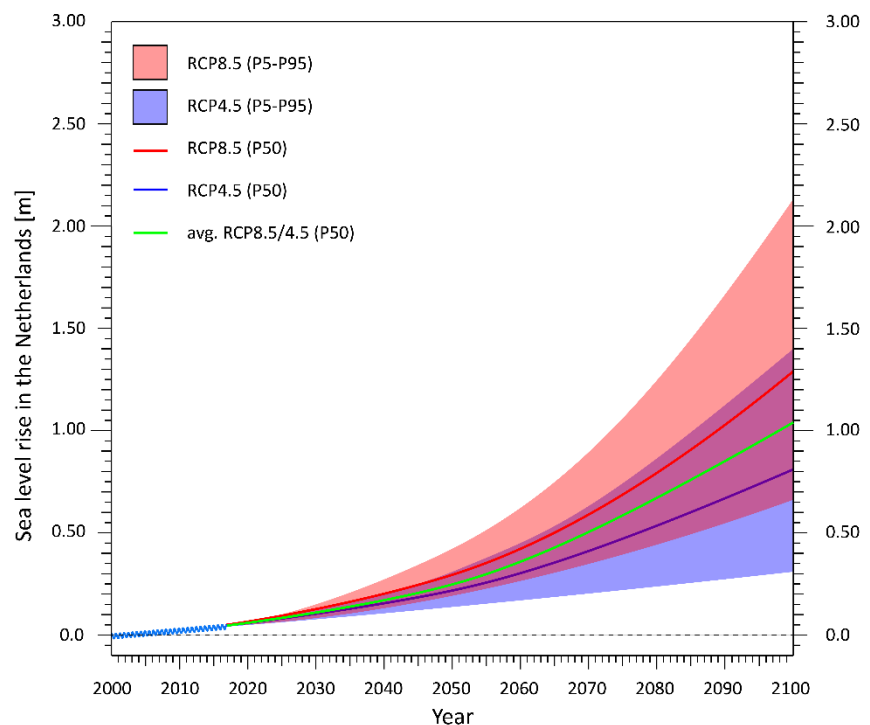


Figure 5.19: Absolute sea level projection for the Netherlands. Red: range of sea level rise for RCP8.5. Blue: range of sea level rise for RCP4.5. Green: likely sea level rise (P50).

# 6. Hydraulic requirements

Chapter 6 is predominately about the identification of relevant parameters that influence the hydraulic loads of the Maeslant Barrier (MLK) and the Eastern Scheldt Barrier (OSK). Chapter 5 concludes that uncertainty in Antarctic ice sheet dynamics dominates the uncertainty of sea level rise projections. The implication for regional sea level rise scenarios is that the range of possible sea level change trends for the long-term increases significantly. Increasing contribution from Antarctica to sea level rise might lead to even more regional sea level rise in the Netherlands than the global average due to gravitational effects. Particularly, the high-end estimate of regional sea level rise increases to a large extent. This is relevant for flood risk management because critical threshold values are exceeded more frequently during extreme events when sea level rise accelerates. The focus of Chapter 6 is on the new hydraulic loads according to new sea level rise scenarios applicable to the Netherlands which are described in Chapter 5. Other contributors such as wind changes, storm surges, precipitation and river discharge are not changed according to the KNMI'14. More research is required into other contributors to be able to examine significant changes.

Important to note, the focus of this chapter is on the hydraulic requirements for the MLK, OSK and the dykes in the hinterland which are part of the inherent water systems. These flood defences will be assessed partly according to WBI-2017 (Dutch: "Wettelijk Beoordelings Instrumentarium"). The hydraulic requirements refer to the required height of the flood defences in order to provide sufficient safety against accelerated sea level rise. The study does not contain a full probabilistic assessment including all relevant failure mechanisms. The MLK and OSK have unique characteristics and should be assessed individually and on expert judgement.

Wave overtopping is one of the three dominant failure mechanisms for the storm surge barriers and the dykes in the hinterland. This failure mechanism is included in this analysis. The stability of the storm surge barriers is described in less detail in Section 7.1.3. The assessment of macro-instability and piping of the dykes are beyond the scope of this research. For a complete assessment of the dykes in the Rhine-Meuse Delta and the Eastern Scheldt, it is recommended to perform a probabilistic assessment in Assessment Program RiskKeer.

## 6.1 Statutory Assessment instruments

This section describes the steps for a complete analysis of the storm surge barriers. The current assessment round of all flood defences is started in January 2017 and will last at least until 2023.

The Water Act prescribes that operators of primary flood defences should assess at least once every twelve years whether their flood defences meet the statutory safety requirements. The way in which this assessment must be carried out is laid down in a legal instrument. Flood defences will be assessed with the use of the statutory assessment tools (WBI). WBI-2017 contains the methods and rules that flood defence managers use to assess the primary flood defences in the assessment round. Rijkswaterstaat is updating this set of instruments for each round on behalf of the Ministry of Infrastructure and Water Management. This is done on the basis of new knowledge, insights from research and experiences with the previous instruments.

For the upcoming assessment round, which started in 2017, the update is changed more radically than during the previous editions. The reason for this change is the new safety standards that were introduced on 1 January 2017. This standard is based on a flood risk approach, which examines not only the probability of flooding but also the consequences. For information about this new flood safety policy can be found in Section 3.2.4. By 2050, all primary flood defences in the Netherlands should meet the new safety standards. The instruments for the upcoming assessment round, the WBI-2017, are entirely based on the new standards (Rijksoverheid, 2017).

## 6.1.1 Assessment process

The assessment process takes place in three phases: preparation, execution and reporting (Rijkswaterstaat, 2017c).

### 6.1.1.1. Preparation phase

The preparation phase is primarily for data management. A significant amount of data is required to assess flood defences. The change in the assessment of the probability of flooding instead of the exceedance probability means that the required data and information for the assessment will change significantly. The required information that is needed for the assessment is laid down in the statutory assessment instruments tools (WBI-2017). Uncertainties are explicitly included in the WBI-2017, and it is important that the information is used correctly and taken into account for the assessment.

### 6.1.1.2. Execution phase

In the execution phase, the dyke trajectory or hydraulic structure will be tested. The OSK and MLK are storm surge barriers with unique characteristics and should, therefore, be assessed in a customized model. The WBI software is fully probabilistic that there are multiple variables and outcomes in the model, each having degrees of certainty or uncertainty of its occurrence. The focus of this research is on the following Assessment Tracks (Dutch: "Toetssporen"):

- hydraulic structures: contribution to the failure of dykes in the hinterland;
- height and wave overtopping.

The variables that will be examined during the assessment of the storm surge barriers are extreme water levels, wave overtopping and reliability of the closing floodgates. Sea level rise scenarios cannot be probabilistically modelled yet within WBI-2017 and will include assumptions. Assessment of dykes can be done probabilistically for hydraulic loads and to determine the required crest height. Other aspects such as macro-stability, piping and dyke coverings can only be determined semi-probabilistically. The focus of this study is predominantly on the storm surge barriers and therefore only the required height of several dykes which are part of the inherent water system will be examined. The assessment in this study will, therefore, be a simplification of the required analysis because the revised WBI-2017 software is not complete.

### 6.1.1.3. Reporting

The operator of the flood defences is obligated to report the results of the assessment. The report should contain a description of the trajectory combined with the results of the assessment with the following supplements:

- the gained experiences with the assessment;
- the conducted management of the flood defences;
- a plan of action for improvements in the case of sections with a final score of 'unsatisfactory';
- a plan of action for the next assessment in case a judgment is not possible so that the next assessment can be awarded a final score (Rijkswaterstaat, 2017c).

It is required to make a plan of action in the case when both storm surge barriers are not according to the safety standards. The sea level rise scenarios are predominantly important in this analysis but are still very uncertain. Therefore, it is impossible to conclude with certainty whether the MLK and OSK will be rejected before the end of their predefined lifetime.

## 6.1.2. Hydra-NL

Hydra-NL is a probabilistic model which calculates the hydraulic loads (water level, wave conditions, wave overtopping) for a predefined exceedance probability. Hydra-NL can be used for the assessment of the primary dykes and hydraulic structures in the Netherlands. The results of this chapter are derived using Hydra-NL version 2.3.5 (August 2017). The model and used statistics are explained in more detail in Appendix I.

The following aspects will be calculated for several locations using Hydra-NL:

- High-water level (for each exceedance probability) [m NAP];
- wave height [m];
- hydraulic load level, as a measure of the required height of the structure [m NAP];
- the volume of water overrun and wave overtopping [m<sup>3</sup>/s].

In addition, Hydra-NL provides insight into exceedance probabilities for failure mode “wave overtopping” at given crest height, maximal rate of overtopping and dyke profile. Hydra-NL is consistent with WBI-2017, which means that the same data is used and that there are no more surcharges. These are integrated into the statistics and model uncertainty of the model.

Hydra-NL can perform calculations of the hydraulic loads for the dykes behind the MLK and OSK while incorporating the influence of these storm surge barriers in storm conditions. The MLK has a substantial effect on the temporary water basin behind the barrier during a closure. The influence of river discharge but also water leakage through the barrier and wave overtopping determine the water levels in the water system and the permissible time that the barrier should be closed. The risk of flooding increases if the barrier is closed for a more extended period because of the water level within the water system increases by blocking the water supply of the river. In the Eastern Scheldt, water levels are not only reliant on wind patterns and sea levels, but also on the storm surge barrier, storm duration and tidal phase. Furthermore, the maximum water levels are influenced by the closing regime and current reliability of the barrier (number of failing gates). Hydra-NL can calculate the hydraulic loads for above cases.

It is essential to understand the impact of SLR on the hydraulic loads for the barriers and the dykes in the hinterland. This study will compute these hydraulic loads to be able to conduct strategic advice on how to deal with accelerated sea level rise in the RMD and the Eastern Scheldt and the inherent storm surge barriers.

Within the framework of the WBI-2017, the statistics of the threats have been updated in Hydra-NL. Longer measurement series have been used for the wind speed and the wind direction, making the wind statistics more accurate. For the Eastern Scheldt, this means that the chance of high wind speeds from the northwest increases compared to the previous standards, while the probability of high wind speeds from the westerly to southwestern directions slightly decreases.

The threat to the dykes around the Eastern Scheldt and the RMD is formed by a high sea level and the wind (both wind speed and direction). For the RMD, also a modest sea level and high river discharge can be a threat to water safety.

The hydraulic loads are probabilistically determined at various locations by making production calculations. The model IMPLIC is used to compute the water level at a specific location in front of the flood defence based on the sea water level, and the waves are computed with the model SWAN.

Hydra-NL uses the WBI-2017 database for hydraulic loads. The prevailing level statistics in Hydra-NL were based on the year 1985. The model and water levels are updated to comply with the changing local environment and measured sea level rise. This model includes 8 cm sea level rise from the year 1985 to 2023 in the water level calculations. Most sea level rise scenarios are compared to the reference year 2000, including the new sea level scenarios of this study (Section 5.7.2). To avoid double counting for sea level rise between the year 2000 and 2023, 5 cm should be subtracted from the Hydra-NL calculations.

To conclude, the following aspects will be assessed using Hydra-NL:

- required height of storm surge barriers and dykes in the hinterland;
- wave overtopping and water overrun over the storm surge barriers and dykes for extreme situations;
- impact of the closing reliability of the storm surge barrier to the maximum water level in the hinterland.

The results are shown in Section 6.4 and analyzed in more detail in Chapter 7.

## 6.2. Hydraulic load factors

It is essential to determine the hydraulic loads, in terms of water levels and wave parameters such as height, period and direction to calculate the probability of flooding. The calculation of the hydraulic loads is done with Hydra-NL and by defining the most critical threats. Threats to flood defences might be the sea level, water level within the water system, wavers, river discharge and the failure rate storm surge barriers. Combinations of these threats usually increase the probability of flooding, depending on the degree of dependency. The required height can be calculated by combining the threats and their specific likelihood and translating these combinations to hydraulic loads on the flood defences.

Extreme sea level events arise during storms. This study computes the hydraulic loads for both the Maeslant Barrier and the Eastern Scheldt Barrier to be able to conclude whether these storm surge barriers meet the requirements in the long-term. Sea level extremes are composed of storm surge and tides. These aspects are briefly described in Appendix J. Sea level extremes are sea water levels that can be significantly higher than the average sea level but are relative. Flood defences in the Netherlands have been designed for extreme water levels and should, therefore, be resistant to storms that statistically occur once in the thousands of years. Hydra-NL (WBI software) contains climate data of the KNMI'14 report to compute the extreme sea level with a pre-defined likelihood of occurrence. However, the climate data does not describe long-term changes in wind, storm surge, tides, and waves due to climate change. Rising regional sea level could also influence storm surge, tides, and waves. Climate change may potentially lead to increasing wind speeds (hurricanes) which increase storm surge. Hydra-NL includes the climate statistics and uncertainty of all these aspects according to the KNMI'14 scenarios.

However, some studies indicate that climate change also results in more frequent storms including more storm surge and higher waves. This is an additional risk for water safety and should be implemented in future analysis. Therefore, it is recommended to perform more research on the effects of climate change on the Metocean statistics such as; wind, storm surge, tides, and geomorphological processes.

### 6.2.1. Sea level rise and sea level extremes

Before 2017, flood defences in the Netherlands are designed to resist certain threshold water levels with a predefined statistical yearly probability to occur. Sea level rise was incorporated by adding a fixed value to the threshold value based on the *high-end* estimate of the KNMI scenario '06 or '14 scenarios. This method results in extra safe flood defences; up to 20 times safer than required at that time.

Recent studies show that sea level rise might accelerate to a much larger extent than initially thought. The mean value of the new scenario that is proposed (Chapter 5) is higher than the old high-end value of KNMI'14. The sea level projections for the year 2100 compared to the year 2000 are shown in Table 6.1.

Table 6.1: Regional sea level scenarios for the Netherlands between the year 2000 and 2100. KNMI'06 presents SLR scenarios between 1990 and 2100. \* refers to P10 and P90.

SLR [m]	LANDT'18		IPCC AR5 (Global)		KNMI'06		KNMI'14	
RCP	RCP4.5	RCP8.5	RCP4.5	RCP8.5	G <i>RCP4.5</i>	W+ <i>RCP8.5</i>	G <i>RCP4.5</i>	W <i>RCP8.5</i>
Low (P5)	0.31	0.63	0.38	0.52	0.35*	0.40*	0.30	0.50
Mean (P50)	0.81	1.28	0.55	0.74	0.47	0.62	0.52	0.75
High (P95)	1.40	2.14	0.73	0.98	0.60*	0.85* 0.95	0.75	1.00

For determining the hydraulic loads, it is proposed to take the full bandwidth of the sea level probability distribution. This implies that it is advised to use sea level rise scenarios probabilistically instead of one fixed high-end value to examine the realistic flooding risk. Sea level rise will be included in other sea level statistics with a likelihood of 1. Current sea level rise scenarios were included with a fixed (high-end) value of 0.85-1 m for sea level rise according to the KNMI'06, or '14 scenario was used in the assessment. The likelihood of high-end sea level rise is just 5% which over-estimates the hydraulic requirements. Current WBI software is not intended yet to incorporate a probability distribution for sea level rise. It is required to include sea level rise

probabilistically to compute the hydraulic requirements accurately. The 50<sup>th</sup> percentile (P50) of the sea level rise probability distribution gives a general indication of the hydraulic requirements, but the spread of the distribution is essential to indicate the total uncertainty. It is not sufficient to only use the P50 because high-end SLR (P95) is also a possibility which can result in different more severe consequences of flooding. This implies that it is advised to compute the hydraulic loads for high-end sea level rise as well.

## 6.2.2. Water overrun and leakage

It is important to determine the effects of sea level rise on the storm surge barriers but especially for the dykes in the hinterland. The storm surge barriers reduce the water levels for backward dykes significantly. It is required to calculate overrun and overtopping of water over the barrier for the assessment of the required height of both the MLK and OSK. Overrun and leakage is acceptable due to the presence of a water storage basin. The basins behind both the MLK and the OSK have a certain amount of capacity left to store overtopping sea water and leakage through the barriers. In contrast to the Eastern Scheldt estuary, the Rhine-Meuse Delta (RMD) will also receive water from the main rivers in the Netherlands. The Waal, Meuse and Lek continuously increase the water level of the basin due to the closed barriers (MLK, Hartel Barrier and Haringvlietdam). All these effects will be included in the analysis.

## 6.3. Probabilistic model and test locations

The hydraulic loads of the MLK, OSK and the dykes behind both storm surge barriers will be calculated with the probabilistic model Hydra-NL. The results will be used to assess whether the storm surge barriers and dykes do comply with the new standards of the latest regulation change. The calculations will be carried out for Assessment Track (Dutch: “Toetsspoor”) “Height” which is part of the Legal Assessment 2017. Height is one of the three primary failure modes of dykes, and the effects of the MLK and OSK are very important in assessing the required height of the dykes in both estuaries.

The hydraulic loads will be assessed for both the MLK and OSK and for several dyke sections within the influence area of the storm surge barriers for several sea level rise scenarios. The advanced assessment (Dutch: “Geavanceerde Toets”), including sea level rise scenarios (Section 5.7.2), will be carried out with the Test Mode of Hydra-NL. Hydra-NL computes the following:

- water levels; sea water levels and water levels at different locations;
- waves; at sea and in the estuary;
- hydraulic load level; the required height of the storm surge barriers and dykes;
- wave overtopping and water overrun; the amount of overflowing water over the barriers and dykes.

The conditions above will be calculated for exceedance frequencies ranging from 1/10 per year to 1/100.000 per year. Before the regulations changes in the year 2017, most dykes behind the MLK and OSK were designed to withstand a certain water level that statistically occurs once in the 10,000 years and 4,000 years respectively. New regulations set the maximum allowable probability of flooding of a specific area ranging from 1/300 to 1/30,000 per year. Dykes can fail in several ways, including overtopping, stability and piping, which generally narrows the total the total acceptable probability.

The dyke rings are divided into dyke trajectories with specific boundary conditions depending on the probability and consequences of flooding. Therefore, each trajectory has a predefined maximum acceptable risk of flooding. The focus of this study is predominately on failure mechanism wave overtopping over the barrier and dykes to give an impression of the robustness of the flood defences in terms of height. The results give insight into the technical capabilities of both the storm surge barriers and the hydraulic loads of the dykes in the delta with various sea level rise scenarios.

Trajectories which do not meet the requirements should be strengthened. However, it is also possible that other trajectories meet the overtopping and overrun requirements, fail on mechanisms macro-stability or piping. Therefore, it is advised to perform an entirely probabilistic calculation that includes all relevant failure mechanisms to be able to give advice on the required reinforcements. It is important to note that results are based on a model, which have several limitations compared to real situations. For instance, the results only show

the maximum values, even if they can only occur for a few seconds. Dykes and flood defences can often withstand a higher water level for a very short period, but a lower load that occurs for a few hours may be decisive.

The maximum permissible yearly probability of flooding is 1/30,000 in Rotterdam which is protected by the MLK and 1/10,000 for some dykes behind the OSK. These requirements are generally stricter than according to the previous requirements. Some other dyke trajectories around the Eastern Scheldt should be less safe with an exceedance frequency of 1/300 per year instead of 1/4,000 per year. Therefore, it is expected that trajectories with stricter safety standards are disapproved in the assessment.

### 6.3.1. Test locations

The focus of this study is on water safety of the MLK, OSK and both estuaries in the hinterland which are protected by these storm surge barriers. After all, these both storm surge barriers have the function to protect the hinterland against high water levels from the sea, resulting in reduced hydraulic loads for the dykes in the temporarily closed estuary. The hydraulic loads will be computed at various locations divided over four areas:

- Maeslant Barrier
- Eastern Scheldt Barrier
- Rhine-Meuse Delta (influenced by MLK)
- Eastern Scheldt (influenced by OSK)

The test locations of the assessed flood defences are presented in Figure 6.1, 6.2 and Appendix K.

The test locations for the MLK and OSK are located on the seaward side to determine the hydraulic loads and effects of SLR for both storm surge barriers. Test locations MLK-2 and OSK-4 are used within this assessment and are shown in Appendix K.

In addition, the effects of SLR on the inherent water systems should be determined. Therefore, various dyke sections around the Rhine-Meuse Delta and the Eastern Scheldt are re-assessed against increased hydraulic loads and the changed safety standards.

Within the RMD, seven dyke sections are tested against the new sea level scenarios. The locations are labelled as RMD-1 to RMD-7 and are presented in Figure 6.1. The locations have been carefully chosen, based on flood risk and required safety standard, to make an impression of the total Rhine-Meuse Delta.

Twelve dyke sections will be assessed around the Eastern Scheldt to determine the effect of SLR on the storm surge barrier which affects water safety in the hinterland. Test locations OS-1 to OS-12, are distributed over the Eastern Scheldt and include most dyke sections (Figure 6.2).

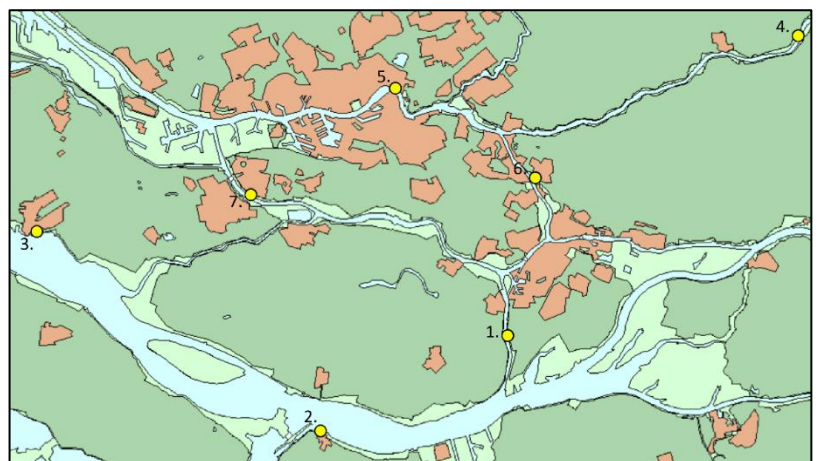


Figure 6.1: Test locations (RMD-1 to RMD-7) to determine hydraulic loads for several dyke sections in the Rhine-Meuse Delta (Hydra-NL).



Figure 6.2: Test locations (OS-1 to OS-12) to determine hydraulic loads for most dyke sections in estuary of the Eastern Scheldt (Hydra-NL).

### 6.3.1.1. Limit values and signalling values

As explained in Section 3.2.4.1 each dyke section should meet the requirements of a prescribed maximum yearly probability of flooding. This safety standard consists of a limit safety value and a signalling value. The signalling value is stricter than the required minimum safety (limit value) and is meant to warn the dyke operator that the flood defence structure probably will no longer meet the minimum required protection level in the foreseeable future. The limit values and signalling for all relevant flood defences are presented in Appendix K.

## 6.4. Hydraulic loads

This section explains the hydraulic loads on the MLK, OSK and the mentioned test locations in the hinterland. The results are obtained by using Hydra-NL and does not include vertical land movement. The used method and parameters of Hydra-NL are described in Appendix I. The calculated locations and exceedance frequencies are described in Appendix K.

### 6.4.1. Storm surge barriers

The storm surge barriers are of primary importance as the first line of defence for the dykes in the hinterland. The storm surge barriers should be assessed on the same safety standard as the heaviest norm for a dyke section in the hinterland. The MLK and OSK were initially designed for a water level which statically occurs 1/10,000 per year and 1/4.000 per year respectively (Rijkswaterstaat, 2007).

After the regulation change in 2017, the norm has been changed for both storm surge barriers. The MLK should be able to protect areas in Rotterdam with an average return period of 30,000 years ( $T=30,000$ ). As for the OSK, who should be able to prevent flooding of several areas in the hinterland with  $T=10,000$ .

This section describes the hydraulic loads on the MLK and OSK. Subsequently, the hydraulic loads for the dykes are calculated on the basis of the performance of the storm surge barriers. It is important to note that these results give input to the risk analysis in Chapter 7. The results are explained in more detail in this section.

#### 6.4.1.1. Extreme sea levels

Extreme sea levels occur in the North Sea often in combination with spring tide during north-western storms. Storm surge only appears in shallow waters that can increase local sea level by several meters. Sea level rise linearly increases the maximal water level according to the WBI software Hydra-NL. At the MLK, this increase in water level is not entirely linear with sea level rise, due to the changing conditions for seiches. The influence of seiches on the maximum water level decreases with increasing water depth. It should be noted that the extreme sea level in front of the MLK is at least 50 cm higher compared to the sea level at Hoek van Holland due to extra storm surge and water impoundment because of the closed barrier. At the OSK, the maximum water level increases linearly with sea level rise because seiches are not expected to occur. The effects of sea level rise on storm surge and the tidal wave are expected to be small (KNMI, 2014). Chapter 5 and Appendix J describe all uncertainties around sea level rise and temporarily extreme sea levels.

The effects of sea level rise increase the hydraulic loads for both storm surge barriers significantly. Water levels are computed at different locations near the MLK and OSK to specifically examine the hydraulic loads which are spatially different due to bathymetry and geological differences. The water levels for the storm surge barriers for an exceedance frequency of 1/10,000 per year are given in Table 6.2.

Table 6.2: Extreme sea levels for MLK and OSK calculated by Hydra-NL using the sea level projections of Section 5.7.

Extreme sea level ( $T=10,000$ )		
Sea level rise scenario <i>Reference period 2000</i>	MLK [NAP]	OSK [NAP]
0.05 m	+5.70 m	+5.44 m
0.81 m <i>RCP4.5 (P50)</i>	+6.36 m	+6.20 m
1.28 m <i>RCP8.5 (P50)</i>	+6.79 m	+6.67 m
1.40 m <i>RCP4.5 (P95)</i>	+6.90 m	+6.75 m
2.14 m <i>RCP8.5 (P95)</i>	+7.62 m	+7.53 m

Despite the higher tidal amplitude at the OSK, the maximal sea water levels are lower than at the MLK. The consequences of the hydraulic loads for the storm surge barriers are described below.

### 6.4.1.2. Maeslant Storm Surge Barrier

The hydraulic loads with various SLR scenarios are calculated for the MLK using Hydra-NL. The used test locations applicable for MLK are visualized in Figure 6.3 and Appendix K. Several locations have been calculated to analyze the development of water levels and waves accurately and to be able to record deviations from the results. For instance, the hydraulic loads at location MLK-1 are significantly higher than at the other locations for relative short return periods (10-1,000 years). It is assumed that the results for these return periods on location 1 are not accurate and are left out the analysis.

As a reference, points MLK-2,3 and 4 show the progression of water levels and waves at sea and in the port of Rotterdam. The water level increases significantly in the port of Rotterdam due to extra storm surge, seiches and the sea water impoundment caused by the closed floodgates. The difference in sea level at sea and in front of the MLK can be 50 cm.

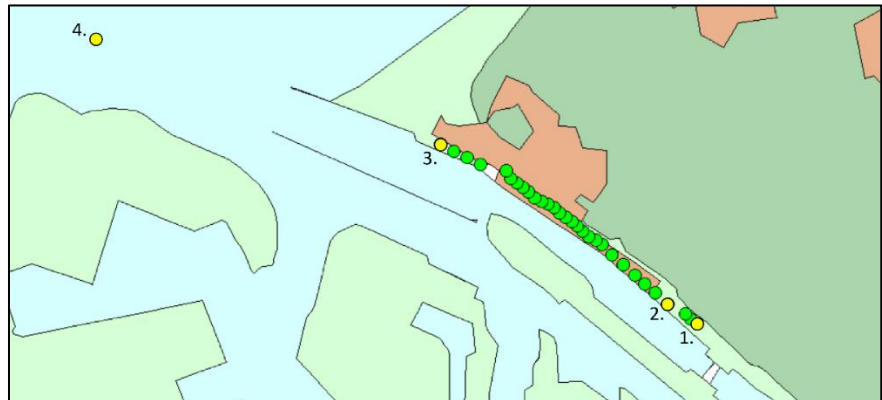


Figure 6.3: Test locations (MLK-1 to MLK-4) to determine hydraulic loads for the MLK (Hydra-NL).

The hydraulic loads are referred to a required height of the barrier to be able to constrain water overrun by a certain amount. The MLK is a hydraulic structure designed to survive significant water overflow during extremely high-water events. Water overflow is considered as the sum of the volume of wave overtopping and water overrun. There is no explicit precondition for the maximum volume of wave overtopping and water overrun for the MLK, but this depends on the strength and stability of the structure and also on the storage capacity in the Rhine-Meuse Delta (RMD) behind the storm surge barrier. However, the maximal allowable difference between the sea level and the water level on the landward side is relatively limited. A large quantity of water overflow increases the load on the barrier significantly. As a consequence, the water level at the inside should also be increased to reduce to forces on the barrier. This calculation assumes a strong barrier that is able to close under all conditions and continues to fulfil function the function of reducing inland water levels. The analysis of the strength of the MLK is discussed in Section 7.1.3.1. The focus of this chapter is only on the hydraulic loads and the required height of the barrier.

The degree of wave overtopping and overrun is calculated by combining extreme water levels and waves in a probabilistic way and then calculating a theoretical return period. The water levels for  $T=10,000$  and  $T=30,000$  are the most interesting due to the safety requirements and the regulation changes. The MLK closes together with the HK to prevent a large area composed of rivers and lakes from exceeding threshold water levels. The failure rate of the MLK is set on 1/100 for each closure. This failure rate substantially influences the hydraulic loads for the dykes in the hinterland which is discussed in Section 7.1.5.1.

The hydraulic loads are given for the MLK for various exceedance frequencies in Table 6.3 (p. 69). The results are calculated at location MLK-2. Table 6.3 shows the sea water level, overflow, wave height and the required height of the MLK to limit overflow to 1,000 l/s/m for different return periods varying from 10 years to 30,000 years. In addition, the results are shown for different sea level rise scenarios. These scenarios are determined in Chapter 5. Sea level rise generally increases the loads for the MLK. As a reference, also the 3 m sea level rise scenario is included, which is the upper limit in the confidence interval of the sea level scenarios. Important to note, is that the base scenario with 0 m sea level rise is applicable for the year 2000. This implies that all scenarios include 5 cm sea level rise between the year 2000 and 2023.

Table 6.3: Hydraulic loads MLK. Red: Wave overtopping >2,000 l/s/m. Values above 2,000 l/s/m are calculated using formula [6] in Appendix M. Orange: Wave overtopping >1,000 l/s/m.

Maeslant Barrier								
Test location	MLK-2 (crest height: +5.0 m NAP)							
Sea level scenario (2100)	Exceedance frequency per year	1/10	1/100	1/300	1/1,000	1/3,000	1/10,000	1/30,000
<b>0.05 m</b> (Year 2023) Mean value	Sea level [m NAP]	3.87	4.44	4.65	4.95	5.30	5.70	6.07
	Required height [m NAP] (Hydraulic load level 1000 l/s/m)	3.23	3.79	4.02	4.34	4.72	5.17	5.59
	Overflow [m <sup>3</sup> /s/m]	<0.001	<0.001	0.019	0.062	0.478	1,344	≈2.73
	Wave height [m]	0.55	0.80	0.90	1.01	1.11	1.22	1.34
<b>0.81 m</b> RCP4.5 Mean value (P50)	Sea level [m NAP]	4.50	4.99	5.30	5.66	5.98	6.36	6.74
	Hydraulic load level 1000 l/s/m [m NAP]	3.86	4.37	4.71	5.11	5.47	5.89	6.33
	Overflow [m <sup>3</sup> /s/m]	<0.001	0.069	0.455	1.225	≈2.36	≈3.62	≈5.05
<b>1.28 m</b> RCP8.5 Mean value (P50)	Sea level [m NAP]	4.83	5.43	5.73	6.07	6.39	6.79	7.20
	Hydraulic load level 1000 l/s/m [m NAP]	4.20	4.84	5.18	5.55	5.91	6.36	6.83
	Overflow [m <sup>3</sup> /s/m]	0.003	0.680	1.377	≈2.58	≈3.66	≈5.19	≈6.92
<b>1.40 m</b> RCP4.5 High-end (P95)	Sea level [m NAP]	4.94	5.54	5.84	6.17	6.49	6.90	7.32
	Hydraulic load level 1000 l/s/m [m NAP]	4.30	4.96	5.29	5.66	6.03	6.49	6.95
	Overflow [m <sup>3</sup> /s/m]	0.026	0.901	1.650	≈2.89	≈4.02	≈5.62	≈7.45
<b>2.14 m</b> RCP8.5 High-end (P95)	Sea level [m NAP]	5.63	6.19	6.48	6.84	7.20	7.62	8.04
	Hydraulic load level 1000 l/s/m [m NAP]	5.04	5.65	5.98	6.38	6.78	7.26	7.73
	Overflow [m <sup>3</sup> /s/m]	1.059	≈2.85	≈3.88	≈5.28	≈6.81	≈8.76	≈10.88
<b>3.05 m</b> RCP8.5 High-end	Sea level [m NAP]	6.41	7.02	7.35	7.72	8.09	8.51	8.93
	Hydraulic load level 1000 l/s/m [m NAP]	5.86	6.53	6.89	7.31	7.72	8.20	8.68

The height of a fully closed MLK is +5.00 m NAP which corresponds to a water level in the Rotterdam Waterway (NWW) that occurs on average once in every 1000 years. The MLK is designed to reduce maximal water levels in Rotterdam and Dordrecht. The yearly probability of flooding of dyke-ring 14, which inhabits 4 million people, is recently set on 1/30,000. Old regulations correspond to a water level with an annual exceedance probability of 1/10,000.

The flood of 1953 resulted in a sea level of +3.85 m NAP at Hoek van Holland, which was the highest recorded water level. According to the program Hydra-NL, that storm had a return period of 50 years. In front of a closed storm surge barrier, a similar storm might have reached a level of +4.31 m NAP due to 15 cm sea level rise between the year 1953 and 2023 and additional storm surge over the watercourse. Also, a potential seiche has a substantial contribution.

A storm event with an average return period of 30,000 years can cause a sea level of +6.07 m NAP which results in enormous water overrun, corresponding to an overflow of more than 2,000 l/s/m. This value combines overrun and wave overtopping. Further research will have to show whether the barrier can withstand such loads, especially in terms of stability and strength. This is analyzed in the risk analysis (Section 7.1.3.1). Waves are relatively small at the MLK because the sea waves are weakened due to reflection on the quays. The maximal wave height is 1.34 m during the extreme storm event.

Approximately 70 cm water overrun resulting in a rate of overtopping of 1,344 litres per second per meter is expected to flow over the arc-shaped floodgates for T=10,000. The barrier should be able to withstand such a

quantity of water overflow and should provide sufficient protection to the hinterland. Still, 62 l/s/m of wave overtopping is expected at a water level of +4.95 m NAP (T=1,000).

The calculated sea level can vary significantly over small distances. It seems that the effects of seiches can be significant. Table 6.4 features the effect of seiches on the sea level during high-water event for different return periods. According to the figures, seiches can increase the sea level by 21 to 34 cm.

Table 6.4: Seiche effect on the peak sea level in front of the MLK for various situations.

Maeslant Barrier								
Test location	MLK-2 (crest height: +5.0 m NAP)							
Sea level scenario (2100)	Exceedance frequency per year	1/10	1/100	1/300	1/1,000	1/3,000	1/10,000	1/30,000
<b>0.05 m</b> <i>(Year 2023)</i>	Sea level excl. seiches [m NAP]	3.64	4.13	4.32	4.61	4.97	5.38	5.79
	Mean value	Seiche effect [m]	0.24	0.31	0.33	0.34	0.33	0.32
<b>0.81 m</b> <i>RCP4.5</i>	Sea level excl. seiches [m NAP]	4.18	4.65	4.97	5.34	5.69	6.12	6.53
	Mean value (P50)	Seiche effect [m]	0.32	0.34	0.34	0.32	0.29	0.24
<b>1.28 m</b> <i>RCP8.5</i>	Sea level excl. seiches [m NAP]	4.49	5.10	5.42	5.79	6.15	6.57	6.99
	Mean value (P50)	Seiche effect [m]	0.34	0.33	0.32	0.28	0.24	0.22
<b>1.40 m</b> <i>RCP4.5</i> <i>High-end (P95)</i>	Sea level excl. seiches [m NAP]	4.59	5.21	5.53	5.90	6.27	6.69	7.10
	High-end (P95)	Seiche effect [m]	0.34	0.33	0.31	0.27	0.23	0.22
<b>2.14 m</b> <i>RCP8.5</i> <i>High-end (P95)</i>	Sea level excl. seiches [m NAP]	5.30	5.92	6.25	6.62	6.98	7.41	7.83
	High-end (P95)	Seiche effect [m]	0.33	0.26	0.23	0.22	0.21	0.22
<b>3.05 m</b> <i>RCP8.5</i>	Sea level excl. seiches [m NAP]	6.18	6.81	7.13	7.51	7.87	8.30	8.71
	RCP8.5	Seiche effect [m]	0.23	0.21	0.21	0.21	0.22	0.22

As a reference, MLK-4 (at sea) indicates that the water levels are 60 cm lower at sea. At this location, a sea level of +5.04 m NAP will be reached for T=10,000. Sea level rise significantly increases the hydraulic loads for the MLK. The expected average sea level rise 0.81 m to 1.28 m for RCP4.5 and RCP8.5 respectively at the end of this century. Also, the degree of uncertainty is large and more than 2 m sea level rise in 2100 cannot be ruled out.

For 0.81 m sea level rise, the maximum water level of +5 m NAP that can be withstood by the floodgates is expected to occur once in the 100 years. For 1.28 m sea level rise, the crest height of the barrier can be reached every 20 years. This analysis indicates that the MLK must be able to withstand large amounts of water overrun and overtopping to reach the end of its intended lifetime, considering accelerated sea level rise. The other effects of SLR on the barrier are analyzed in Chapter 7.

### 6.4.1.3. Eastern Scheldt Storm Surge Barrier

The OSK consists of three sections with floodgates and a part with sea dykes. The focus of this study is only on the concrete structures and the floodgates because of its complexity and constraints to be reinforced. Section Roompot (location OSK-4) has the heaviest hydraulic loads which are presented in Table 6.5.

The OSK is designed to withstand a certain water level that statistically occurs once in the 4000 years. After the regulation change in 2017, this changed to a maximal probability of flooding of 1/10,000 per year. It is expected that overrun and overtopping over the storm surge barrier is the determining factor for the OSK.

The results show that a sea level +5.18 m NAP can occur for a yearly exceedance probability of 1/4,000 around the year 2023. At this year, only 5 cm of SLR is included in the probabilistic model. The storm surge barrier has a crest height of +5.8 m NAP at this section, which implies that water overrun does not occur. However, waves with a height of 3.86 m cause a significant amount of overtopping of 1,251 l/s/m.

The expected rate of wave overtopping is similar for location Hammen (OSK-2) and Schaar (OSK-3), referring to an overtopping of 1,229 and 996 l/s/m respectively.

For T=10,000, water levels are 26 cm higher for all sea level rise scenarios compared to T=4,000. Without sea level rise, overtopping increases to 1,692 l/s/m at Roompot, 1,611 l/s/m at Hammen and 1,372 l/s/m at Schaar. Sea level rise significantly increases overrun and overtopping above 2,000 l/s/m which should be calculated by using Formula [6] in Appendix M.

Further analyzes are needed to prove how much water overflow and leakage is acceptable to limit the effect to the dykes around the Eastern Scheldt. It should be clear that the hydraulic loads for these dykes are increased with an additional increase in the water level in the Eastern Scheldt.

Table 6.5: Hydraulic loads OSK Roompot OSK-4. Values above 2,000 l/s/m are calculated using formula [6] in Appendix M \*: hydraulic loads with small assumption.

Eastern Scheldt Barrier								
Test location	OSK-4 Roompot (crest height: +5.8 m NAP)							
Sea level scenario (2100)	Exceedance frequency per year	1/10	1/300	1/1,000	1/3,000	1/4,000	1/10,000	1/30,000
<b>0.05 m</b> (Year 2023) Mean value	Sea level [m NAP]	3.60	4.48	4.80	5.10	5.18	5.44	5.77
	Hydraulic load level 1000 l/s/m [m NAP]	3.86	5.14	5.63	6.08	6.20	6.60	7.09
	Overflow [m <sup>3</sup> /s/m]	0.08	0.484	0.770	1.134	1.251	1.692	≈3.63
	Wave height [m]	2.63	3.32	3.57	3.81	3.86	4.06	4.30
<b>0.81 m</b> RCP4.5 Mean value (P50)	Sea level [m NAP]	4.36	5.24	5.59	5.86	5.94	6.20	6.53
	Hydraulic load level 1000 l/s/m [m NAP]	4.73	6.03	6.53	6.99	7.12	7.52	8.03
	Overflow [m <sup>3</sup> /s/m]	0.262	1.084	1.637	≈3.30	≈3.44	≈4.07	≈5.09
<b>1.28 m</b> RCP8.5 Mean value (P50)	Sea level [m NAP]	4.83	5.71	6.03	6.33	6.41	6.67	7.00
	Hydraulic load level 1000 l/s/m [m NAP]	5.27	6.59	7.09	7.56	7.69	8.10	8.61
	Overflow [m <sup>3</sup> /s/m]	0.475	1.743	≈3.35	≈4.16	≈4.41	≈5.31	≈6.57
<b>1.40 m</b> RCP4.5 High-end (P95)	Sea level [m NAP]	4.95	5.78	6.10	6.41	6.53	6.75	7.08
	Hydraulic load level 1000 l/s/m [m NAP]	5.41	6.73	7.23	7.71	7.83	8.25	8.76
	Overflow [m <sup>3</sup> /s/m]	0.548	1.956	≈3.48	≈4.37	≈4.72	≈5.56	≈6.88
<b>2.14 m</b> RCP8.5 High-end (P95)	Sea level [m NAP]	5.69	6.57	6.89	7.19	7.27	7.53	7.86
	Hydraulic load level * 1000 l/s/m [m NAP]	6.25	7.60	8.11	8.59	8.73	9.15	9.67
	Overflow [m <sup>3</sup> /s/m] SLR = 2 m	1.216	≈4.36	≈5.55	≈6.80	≈7.15	≈8.36	≈9.99

## 6.4.2. Water levels in the Rhine-Meuse Delta and Eastern Scheldt

The storm surge barriers are the first line of defence for the dykes in the hinterland. This section describes the hydraulic loads on the dykes which are located at the landward side of the storm surge barriers. The MLK and OSK largely determine the water levels in the Rhine-Meuse Delta and the Eastern Scheldt. Important to note that these results give input for the risk analysis in Chapter 7. The results are explained in more detail in this section.

### 6.4.2.1. Rhine-Meuse Delta

The MLK together with the HK has the function to reduce the water level for hundreds of kilometres of dykes in the RMD during extreme storm events. The consequences of SLR and the closing frequency of the storm surge barriers have been analyzed for seven dyke-sections which are located within the Rhine-Meuse Delta. The locations and corresponding required safety standards are explained in Appendix K.

The river discharge slowly increases the water level during a storm closure. Usually, river-dykes are constructed with a maximally acceptable volume of wave overtopping of 0.1 or 1 l/s/m. Otherwise, the soil and body of the dyke might become saturated which reduces the stability and water-retaining capability.

The hydraulic loads are computed for all seven locations (RDM-1 until RDM-7) including five sea level scenarios. The required safety standard for the dyke section varies from T=300 in Willemstad (RDM-2) to T=30,000 in Rotterdam (RDM-5). The results are shown in Table 6.6 for the predefined safety standard.

Crest heights of the dykes are between +3.76 m NAP in Alblasterdam and +5.79 m NAP in Schoonhoven. The required dyke height is determined on the basis of a maximal 1 l/s/m overtopping. Important to note is that the results are determined for the condition of a maintained closing regime of the storm surge barriers. This implies that the barriers close if the forecasted water level exceeds +3.00 m NAP in Rotterdam or +2.90 m NAP in Dordrecht. Sea level rise results in more frequent closures but according to Hydra-NL, the hydraulic loads do not increase significantly. The maximum water levels in the delta increase on average by a fraction of 35% compared to sea level rise. However, the maximum water levels at RMD-5 (Rotterdam) increase by a fraction of 70%.

The observed increased hydraulic loads for the different sea level rise scenarios for the dykes is caused by increased flood risk due to more frequent high-water levels. In addition, increasing water overrun, wave overtopping and leakage of both the MLK and HK will slightly raise the maximum water level in the RMD. The results are only realistic during optimal operation of the storm surge barriers. These barriers must, therefore, be robust enough to be operational at all cost, also with the significant increase in sea level rise. The complete analysis of the effects of SLR on the MLK and hinterland is performed in Chapter 7.

Table 6.6: Water levels and hydraulic loads for locations RMD-1 till RMD-7 for different sea level scenarios. Red: wave overtopping >5 l/s/m. Orange: wave overtopping >1 l/s/m. \*: dyke profile with a small deviation in geometry.

Rhine-Meuse Delta								
Sea level scenario (2100)	Test location	RMD-1	RMD-2	RMD-3	RMD-4	RMD-5	RMD-6	RMD-7
	Standard (WBI-2017)	1/1,000	1/300	1/300	1/10,000	1/30,000	1/10,000	1/1,000
	Crest height [m NAP]	4.7	3.8	4.35	5.79	5.23	3.76	5.53
	Geometry	*	*	*	*		*	*
<b>0.05 m</b> (Year 2023) Mean value	Water level [m NAP]	3.02	2.86	2.74	5.16	3.93	2.20	3.31
	Hydraulic load level (1 l/s/m) [m NAP]	3.31	3.01	3.26	5.68	7.36	2.70	3.94
	Overflow [l/s/m]	<0.1	<0.1	<0.1	0.25	8.22	<0.1	<0.1
	Wave height [m]	0.94	0.82	1.17	1.07	1.962	1.05	1.01
<b>0.81 m</b> RCP4.5 Mean value (P50)	Water level [m NAP]	3.26	3.08	2.97	5.32	4.46	3.57	3.54
	Hydraulic load level (1 l/s/m) [m NAP]	3.51	3.20	3.51	5.82	7.451	4.14	4.19
	Overflow [l/s/m]	<0.1	<0.1	<0.1	0.59	19.202	14.60	<0.1
<b>1.28 m</b> RCP8.5 Mean value (P50)	Water level [m NAP]	3.41	3.22	3.10	5.42	4.81	3.95	3.73
	Hydraulic load level (1 l/s/m) [m NAP]	3.68	3.33	3.64	5.91	7.55	4.58	4.34
	Overflow [l/s/m]	<0.1	<0.1	<0.1	1.17	56.46	153.33	<0.1
<b>1.40 m</b> RCP4.5 High-end (P95)	Water level [m NAP]	3.46	3.26	3.15	5.45	4.90	4.03	3.80
	Hydraulic load level (1 l/s/m) [m NAP]	3.73	3.37	3.68	5.94	7.594	4.67	4.40
	Overflow [l/s/m]	<0.1	<0.1	<0.1	1.47	75.56	203.63	<0.1
<b>2.14 m</b> RCP8.5 High-end (P95)	Water level [m NAP]	3.81	3.56	3.46	5.67	5.46	4.46	4.32
	Hydraulic load level (1 l/s/m) [m NAP]	4.09	3.69	3.93	6.16	8.13	5.13	4.92
	Overflow [l/s/m]	<0.1	<0.1	<0.1	8.66	433.37	674.00	0.1
<b>3.05 m</b> RCP8.5	Water level [m NAP]	4.25	4.02	3.92	6.00	5.90	4.99	4.95
	Overflow [l/s/m]	<0.1	25.64	0.33	167.87	1668.21	>2000	<0.1

The assessed dyke sections, except for Rotterdam, meet the requirement of a maximum wave overtopping of 1 l/s/m for the year 2023. The maximal water level at location Rotterdam is +3.93 m NAP. The dyke height is +5.23 m NAP, but the waves result in an overtopping of 8 l/s/m. This is higher than the requirement of 1 l/s/m, but this specific dyke located in the urban area is not a typical dyke covered in grass. This particular dyke is a multifunctional dyke with a road composed of asphalt which should withstand a higher value of wave overtopping. However, the previous critical water level (MHW) of +3.60 m NAP is exceeded in that situation. It is

not certain what the new critical water level will be after the assessment according to WBI-2017. Critical water levels are discussed in more detail in Section 7.1.2.1. Still, a chance exists that RMD-5 should be strengthened to the safety standard of  $T=30,000$  because of the increased maximal water level relative to the previous MHW. It should be noted that the results probably underestimate the water level at Alblasterdam (RMD-6) due to the presence of a foreland. As a result, water levels below 3 m NAP are not calculated correctly for this specific dyke section. The actual water level for  $T=10,000$  should be around +3.0 m NAP.

At 0.81 m sea level rise, also the dyke (RMD-6) in Alblasterdam fails to the requirement of wave overtopping. This dyke is relatively low and should be heightened to reduce wave overtopping. For more sea level rise, also water overrun might occur at this location which significantly increases the rate of overflow. The change of the safety standard from  $T=4,000$  to  $T=10,000$  also has a substantial contribution to the increased hydraulic loads.

More issues arise at 1.28 m SLR, where the dykes in Rotterdam, Alblasterdam and the river dykes around the Lek will not meet the requirements. An amount of wave overtopping of 1.2 l/s/m at the Lek-dyke might not be acceptable. The primary failure mechanisms of river dykes such as piping and water overrun should be prevented at all cost. Furthermore, this dyke prevents a large economically valuable area from flooding. At Rotterdam, the maximal water level increases to +4.81 m NAP which is significantly higher than the previous MHW of +3.60 m NAP. In that case, all other dykes, except RMD-7, will fail due to overtopping. However, this is generally accepted because the minimal safety standard for these locations is significantly lower compared to the required safety standard of dykes in Rotterdam.

In summary, it is clear that the effects of SLR are transferred for 30-40% to the hinterland if the storm surge barriers continue to function as planned. This implies that the effectivity of the storm surge barrier might increase by accelerated sea level rise. However, Hydra-NL is prone to limitations who underestimate the hydraulic loads for dykes in the hinterland which is discussed in Appendix I.

#### **6.4.2.2. Eastern Scheldt**

The Eastern Scheldt Barrier (OSK) has the function to reduce the hydraulic loads for dykes in the Eastern Scheldt estuary during extreme storms events. The OSK should meet the enhanced safety standard of  $T=10,000$  after the regulation change.

This section explains the hydraulic loads for the dykes around the Eastern Scheldt, with the condition that the OSK meets the requirements and continues to function in accordance with the predefined safety standards and protocols. Another assumption is that the barrier remains intact under the most extreme storm conditions in combination with SLR. This implies that the OSK will be closed in advance if the forecasted water level in the Eastern Scheldt exceeds +3.00 m NAP. The aim is to achieve a water level of +1 m NAP on the Eastern Scheldt during a closure. However, the probabilistic model also includes the effects of an emergency closure of the OSK. An emergency closure is automatically activated when the measured sea level at the OSK exceeds +3.00 m NAP. In addition, leakage and wave overtopping of the OSK and other effects such as storm surge results in spatially different water levels in the Eastern Scheldt, are included in the model.

In reality, it appears that the barrier will usually close at the aimed water level of +1 m NAP, in order to reduce loads of the dykes around the Eastern Scheldt. This closing procedure will usually ensure that the actual load may be significantly lower than calculated according to the model. More information about the closing regime can be found in Section 7.1.4. The consequences of sea level rise (SLR) and changing safety standard are analyzed for twelve dyke sections located in the Eastern Scheldt. The test locations (OS-1 to OS-12) and corresponding limit values are explained in Appendix K. The results are revealed in Table 6.7. The table includes water levels, wave heights, overtopping and required dyke height for each location and multiple SLR scenarios.

Table 6.7: Water levels and hydraulic loads for locations OS-1 till OS-12 for different sea level scenarios. Red: wave overtopping >5 l/s/m. Orange: wave overtopping >1 l/s/m. \*: dyke profile with a small deviation (conservative geometry).

Eastern Scheldt Estuary													
Sea level scenario (2100)	Test location	OS-1	OS-2	OS-3	OS-4	OS-5	OS-6	OS-7	OS-8	OS-9	OS-10	OS-11	OS-12
	Standard (WBI-2017)	1/300	1/300	1/3,000	1/10,000	1/10,000	1/10,000	1/10,000	1/3,000	1/10,000	1/3,000	1/3,000	1/1,000
	Crest height [m NAP]	7.00	6.60	7.10	6.00	6.40	6.40	6.60	6.30	6.60	6.09	7.25	6.77
	Geometry	*	*	*	*			*	*	*			
<b>0.05 m</b>  <i>(Year 2023)</i> <i>Mean value</i>	Water level [m NAP]	3.29	3.44	3.86	4.17	3.90	3.84	4.14	3.88	3.95	3.74	3.57	3.41
	Hydraulic load level (1 l/s/m) [m NAP]	5.28	5.92	6.17	8.90	6.55	6.37	6.10	5.10	7.08	6.07	7.31	5.85
	Hydraulic load level (5 l/s/m) [m NAP]	4.71	5.27	5.56	7.84	5.82	5.72	5.60	4.73	6.29	5.48	6.37	5.03
	Overflow [l/s/m]	< 0.1	0.27	0.25	78.72	2.10	1.09	0.36	< 0.1	3.56	0.71	1.39	0.22
	Wave height [m]	0.96	1.39	1.48	2.25	2.75	2.13	1.66	1.07	1.83	1.30	2.71	1.83
<b>0.81 m</b> <i>RCP4.5</i> <i>Mean value (P50)</i>	Water level [m NAP]	3.43	3.51	3.88	4.20	3.93	3.92	4.24	3.93	4.02	3.78	3.62	3.56
	Hydraulic load level (1 l/s/m) [m NAP]	5.41	5.99	6.23	8.94	6.90	6.43	6.18	5.14	7.16	6.16	7.43	6.29
	Hydraulic load level (5 l/s/m) [m NAP]	4.82	5.34	5.61	7.87	6.11	5.78	5.68	4.77	6.36	5.56	6.47	5.39
	Overflow [l/s/m]	< 0.1	0.39	0.28	80.84	4.18	1.28	0.41	< 0.1	4.11	0.93	1.76	0.62
<b>1.28 m</b> <i>RCP8.5</i> <i>Mean value (P50)</i>	Water level [m NAP]	3.55	3.54	3.91	4.30	4.11	4.13	4.33	4.00	4.19	3.88	3.78	3.72
	Hydraulic load level (1 l/s/m) [m NAP]	5.43	6.08	6.27	8.98	6.92	6.50	6.23	5.18	7.18	6.22	7.44	6.52
	Hydraulic load level (5 l/s/m) [m NAP]	4.84	5.41	5.63	7.91	6.14	5.86	5.73	4.82	6.38	5.62	6.49	5.59
	Overflow [l/s/m]	< 0.1	0.58	0.31	84.32	4.40	1.48	0.42	< 0.1	4.21	1.14	1.82	1.06
<b>1.40 m</b> <i>RCP4.5</i> <i>High-end (P95)</i>	Water level [m NAP]	3.60	3.54	3.94	4.37	4.20	4.23	4.38	4.05	4.28	3.95	3.86	3.80
	Hydraulic load level (1 l/s/m) [m NAP]	5.43	6.08	6.28	9.00	6.92	6.54	6.26	5.20	7.18	6.26	7.45	6.51
	Hydraulic load level (5 l/s/m) [m NAP]	4.85	5.41	5.64	7.93	6.14	5.90	5.76	4.84	6.38	5.66	6.49	5.59
	Overflow [l/s/m]	< 0.1	0.58	0.31	86.15	4.42	1.62	0.45	< 0.1	4.27	1.31	1.84	1.05
<b>2.05 m</b> <i>RCP8.5</i> <i>High-end (P95)</i>	Water level [m NAP]	3.94	3.89	4.35	4.91	4.71	4.78	4.86	4.53	4.82	4.48	4.41	4.33
	Hydraulic load level (1 l/s/m) [m NAP]	5.49	6.17	6.36	9.28	6.94	7.01	6.58	5.46	7.24	6.78	7.48	6.67
	Hydraulic load level (5 l/s/m) [m NAP]	4.92	5.49	5.74	8.23	6.17	6.42	6.11	5.15	6.46	6.17	6.54	5.73
	Overflow [l/s/m]	< 0.1	0.75	0.36	> 100.0	4.66	4.10	0.77	< 0.1	4.87	4.86	1.95	1.40

The dyke height around the Eastern Scheldt varies between +6.0-7.25 m NAP. The most common slope of the dykes is 1/3. It can be concluded that the water level for all locations has increased compared to the prevailing safety standard. This is mainly due to modified surcharges in WBI-2017. The orange and red shaded values represent the dyke sections with significant wave overtopping of more than 1 l/s/m and 5 l/s/m respectively. The maximal acceptable wave overtopping is set on 5 l/s/m due to fragile grass cover on the crest of the dykes. The maximum allowable value was earlier 1 l/s/m according to the previous standard (Rijkswaterstaat, 2007), (Witteveen+Bos, 2017). It is expected that, according to the results of Hydra-NL, at least the red shaded sections should be reinforced after the next assessment round.

First, all locations are calculated using a dyke profile without incorporating a foreland composed of sand. The Eastern Scheldt is full of sand plates that reduce waves in storm conditions. Sand plates located in front of the dyke which significantly reduces the waves, but this foreland is very dynamic and can change due to currents and wind effects. The condition is that the foreland must be well maintained (at height and volume) if it is included as part of the flood defence. Locations OS-1, 2, 3, 7 and 8 scored well and are approved in terms of height and wave overtopping without including a foreland. It is plausible that these dykes might be considerably stronger than according to the results. The other dyke sections did not meet the requirements for wave overtopping, under these conditions and should be assessed more specifically.

In advance, accurate dyke profiles, including a foreland, have been used for test locations OS-5, OS-6, OS-10, OS-11 and OS-12. OS-10 and OS-12 do only meet the standard under the condition that the foreland is part of the flood defence and should be maintained according to the current state. The other flood defences should be reinforced in all cases.

The accurate geometry of the dyke profile and foreland was missing for locations OS-4 (Oesterdam) and OS-9 (Philipsdam). These dams do not meet the requirements for wave overtopping without incorporating a foreland. Wave overtopping might not be an issue in these cases, due to the water storage capacity behind the dams. These dams protect the second row of dykes which generally have an increased crest height. Therefore, it is assumed that significant wave overtopping is accepted over the Oesterdam and the Philipsdam. Nevertheless, it can be expected that these dams should be reinforced in the short-term due to the regulation change. More specific data and research are required to assess these dams accurately.

Upon further analysis of the results, the first conclusion is that several dykes do not meet the requirement of overtopping, mainly because of the increased safety standard after the regulation change. This means that most dykes with a safety standard of T=10,000 should be reinforced to meet the standard in terms of wave overtopping. The only dykes that will withstand a high water with an average return period of 10,000 years storm are OS-1, 3, 7 and 8.

Also, the location is decisive in determining the tides and waves. Storm surge in the Eastern Scheldt estuary increases the water level in the south-east by 20-30 cm, due to the most common north-western wind direction. This also corresponds to the waves, which increase in height to maximal 2.75 m at the eastern side of the Eastern Scheldt for T=10,000.

According to the results in Table 6.7, dyke sections OS-5, 6 and 11 should be heightened to meet the location specific requirements of wave overtopping of 1 l/s/m. If the requirement for wave overtopping changes to 5 l/s/m, it is not required to reinforce these dykes.

In contrast to the rising water level during daily conditions under sea level rise, the effects of SLR are barely noticeable (15%) during storm events in Eastern Scheldt. The water level is only 5-25 cm higher among the locations for the year 2100 in the 1.28 m SLR scenario. This can be explained by the effectiveness of the OSK. In the case of an unchanged closure regime, the barrier is closed at an expected water level higher than +3.0 m NAP. The water level of the Eastern Scheldt will not increase linearly with SLR due to the current closing regime. The major aspects which increase the maximum water level of the Eastern Scheldt are leakage, wave overtopping, storm surge, oscillations and the effects of a closing failure of the OSK. Also, SLR leads to a higher closing frequency of the OSK because the water level higher than +3.0 m NAP will be exceeded more often. All these effects are being processed in the probabilistic model.

To conclude, if the OSK is resistant to significant sea level rise and can continue to perform according to the standards in the long-term, the effects on the dykes around the Eastern Scheldt will be limited. Apart from a few reinforcements, the dykes will meet the standards for failure mechanism wave overtopping.

The worst situation for the dykes can occur with a sea level of just below +3 m NAP meaning that the floodgates of the OSK do not close. The maximum water levels in the Eastern Scheldt will, therefore, exceed the +3 m NAP significantly caused by storm surge in the Eastern Scheldt. If the conditions at sea exceed these threshold values, the floodgates close at a water level of +1 m NAP which results in a substantial lower load on the dykes. Sea level rise mainly ensures that both situations will occur more often, without significantly increasing the load on the dykes.

### 6.4.3. Limitations of the results

The results of the hydraulic loads for the flood defences explained in the section are prone to limitations.

First, the used geometry of the dykes behind the storm surge barriers has a deviation compared to the reality. The profiles that had been requested were not always accurate. Especially the used dyke profiles for the dykes around the Eastern Scheldt were schematized very conservatively. This means that if the calculation shows that the dyke meets the boundary condition for overtopping, this is likely to be correct. However, various dyke sections scored very badly. Therefore, the geometry of the dykes was checked for validation proposes. It turned out that most dyke sections have a foreland that significantly reduces the wave impact. Also, the used geometry for the dyke locations in Rhine-Meuse Delta was slightly simplified. Location RMD-5 is recalculated according to the actual geometry.

Due to time constraints, it was not possible to recalculate all dyke section, but locations OS-5, 6, 10, 11 and 12 are recalculated with the actual dyke geometry. The dams (OS-4 and 9) score insufficient, but more accurate data of the geometry of the eventual foreland was not available. Therefore, it might be the case that the actual overtopping is significantly lower at these locations.

Second, the water levels and hydraulic loads for the dykes are underestimated for the various sea level rise scenarios. Hydra-NL computes the water levels in the closed basins including water supply of the rivers, leakage and wave overtopping over the storm surge barriers. However, the maximal value for wave overtopping in the model is 2,000 l/s/m. A manual calculation is used to compute the rate of overtopping above 2,000 l/s/m (Appendix M). The actual volume of overtopping could be more significant with accelerated SLR, which is not incorporated in the results. The effects of this additional supply of water for the storage capacity and water level will be analyzed in Section 7.1.2.

Third, the rate of overtopping in l/s/m for the dykes in the Rhine-Meuse Delta does not include model uncertainty. The calculation time for this parameter was not appropriate within this scope. However, the required dyke height does include model uncertainty, which gives more accurate results.

Fourth, the results are only valid under the condition of outstanding functioning storm surge barriers. Small adjustment to the closing criterion or a late closure of the barrier has significant consequences for the hydraulic loads for the backward dykes. SLR will also increase the low tide, which implies that closing in advance can result in a higher water level in the delta. This is currently not included in Hydra-NL and is investigated in Section 7.1.4.

Furthermore, the probabilistic model Hydra-NL have more model limitations and uncertainties. These deviations can influence the accuracy of the results and are summarized in Appendix I.

To conclude, the hydraulic loads give a clear indication of the current state of the flood defences in terms of the required dyke height. However, this analysis does not provide information about the other failure mechanisms. As a result, no conclusive judgment can be given about the strength and capacity of these assessed flood defences.

# 7. Risk analysis

This chapter is about determining the remaining lifetime of the MLK and OSK. This depends on various risks which will be analyzed in this chapter. It should be emphasized that this risk analysis needs to be used as an addition to the full assessment method of the WBI-2017. Therefore, it is advised to perform a customised assessment (Dutch: “Toets op Maat”) using the WBI-Software Ringtoets. This probabilistic program assesses the storm surge barriers according to the WBI-2017 requirements. However, more insight into the parameters is required to be able to make a complete analysis of the possible failure mechanisms. This analysis can help to give a policy advice for the remaining lifetime of the storm surge barriers for different sea level scenarios and helps to find the appropriate parameters as input for the model.

The focus of this chapter is primarily on technical factors that contribute to the tipping point of both the MLK and OSK. The goal of the tipping point analysis is to project the remaining lifetime of the storm surge barriers and to recommend measures to extend the operating lifetime if this is needed. The initially planned lifetime is 100 years for the MLK, which is built in 1997. The OSK is constructed in the year 1986 and has a designed lifespan of 200 years. The expectation is that accelerated sea level rise shortens the remaining lifetime considerably due to increasing hydraulic loads.

WBI-2017 program Hydra-NL is used for the identification of relevant parameters that influence the hydraulic loads of the MLK and OSK and the dykes of the inherent water system in the hinterland for various sea level rise scenarios. Hydra-NL is used to determine the water levels and waves probabilistically at various locations for several exceedance frequencies of the safety standard. These values are used to test the dykes against the maximal wave overtopping requirements.

The remaining lifetime of the MLK and OSK depend on various risk factors which might affect the decision-making for the long-term strategy of the storm surge barriers. Sea level rise is a very uncertain phenomenon, which predominantly affects the technical tipping point of the storm surge barriers. Also, the risks of sea level rise are appointed for flood risk management in the Netherlands including the dykes in the RMD and Eastern Scheldt.

Table 7.1 summarises the risks and responses that will be analysed in Chapter 7. The described risks in the risk register are assumed to be the foremost contributors that affect the remaining lifetime of the MLK and the OSK. The table describes the main risk events, causes and expected consequences for the functionality of both storm surge barriers. The assessment is performed in the next sections of this chapter for each of the described risks. The total assessment including all risk events determine the technical tipping points of the current status of both storm surge barriers. The tipping point analysis and strategies are provided in Section 7.2 and 7.3.

It should be emphasised that the focus will be mainly on the hydraulic loads and less on the strength of the construction. Important to note is that the given functional lifetime of the storm surge barriers does not indicate that all dykes in the hinterland meet the requirements according to WBI-2017. The remaining lifetime of the storm surge barrier will be determined, for the condition that dykes in the hinterland have to be reinforced to the updated safety standard. This implies that first relatively small dyke improvements will be made to prevent expensive adjustments to the storm surge barriers.

As a response to the possible shortened lifetime of the barriers due to the risk events, measures are analyzed that can extend the remaining lifetime. If these measures have a positive effect on the technical tipping point and are financially feasible, these response measures are recommended to be implemented.

The risks and response measures are summarised in Table 7.1 and described in later in this chapter. Hence, there are many dependencies between the risk events. Risk responses to one risk event might also affect the probability and/or impact of other risks which should be investigated by conducting a trade-off analysis.

Table 7.1: Risk register; effect of risk factors to the performance and lifespan of the Maeslant Barrier and Eastern Scheldt Barrier. The register includes risk responses that can reduce risk and therefore extend the remaining lifetime of the storm surge barriers.

Nr.	Category	Risk Description			Pre-response Assessment				Risk Response	Post-Response Assessment			
		Cause	Risk Event	Consequence	Probability		Impact			Probability	Impact	Post-response action	Secondary risk
					MLK	OSK	MLK	OSK					
1	Climate <i>Sea level rise</i>	Uncertainty in the future rate of carbon emissions and the rate of sea level rise	SLR might accelerate faster than previously expected	The hydraulic loads increase which leads to a shortened lifespan of the storm surge barriers	High	Med	Very high	Very high	Reduce the risk by conducting more research to future SLR and develop mitigation measures in advance	Med	High	Implement surcharges in the design of flood defences to compensate for climate uncertainty	Reinforced flood defences may be over-dimensioned if SLR appears to be lower than projected
2	Technical <i>water-retaining height</i>	Sea level rise and more extreme storms result in increased peak water levels and hydraulic loads	The height of both barriers might not be sufficient regarding water overrun	Storm surge barriers are disapproved before the end of their planned lifetime	High	High	Med	Med	Reduce the risk by increasing the height of the dykes behind the barriers.	Med	Med	Investigate the maximum acceptable rate of water overrun	n/a
3	Technical <i>Construction</i>	Sea level rise and more extreme storms result in increased hydraulic loads to the construction	The construction and stability of the barriers might be insufficient against increasing hydraulic loads	Storm surge barriers are disapproved before the end of their planned lifetime	Very high	Very low	Very high	Very high	Reduce the risk by lowering the horizontal loads by partially raising the floodgates	MLK: Med	Very high	Investigate if the soil protection behind the floodgates should be reinforced	Increased hydraulic loads to the dykes in the hinterland. Increased load on the top layer of the soil protection behind the floodgates
										OSK: Very low			
4	Operation <i>Closing procedure</i>	Closing the MLK takes approximately 120 minutes for the MLK and 82 minutes for the OSK	The storm surge barrier might close too late due to an inefficient closing procedure	Water levels behind the barrier temporarily exceed the maximum allowable levels	Very high	Low	High	High	Reduce the risk by minimizing delays to make the closing procedure more efficient	Low	High	Perform always a turnaround closure to lower the water level of the water system	n/a
5	Operation <i>failure rate closure</i>	The failure probability of the MLK is 1/100 per closure and closing the OSK is not 100% reliable	The barriers could fail to close during a high-water situation	Water levels behind the barrier exceed the critical levels and increase the risk of flooding	Med	Very low	High	Med	Reduce the risk of failure by reducing maintenance intervals and installing backup systems ( <i>only for MLK</i> )	MLK: Med	MLK: Med	n/a	n/a
										OSK: Very low	OSK: Med		
6a	Economic <i>Closing frequency</i>	Sea level rise results in more frequent closures which increase waiting time of the transport sector	The Maeslant Barrier might not be economically beneficial for more frequent closures	Financial losses for transport companies in the port of Rotterdam and reducing employment opportunities	Med	-	Med	-	Reduce the risk by optimising the time to close. Adapt harbour activities to closing forecast	MLK: Med	MLK: Low	n/a	n/a
6b	Nature <i>Closing regime</i>	Sea level rise cause more frequent closures which diminish tidal activity in the estuary	The Eastern Scheldt Barrier might affect the ecology by more frequent closures	Reduced salt water interaction results in changes of flora and fauna and sea level rise results in diminished sand plates	-	High	-	High	Sand nourishments and other investments are required to restore the ecology	OSK: Med	OSK: Med	n/a	n/a
7	Technical <i>soil subsidence</i>	Natural geological processes and anthropogenic process cause vertical land movement	The water-retaining height of the storm surge barriers could reduce due to vertical land movement	The hydraulic loads increase during storm events due to the reduced height	Low	Low	Low	Low	Accept the risk and take soil decline into account surcharges during the design of flood defences	Low	Low	n/a	n/a
8	Legal <i>Changing safety standard</i>	Safety standards are determined by economic activity and potential victims in the area	Storm surge barriers can be disapproved due to more strict safety standards	Storm surge barriers should be reinforced or should be replaced	Med	Med	Med	Med	Reduce the impact by effective adjustments which extent the technical tipping point	Med	Low	n/a	n/a
9	Economic <i>Cost / Benefit</i>	Increasing hydraulic loads lead to performance loss and increase maintenance costs	The storm surge barriers might not be financially adequate to deal with climate change	Other structures will be build which are more effective	Low	Very Low	High	Very high	Accept	MLK: Low	MLK: High	n/a	n/a
										OSK: Very low	OSK: Very high		

## 7.1 Risk analysis of the storm surge barriers

This section investigates the main risks that can potentially affect the remaining lifetime of the Maeslant Barrier and the Eastern Scheldt Barrier which are summarized in Table 7.1. The technical analysis will contribute to the understanding of the parameters and physics who can influence the performance of the storm surge barriers. Furthermore, the technical analysis describes the risks of the failure mechanisms of the storm surge barriers. This study can be used as policy advice to indicate the risks of sea level rise to the storm surge barriers and to find appropriate response strategies to extend the remaining lifetime.

This analysis uses the results of Hydra-NL, consisting of critical water levels and wave heights, to quantify the high-end conditions for the storm surge barriers. However, the results of Hydra-NL are prone to limitations which can underestimate the hydraulic loads for the hinterland in case of accelerated SLR. Various adjustments such as; the closing procedure and leak opening cannot be changed in Hydra-NL, while these aspects could have one significant role in the tipping point analysis. Therefore, insight is needed in the contributing factors to determine the technical tipping point and to formulate substantiated recommendations to improve the performance and remaining lifetime of the storm surge barriers.

### 7.1.1 Climate change and sea level rise

Both the MLK and OSK are designed for a relatively limited amount of sea level rise. Specialists indicate that 50 cm SLR has been implemented in the design of the MLK, but one prescribed design requirement was not considered. Moreover, the OSK should be operational for 200 years, but only 40 cm relative sea level rise was included in the design.

Global warming results in sea level rise by melting ice-sheets, glaciers, steric effects, and land water changes. Sea level rise directly influences the coastal environment and results in higher flood risk. Recent projections suggest that sea level rise probably increases to a large extent. More than 1 m sea level rise might be expected at the end of this century, according to the latest insights. Furthermore, the sea level scenarios are more uncertain than previously thought and 2 m sea level rise cannot be ruled out by the year 2100.

Therefore, the risk for the remaining lifetime of the storm surge barriers is the following:

*“Sea level rise might accelerate more than previously expected.”*

The consequence might be that the remaining lifetime of the MLK and OSK shortens significantly, depending on the rate of future SLR. Sea level rise also triggers various other risk factors such as the limited height and strength of the construction which can further affect the hydraulic loads for the dykes in the hinterland.

The risk of accelerated sea level rise has been analyzed extensively in Chapter 5. Table 7.2 shows the sea level projections for the Netherlands for the year 2100 which are constructed in Section 5.7 p. 60.

*Table 7.2: Projected regional sea level rise [cm] by the year 2100 compared to 2000 including uncertainty range according to reference studies.*

Percentiles [%]	RCP4.5	RCP8.5	Average RCP8.5 & RCP4.5
P5	31	63	47
P17	52	87	70
P50	81	128	104
P83	114	175	144
P95	140	214	177
P99	168	258	213

According to the results DP16, the projected rate of sea level rise mainly depends on the amount of (future) carbon emissions. Earlier studies argued that the “business as usual” scenario RCP8.5 is likely by proceeding current global emission trend, but recent technological innovations and the reducing dependency on fossil energy indicate that a slightly lower emission scenario between RCP8.5 and RCP4.5 is more likely to occur (Raftery et al., 2017). Therefore, the most likely sea level rise to be expected is the average between RCP4.5 and

RCP8.5 which is 1.04 m (50%) at the end of this century. Figure 7.1 shows the projected rate of SLR for emission scenario RCP4.5 and RCP8.5. As featured in the graph, substantial acceleration of the rate of sea level rise is expected to start after 2050. The expected rate of sea level rise is 25 mm per year in 2100 for RCP8.5. For RCP4.5, the expected rate of sea level rise is 15 mm per year in the year 2100. The high-end estimate suggests a rate of 25 mm per year to 40 mm per year for RCP4.5 and RCP8.5 respectively.

The root cause of the significant increase in sea level projections is the new knowledge about the processes of the Antarctic ice sheet. This new knowledge shows that sea level scenarios are relatively uncertain, and that high-end sea level rise is a possibility. It is essential to include the uncertainty of sea level rise in the flood risk analysis for low-lying areas in the Netherlands. This study will cope with the risks and uncertainty of high-end sea level rise by making a response plan for the Dutch storm surge barriers.

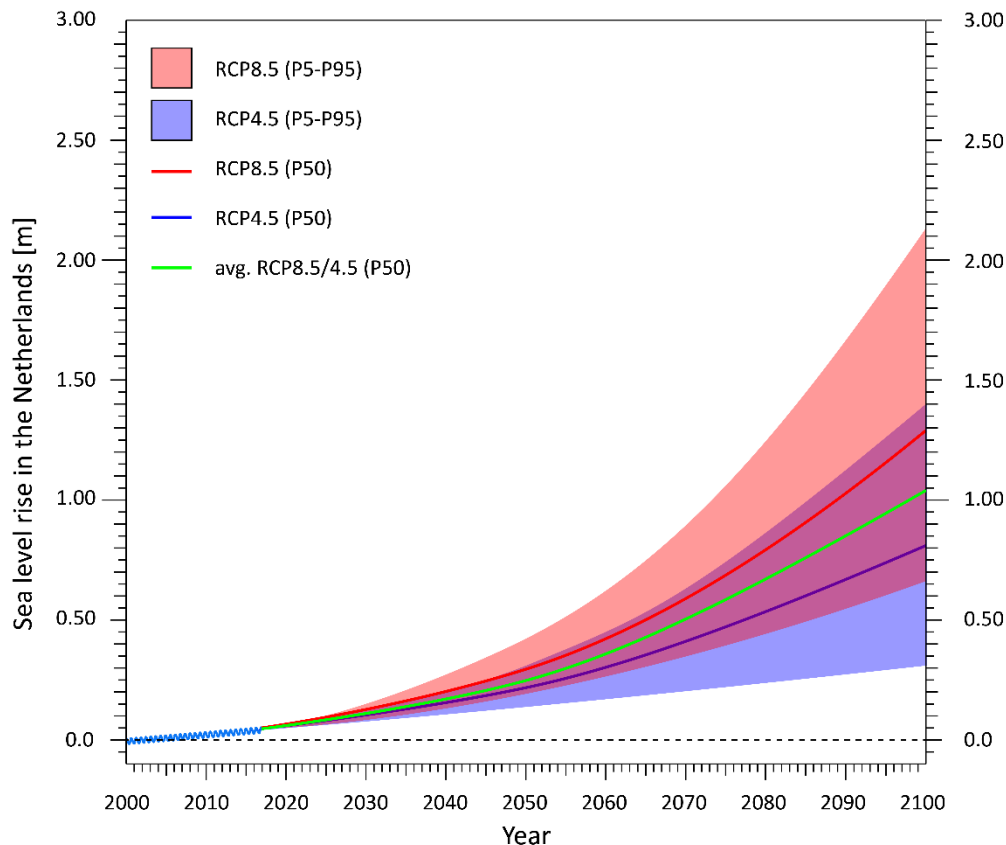


Figure 7.1: Absolute sea level projection for the Netherlands. Red: range of sea level rise for RCP8.5. Blue: range of sea level rise for RCP4.5. Green: likely sea level rise (P50).

### 7.1.2 The water-retaining height of the storm surge barriers

Both the MLK and OSK are designed for a high-water event with a very small probability to occur. Also, both barriers should be able to withstand a significant amount of wave overtopping. Preconditions for the maximal volume of wave overtopping were not specified, but the MLK should be able to withstand more than 1,000 l/s/m based on the design requirements of the maximum sea level and wave height. For the OSK, this is more than 6,000 l/s/m due to the relatively large waves.

Sea level rise increases the probability of a high-water event and could also increase the hydraulic loads beyond the design requirements of these storm surge barriers. This does not imply that the storm surge barriers are immediately rejected if sea level rise appears to be accelerating. Storm surge barriers are expensive constructions which have various safety surcharges in the design to minimize the risk of a collapse. Nevertheless, sea level rise and legislation changes increase the risk that the limited height of the storm surge barriers results in disapproved flood defences before the end of their projected lifetime.

Sea level rise does have consequences for the volume of wave overtopping and water overrun which has an impact on the storage capacity of the backward water system. If the water levels in the hinterland increase, also the hydraulic loads for the dykes on the landward side could increase significantly. Also, significant wave overtopping might result to erosion of the soil protection which might affect the stability of the construction. The construction of the storm surge barriers should be resistant to a large volume of water overrun. Therefore, it is not expected that a failure of the construction is the dominant failure mechanism. However, at a rate of water overflow of 1,000 l/s/m or more, vibrations might occur in the floodgates of hydraulic structures (Rijkswaterstaat, 2017d). This might be an issue for the MLK, due to the turning barrier. Therefore, it is advised to perform in-depth analysis of this failure mechanism to determine the maximum allowable rate of overflow for the construction. The Fault Tree analysis for the assessment track “height” is given in Figure 7.2.

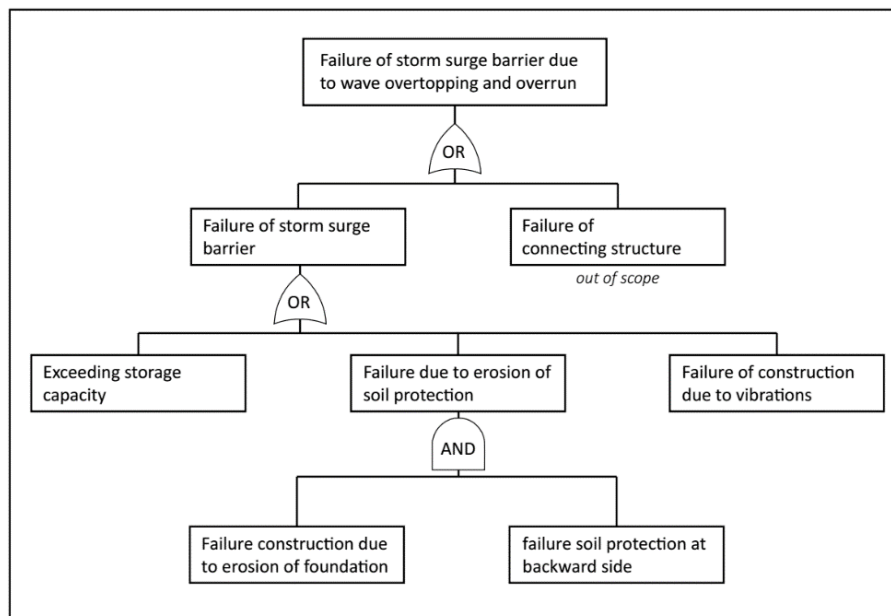


Figure 7.2: Fault tree of failure mechanism: water overflow.

This section focusses on the effects of the constraining height of the storm surge barriers to the tipping point analysis and to project the remaining lifetime. Important to note is that the emphasis is only on the storm surge barriers and not on connecting structures. It is assumed that these connecting dykes and structures can be reinforced separately without affecting the technical tipping point of the storm surge barriers.

The focus is predominately on the risk of exceeding the storage capacity due to sea level rise which affects the performance of the storm surge barriers. This risk is also influenced by the closing regime and failure rate of the storm surge barrier which is investigated in Section 7.1.4 and 7.1.5.

### 7.1.2.1 Risk of exceedance of the storage capacity

The storage capacity is determined by the characteristics of the water system of the delta behind the closed storm surge barriers. This concerns the maximum accepted increase of the water level within the water system over the total surface area of the water system. River discharge, leakage and wave overtopping contribute to the incoming volume of water in the delta. If the total storage capacity, substantial consequences may occur in the hinterland, such as dyke breaches and floods. Both the Maeslant Barrier and Eastern Scheldt Barrier close-off an extensive water system during a high-water event. Furthermore, the required duration of the closure depends on the high-water situation. The used calculation methods to determine the storage capacity and the required closing time are explained in Appendix L in more detail. This section describes the risk of exceeding the storage capacity of the Rhine-Meuse Delta and the Eastern Scheldt.

## Rhine-Meuse Delta

This section describes the risk of exceeding the storage capacity of the Rhine-Meuse Delta (RMD) during the closed Maeslant Barrier. First, the contributing factors are analyzed to determine the rate of water level increase in the RMD. The results will feature the maximum water levels and the rate of the rise for various situations.

### **Maximum water levels and surface area of the Rhine-Meuse Delta**

The MLK together with the Hartel Barrier (HK) prevents the Rhine-Meuse Delta from exceeding critical water levels (MHW) during high-water events. This is the maximum permissible water level that can statistically occur at a specific location (Rijksoverheid, 2016). Before the regulation change in 2017, the MHW was decisive for determining the locally required height of the flood defences.

The new assessment methodology computes the probability of flooding based on various failure mechanisms. Some of these failure mechanisms may also occur at different hydraulic conditions. Therefore, it is not required to test flood defences to one specific critical water level (MHW). However, in the context of this research into the storage capacity during a closure, a maximum water level should be chosen.

The critical water levels before the regulation change are given in Table 7.3 and are obtained from (Rijkswaterstaat, 2007) and (HKV, 2015). The threshold values after changing the regulations in 2017 are estimated using Hydra-NL including the statistical- and model uncertainty of WBI-2017. Table 7.3 also features the assumed MHW according to the new assessment methodology (WBI-2017) using Hydra-NL. This critical water level is calculated for the changing safety standard at the test locations. The results show that the critical water levels are higher than for the previous safety standard. It is compulsory to reinforce all dyke sections, if needed, according to the new norm before the year 2050 (Section 3.2.4). Therefore, it is assumed that the dykes in the RMD will be reinforced in the short-term which might result in a slightly increased maximum acceptable water level. Due to the uncertainty in the assessment, a range is given for the new critical water levels which are between the previous MHW and the maximum water level computed by Hydra-NL. This does not mean that the results in Table 7.3 will be the actual new critical water levels. This will have to be determined with an extensive probabilistic assessment of the dyke sections in the RMD.

*Table 7.3: Critical water levels of the RMD locations (Rijkswaterstaat, 2007) and (HKV, 2015). MHW after 2017 is assumed based on calculated water levels of the changed safety standard (Hydra-NL). \*: assumed water level.*

MWH of the RMD Location	Safety standards in 2006		Safety standards in 2017	
	Annual exceedance frequency	Critical water level (MHW) [m NAP]	Annual exceedance frequency	<i>Assumed Critical water level</i> (MHW) [m NAP]
Dordtsche Kil (RMD-1)	1/2,000	2.8	1/1,000	2.8-3.0
Willemstad (RMD-2)	1/2,000	2.6	1/300	2.6-2.9
Hellevoetsluis (RMD-3)	1/4,000	2.6	1/300	2.6-2.7
Lek (RMD-4)	1/10,000	5.2	1/10,000	5.2-5.2
Rotterdam (RMD-5)	1/10,000	3.6	1/30,000	3.6-3.9
Alblasserdam (RMD-6)	1/4,000	3.1	1/10,000	3.1-3.4*
Hoogvliet (RMD-7)	1/4,000	3.1	1/1,000	3.1-3.3

Table 7.4 (p. 83) shows the maximum accepted peak average water levels of the entire RMD for T=10,000 and T=30,000. These values are used as upper limit in calculating the risk of exceeding the storage capacity of the RMD. The calculations of the water storage in Table 7.8 and the tipping point analysis (Section 7.2.1) does not include aspects such as storm surge within the delta, river water impoundment and the tidal wave and translation wave (Appendix L). These aspects can temporarily increase the peak water level by 0.2-0.5 m at Rotterdam (RMD-5). Therefore, the peak water levels which are used in the calculations of the water storage presented are slightly lower than the critical water levels given in Table 7.3. An uncertainty bandwidth of 10cm is maintained in the tipping point analysis of the water storage which is conducted on pp. 115-119.

Table 7.4: Critical peak water level average in the Rhine-Meuse Delta.

Return period	Peak water level RMD (including uncertainty)
T=10,000	+3.4 m NAP ( $\pm 0.1$ m)
T=30,000	+3.6 m NAP ( $\pm 0.1$ m)

The surface area of the MLK increases at a higher water level due to extra storing capacity in the rivers and floodplains. The surface area of the Rhine-Meuse Delta is given in Table 7.5 and is used in the calculation.

Table 7.5: Surface area of the RMD at various heights (Rhine-Meuse Delta) (Rijkswaterstaat, 2006).

Water level [+m NAP]	0	0.5	1.0	1.5	2.0	2.5	3.0	3.5
Surface area [km <sup>2</sup> ]	219	240	276	317	327	339	347	360

### The rate of water level increase in the Rhine-Meuse Delta

The critical water levels and surface area are used to determine the acceptable volume of incoming water in the RMD. This is calculated by using Formulas [3,4,5,20] in Appendix L and Q. Then the volume of incoming water that reduces the remaining storage capacity of the RMD, can be determined by calculating the following aspects:

- river discharge;
- wave overtopping and water overrun;
- leakage of seawater through the arc-shaped doors.

These aspects will be discussed in the next section.

### River discharge

The Rhine-Meuse Delta is supplemented with water from the Rhine and the Meuse. The Rhine branches into the IJssel, Lek and Waal, whereof the last two supply water to the Rhine-Meuse Delta. The Meuse, on the other hand, flows entirely to the RMD. The maximum discharge of the Rhine (Lobith) is approximately 16,000 m<sup>3</sup>/s and 4,000 m<sup>3</sup>/s of the Meuse for a return period of 10,000 years (Deltares, 2017b).

Hydra-NL calculates the critical river discharge in combination with a sea level for various return periods. Both factors are independent which implies that it is improbable that an extreme high-water event and extreme river discharge coincide at the same moment. The relationship between river discharge, sea level and wind direction has been calculated for each location in Hydra-NL. As an example, the results are shown in Table 7.6 for location Rotterdam (RMD-5) during a closed MLK. More than 1.4 m SLR is left out the analysis as this will lead to a significant exceedance of the critical water level which is shown in Table 7.9.

Hydra-NL has an essential limitation because the statistics of the river discharge of the Meuse are not included in the model. That is a compelling reason why it is recommended to make a manual calculation. The discharge of the Rhine is measured at Lobith whereof a small volume flows to the IJssel and will not reach the RMD. On the other hand, the river discharge of the Meuse should be added to the total river supply towards the RMD. The total incoming river supply increases 5-7% compared to the river discharge of the Rhine at Lobith which is included in Table 7.9 (p. 85).

Also, the situation with an extreme sea level and average river discharge, which is not considered to be critical in Hydra-NL, will be computed in the manual calculation.

Table 7.6: Probabilistic distribution of river discharge and sea level for location RMD-5 (Hydra-NL).

Sea level rise [m]	Return Period [yr.]	Sea level [+m NAP]	River discharge Rhine at Lobith [m <sup>3</sup> /s]	Wind direction [r]	Water level [+m NAP] RMD-5
0	10,000	3.72	12,550	NW	3.80
0	30,000	3.89	12,950	NW	3.93
0.81	10,000	4.13	13,000	NW	4.20
0.81	30,000	4.38	13,950	NW	4.46
1.40	10,000	5.04	15,223	WNW	4.64
1.40	30,000	5.33	15,950	WNW	4.90

### Water overrun and overtopping

Water overrun can occur during extreme high-water events of +5.00 m NAP or more over the top of the floodgates of the MLK. At the Hartel Barrier (HK), water overrun already occurs at a sea level of +3.00 m NAP. Therefore, wave overtopping and water overrun at the HK cannot be omitted. Wave overtopping might also take place at the dykes which are part of the Europort Barrier. These influences will be included in the calculation of the rate of water level increase in the RMD during a storm closure. The combination of overrun and wave-overtopping of the MLK and the dykes in the hinterland is calculated with the use of Hydra-NL. The limitation of this model is that the amount of overflow above 2,000 l/s/m, cannot be calculated with Hydra-NL. Therefore, a manual calculation is made to give an indication of a larger flow rate over the top of the vertical barriers (Appendix M). The results are shown in Table 6.3 (Chapter 6). For very long return periods, the amount of water overflow is significant. An overflow of more than 2,000 l/s/m is not an exception to the MLK.

### Leakage

Leakage through the MLK is another factor that contributes to the water level increase in the Rhine-Meuse Delta. The doors do not close completely to prevent a potential collision. Therefore, a gap of 80 cm is being held between the doors. Also, the construction does not provide a complete connection to the quays. The total leak opening is approximately 100 m<sup>2</sup> which leads to a considerable amount of leakage. Also, the HK has a significant leakage during the closure due to the leak opening of 47 m<sup>2</sup> (Slomp, Geerse, & de Deugd, 2005).

The amount of leakage also depends on the water level difference and river discharge. A relatively high river discharge reduces the potential energy height loss (H) due to the seaward pressure. The volume of the leakage per second for both the MLK and HK is given in Table 7.7 and 7.8.

Table 7.7: Average leakage through MLK for different situations using a leak opening of 100 m<sup>2</sup> (Slomp et al., 2005).

Leakage MLK [m <sup>3</sup> /s]	Sea level [m NAP]				
River discharge (Q) [m <sup>3</sup> /s]	2.00	3.00	4.00	5.00	6.00
2,000	n/a	352	480	607	694
4,000	n/a	334	448	575	669
6,000	300	391	448	556	639
8,000	297	376	392	526	603
10,000	261	390	447	489	577
13,000	194	349	412	511	528
16,000	73	308	390	479	545

Table 7.8: Average leakage through HK for different situations using a leak opening of 47 m<sup>2</sup> (Slomp et al., 2005).

Leakage HK [m <sup>3</sup> /s]	Sea level [m NAP]				
River discharge (Q) [m <sup>3</sup> /s]	2.00	3.00	4.00	5.00	6.00
2,000	n/a	122	167	207	229
4,000	n/a	101	159	195	220
6,000	91	126	144	182	209
8,000	78	114	122	172	199
10,000	68	112	125	155	190
13,000	61	103	117	147	167
16,000	31	78	113	135	167

### Results

This section expresses the storage capacity and rate of water level increase in the RMD for various sea level scenarios. The results are calculated according to the Formulas [3,4,5,20] and information provided in Appendix L. Consequently, the results are compared with the outcomes of hydra-NL for the long return periods.

The average peak water level in the RMD during the closure of the MLK is given in Table 7.9 column J. This is the peak water level in the RMD, averaged over the total surface area, for different sea level rise scenarios (A) and the highest safety standards (C). These water levels apply under the condition of a 100% reliable storm surge barrier which closes according to closing protocol. Column K presents the maximum water level at Rotterdam

(RMD-5) and Alblasterdam (RMD-6) for similar conditions but also includes the effects of the failure rate of the MLK. These locations should meet the hydraulic loads that can occur with an annual probability of 1/30,000 and 1/10,000 respectively. It is considered that these relatively long return periods determine the tipping point of the remaining lifetime of the MLK. The maximum accepted average peak water level is +3.4 m NAP for T=10,000 and +3.6 m NAP for T=30,000 according to Table 7.4. A further increase is expected to exceed the critical water level due to the following aspects which are not included:

- storm surge within the RMD;
- river water impoundment;
- tidal wave and translation wave.

Table 7.9 includes two situations (S) (column B) for each scenario and safety standard which are assumed to be the critical situations. Situation 1 projects the storage capacity for a high river discharge condition. Situation 2 describes the storage capacity during an extreme high-water event combined with modest river discharge.

*Table 7.9: Water level increase in the RMD during a closure for situation (S) 1 and 2. \*: Assumed water level due to deviation in dyke geometry (Hydra-NL). Orange: maximal acceptable water level. Red: exceedance of the storage capacity.*

SLR [m] (A)	S (B)	Return Period (T) [yr.] (C)	Sea-level [+m NAP] (D)	River discharge Rhine (Lobith) [m <sup>3</sup> /s] (E)	Total River discharge incl. Meuse [m <sup>3</sup> /s] (F)	Leakage +overtopping MLK & HK [m <sup>3</sup> /s] (G)	Closure water level [+m NAP] (H)	Closure time[hr.] (I)	Average peak water level of RMD [+m NAP] (J)	Water level [+m NAP] RMD-5 & 6 (Hydra-NL) (K)
0.05	1	10,000	3.72	12,550	13,354	572	1	10	2.56	3.80 & 3.00*
0.05	2	10,000	5.70	3,500	3,582	1,478	2	20	3.07	n/a
0.05	1	30,000	3.89	12,950	13,779	616	1	10	2.61	3.93 & 3.06
0.05	2	30,000	6.07	4,000	4,134	1,894	2	20	3.28	n/a
0.81	1	10,000	4.13	13,000	13,832	709	1.76	10	3.31	4.20 & 3.57
0.81	2	10,000	6.36	3,500	3,582	2,136	2.1	20	3.31	n/a
0.81	1	30,000	4.38	13,950	14,849	807	1.76	10	3.43	4.46 & 3.89
0.81	2	30,000	6.74	4,000	4,134	2,520	2.25	20	3.64	n/a
1.40	1	10,000	5.04	15,223	16,213	1063	2.35	10	4.11	4.64 & 4.03
1.40	2	10,000	6.90	3,500	3,582	2,681	2.5	20	3.79	n/a
1.40	1	30,000	5.33	15,950	16,921	1,193	2.35	10	4.19	4.90 & 4.26
1.40	2	30,000	7.32	4,000	4,134	3,151	2.5	20	3.99	n/a

The results show that a water level of +3.6 m NAP will be reached at 0.75 m sea level rise for T=30,000 during a high-water event (situation 2) in case of a successful closure. The closing levels (column H) are highly influenced by SLR. As a result, more SLR will lead to substantially increased hydraulic loads for backward dyke trajectories. This implies that the MLK fails for more than 0.75 m SLR according to the statement described on p. 115. However, these values do not include the failure rate and the risks of the closing procedure which have a significant effect on the tipping point. The effects of these risks are described in Section 7.1.4, 7.1.5 and included in the tipping point analysis of the storage capacity (7.2.1). The results in case of a successful closure of the Maeslant Barrier are described below for both situations.

#### Situation 1: High river discharge

Situation 1 is the dominant situation according to the probabilistic calculation made with Hydra-NL. The choice was made to compare both critical situations due to the simplifications and limitations of implementing the closing regime, storm duration and maximal volume of wave overtopping in Hydra-NL.

The previous critical water level in Rotterdam was +3.6 m NAP (HKV, 2015) which is considered as the acceptable upper limit for T=30,000. According to Hydra-NL, this threshold value will be exceeded for T=10,000 and T=30,000 without sea level rise. However, the results of Hydra-NL tend to be too conservative. The water level in Rotterdam is even higher than at sea (D), which makes closing the MLK almost irrelevant in this situation. According to the results of the manual calculation (J), the peak water level in the RMD should be around +2.56-

2.61 m NAP if the MLK closes as planned due to the relatively short closing period of 10 hours. The sea level (D) is relatively limited in this situation, leading to the opening of the floodgates after one tide. It can, therefore, be determined that the threshold water level will not be exceeded for this situation. This situation is visualised in Figure 7.3. Consequently, it can be assumed that the maximum water level in Rotterdam is largely determined by a failing storm surge barrier which will be discussed in Section 7.1.5.

Sea level rise (0.8 m) has a substantial reducing effect on the storage capacity during high river discharge due to the higher closing level of a turnaround closure. This type of closure is explained in Section 7.1.4 and Appendix H. It is assumed that floodgates can only close at +1.76 m NAP in this situation due to sea level rise. The higher closing level is the main contributor to the increased peak water level in the RMD of +3.31-3.43 m NAP (J).

The maximum water level of +3.4 m NAP in the RMD for T=10,000 will be reached at 0.89 m SLR. It is expected that this amount of sea level rise is the limit to avoid significant exceedance of the maximum storage capacity. This is also shown in Figure 7.3. More sea level rise leads to a substantial increase of the water level of the RMD, which means that the MLK fails according to the Water Act Art. 1.1.1. The maximum acceptable extent of sea level rise is 0.91 m for T=30,000. More sea level rise could lead to an exceedance of the maximum acceptable hydraulic loads for the dykes in Rotterdam (RMD-5) during a high river supply in combination with a required closure of the MLK.

#### Situation 2: Extreme sea level

The consequences for the storage capacity of the RMD are significant at an extreme sea level due to leakage, water overrun and river discharge. This is in contrast to the results of Hydra-NL, which indicate that situation 1 is decisive in determining the maximum water level in the water system. This implies that the rate of wave overtopping over the MLK and HK does increase the risk of exceeding the storage capacity. This is mainly because the floodgates must be closed for a longer period because of the relatively large difference between the sea level and water level in the RMD. As a result, the floodgates should close for 20 hours because opening during ebb (between two high-waters) is not possible. This is visualized in Figure 7.3.

Nevertheless, the maximal accepted water level of +3.6 m NAP (Table 7.4) will not be exceeded in this situation. The maximal average water level in the RMD is expected to be +3.07 m NAP for T=10,000 and +3.28 m NAP for T=30,000. The current procedure of closing at a water level of +2 m NAP can be maintained. The closing procedure is explained in Section 7.1.4 and Appendix H. Performing a prescribed water level closure of +2 m NAP might be impossible after 0.81 m SLR. This is because the minimum sea level, during ebb and an approaching high-water, will increase considerably. Also, it can be recognized that the maximum difference between the sea level and the backward water level is 4 m due to the construction requirement. If it is expected that the high-water event exceeds +6 m NAP, the operational team is obliged to close at a later stage. Otherwise, the force on the construction of the MLK could be too large. The consequence is that the maximal storage capacity of the RMD will decrease.

Based on situation 2, maximal 0.93 m SLR is allowed for T=10,000. The critical water level is higher for Rotterdam and the storage capacity will be exceeded at 0.72 m sea level rise for T=30,000 years. Various situations are visualized in Figure 7.3. Despite the necessity to execute multiple significant dyke reinforcements at RMD 6, it is expected more SLR will lead to a disapproved MLK due to exceeding the storage capacity during an extreme high-water event. It turns out that a closure during a high-water event (situation 2) results in higher water levels in the RMD than a closure during a high river discharge (situation 1) for T=10,000.

Ultimately, it is a trade-off between increasing the storage capacity (closing at a lower level) and strength of the construction which both are determined in the tipping point analysis. It is recommended to check and adjust, if necessary, the parameters and variables for minimum closing water levels, duration of the closure and rate of overtopping in Hydra-NL. It might be the case that, after probabilistic modelling, the dominant situation is between both extreme situations (1 and 2). The described conditions including water levels and the duration of the required closure are visualised in Figure 7.3.

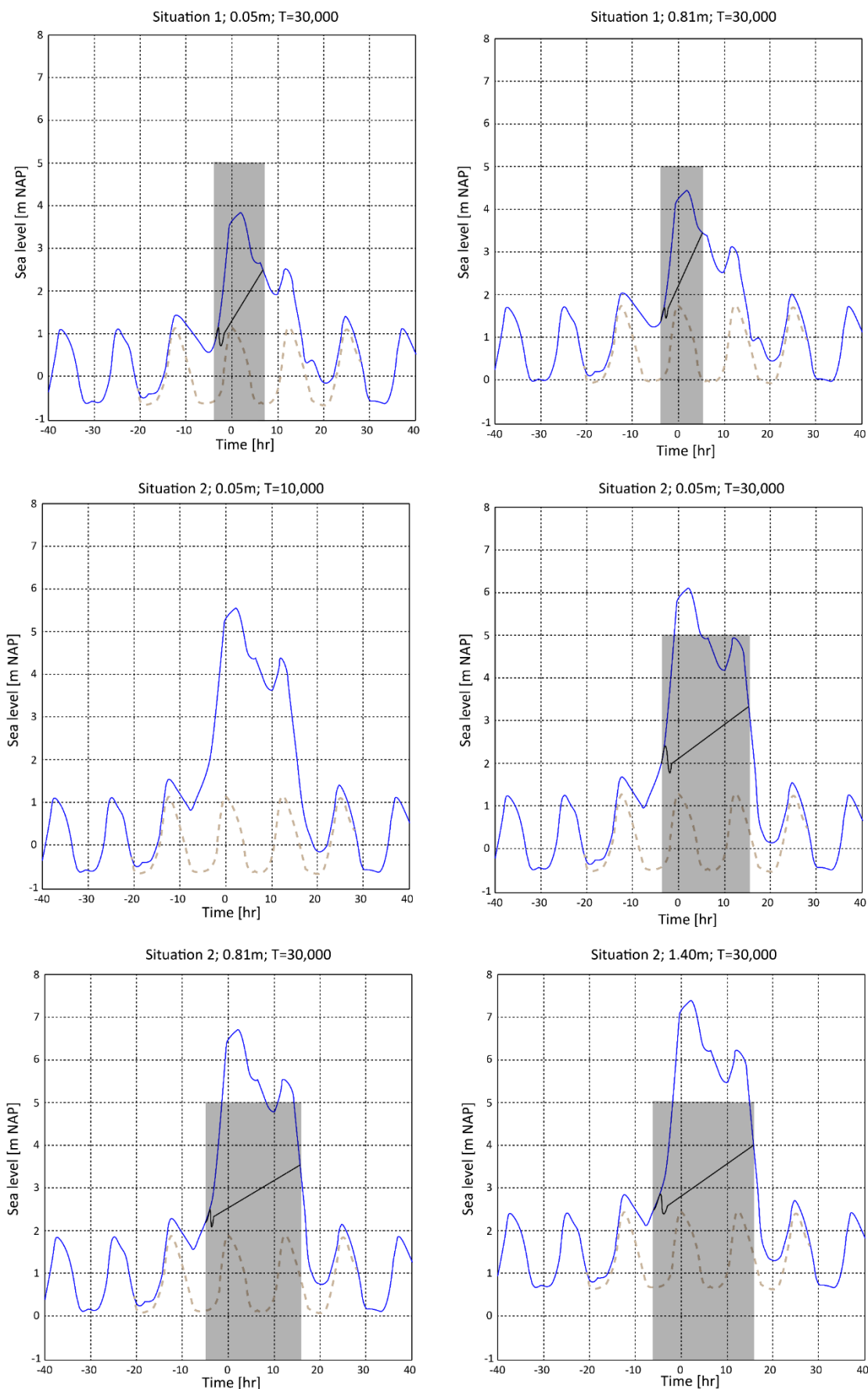


Figure 7.3: High-water event for the MLK including the closing time and water level increase in the RMD. Black: water level increase during the closure. Blue: sea level. Shaded grey: closed period of the MLK.

## Eastern Scheldt

This section describes the risk of exceeding the storage capacity for the Eastern Scheldt estuary (OS). First, the contributing factors are analyzed to compute the rate of water level increase in the OS. The results show the maximum water levels and the rate of this increase for the entire estuary.

### **Maximum water levels and surface area of the Eastern Scheldt**

The OSK prevent the Eastern Scheldt from exceeding critical water levels during high-water events. The critical water levels (MHWs) before the regulation change are given in Table 7.10 and are obtained from (Rijkswaterstaat, 2007). The threshold values after the regulation change in 2017, are unknown yet.

The upper range of the critical water level after changing the assessment methodology is determined by Hydra-NL. It is assumed that the dykes around the Eastern Scheldt will comply with the new safety standard before the year 2050. This implies that the critical water level might increase slightly after the reinforcements. The technical tipping point of the OSK is expected to be reached after this timeframe which indicates that the dykes should be able to withstand slightly increased hydraulic loads. Due to the uncertainty in the assessment, a range is given for the new critical water levels which are between the previous MHW and the maximal water level computed by Hydra-NL. Table 7.10 shows the assumed critical water levels for the flood defences that have a safety standard of T=10,000. This does not mean that the results in Table 7.10 will be the actual new critical water levels. This will have to be determined with an extensive probabilistic assessment of the dykes around the Eastern Scheldt.

*Table 7.10: Critical water levels of OS locations with exceedance frequency 1/10,000 per year (Rijkswaterstaat, 2007). MHW after 2017 is assumed based on calculated water levels of the changed safety standard (Hydra-NL).*

MWH (OS)	Safety standards in 2006		Safety standards in 2017	
Location	Annual exceedance frequency	Critical water level (MHW) [m NAP]	Annual exceedance frequency	<i>Assumed Critical water level</i> (MHW) [m NAP]
Oesterdam (OS-4)	1/4,000	4.0	1/10,000	4.0-4.2
Scherpenissepolder (OS-5)	1/4,000	3.8	1/10,000	3.8-3.9
Moggershilpolder (OS-6)	1/4,000	3.6	1/10,000	3.6-3.8
Van Haftenpolder (OS-7)	1/4,000	3.9	1/10,000	3.9-4.1
Philipsdam (OS-9)	1/4,000	3.7	1/10,000	3.7-3.9

Table 7.11 shows the peak water levels of the Eastern Scheldt for T=10,000 and T=30,000 which are used as upper limit in the calculations of the water storage in Table 7.13, 7.14 and the tipping point analysis which is conducted in Section 7.2.1 (pp. 119-121). The peak water levels include a safety margin and an uncertainty bandwidth of 10 cm to compensate for uncertain regional effects such as local storm surge in the Eastern Scheldt.

*Table 7.11: Critical peak water level in the Eastern Scheldt (OS).*

Return period	Peak water level OS (including uncertainty)
T=4,000	+3.6 m NAP ( $\pm 0.1$ m)
T=10,000	+3.7 m NAP ( $\pm 0.1$ m)

It is difficult to estimate the surface area of the Eastern Scheldt for low water levels due to the changing sand plates. It can be assumed that the entire surface area of the Eastern Scheldt can be used for water storage starting at a water level of +1 m NAP. The used surface area is 343 km<sup>2</sup> (Google, 2018).

### **The rate of water level increase in the Eastern Scheldt**

The Eastern Scheldt estuary only exchanges water through the OSK. The volume of water exchange through the shipping locks is negligible within this context. Also, precipitation can increase the volume of water with several millimeters in the Eastern Scheldt when the OSK is closed, but this factor is also neglected. The dominant contributors to the volume change of the Eastern Scheldt basin are:

- wave overtopping and water overrun;
- leakage of seawater through the floodgates.

Also, the failure rate of closing the floodgates influence the water storage of the Eastern Scheldt. This factor is analysed separately in Section 7.1.5.2. Hydra-NL calculates hydraulic load levels for the dykes in the Eastern Scheldt estuary in combination with an optimal functional storm surge barrier. The model includes overtopping and leakage through the barrier. According to the probabilistic model, the effects are relatively limited for accelerated SLR. However, various aspects might change the results of Hydra-NL. This section analyses the impact on the water storage in the Eastern Scheldt differently.

### **Wave overtopping and water overrun**

In a situation of the OSK, water overrun can occur during extreme high-water events of +5.60-5.80 m NAP or more, depending on the location. The volume of wave overtopping and water overrun increase the water level of the Eastern Scheldt during a closure which is calculated by Hydra-NL (Chapter 6) and using standard Formula [6]. In contrast to Hydra-NL, the manual calculation also include the effects of a high flow rate (>2000 l/s/m) over the top of a vertical barrier, which can occur during extreme high-water events (Appendix M). The results of Hydra-NL are shown in Table 6.5 (p. 71).

### **Leakage**

Leakage of seawater through the OSK is a leading contributor to the risk of exceeding the storage capacity of the Eastern Scheldt. The leak opening of the OSK is estimated at 1,250 m<sup>2</sup> in the current situation (Rijkswaterstaat, 2015b). This has a significant impact on the water storage in the Eastern Scheldt. The flow velocities shown in Table 7.12 have been determined by using flow rate Formulas [9-14] which are explained in Appendix N.

Table 7.12: Flow velocities through the leak opening in the OSK.  $\xi_c=0.44$ ,  $\xi_k=1.1$   $\xi_w=0.42$  and  $\xi_u=1$ . <sup>1</sup>Leak opening 1250 m<sup>2</sup>, <sup>2</sup>Leak opening 600 m<sup>2</sup>.

Water level difference $\Delta H$ [m]	1	2	3	4	5	6
Flow rate [m/s] <sup>1</sup>	2.57	3.64	4.46	5.14	5.76	6.31
Flow rate [m/s] <sup>2</sup>	2.29	3.24	3.97	4.58	5.12	5.61

The leakage volume can be diminished by reducing the leak opening which is part of the preferred strategy. Reducing the leak opening to 350 m<sup>2</sup> is considered to be too optimistic. Nevertheless, it is expected that it is possible to reduce the leak opening to 600 m<sup>2</sup>. However, when the leak volume is reduced by adequate measures, the failure probability of closing the floodgates could increase (Rijkswaterstaat, 2015b). Still, it is considered that this effect of the failure rate is relatively small. It is advised to investigate the potential consequence.

### **Results**

This section expresses the storage capacity and rate of water level increase in the Eastern Scheldt. The results are calculated according to Formulas [9-14] and information provided in Appendix L. Subsequently, the results are compared with the values of hydra-NL for the long return periods (Chapter 6).

The maximal average water level in the Eastern Scheldt during a closure is given in Table 7.13 column I. This is the average peak water level in the estuary for different sea level rise scenarios (A) and two exceedance frequencies (B). Column J gives the maximum water levels in the estuary according to Hydra-NL for the long return periods. The remaining lifetime of the OSK should be determined by using the 10,000-year return period according to the new hydraulic requirements of WBI-2017. The peak water levels (J) at the east side of the estuary are slightly higher than the maximum average water level (I) due additional storm surge during a western wind.

Table 7.13 includes two situations. Situation 1 projects the effects for the remaining storage capacity with the current leak opening of 1,250 m<sup>2</sup>. Situation 2 projects the effects for the remaining storage capacity with an adjusted leak opening of 600 m<sup>2</sup>.

The dykes around the Eastern Scheldt are designed to prevent failure mechanisms wave overtopping and macro-instability in particular. Macro-instability is beyond the scope of this research. However, it can be noted that all dyke sections should be re-assessed according to WBI-2017 due to the following:

- changes of the model and assessment method;
- increased hydraulic requirements;
- increased safety factors (Witteveen+Bos, 2017).

Failure mechanism piping is probably not an issue for the Eastern Scheldt dykes (Witteveen+Bos, 2017).

It can be considered that the hydraulic loads for some dykes become too high at an average water level of +3.60 and +3.70 m NAP or more, in terms of wave overtopping and macro-instability for T=4,000 and T=10,000 respectively (Table 7.11). The maximum water levels among 12 locations on the Eastern Scheldt according to Hydra-NL, are provided in Chapter 6. The results of the manual calculation are shown in Table 7.13 and 7.14 and Figure 7.4.

Table 7.13: Results water level and storage capacity of Eastern Scheldt. [1] Leak opening of 1250 m<sup>2</sup>. Red: exceedance of the storage capacity.

Sea level rise [m] (A)	Return Period [yr.] (B)	Sea level [+m NAP] (C)	Average flow velocity [m/s] (D)	Leakage [m <sup>3</sup> /s] (E) [1]	Average overtopping [m <sup>3</sup> /s] (F)	Closure water level [+m NAP] (G)	Closure time [hr.] (H)	Average peak water level of OS [+m NAP] (I)	Water level [+m NAP] OS 1-12 (Hydra) (J)
0.05	4,000	5.18	4.82	6,025	1,318	0.5	20	2.04	3.40-4.11
0.05	10,000	5.44	4.96	6,200	1,782	0.5	20	2.18	3.48-4.17
0.81	4,000	5.94	4.82	6,025	3,628	1.26	20	3.29	3.66-4.16
0.81	4,000	5.94	5.20	6,500	2,419	0.5	30	3.31	3.66-4.16
0.81	10,000	6.2	4.96	6,200	4,293	1.26	20	3.46	3.78-4.24
1.28	4,000	6.41	4.82	6,025	4,651	1.73	20	3.97	3.87-4.22
1.28	10,000	6.67	4.96	6,200	5,600	1.73	20	4.21	4.06-4.33
1.40	4,000	6.53	4.82	6,025	4,978	1.85	20	4.16	3.95-4.26
1.40	10,000	6.75	4.93	6,163	5,864	1.85	20	4.37	4.17-4.38

The values in column I feature the maximum water levels in the OS under the condition of a fully reliable closure procedure. The effect of the failure rate of the floodgates of the OSK is computed in Section 7.1.5. The aim is to reach a water level of +1 m NAP in the OS during a closure. Based on the data of previous closures, the floodgates usually close at a sea level of 0.5 m NAP (Appendix Q). It is considered that this is still possible during ebb before the start of an extreme high-water event. The result is that the water level at the end of the storm is just above +2 m NAP due to leakage and wave overtopping. This gives a considerable margin, meaning that it is also allowed to close at +1 m NAP. It should be noted that this value only applies to an optimally functioning closure of the OSK. The results of column J expresses the maximal water levels obtained from Hydra-NL. These values include the likelihood of an emergency closure (starting at +3 m NAP) and a non-closure. Water levels in the Eastern Scheldt may exceed the closing requirement of +3.00 m NAP by 0.6-1.2 m without exceeding the critical water level (Table 7.10). An emergency closure is not assessed in this analysis but is included in the tipping point analysis.

Sea level rise leads to an increased closing water level or a substantial longer closure period. At 0.81 m sea level rise, the difference between the outcomes of the calculation and Hydra-NL reduces significantly. The calculated maximum water level averaged over the Eastern Scheldt is +3.46 m NAP (T=10,000). Closing 10 hours in advance at a lower sea level of +0.5 m NAP is not beneficial due to the increased volume of leakage. This is shown in Table 7.13 for scenario (SLR: 0.81 m; T=4,000). These results show that it is preferred to close as late as possible to reduce the total leak volume during the closure. The consequence is that the floodgates cannot close at a water

level lower than +1.26 m NAP (0.81 m SLR). This is also visible in Figure 7.4. It can be concluded that the storm surge barrier cannot fulfil the requirements for the storage capacity for approximately 0.95 m SLR for T=10,000, without significant reinforcements of all dykes around the Eastern Scheldt.

However, reducing the leak opening of the barrier lowers the maximum water levels in the Eastern Scheldt significantly during a closure. Table 7.14 shows the results of the water level and storage for a reduced leak opening of 600 m<sup>2</sup>. The reduction of the water levels in the Eastern Scheldt is at least 0.72 m. This adjustment improves the effectivity of the OSK considerably. The water levels in the Eastern Scheldt (T=10,000) are expected to reach the critical limit of +3.7 m NAP after 1.43 m SLR (Figure 7.4).

However, if the choice is made to close 10 hours earlier at a low water level of 0.75 m NAP, the storage capacity will not be exceeded for more than 1.5 m SLR (Figure 7.4).

It can be concluded that the risk of exceeding the storage capacity reduces considerably after reducing the leak opening of the storm surge barrier. However, the consequence is that the OSK must be closed very often by more than 1 m SLR which is calculated in Section 7.1.6. Furthermore, the risk of a non-closure also increases to a large extent due to the higher sea level and more required closures which is calculated in Section 7.1.5 and included in Section 7.2.1.

In the end, it can be stated with some certainty that the risk of exceeding the storage capacity will not form a tipping point for the OSK after adjusting the leak opening to 600 m<sup>2</sup>.

Table 7.14: Results water level and storage capacity of Eastern Scheldt. [2] Leak opening of 600 m<sup>2</sup>.

Sea level rise [m] (A)	Return Period [yr] (B)	Sea level [+m NAP] (C)	Average flow velocity [m/s] (D)	Leakage [m <sup>3</sup> /s] (E) [2]	Average overtopping [m <sup>3</sup> /s] (F)	Closure water level [+m NAP] (G)	Closure time [hr.] (H)	Average peak water level of OS [+m NAP] (I)	Water level change compared to [1] [m]
0.05	4,000	5.18	4.29	2,574	1,318	0.5	20	1.32	-0.72
0.05	10,000	5.44	4.41	2,646	1,782	0.5	20	1.43	-0.75
0.81	4,000	5.94	4.29	2,574	3,628	1.26	20	2.56	-0.73
0.81	10,000	6.2	4.41	2,646	4,293	1.26	20	2.72	-0.74
1,28	4,000	6,41	4,29	2,574	4,651	1,73	20	3,25	-0.72
1.28	10,000	6.67	4.39	2,634	5,600	1.73	20	3.46	-0.75
1.28	4,000	6.41	4.78	2,868	3,101	0.6	30	2.48	-1.49
1.28	10,000	6.67	4.89	2,934	3,733	0.6	30	2.7	-1.51
1.40	4,000	6.53	4.29	2,574	4,978	1.85	20	3.44	-0.72
1.40	10,000	6.75	4.39	2,634	5,864	1.85	20	3.63	-0.74
1.40	4,000	6.53	4.77	2,862	3,319	0.75	30	2.70	-1.46
1.40	10,000	6.75	4.86	2,916	3,909	0.75	30	2.90	-1.47
1.50	4,000	6.63	4.29	2,574	5,287	1.95	20	3.60	-0.72
1.50	10,000	6.89	4.41	2,646	6,319	1.95	20	3.83	-0.75
1.50	4,000	6.63	4.77	2,862	3,525	0.85	30	2.86	-1.46
1.50	10,000	6.89	4.88	2,928	4,213	0.85	30	3.10	-1.48
1.6	4,000	6.73	4.29	2,574	5,608	2.05	20	3.77	-0.72
1.6	10,000	6.99	4.41	2,646	6,680	2.05	20	4.01	-0.74
1.6	4,000	6.73	4.77	2,862	3,739	0.95	30	3.03	-1.46
1.6	10,000	6.99	4.88	2,928	4,453	0.95	30	3.27	-1.48

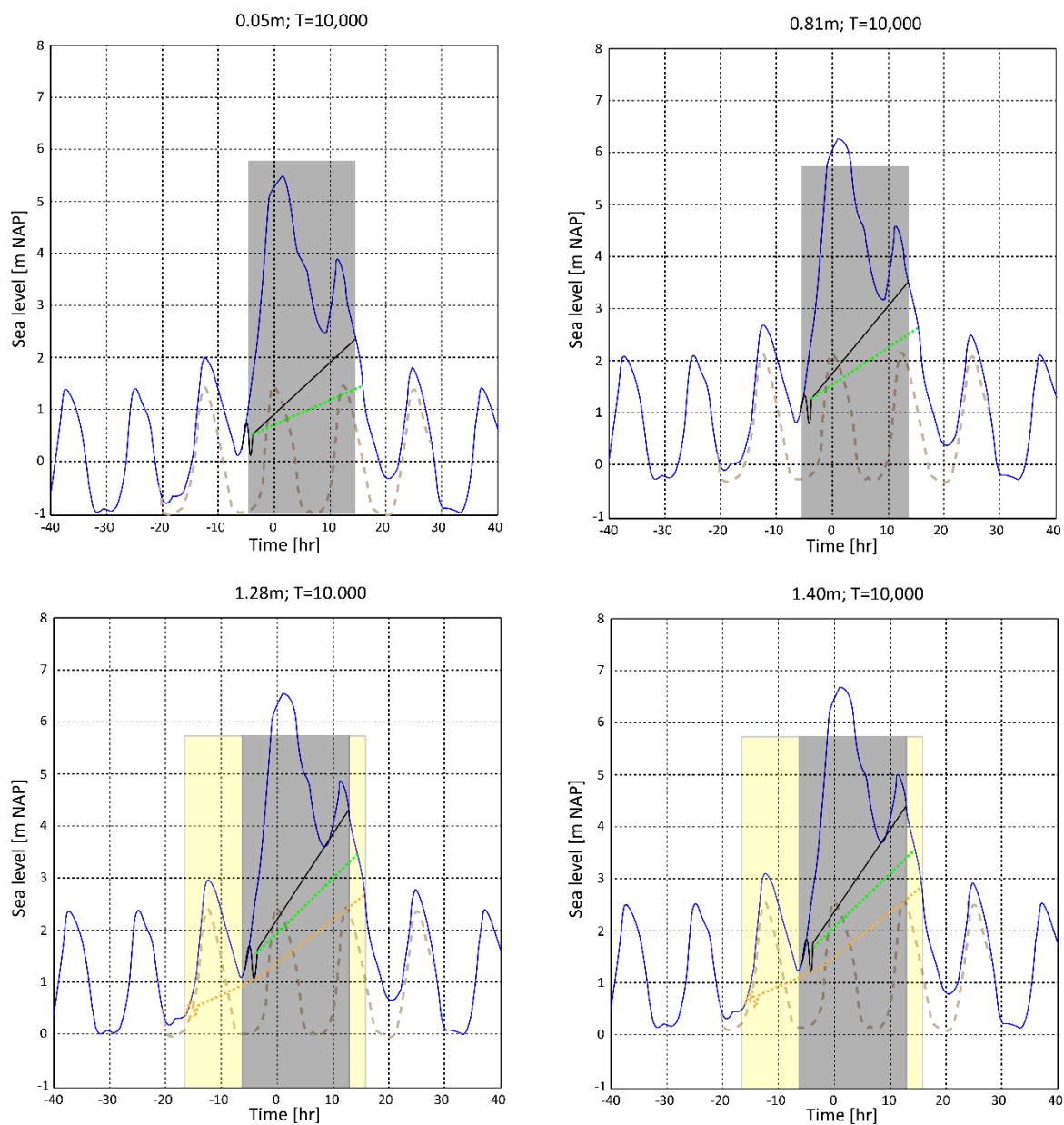


Figure 7.4: High-water event for the OSK including closing time and water level increase in the Eastern Scheldt. Black: leak opening 1250 m<sup>2</sup>, green: leak opening 600 m<sup>2</sup>, orange: leak opening 600 m<sup>2</sup> and an early closure. Blue: sea level. Shaded grey: closed period. Shaded yellow: potential additional closing time.

### **7.1.2.2 Risk of erosion to the soil protection due to water overrun**

Another potential risk is erosion of the soil protection behind the barrier due to water overrun. Failing soil protection might undermine the construction which leads to instability of the construction.

A manual calculation is made to quantify the risk of failing soil protection under maximal hydraulic loads, according to the requirements of WBI-2017 (Appendix M). The top layer of the soil protection of the MLK consists of large stones with an estimated weight between 3,000-6,000 kg. The maximum stone grading behind the floodgates of the OSK is 6,000-10,000 kg.

Water overrun over the top of the vertical barrier can lead to turbulence behind the floodgates, but the load on the soil protection is considerably lower than in the case of failing or semi-closed floodgates. In addition, the large water depth behind the barrier decreases the force of the overtopping water to a large extent. The calculation is made by considering the most extreme high-end situation (>10,000 l/s/m overtopping). Based on the results of Appendix M, the risk of this failure mechanism is negligible for both the Maeslant Barrier and Eastern Scheldt Barrier. It should be noted that partially opening the floodgates during a high-water event is a risk to the storm surge barriers, which is discussed in Appendix P.

### **7.1.2.3 Risk of construction failure due to vibrations**

Massive overrun of water over the top of storm surge barriers can result in vibrations in the structure which have not been analysed yet. The maximal overtopping requirement for the floodgates of shipping locks is 1,000 l/s/m because more overtopping can result in vibrations in the gates and hydraulic structure (Rijkswaterstaat, 2017d). The design requirements of the MLK and OSK does not specify a maximum rate of water overrun and wave overtopping

Important to note is that the behaviour of the construction is difficult to predict in a high-end situation with the massive amount of overflowing water. The combination of overflow and wave impacts can lead to a higher load than currently provided in the design.

The Maeslant Barrier could be relatively susceptible to vibrations because of the moving floodgates. Also, the MLK is entirely made of steel, which is considered relatively vulnerable to vibrations compared to the concrete construction and horizontally fixed floodgates of the OSK. The MLK is designed for 50 cm sea level rise and should, therefore, be resistant to a higher volume of overtopping than 1,000 l/s/m if the water level difference (hydraulic head) stays below 4 m. The MLK is a unique construction where expert judgment should determine the requirements.

Nevertheless, vibrations remain a significant risk to the performance of the MLK and should be investigated explicitly. Further research will have to point out which allowances should be enforced. The recommended adjustment which limits wave overtopping to a large extent is described in Section 7.1.3 and 7.2.1.

The construction of the OSK was originally not intended for substantially increased hydraulic loads caused by the accelerated sea level rise. However, the structure is designed for significant wave overtopping. The construction is calculated on waves of 6.2 m high and a water level equal to the crest height which is +5.8 m NAP (Rijkswaterstaat, 1991). This corresponds to a volume of wave overtopping of approximately 6,200 l/s/m according to Formula [6] which is described in Appendix M. The design waves are much larger than in the actual situation. Also, considerable safety surcharges have been applied during the design. More information can be found in Section 7.1.3.

Therefore, it is assumed that significant amount of overflow is acceptable for the OSK because of the margins in the strength of the construction. It is assumed that this failure mechanism is not decisive for the tipping point analysis of the OSK because it is unlikely that vibrations will occur in high-end situations. Nevertheless, it is recommended to investigate the effects on the construction with a large volume of water overrun.

### 7.1.3 The risk to the construction of storm surge barriers

The strength and stability of the construction of the storm surge barriers are one of the most critical aspects in the analysis of the remaining lifetime. This section will describe the strength generally because the strength and stability are not the primary focus of this research.

However, after discussions with specialists, it appeared that the strength of the MLK could be decisive in the tipping point analysis. The strength is related to water levels and hydraulic loads because the storm surge barriers have to absorb the forces of the difference between the sea level and the water level on the landward side (hydraulic head). A change to the landward water level, therefore, influences the maximum sea level that the flood defence could withstand. The OSK, on the other hand, is relatively robust so that the strength and stability should not be an issue during significant sea level rise. The state and robustness of the soil protection are also important in determining the stability of the storm surge barriers.

The primary risk for the construction of the storm surge barriers is the following:

*“The construction and stability of the barriers might be insufficient against increasing hydraulic loads.”*

The cause of this risk event is the increasing hydraulic load on the storm surge barriers under extreme high-water events due to sea level rise and climate change. The main consequence might be that these storm surge barriers are disapproved before the end of their lifetime.

#### 7.1.3.1 The risk to the construction of the Maeslant Barrier

The Maeslant Barrier is a unique construction that is open during daily conditions and can close during storm conditions. During the storm closure, the difference between the outside and the inside water level will increase. As a result, the forces on the ball-shaping joint will increase significantly.

The ball joint is a very complicated component of the MLK with a maximal design load of 30,000 tons each. This corresponds to a difference in water level of more than 4 m, including a significant safety surcharge. This load will be absorbed by the fixed bearing part “achterstoel” located behind the joint. The fixed bearing part and the total construction including the foundation is designed to absorb 35,000 tons of positive water pressure.

The ball joint is not designed for a large negative force, exerted by a higher water level of the river. This pulling force (negative water level difference) is absorbed by the “voorstoel”, which is much smaller. The maximal acceptable positive pressure is 6,500 tons, translated to a difference in water level of 1.5 m. Therefore, it is necessary to open the doors quickly at a lower sea water level.

It can be assumed that the joint is the weakest component in the construction. Therefore, the design load of 30,000 tons should never be exceeded during a closure. The difference between the inside and outside water level determines the forces on the flood defence. This is also the main reason that two closing criteria have been established to minimize the load on the joint. These criteria are discussed in Section 7.1.4 and Appendix H.

An important fact during the closure is to minimise the loads exerted on the concrete threshold block on the bottom of the river. This has been done to minimise settlement of the blocks. This can be achieved by partly filling the floodgates with water to limit the weight. The blocks are calculated on a total load of 10,000 tons.

It can be presumed that all forces are transferred to the ball-shaped joint and that no shear force is exerted on the bottom (Figure 7.5). An additional advantage is that the barrier can float quickly due to the minimal volume of water stored inside the doors. At very high-water levels, the doors should be entirely full-pumped to be able to sink. Also, in this extreme situation, the shear stress on the threshold blocks is negligible.

Another aspect is that fatigue damage can occur in some components if the barrier closes very often during heavy loads. However, it is considered that fatigue damage is not an issue in the strength of the barrier because many elements could be maintained or replaced.

Failing soil protection does not entirely determine the stability of the storm surge barrier. The joint, located on land determines the actual strength of the barrier. Failing soil protection might lead to deviations between the concrete threshold blocks but is not considered to collapse the storm surge barrier. The assessment of the soil

protection is performed in Appendix M and P. Any deviations between the blocks can only affect the height of both floodgates. Therefore, it can be concluded that the water level difference (hydraulic head) is decisive in the analysis of the strength of the MLK.

Figure 7.5 and 7.6 show an implied scheme of the floodgate and the horizontal forces exerted on the doors. It is stated in the design handbooks that the barrier is designed to withstand a water level difference of 4 m according to figure 7.5. Figure 7.6 features a higher sea level that might occur with sea level rise. Water overrun significantly increase the hydraulic pressure on the floodgates which is visualised in Figure 7.6.

The water level in front of the barrier reduces during large volume of water overrun, which reduces the hydraulic load of the floodgates. However, this is not included in the calculation.

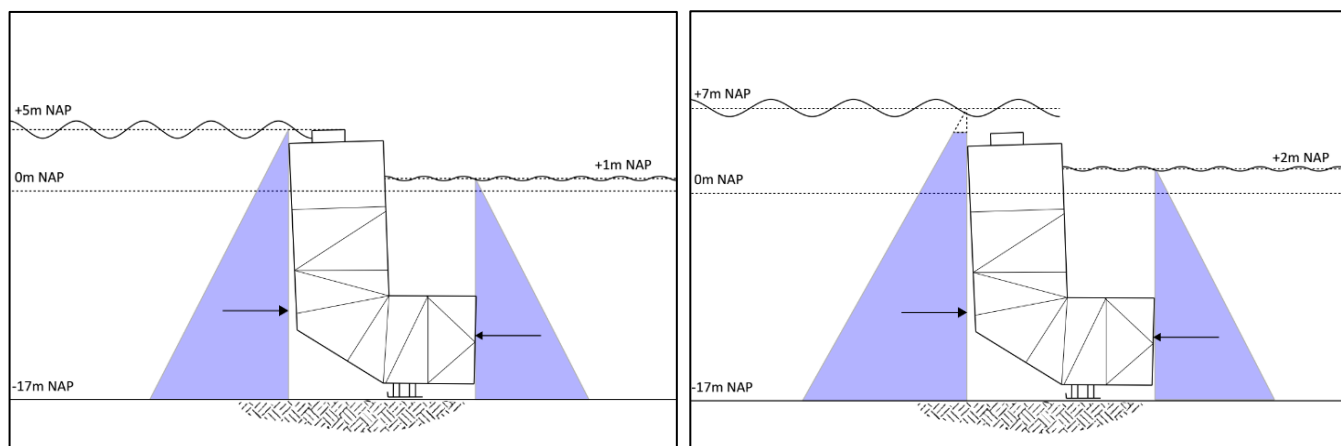


Figure 7.5: Schematic view of the hydraulic loads on the floodgates without water overrun.

Figure 7.6: Schematic view of the hydraulic loads on the floodgates including water overrun.

## Results

The results for the horizontal load on the ball-shaped joint are shown in Table 7.15. The values are calculated using the input parameters described in Appendix O which also features more high-water situations.

Table 7.15: Horizontal load on the floodgates of the MLK for different water levels. The safety margin (%) and uncertainty factors  $\gamma=1.2-1.5$  are applied to include uncertainty factors.

Sea level [m NAP]	Inland water level [m NAP]	Difference [m]	Total load on the ball-joint [ton]			Acceptable?
			$\gamma=1.2$	$\gamma=1.5$	Margin	
5.0	1.0	4.0	45,022	56,277	37.47%	Yes
5.5	1.0	4.5	50,921	63,651	29.28%	Probably
5.5	1.5	4.0	38,455	57,683	35.91%	Yes
6.0	2.0	4.0	47,141	58,926	34.53%	Yes
6.5	2.0	4.5	53,040	66,300	33.33%	Probably
7.0	1.5	5.5	63,844	79,805	11.33%	No
7.0	2.0	5.0	58,938	73,673	18.14%	Probably
7.5	2.0	5.5	64,837	81,047	9.95%	No

The results of Table 7.15 specify that the MLK can withstand a water level difference (hydraulic head) of 4 m. Also, a hydraulic head of 5 m should be possible. However, the safety margins are relatively limited in that case. The translation wave behind the barrier increases the water level difference and, therefore, increase the load on the barrier. This wave can temporarily lower the water level by more than 50 cm just behind the floodgates. This can significantly increase the load on the barrier.

Water overrun occurs in addition to wave overtopping at a water level above +5 m NAP. The extra hydraulic horizontal pressure on the doors is significant in that situation. It can be concluded that the MLK can withstand a maximum sea level of +6.5 m NAP under the condition that the river water level should be less than +2.5 m NAP at the same moment. It is eventually possible to close-off an even higher sea water level, but the safety margin decreases to less than 26%. A sea level of +7.5 m NAP is the absolute upper limit of the MLK combined with an inside water level of +2.5 m NAP. However, due to the uncertainty of the exact water level close to both sides of the MLK and the additional hydraulic load caused by waves, a hydraulic head of 4 m will be used as the critical limit.

Important to note is that the behaviour of the construction is difficult to predict in such high-end situation. The combination of overflow and wave impacts can lead to a higher load than currently provided. However, a large volume of water overrun will reduce the water level in front of the MLK due to the flow speed.

### **Consequence**

Two closing criteria have been established to minimise the load on the construction of the MLK:

- *Water level closure* (Dutch: “Peilsluiting”); closure starts at a water level +2.0 m NAP during a river discharge of <6,000 m<sup>3</sup>/s.
- *Turnaround closure* (Dutch: “Kenteringsluiting”); closure starts at the turning point from ebb to flood. The closure starts at roughly +0.5-1 m NAP during a river discharge of >6,000 m<sup>3</sup>/s.

More information about these criteria is given in Appendix H. The water level closure is intended to reduce the load on the barrier during the closure. The barrier must be able to withstand a water level of at least +6 m NAP by implementing this type of closure. A turnaround closure will lead to a higher load on the barrier due to the aimed low-water closure. The water level can increase by more than 5 m during one tidal period with springtide and increasing storm surge. The contribution of the tidal wave is about 3 m and storm surge could be 2 m. The hydraulic loads may be too high to bear for the storm surge barrier for a turnaround closure if certain extreme high water levels are expected. A solution for this is proposed on p. 98.

An additional strategy can be implemented to reduce the risk of a collapse of the storm surge barrier by temporal exceedance of the maximal water level difference. It is advised to adjust the closing regime (closing time) to the forecasted sea water level during an extreme high-water event. In addition, it is required to implement an additional condition for the closing criteria:

- maximize the water level difference (hydraulic head) to 4 m.

This condition mainly relates to the turnaround closure. It is essential to analyse and minimise the hydraulic head between both sides of the floodgates. The current prevailing closing criteria should be sufficient for moderate storms, but the prescribed extra condition is required for the extreme situations.

The floodgates should be partially raised to reduce the horizontal load if the difference in water level threatens to exceed 4 m. The functionality of the MLK will decrease slightly but should be enough to prevent unusually high-water levels in the delta. Another option might be to install valves (Dutch: “doorlaatopeningen”) within the floodgates to allow a water passage to reduce the horizontal load on the floodgates. It is advised to evaluate both options as potential solutions to the strength limitation of the MLK.

It can be argued that the exceedance of some critical water levels in the RMD is preferable compared to the collapse of the MLK, making this condition necessary. The consequence for the hinterland is that water levels will increase with sea level rise and more heavy storms might occur in the future. This risk is related to the risk of exceeding the storage capacity, where the required height of the dykes is central. This condition will be included in the analysis of the dykes in the hinterland.

It is worth mentioning that a considerable safety margin has been included in the given conditions. The barrier could theoretically withstand a hydraulic head of 5.5 m. However, wind waves and a translation wave can increase the hydraulic load. Also, the water levels are measured at 500 m from the floodgates, which means that the actual water level difference could be higher. As a result, the boundary condition has been set at 4 m. More research should be performed to investigate whether this requirement can be changed.

### **The tradeoff between construction and storage capacity**

The limited strength of the ball-joint has a large influence on the tipping point analysis which is based on the expected high-water levels for T=10,000 and T=30,000. This implies that the closing level is very important in the analysis of the storage capacity and the horizontal force on the storm surge barrier. A tradeoff should be made between the load on the construction and the storage capacity by modifying the closing water level.

The data of the closure of November 2007 (Appendix Q) shows that the stabilized water level in the RMD (two hours delayed due to the closing procedure) is 20 cm higher than the sea level at the start of the closure. However, this was for a relatively low water closure (turnaround closure). On the other hand, the water level closure of 2018 showed that the water level in the RMD stabilizes at a lower level +1.50 m NAP despite the start of the closure at +2 m NAP. All closures have been analyzed in Appendix Q.

The sea level peak will probably occur circa 2-3 hours after the start of the closure, similar to the stabilization point of the water level in the RMD. According to Section 7.1.4, the maximal water level closure can take place at an average water level of +2.25 m NAP in the RMD during a high-water event with T=30,000. This can only be obtained during a late closure and slow sinking process because otherwise, a lower water level will be achieved in the water system which can damage the MLK during extreme conditions.

If the actual water level after closing is lower than the required 2.25 m NAP, the doors should be partially raised by 2 m during the high-water peak in front of the barrier to lower the horizontal force on the floodgates. It is not expected that the floodgates of the HK should be raised. Combining all aspects of both risk factors result in the following tipping points, provided in Table 7.16.

*Table 7.16: Tipping points in terms of the combination of risk 1 and 2. Green: acceptable situation. Orange: Critical situation. Red: exceedance of the horizontal load requirement ( $\Delta h > 4$  m).*

Exceedance frequency [1/yr]	SLR [m] Compared to the year 2000	Closing level [m NAP]	Sea level peak [m NAP]	Water level in RMD during peak [m NAP]	Maximal water level difference [m]
1/10,000	0.05 m	2.00	5.70	2.00	3.70
1/30,000	0.05 m	2.00	6.07	2.25 (slow sinking process)	3.82
1/10,000	0.30 m	2.00	5.90	2.00	3.90
1/30,000	0.30 m	2.00	6.27	2.25 (slow sinking process)	4.02
1/10,000	0.65 m	2.25	6.20	2.25	3.95
1/30,000	0.65 m	2.25	6.58	2.25	4.33

It will be supposed that 4 m water level difference between the sea level and the water level behind the floodgates is the maximum permissible hydraulic head. Implementing this requirement has a large effect on the remaining lifetime of the MLK. The tipping point for the construction is 30 cm SLR for T=30,000. However, the tipping point is 65 cm sea level using the exceedance frequency of 1/10,000 per year. Important to note is that these results are the optimum of the tradeoff between the construction and the storage capacity and under the condition of changing the closing process to the expected conditions. The impact of the other risks to the tipping points are assessed in the next sections.

To conclude, it is of primary importance to adjust the sinking process of the MLK to limit the hydraulic head to maximal 4 m and to partially raise the floodgates if this value tends to be exceeded during extreme conditions. Without changing the sinking process, a risk exists that the MLK will be disapproved in the next assessment round.

### ***Response: Temporarily raise the floodgates during high-water peak***

The tipping point of 30 cm sea level rise for T=30,000 is the decisive factor in the tipping point analysis of the Maeslant Barrier. The peak water level in front of the MLK can reach +6.27 m NAP in that situation. Peak water levels occur for only 2-3 hours. It may, therefore, be effective to raise the floodgates partially during peak water levels to prevent an exceedance of the maximum horizontal load on the floodgates. This adjustment can extend the tipping point considerably. The recommended measure is the following:

- Temporarily raise the floodgates by 1-2 m during peak water levels of more than +5 m NAP.

The MLK can withstand a higher water level when the floodgates are raised during the high-water peak. The force on the construction reduces to a large extent due to the water discharge underneath the floodgates. By raising the floodgates with 2 m, the water-retaining height increases to +7 m NAP. This reduces the volume of wave overtopping significantly, making the risk of vibrations, caused by water overrun, irrelevant.

The construction should be able to withstand a water level of +6.50 m on the outside with a water level of +2 m NAP at the inside when the floodgates partially float. Also, the significant flow under the doors will reduce the actual water level against the floodgates. Therefore, the effective sea level which should be acceptable is +6.75 m NAP. This corresponds to 0.8 m SLR for T=30,000 and 1.2 m SLR for T=10,000.

The discharge increases the water level in the Rhine-Meuse Delta during the temporarily rise of the floodgates. The specific discharge per meter width can be calculated using the following formula:

$$q = \mu h_s \sqrt{2g(\Delta H)} \quad [1]$$

- $q$ : specific discharge [ $\text{m}^2/\text{s}$ ];
- $\mu$ : contraction coefficient [-];
- $h_s$ : opening gap of the floodgates [m];
- $\Delta H$ : energy head difference [m];
- $g$ : gravitational acceleration [ $\text{m}/\text{s}^2$ ].

The results are calculated in Appendix P. The average water level difference during the opening is 4 m, resulting in a specific discharge of 15.95  $\text{m}^2/\text{s}$  and a flow velocity of 8.86  $\text{m}/\text{s}$ . The floodgates should be raised by 2 m for roughly 3 hours according to the model storm for 0.81 m SLR and T=30,000. The total discharge is 5741  $\text{m}^3/\text{s}$  and a contribution of 25 cm to the water level in the RMD. However, the net contribution is 17 cm due to the much lower volume of wave overtopping over the top of the MLK for both T=30,000 and T=10,000. This result is equivalent to the results of Rijkswaterstaat (2006).

In addition, the floodgates can close considerably earlier in the case of an approaching extreme high-water event due to the larger margin in the strength of the MLK. Instead of closing at +2.25 m NAP, the doors are able to close at 2 m NAP or lower, increasing the storage capacity by at least 25 cm.

The recommendation to raise the floodgates temporarily with 2 m during very high-water level leads to an increased load on soil protection. The required stone grading is calculated in Appendix P using formulas of Izbash [15] and Shields [19]. It appears that a hydraulic head of more than 3.5 m results to small movements of the stones of the top layer (shields parameter ( $\Psi$ ) >0.032). However, it is not expected that damage occurs for a water level difference lower than 3.5 m.

Damage can occur for a water level difference of 3.5-4.5 m, but a collapse is not expected. The collapse criterium is a Shields parameter ( $\Psi$ ) of 0.045 [-], resulting in a loss of stones but not a collapse of the soil protection of the MLK. Nevertheless, raising the floodgates at a peak water level of more than +5 m NAP increase the risk for the soil protection, but a failure is not expected. In addition, peak levels of more than +5 m NAP are rare and therefore, it might be allowed to damage the soil protection to a small extent. Ultimately, this consideration should be discussed in more detail.

### 7.1.3.2 The risk to the construction of the Eastern Scheldt Barrier

The concrete structure of the Eastern Scheldt Barrier (OSK) is fixed and therefore relatively robust compared to the flexible ball-shaped joint of the MLK. The 62 floodgates of the OSK can move vertically only within the 65 concrete pillars. The elements of the construction are described in more detail in Appendix H. This section is about the strength of the storm surge barrier during extreme hydraulic loads to assess the robustness to SLR.

It is assumed that the technical tipping point is not influenced by the soil protection. Increased hydraulic loads due to SLR will increase the flow velocity during a failing floodgate (failed to close) but will probably not damage the soil protection to such an extent to threaten the barrier. The current state of the soil protection will be extensively monitored and maintained. Further research should indicate the potential tipping point of the soil protection.

The OSK is designed according to various design formulas given in the design handbooks (Rijkswaterstaat, 1991).

The water-retaining height of the OSK is +5.6-5.8 m NAP, depending on the location. The design incorporated 40 cm relative sea level rise during the planned 200-year lifetime of the storm surge barrier. Sea level rise will probably increase significantly beyond this design criteria. Also, the recent legislation changes result in a stricter safety standard for the OSK. Therefore, it is required to analyse the used design conditions and the current projections of future SLR to project the technical tipping point of the construction.

In the design philosophy of the storm surge barrier, extreme hydraulic loads were used which have an exceedance frequency of 1/4,000 per year. The following surcharge has been implemented to guarantee that the barrier does not collapse under extreme hydraulic loads:

$$Q_c = 1.4Q_e; \quad [2]$$

$Q_c$ : hydraulic load for a collapse;  
 $Q_e$ : extreme hydraulic loads (1/4,000 per year).

Formula [2] specifies that the construction is designed for a 40% greater load than assumed for the average return period of 4,000 years.

The extreme hydraulic load level includes a maximal water level difference of 6.2 m between both sides and a wave height of 6.2 m (Rijkswaterstaat, 1991). The design assumed a sea level of +5.5 m NAP and a water level of -0.70 m NAP in the Eastern Scheldt. The estimated wave height for the extreme situation was 5.3 m for Roompot and 4.1 m for Hammen and Schaar. In the design, these values have been increased to 6.2 m to incorporate various uncertainties. A considerable volume of wave overtopping is acceptable in that situation.

Furthermore, a safety margin of 50% in the design has been implemented to prevent instability (tilt) from the massive hydraulic horizontal loads (Rijkswaterstaat, 1991). This surcharge compensates for the increased moment force on the barrier due to the higher sea level.

The used hydraulic loads in the design and the revised standard (WBI-2017) are compared to each other in Table 7.17. Sea level rise is not included in these hydraulic loads.

Table 7.17: Water-retaining height of the sections of the OSK and the hydraulic loads (extreme sea level and wave height) excl. sea level rise for  $T=4,000$  and  $T=10,000$ . \*: Design books (Rijkswaterstaat, 1991).

	Section (location)	Hammen	Schaar	Roompot
	Height [m NAP]	5.6	5.80	5.80
Extreme sea level [m NAP]	Exceedance frequency 1/4,000 per year. (1986) *	5.30	5.50	5.50
	Exceedance frequency 1/4,000 per year. (WBI-2017)	5.13	5.14	5.18
	Exceedance frequency 1/10,000 per year. (WBI-2017)	5.40	5.40	5.44
Wave height [m]	Exceedance frequency 1/4,000 per year. (1986) *	6.20	6.20	6.20
	Exceedance frequency 1/4,000 per year. (WBI-2017)	3.81	3.57	3.86
	Exceedance frequency 1/10,000 per year. (WBI-2017)	3.98	3.75	4.06

It can be concluded that the design is relatively robust, despite the low surcharge for sea level rise. The wave load is over-estimated in the design, making the construction resistant to a large volume of wave overtopping.

Sea level rise linearly increases the water level in front of the storm surge barrier (Hydra-NL). The following section analyses whether the construction can withstand more SLR than included in the design.

### Consequences

The consequences of increasing hydraulic loads in the future for the OSK are only considered for the three water-retaining sections (Hammen, Schaar and Roompot). Other elements of the construction are not part of the analysis.

The maximal water level difference of 6.2 m is an essential indicator of the strength of the construction. The aim is to achieve a water level of +1 m NAP in the Eastern Scheldt (during the first high-water closure) which is significantly higher than the design condition (-0.7 m NAP). As a result, the actual hydraulic loads will be considerably lower than calculated in the design. A significant amount of water overrun may be allowed, on the condition that the current closure water level of minimal +1 m NAP in the Eastern Scheldt will be maintained.

In addition, the expectation is that one exceptionally high peak sea level (T=10,000) leads to reduced wave load on the construction. At a sea level of more than +5.8 m NAP, a substantial part of the wave energy passes over the top of the beams of the storm surge barrier (water overrun). A lower water level is then assumed to have a more significant impact on the construction. However, significant water overrun is not encompassed in the design. Therefore, it is difficult to predict the behaviour of the construction for a large volume of water overrun. The combination of overrun and overtopping might lead to vibrations in the construction which are not implemented before (Witteveen+Bos, 2017). Nonetheless, it is expected that water overrun is acceptable because of the large design surcharges. Still, it is recommended to investigate the risk of water overrun for the construction of the OSK.

If vibrations do not have an adverse contribution to the strength, the extreme sea level may be considerably higher than the set standard of +5.3-5.5 m NAP. The condition is that the water level difference between both sides does not exceed 6 m. Therefore, it is advised to implement an additional requirement for the closing criteria:

- Maximize the water level difference to 6 m between the sea level and the water level of the Eastern Scheldt.

Based on the used surcharges, it is assumed that the stability and strength of the concrete construction are not the determining factors in the tipping point analysis. The OSK is probably resistant to a peak sea level of +6.70 m NAP under the assumption that the calculations made during the design are valid. This is comparable to an extreme sea level (T=10,000) combined with 1.35 m sea level rise. Hydra-NL indicates that 1.57 m SLR is required to reach such a sea level peak for T=4,000. It should be noted that the hydraulic loads of a sea level of +6.70 m NAP in combination with 4.4 m waves are comparable to the design requirement given in Table 7.17. Therefore, it is assumed that the OSK can withstand a higher sea level than considered in the design due to the large design surcharges.

### 7.1.4 Closing procedure

This section analyses the risks that may occur during the closure of the storm surge barriers. The focus of this aspect is about the closing criteria and the required time to close the Maeslant Barrier and the Eastern Scheldt Barrier. The primary risk of the closing procedure is the following:

*“The storm surge barrier might close too late due to an inefficient closing procedure”.*

This risk is relevant because the closing procedure might have a substantial contribution to the assessment of the storm surge barriers. The closing procedure should be adaptive and efficient to cope with SLR rise and high-water events because more frequent closures under more severe conditions can take place. This section describes the cause and consequences of this risk. Adjustments to the closing procedure should be made when the risk is relatively significant and contributes to the tipping point of the barrier.

### 7.1.4.1 Closing procedure Maeslant Barrier

The closing procedure might have a significant effect on the effectiveness of the Maeslant Barrier. The closing process takes a relatively long time, and the margins for the dykes in the hinterland are relatively small.

The storm surge barrier closes in advance if the forecasted water level reaches +3.00 m NAP at Rotterdam or +2.90 m NAP at Dordrecht. These two locations are representative of the entire water system of the Rhine-Meuse Delta (RMD). The condition is, therefore, that the barrier must be closed in time to prevent high water levels in the RMD. Urban areas which are not protected by dykes (Dutch: “buitendijkse gebieden”) will flood for water levels above +2.8-3.0m NAP. Hence, it is desirable to avoid a water level of +3.00 m NAP in the RMD.

The dykes are designed to withstand higher water levels to protect low-lying areas against flooding. A safety margin is required to store incoming water from the rivers during a closure of the MLK. The maximum allowable water level in Rotterdam was +3.60 m NAP, emerged from the last assessment round before the regulation change. The required storage height reduces further away from the MLK for areas with a lower prescribed safety standard.

The total time to close (departure and sinking) takes approximately 2 hours. The closing time can be accelerated to 1.5 hours, but this can result in a large translation wave in the harbour of Rotterdam. This accelerated closure took place during the closure on 3 January 2018. It is, therefore, required to start the closure in advance of an approaching high-water to avoid exceeding the maximum water levels in Rotterdam or Dordrecht.

It is necessary to close earlier to increase the margin for the storage capacity during a closure. On the other hand, it is recommended to minimise the water difference between the sea and the river to prevent potential damage to components of the storm surge barrier. This tradeoff is discussed extensively in Chapter 7.1.3.1. To make a consistent judgement; two criteria have been established:

- *Water level closure*: closure starts at a water level +2.0 m NAP during a river discharge of < 6,000 m<sup>3</sup>/s.
- *Turnaround closure*: closure starts at the turning point from ebb to flood. The closure starts at roughly +0.5-1 m NAP during a river discharge of > 6,000 m<sup>3</sup>/s.

The automatic operating system (BOS) of the Maeslant Barrier uses information and statistics of the forecasted water levels, wind speeds and the river discharges to decide which type of closure is required and how long the barrier should be closed.

Normally, the river discharge will be below 6,000 m<sup>3</sup>/s whereby the barrier starts to close at a water level of +2.0 m NAP. This closure provides a relatively low load on the barrier, but the water levels in the hinterland will be relatively high. It takes roughly 2 hours before the barrier is completely closed, resulting in a significant supply of seawater to the water system. This type of closure (water level closure) has recently been implemented in January 2018. This is also the type of closure that poses the risk of (temporarily) exceeding the critical water levels in the Rhine-Meuse Delta. All previous closures of the MLK have been analysed in Appendix Q.

The closure takes on average 130 minutes depending on the situation. The start of the closure begins with the departure of the floodgates. After closing the doors (turning), the floodgates sink to the threshold blocks to complete the closure. A part of the closing procedure is shown in Table 7.18. More information about the closing criteria can be found in Appendix H.

Table 7.18: Time to close the Maeslant Barrier.

-	Start horizontal departure arc-shaped doors (begin with the closure)
+0:30	Floodgates are in place to start sinking process
+0:30 +1:40	The sinking of floodgates is completed, MLK is closed

The turning of the arc-shaped doors takes 30 minutes and cannot be accelerated without significant adjustments. This speed depends on the performance of the “locomobiles” that provides the drive. The sinking can be accelerated to about 60 minutes, but this does result in a translational wave in the harbour. The sinking is controlled by opening different valves which are controlled by the BOS system. The total closing process takes at least 1.5 hours.

The analysis of the closure on 3-1-2018 showed that the floodgates started to close at least 30 minutes later than according to the protocol. This contributes to the fact that considerably high-water levels were achieved in Rotterdam due to the incoming tidal wave (Appendix Q). In this situation, the delay was not a problem for water safety, but the consequences may be more significant in more severe high-water situations.

### ***Analysis of the closure on 3-1-2018***

The cause of the late closure on 3 January 2018 was found after further analysis and inquiries with specialists from the operating team. The full analysis is given in Appendix Q.

First, the used water level statistics measure the average water level for each 10 min. Second, it takes several minutes before the data is received in the BOS system. Third, it takes a while for BOS to calculate the required moment to begin the closure. Fourth, the system is set in such a way that the barrier can only close every 10 minutes. In the end, the delay of the start of the closure is 30-40 minutes. Table 7.19 shows the measured water levels and time before the start of the closure on 3-1-2018 and show the causes of the delayed closure.

Table 7.19: Closing time MLK during the closure of January 2018.

Water levels at the MLK during the closure of 3-1-2018				
Time (measure period)	14:10 (14:05-14:15)	14:20 (14:15-14:25)	14:30 (14:25-14:35)	14:40 (14:35-14:45)
Measured water level [+m NAP]	1.97	2.13	2.25	2.32
Time of received data in BOS	~ 14:20	~ 14:30	~ 14:40	~ 14:50
Calculation in BOS completed	~ 14:25	~ 14:35	~ 14:45	~ 14:55
Closing time	-	<b>14:40</b>	-	-

At 14:10, the water level at the MLK exceeded +2 m NAP. The closure started at 14:40 and the total closure took in total at least 2:15 hours. Table 7.19 indicates that the actual closing water level was +2.3 m NAP due to the delay. The result is that the tidal wave moves through the harbour without resistance. Important to note is that this delay of 30 minutes is *not* included in the probabilistic assessment model, meaning that the effects for the hinterland tend to be underestimated. This has significant consequences for the peak water level in the RMD.

### **Consequences**

The storm of January 2007 showed that the water level could rise by 2.4 m in just two hours through the incoming tide (Appendix Q). An extreme storm with a yearly probability of 1/10,000 might lead to 3 m rise within this timeframe due to the springtide and the rising storm surge. It should be noted that the MLK closes not automatically if a storm during ebb results in a water level slightly below +2 m NAP. The closing process takes at least 1 hour and 40 minutes and another 30 min for the delay. The water level can rise more than 80 cm in 30 minutes, resulting in a start of an actual water level closure of +2.8 m NAP instead of +2 m NAP measured at the MLK. As a result, a temporal exceedance of the maximum water level of +3.00 m NAP cannot be prevented under these hypothetical conditions. A water level of more than +4.0 m NAP might occur under such circumstances in Rotterdam which is higher than the previous critical water level (MHW) of +3.6 m NAP.

Figure 7.7 (p. 103) features the effect of the late closure to the water level in Rotterdam during a model storm (T=30,000). These water levels are relatively short-lived and occur approximately for one hour. Such situations can also take place during more modest high-water events (+4 m NAP; T=1,000) and much more frequently in the event of a significant sea level rise. This risk significantly affects the performance of the MLK and might have an effect on the tipping point.

Important to note is that the operation team can intervene in time if the forecasted water levels are extremely high. As a result, the consequences for the hinterland might be significantly reduced. After the closure, the water will spread over the entire water system (RMD) and stabilizes at a lower water level. This is also visible in the graph of the closure 3-1-2018 (Appendix Q).

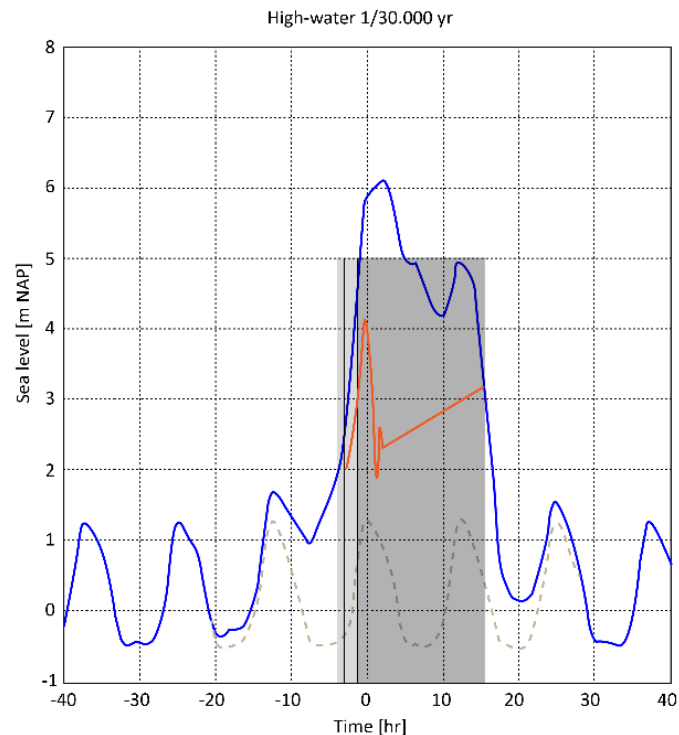


Figure 7.7: Extreme high-water event in front of the MLK including effect for water level of Rotterdam (RMD-5) due current closing procedure (orange). Light gray: time to close.

### **The effect of the tipping point analysis.**

The analysis of the storage capacity and horizontal forces on the construction show that the limited strength of the Maeslant Barrier determines the tipping point. However, the risk of temporarily exceeding critical water levels increase the risk of dyke failures and have an effect on the storage capacity. The probability of this risk is difficult to estimate because of the uncertainties in potential failure mechanisms, high-water statistics and model parameters. Because of the various uncertainties, this effect is not considered decisive in the tipping point analysis of the Maeslant Barrier. Nonetheless, a temporal exceedance of the maximum water level increases the risk of dyke failures. Therefore, it is highly recommended to optimise the closing process of the MLK.

In addition, this temporary high water will occur much more frequently with sea level rise if no adjustments are made to the closing procedure.

### **The effect to the storage capacity**

The propagation speed of the tidal wave in the port of Rotterdam is 8-10 m/s, while the flow rate caused by incoming tide in the Rotterdam waterway (NWW) (Dutch: “Nieuwe Waterweg”) and Hartel canal (Dutch: “Hartelkanaal”) is significantly lower. The analysis of the flow rate and water level increase is performed in Appendix Q.

During the closure on 3-1-2018, the flow rate of the incoming seawater was maximal 1.8 m/s in the NWW and 1.3 m/s in the Hartel canal. The loss of storage capacity in the Rhine-Meuse Delta is roughly 5 cm, because of the delay of 30 min. During an extreme storm, the delayed closure probably results in a water level increase of 0.1 m due to the higher flow rate. Important to note is that this contribution of 0.1 m is not implemented in the current water storage models. The average water level in the RMD is expected to rise 0.25-0.30 m during the closing process ( $\pm 2$  hours) at an extreme storm event with an average return period of 30,000 years. These effects are not yet included in the calculation of the risk of exceeding the storage capacity in the RMD. The effects for the actual closing level of the MLK for both closing procedures are described below.

### **Turnaround closure**

When the floodgates are closed, the water level in the RMD rises by 16 cm per hour and 17 cm per hour for 1/10,000 and 1/30,000 per year respectively. A significant part of the river supply flows into the sea during the

closing procedure. This will diminish the incoming volume of seawater during the closing process due to the relatively large discharge of water from the rivers. As a result, the increase of the water level in the RMD during the closure of the floodgates will be significantly lower than described above. However, according to the water level statistics of previous storms (Appendix Q), the effect of the lag time of the tide in the RMD results in a higher water level in the RMD than at sea during ebb. This effect increases the actual closing level from +0.75 m to +1 m NAP which is included in the calculation of the storage capacity.

In summary, the additional surcharge to the closing level of the turnaround closure should be 25 cm due to the higher water level in the RMD than at sea at the start of the required closure. Therefore, the average water level in the RMD is +1 m NAP at the beginning of the closure. Each centimeter of future SLR will linearly increase the closing level for a turnaround closure.

### Water level closure

A rapid increase in sea level during the combination of storm surge and tide will raise the water level in the RMD during the closure. The average water level in the RMD is expected to rise 0.25-0.3 m during the closing process ( $\pm 2$  hours) at an extreme storm event with an average return period of 30,000 years during a low river discharge. On the other hand, the average water level in the RMD is +1.5-1.7m NAP at the start of the water level closure. This is because the high water arrives at the MLK first, while the average water level in the RMD is still significantly lower. The start of the closing procedure depends on the moment when the water level exceeds +2 m NAP measured at the MLK. Therefore, it is assumed that the average water level in the RMD is similar to the closing level of a water level closure. The effect of the closing procedure to the performance of the MLK is described in the tipping point analysis (Section 7.2.). Sea level rise reduces the margin to perform a water level closure at +2 m NAP and increase the average water level in the RMD. With more than 0.8 m SLR, the water level closure will automatically switch to a turnaround closure.

### Response

Response strategies can be implemented to reduce the risk of flooding by a temporal exceedance of the critical water levels. It is advised to minimise the delay in the closure by changing the following:

1. change the closing procedure to be able to close at any time;
2. change the interval between the water level measurements to 1 minute instead of 10 minutes.

Based on the knowledge of hydraulic specialists, it should be possible to adjust the closing process to be able to close on every minute, without having to adjust the entire system on a large scale. The costs of this adjustment are relatively low, and the total closing time can be reduced by 1-9 minutes. Also, it should be possible to measure the average sea level at an interval of 1 minute instead of 10 minutes. This adjustment is relatively easy to achieve without changing the system. The BOS system dates from 1997 and has a relatively slow processing speed of data. Renewing this system will save a few extra minutes.

It is essential that both adjustments will be made to the system to improve the closing procedure and to reduce the effect of the tidal wave in the water system. As a result, the maximal water level triggered by the tidal wave can reduce by 0.3-1 m. Furthermore, the storage capacity will increase by 0.1 m for a high-water closure due to the lower closing level. This benefit circa 0.05 m for the turnaround closure (situation 1).

On the other hand, it can be decided to lower the closing level to +1.75 m NAP instead of a renewal of the entire BOS system. Consequently, it is no problem that the system has a delay of a few minutes because the closure can start before exceeding +2 m NAP.

The combination of both measures makes it possible to start the closure at the predetermined times without any delay. These adjustments to the procedure reduce the probability of temporary exceeding the critical water level in the hinterland considerably. In addition, these measures are required to be consistent with the probabilistic model of WBI-2017. These models were already based on a water level closure of 2 m NAP without any delays.

The measures are considered to be increasingly important if SLR accelerates due to the improved efficiency of the closing procedure which increases the storage capacity of the water system.

### 7.1.4.2 Closing procedure Eastern Scheldt Barrier

In total, the OSK was closed 27 times (until 1 February 2018) due to high water levels. Since construction, the highest sea level that led to a closure was +3.69 m NAP (27 February 1990). As a reference, the Flood of 1953 resulted in a water level of +4.55 m NAP at Vlissingen.

When the sea level exceeds +2.75 m NAP, the operating team discusses if a closure is needed. The team is obligated to close the gates if the forecasted sea level on the North Sea exceeds +3.00 m NAP. The total closure time takes 82 minutes, so it is essential to investigate the sea level forecasts several hours in advance. An emergency locking system is operational if all operations fail. When this happens, the doors close automatically when currently measured sea level exceeds +3.00 m NAP (Steeneporte, 2014).

On average once per year it is required to close the floodgates of the OSK. The aim is to achieve a water level of +1 m NAP in the Eastern Scheldt during a closure. This water level will be maintained for approximately 10 hours, as the barrier cannot be reopened until the next low tide. If it is predicted that the next high water also exceeds +3 m NAP, the aim is to limit the water level on the Eastern Scheldt to +2 m NAP after the second closure of the barrier. An eventual third closure will limit the water level again at +1 m NAP (Witteveen+Bos, 2017).

In contrast to the Maeslant Barrier, the closure protocol of Eastern Scheldt Barrier is aimed to close well in advance of a high-water event to reduce the hydraulic load on the dykes. It is expected that no or little fatigue damage will occur during a closure which means that the storm surge barrier can close relatively early. This approach leads to a significant reduction in flood risk. During an extreme storm, the hydraulic loads for the dykes are relatively low due to the maintained water level of +1-2 m NAP on the Eastern Scheldt.

There are two situations in the closure procedure which can increase the risk of flooding.

1. Floodgates do not close at a sea level peak just below +3.00 m NAP.
2. Emergency closure.

The most substantial load on the dykes, therefore, takes place if the floodgates remain open due to a water level slightly below +3 m NAP at the North Sea. Also, an emergency closure can lead to severe loads on the dykes, but this probability is only 1% per closure of the storm surge barrier (Deltares, 2017c).

### Consequences

The results of Chapter 6 show that strategic non-closures also can have a significant effect on the hydraulic loads for the dykes around the Eastern Scheldt. The safety margin for some dykes is relatively limited at a water level of 3 m NAP on the Eastern Scheldt during a storm. During more severe conditions, the storm surge barrier must intervene to reduce the hydraulic loads in the estuary. This small safety margin implies that a small underestimation in the forecast of the sea level can lead to the occurrence of very high-water levels on the Eastern Scheldt. Appendix Q shows that water levels of +3.2 m NAP can occur on the Eastern Scheldt when the floodgates do not have to close.

The chance of an emergency closure is very small (1%), as a result of which it only counts a small amount in the probabilistic model. The protocol suggests that the operating team should intervene in time if the barrier does not close automatically. The failure rate of closing some or all floodgates is treated in Section 7.1.5.2. It should be noted that the water level during incoming high-tide can rise by 1.6 m in the 80 minutes, resulting in a potential water level of more than +4 m NAP in the Eastern Scheldt during an emergency closure. Then leakage and wave overtopping over the barrier can further increase the water level in the Eastern Scheldt which increases the risk of flooding. However, the probability of an extreme high-water event and an emergency closure is very small and therefore acceptable ( $\sim 1/1,000,000$  per year). It is not clear whether the dykes (height 6.0-7.3 m NAP) will fail in case of an emergency failure, but wave overtopping is considerably more than 1 l/s/m.

Sea level rise will lead to more frequent closures, but also non-closures can occur more often which increase the hydraulic loads. Raising the closing level to more than +3.00 m NAP, during sea level rise, will substantially increase the hydraulic loads. Any increase in the closing level will lead to the recommendation to reinforce dykes around the Eastern Scheldt.

## Response

Despite the outstanding performance of the OSK, the loads for the dykes can become significant if the floodgates are not closed. It is not required to lower the required closing sea water level, but this will significantly reduce the loads on the dykes in the Eastern Scheldt.

Accelerating the closing procedure does probably not influence the tipping point of the barrier, because the floodgates usually close well in advance of an incoming high-water. An emergency closure can result in critical water levels in the Eastern Scheldt, but the likelihood of this event is relatively small (1%). This risk does not affect the lifetime of the OSK. Therefore, it is advised to accept the relatively small risk of the current closing procedure.

### 7.1.5 Risk of a closing failure

This section analyses the flood risk of the failure rate to close the floodgates of the storm surge barriers. The focus of this aspect is about the failure rate and the projected effect on the maximal water levels in the hinterland. The risk description of a failing closure is the following:

*“The barriers could fail to close during an extremely high-water situation.”*

This risk is relevant because the failure rate has a substantial impact to the assessment of the storm surge barriers. The main consequence is that the water levels behind the barrier might exceed the maximum allowable level in case of a closing failure. Both the probability and consequence of this risk will be analysed in this section. If the risk is relatively significant and contributes to the tipping point of the barrier, response measures will be proposed to reduce the risk of this event.

#### 7.1.5.1 Maeslant Barrier

The Maeslant Barrier (MLK) should be able to prevent a flood in Rotterdam with a yearly probability of 1/30,000 per year. Therefore, the MLK should reduce the water level in the hinterland to prevent flooding. However, both the MLK and the Hartel Barrier (HK) are complex barriers with reliability lower than 100%. This implies that always a chance exists that one of the barriers can fail during a required closure. The failure rate of the MLK and HK influences the critical water level in the hinterland. The assessment system, therefore, considers the probability that the barrier will not close.

The original design requirement of the MLK was a minimum reliability of 99,9% or a failure rate of 1/1000 per closure. The required reliability should be achieved by a fully automated operation, explained in Appendix H. However, in 2005, it turned out that the actual reliability was circa 90%. Subsequently, large-scale research has been conducted into the chance of failure. Finally, it was decided in 2006 that a failure probability of 1/100 per closure would be acceptable (HKV, 2012). Since then, many improvements and optimisations have been made which result in the actual reliability of at least 99%.

The probability of failure of the MLK is set equal to 1/100 per closure in WBI-2017. This value has been used in the Hydra-NL calculations. The permissible failure probability of the HK is 1/10 per closure. However, the failure rate of the HK has almost no influence (few centimeters) on the critical water levels in the Rhine-Meuse Delta (Deugd, 2007). For technical reasons, the failure rate of the HK is therefore always equated with the probability of failure MLK, which is set on 1/100 per closing question in the Hydra calculations (Deltares, 2017c).

Sea level rise increases the risk of a closing failure significantly. The failure rate to close the MLK is currently 1/100 per closure and the floodgates close on average once per 10 years. Therefore, the probability of one non-closure is 1/1,000 per year. At 1 m sea level rise, the probability of a non-closure increase to 1/25 per year due to the more frequent closures.

Sea level rise is the main reason for the increased hydraulic loads on the dykes in the hinterland. However, the increased failure probability of a non-closure per year does not imply that the likelihood of a non-closure during the most extreme high-water event increase. The probability that the closure fails during more moderate circumstances (sea level of +3.0-3.5 m NAP) will rise significantly due to more frequent closures in the future. More information about the closing frequency can be found in Section 7.1.6.

The effects of the failure rate of the Europort Barrier to the maximal water levels of the test locations in the RMD are calculated in Table 7.20. A considerable gain can still be achieved by further improving the reliability. Results from Hydra-NL indicate that the maximum water level in Rotterdam can reduce by 10 cm when the failure rate of the MLK reduces to 1/10,000 per closure. The storage capacity is calculated in Section 7.1.2 with a 100% reliability of the MLK. Therefore, this factor added in the tipping point analysis of the water storage (Section 7.2.1).

The effect of the failure rate including SLR is substantial for Rotterdam. The surcharge for the water level of RMD-5 ( $T=30,000$ ) is 48 cm at 0.8 m SLR. The effect for the other locations in the RMD, except RMD-6, is almost negligible. For  $T=10,000$ , the surcharge for the water level of RMD-5 is 28 cm. The effect of the failure rate to the water level at RMD-5 is visualized in Figure 7.8. These values should be added to the tipping point analysis.

Table 7.20 also shows the effectiveness of the storm surge barriers regarding reducing the water level in the Rhine-Meuse Delta. The peak water level increase to 5.16 m NAP in Rotterdam (RMD-5) during an extreme high-water event ( $T=30,000$ ) and a failing MLK. Important to note is that a failing MLK results in a large amount of water overrun at RMD-6 during an extreme high-water ( $T=10,000$ ). This result indicates that dyke section 16-2 should be strengthened in the short term.

Table 7.20: Effect of the failure rate of the MLK to the water levels in the RMD. Shaded blue: effects of 0.05 m SLR (2023). Shaded yellow: effects of 0.81 m SLR (P50 RCP4.5).

Rhine-Meuse Delta								
Sea level scenario	Test location	RMD-1	RMD-2	RMD-3	RMD-4	RMD-5	RMD-6	RMD-7
	Standard (WBI-2017)	1/1,000	1/300	1/300	1/10,000	1/30,000	1/10,000	1/1,000
	Crest height [m NAP]	4.70	3.80	4.35	5.79	5.23	3.76	5.53
0.05 m (Year 2023)	Water level [m NAP] 1/100 [1]	3.02	2.86	2.74	5.16	3.93	2.20	3.31
	Water level [m NAP] 1/10,000 [2]	3.02	2.86	2.74	5.15	3.83	1.87	3.30
	No closure [3]	3.31	3.05	2.90	5.48	5.16	4.21	3.81
	Difference [m] ([2]-[1])	0.00	0.00	0.00	-0.01	-0.10	-0.33	-0.01
0.81 m RCP4.5 (P50)	Water level [m NAP] 1/100 [1]	3.26	3.08	2.97	5.32	4.46	3.57	3.54
	Water level [m NAP] 1/10,000 [2]	3.26	3.08	2.96	5.31	3.98	3.08	3.50
	No closure [3]	3.71	3.46	3.31	5.94	5.74	4.61	4.35
	Difference [m] ([2]-[1])	0.00	0.00	-0.01	-0.01	-0.48	-0.49	-0.04

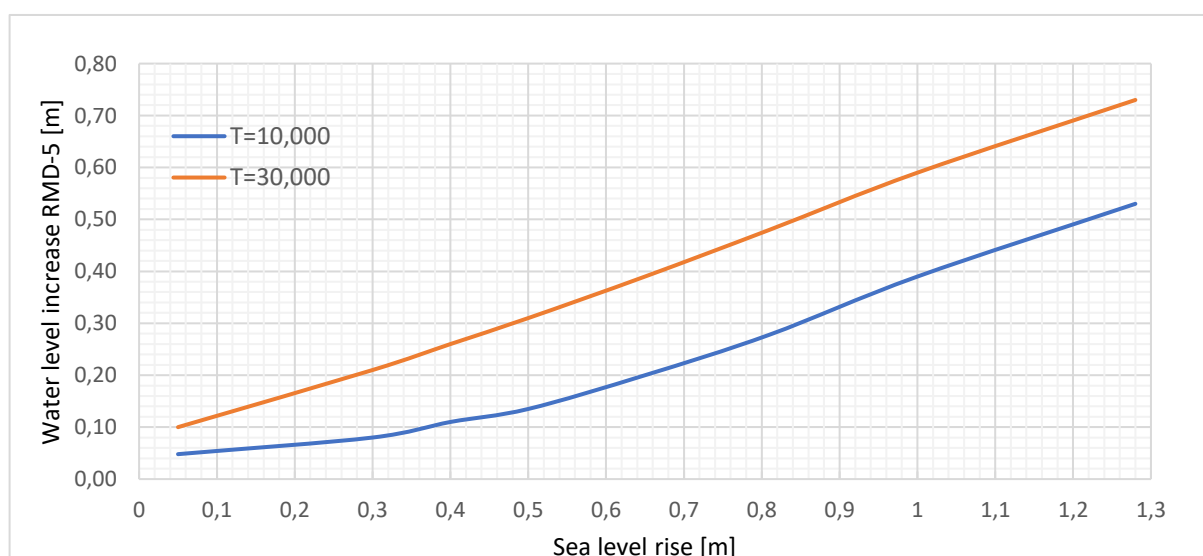


Figure 7.8: Effect of the current failure rate of the MLK to the peak water level of RMD-5 for  $T=10,000$  and  $T=30,000$  (Hydra-NL).

## Response

There are plans to improve the reliability of the MLK to a maximal allowed failure rate of 1/200 per closure. This adaptation has a considerable reducing effect on the hydraulic loads of the dykes in the hinterland which is presented in Table 7.21 for various sea level scenarios. Adjusting the failure rate to 1/200 per closure result in a decline of 6 cm of the maximal water level in Rotterdam. The benefit increases to 16 cm with 0.81 m sea level rise or more. Therefore, it can be considered that reducing the failure rate becomes more beneficial in case of climate change and accelerated sea level rise. The surcharge of a failure rate of 1/200 per closure to the peak water level of RMD-5 is shown in Figure 7.9. Further analysis is required to determine the cost-effectiveness of improving the failure rate.

Table 7.21: Effect to the water levels in the RMD after improving the failure rate of the MLK to 1/200 per closure. The colours refer to the used sea level scenarios.

Rhine-Meuse Delta								
Sea level scenario (2100)	Test location	RMD-1	RMD-2	RMD-3	RMD-4	RMD-5	RMD-6	RMD-7
0 m (Year 2023)	Standard (WBI-2017)	1/1,000	1/300	1/300	1/10,000	1/30,000	1/10,000	1/1,000
	Crest height [m NAP]	4.70	3.80	4.35	5.79	5.23	3.76	5.53
0.81 m RCP4.5 (P50)	Water level [m NAP] 1/100	3.02	2.86	2.74	5.16	3.93	2.20	3.31
	Water level [m NAP] 1/200	3.02	2.86	2.74	5.15	3.87	2.03	3.31
	Difference [m]	0.00	0.00	0.00	-0.01	-0.06	-0.17	0.00
1.28 m RCP8.5 (P50)	Water level [m NAP] 1/100	3.26	3.08	2.97	5.32	4.46	3.57	3.54
	Water level [m NAP] 1/200	3.25	3.08	2.96	5.31	4.30	3.40	3.52
	Difference [m]	-0.01	0.00	-0.01	-0.01	-0.16	-0.17	-0.02
1.40 m RCP4.5 (P95)	Water level [m NAP] 1/100	3.41	3.22	3.10	5.42	4.81	3.95	3.73
	Water level [m NAP] 1/200	3.40	3.21	3.10	5.41	4.65	3.84	3.67
	Difference [m]	-0.01	-0.01	0.00	-0.01	-0.16	-0.11	-0.07
1.40 m RCP4.5 (P95)	Water level [m NAP] 1/100	3.46	3.26	3.15	5.45	4.90	4.03	3.80
	Water level [m NAP] 1/200	3.45	3.25	3.13	5.44	4.74	3.93	3.71
	Difference [m]	-0.01	-0.01	-0.02	-0.01	-0.16	-0.10	-0.09

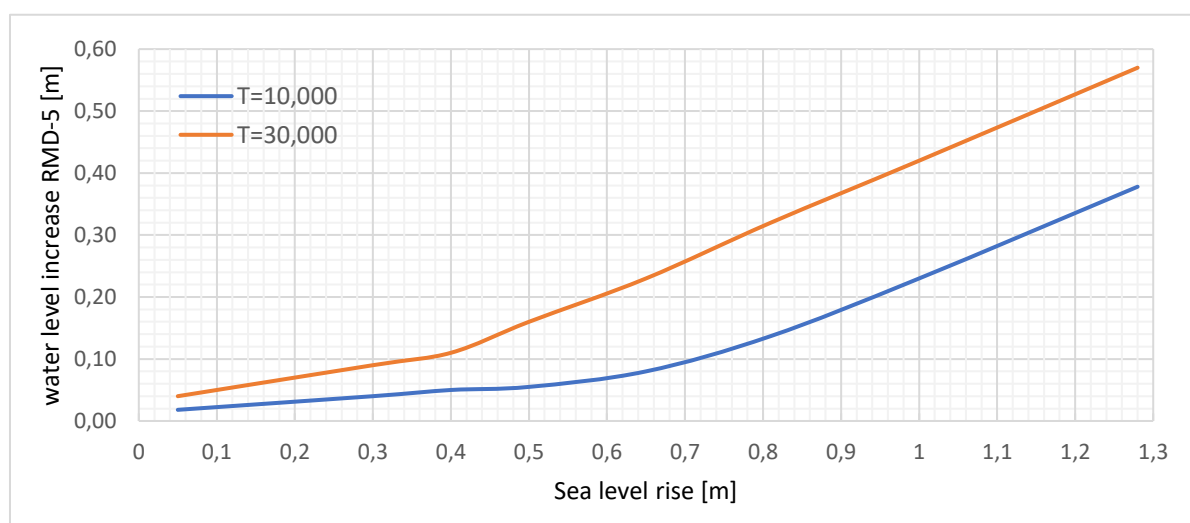


Figure 7.9: Effect of the improved failure rate (1/200) of the MLK to RMD-5 for T=10,000 and T=30,000 (Hydra-NL).

### 7.1.5.2 Eastern Scheldt Barrier

The OSK is a unique storm surge barrier with 62 floodgates that can operate independently. Therefore, it is very complicated to assume the chance of a non-closure very precisely. The consequences of the failure depend on the number of floodgates that do not close, but also on the position of these gates within the barrier. Despite the complexity, the failure rate of one of the floodgates is relatively low.

Table 7.22 shows the failure rate based on the current performance of the OSK for multiple scenarios. Appendix R features all scenarios which are used to compute the effect of the failure rate to the water levels in the Eastern Scheldt.

Table 7.22: failure frequencies floodgates OSK (Deltares, 2014).

# Failing floodgates	Failure rate (Manned operation)	Failure rate (Unmanned operation)
0	0.98647 (reliability)	0.93951 (reliability)
1	0.01180	0.05410
2	0.00038	0.00183
62	0.00002	0.00075

A failure of one floodgate will increase the leakage opening by 200-500 m<sup>2</sup> depending on the sea level (Rijkswaterstaat, 2015b). The effect of one failing floodgate during a high-water closure is substantial. The total leak opening increase by 16-40%, but also the flow velocity is higher due to the larger opening gap. The estimated average discharge through the extra leakage opening is 2,500 m<sup>3</sup>/s for a 10,000-year storm. The total water level increase in the Eastern Scheldt is approximately 52 cm during a 20-hour closure. Based on the presence of the operational team during a closure, only a 1.1% probability exists that one floodgate fails to close. Hence, the likelihood of a failure during an extreme high-water event (T=10,000) is very small. It is assumed that both events occur independently, resulting in a probability of  $1.35 \cdot 10^{-6}$  of one or more failing floodgates during the extremely high-water event. As a result, the effect on the hydraulic loads on the dykes in the hinterland is negligible in the current situation. This statement is confirmed by the results shown in Table 7.23 which are computed by using probabilistic model Hydra-NL.

Table 7.23: Effect of the current failure rate of the OSK to the peak water level of the Eastern Scheldt, averaged over all 12 test locations for different sea level scenarios and for the previous and current safety standard of the OSK. Effect [1]: average water level difference between 100% reliability and the current reliability. Effect [2]: average water level difference between 0% reliability and the current reliability (Hydra-NL).

The average peak water level in the Eastern Scheldt	SLR=0.05 m		SLR=0.81 m RCP4.5 (P50)		SLR=1.28 m RCP8.5 (P50)		SLR=1.40 m RCP4.5 (P95)	
	4,000	10,000	4,000	10,000	4,000	10,000	4,000	10,000
Return period (T) [years]	4,000	10,000	4,000	10,000	4,000	10,000	4,000	10,000
Water level current situation [m NAP]	3.77	3.82	3.85	3.93	3.97	4.14	4.04	4.23
Water level 100% reliability [m NAP] [1]	3.77	3.82	3.83	3.89	3.88	3.95	3.90	3.98
Water level non-closure [2]	5.16	5.40	5.81	6.05	6.21	6.46	6.32	6.56
Effect [m] [1]	0.00	0.00	-0.02	-0.04	-0.09	-0.18	-0.14	-0.25
Effect [m] [2]	1.38	1.58	1.96	2.12	2.24	2.32	2.27	2.33

Sea level rise will increase the effect of the failure rate to the maximal water levels in the Eastern Scheldt significantly. The main reason is the drastically increasing frequency of required closures (Section 7.1.6.2) of the OSK for more than 1 m sea level rise, which increases the likelihood of failing floodgates to a large extent. Table 7.23 features an increase of the effect to the water level in the hinterland of the current failure rate from zero to 0.04 m (SLR: 0.81 m; T=10,000) to 0.25 m for 1.40 m SLR (T=10,000). This effect is visualized in more detail in Figure 7.10. This outcome will affect the technical tipping point and the remaining lifetime of the Eastern Scheldt Barrier significantly which will be discussed in Section 7.2.1. The effects to various dyke sections around the Eastern Scheldt are presented in Appendix R.

In addition, Table 7.23 shows the current effect of the OSK by calculating the difference, in water level, between the current situation and a non-closure. The efficiency of the OSK increases, in terms of water level reduction in the hinterland, from 1.58 m (SLR = 0.05 m) to 2.33 m for 1.4 m SLR (T=10,000).

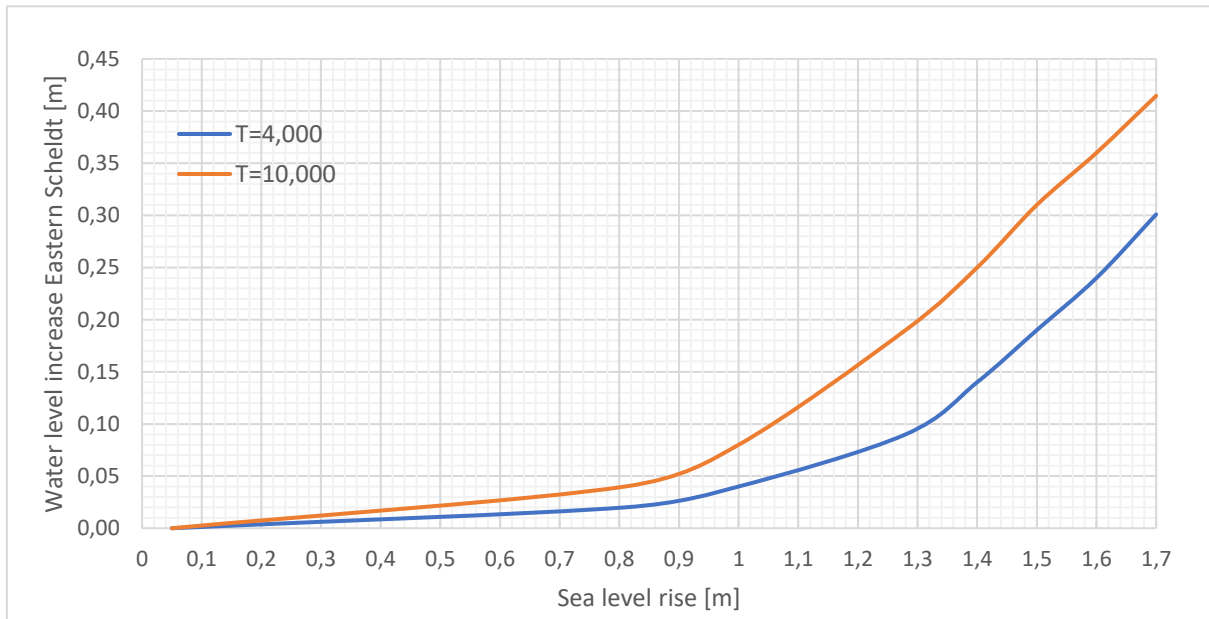


Figure 7.10: Effect of the failure rate of the OSK to the peak water level averaged over the Eastern Scheldt for T=4,000 and T=10,000 (Hydra-NL).

## 7.1.6 Closing frequency

The closing frequency can have a large influence on the remaining lifetime of the storm surge barrier. Sea level rise cause more frequent closures when the current closing strategy will be maintained. The MLK and OSK can technically close many times each year. However, more frequent closures of the MLK have a substantial economic impact for the port of Rotterdam. On the other hand, more frequent closures of the OSK will have a significant impact on the tidal zone in the estuary which affects nature and the environment. The focus of this study is primarily on the technical tipping points of the storm surge barriers, but the closing frequency can have a significant impact on economics and nature which should be addressed as well. The risk description of a failing closure is the following:

*“The Maeslant Barrier might not be economically beneficial by more frequent closures per year.”*

*“The Eastern Scheldt Barrier might have too severe effects on the ecology by more frequent closures per year.”*

The MLK should close on average once in the 10 years according to the sea level statistics. For the OSK this is on average 4 times per 5 years. Concerning sea level rise, the closing frequency of both storm surge barriers will increase to a large extent. Figure 7.11 (p. 111) features the rate of increase of the expected closing frequency during sea level rise for both storm surge barriers. The results are obtained from Hydra-NL and expert judgement of specialists of Rijkswaterstaat.

### 7.1.6.1 Maeslant Barrier

At 0.6 m sea level rise, the MLK will close on average once per year. This might not result in a large economic issue for the port of Rotterdam because nowadays, the barrier closes also every year. Once a year Rijkswaterstaat tests the closure of the MLK and the HK before the start of the storm season. The functional closure is intended to test the storm surge barriers integrally. Both the technology and the people operating the flood defence systems will be tested as well. These functional test closures are required to test the closure because a real required closure is still relatively rare. Since the opening of the Maeslant Barrier in 1997, the floodgates have been closed only twice (2007 and 2018), during storm conditions but at a reduced forecasted water level. In the long run, functional closures should be replaced by the more frequent required storm closures.

The MLK is expected to close on average two times a year at 0.8 m sea level rise. The companies of the port of Rotterdam stands for open access to the port. However, the image of open access to the port with the MLK may not be maintained with accelerated sea level rise. The chance exists that shipping locks replace the open and closable strategy of the Rhine-Meuse Delta in the long-term.

By closing the MLK more frequently, the stagnation effects for the port become over time in the same order of magnitude as locks. If the MLK will be replaced by locks, the ships will have a delay every day. It must, therefore, be investigated in more detail when the economic tipping point is reached.

The MLK is expected to close on average four times a year at 1 m SLR. The total unavailability of the NWW is 60 hours per year at 1 m SLR under the assumption of an average shipping prohibition of 15 hours (10 hours at closure 3-1-2018) for each closure. It is difficult to determine differences in total shipping delay between the Maeslant Barrier and replacing the barrier by constructing shipping locks because this depends on the number of ship movements per ship per year. However, the unavailability of the NWW after the realization of shipping locks will increase considerably. Also, for ships, it is crucial to know in time when the port can be entered and departed. It is expected that this will not be a major problem for ships at on average four closures per year. Therefore, it is projected that the economic tipping point has not yet been reached after 1 m sea level rise. As a result, the technical tipping point will be regarded as normative. It is advised to perform a study to determine the economic tipping point more concretely.

### 7.1.6.2 Eastern Scheldt Barrier

The Eastern Scheldt Barrier closes more frequently than the Maeslant Barrier. As a result, sea level rise will lead to a more considerable increase in the number of closures. More than 7 closures per year are expected at 0.6 m sea level rise. The impact for ecology is probably not outweighing the additional cost of replacing the storm surge barrier at that point (Leeuwdront, 2012). The number of required closures increase to 18 per year at 0.8 m SLR and more than 45 per year at 1 m SLR. It is expected that the OSK should close every day for more than 1.2 m SLR with a massive impact on the tidal activity on the Eastern Scheldt.

It can be concluded that the open-closable strategy of the OSK cannot be maintained at more than 1 m sea level rise without increasing the closing level. It is expected that the ultimate technical tipping point of the OSK will be above this point. Therefore, a trade-off should be made between water safety, costs and ecology to determine the most feasible solution for the Eastern Scheldt when 1 m sea level rise is reached.

If the effect to ecology is too large to bear in the long-term, the possibility exists to increase the closing level in order to maintain the intertidal zone in the Eastern Scheldt. If the closing level will be raised to +3.2 m NAP after 0.6 m sea level rise, the number of closures decreases from on average 8 to 3 times per year. If the raised closing level will be maintained, the number of closures decreases from 45 to 18 times per year at 1 m SLR. The consequence is that most dykes around the Eastern Scheldt should be reinforced if the closing level will be raised.

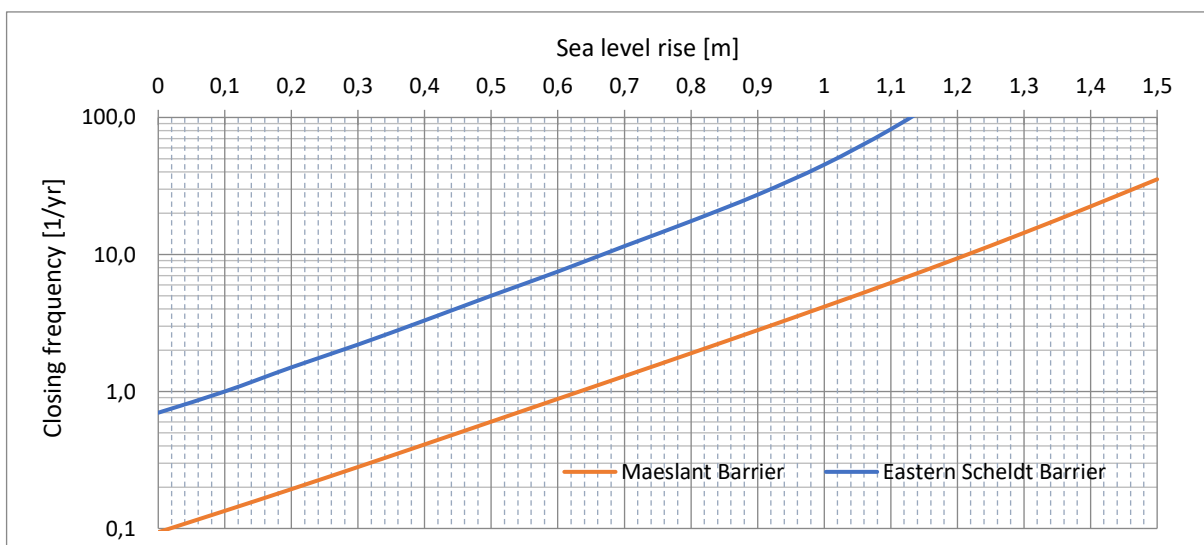


Figure 7.11: Closing frequency of the Maeslant Barrier and Eastern Scheldt Barrier with sea level rise.

## 7.1.7 Soil subsidence

This section analyses the increase in flood risk caused by the vertical decline of the storm surge barriers due to soil subsidence. The risk description of soil subsidence to the technical tipping point is the following:

*“The water-retaining height of the storm surge barriers could reduce due to vertical land movement.”*

Vertical land movement increases the relative sea level rise in a specific area. Relative sea level rise is explained in Section 5.7.1.2 and Appendix B in more detail. Important to note is that absolute sea level rise scenarios are used in Chapter 6 and 7. Vertical land decline reduces the height of the storm surge barriers and, therefore, increases the hydraulic loads to the barrier.

Total vertical land movement includes subsidence caused by geological processes and anthropogenic factors. The full analysis of influencing factors is included in Appendix B.

### 7.1.7.1 Maeslant Barrier

The depth of the threshold blocks determines the water-retaining height of the Maeslant Barrier. Figure 7.12 gives an impression of the location of the threshold blocks and the water-retaining doors. The arc-shaped doors with a height of 21.5 m sink to the threshold blocks which are located at a depth of circa -17 m NAP. An extra wall is placed on top of the doors (not visible in Figure 7.12) making a total height of 22 m. The foundation of the MLK is located on land and does not have a water-retaining function. Therefore, limited soil decline under the foundation does not affect the water-retaining height of the storm surge barrier.

The 65 threshold blocks, with a length and width of 15 by 5.6 meters and a height of 3.2 meters, weighs 630 tons each. The threshold blocks are placed with considerable accuracy at a depth of -16.75 m NAP. It was calculated that the blocks could decline by about 0.17 m after multiple loadings of the floodgates. The current depth of the threshold blocks determines the retaining water height of the MLK and should therefore not move. That is the main reason why the doors are not completely filled with water to minimise the load on the threshold blocks during a closure. It is the intention to transfer all loads of closure to the ball-shaped joint and not by the shear stress on the threshold blocks. The current height of the barrier is circa +5.0 m NAP.

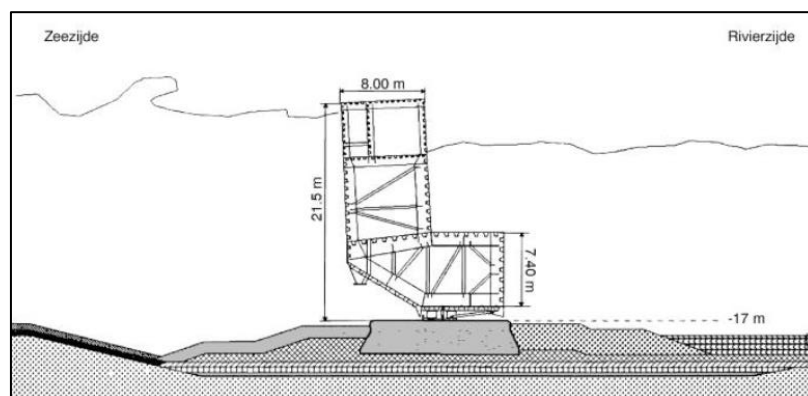


Figure 7.12: Soil protection and threshold blocks (RWS).

The total vertical land decline at the MLK is projected at  $6\pm 8$  cm between 2000 and the year 2100 (Appendix B). It is expected that this decline is smaller than the total settlement of the threshold blocks due to loadings of the massive doors. Due to the increased installation height of the threshold blocks, it is expected that the water-retaining height can remain +5.0 m NAP during its lifetime.

Nevertheless, a reasonable risk exists that the threshold blocks will decline to a greater extent than the projected 17 cm. It has been described in the design requirements that a deviation of more than 10 cm is not allowed. The amount of wave overtopping increase if the height of the barrier decreases to lower than +5.00 m NAP. Nonetheless, the consequence for the hinterland is expected to be very small.

If the deviation of the blocks exceeds 10 cm in the long-term, it can be decided to re-install the threshold blocks on an elevated bottom. This measure can also be implemented to increase the height of the MLK, depending on

the storage capacity and the rate of water overflow. This should be done in consultation with the harbour, which specifies the minimum depth for shipping. The bottom of the Rotterdam Waterway was -14.5 m NAP but is recently dredged to allow access for larger ships.

To conclude, the risk of increased hydraulic loads for the dykes in the hinterland due to vertical land decline of MLK is expected to be very small. If this turns out to be the case in the long-term, the height of the threshold blocks can be increased without replacing the entire barrier.

### **7.1.7.2 Eastern Scheldt Barrier**

The Eastern Scheldt Barrier is located in an area without substantial vertical land decline caused by geological and anthropogenic processes. The OSK is projected to decline with  $3\pm 6$  cm within this century (Appendix B). The OSK was designed for 40 cm relative sea level rise, which includes vertical land movement.

The water-retaining height of the storm surge barrier is +5.8 m NAP at Roompot and Schaar and +5.6 m NAP at Hammen. More technical information about the OSK can be found in Appendix H. Based on the knowledge about vertical land movement a decline of 5 cm should be taken into account for the year 2100. This decline will lower the water-retaining height and slightly increase the rate of wave overtopping. The effect on the water level of the Eastern Scheldt is an increase of 3 cm (SLR: 1.28 m; T=10,000) due to extra overtopping during a closure which takes 20 hours. This value indicates that the risk of a failing OSK due to vertical land movement is minimal. However, vertical land movement reduces the water-retaining capacity which should be included in the tipping point analysis.

Settlement of the construction is another factor that can contribute to a decreasing water-retaining height. Various measures have been taken during the construction to limit settlement of the storm surge barrier. First, sludge and clay have been removed till the sand layer at a depth of -12.5 m NAP. Moreover, the bearing capacity of the sand was considerably increased to keep settlements of the pillar structures as low as possible. Also, the structure is designed with several surcharges to deal with settlement differences between the pillars (Rijkswaterstaat, 1991). In the end, it is assumed that the construction height is only affected by vertical land movement and not by additional settlement due to the precaution measures.

For the year 2100, 5 cm vertical land movement will be included in the technical tipping point analysis of the remaining lifetime of the OSK. It is advised to accept this small increase in flood risk. It is not required to implement an immediate response strategy.

## **7.1.8 Safety standard and legislation changes**

Legislation changes might result in a different assessment method for flood defences which lead to disapproved storm surge barriers. Therefore, legislation changes about flood risk management might shorten the remaining lifetime of the storm surge barriers. The risk description is the following:

“Storm surge barriers can be disapproved due to more strict safety standards in the future.”

The storm surge barriers are the first line of defence for the dykes in the hinterland. Therefore, storm surge barriers should be assessed on the same safety standard as the heaviest norm for a dyke section which is part of the water system. The MLK and OSK were initially designed to protect the hinterland against an extreme sea level with the annual probability of 1/10,000 per year and 1/4,000 respectively (Rijkswaterstaat, 2007).

The norm has been changed for all flood defences in the Netherlands after the alteration of the Water Act in 2017. The probability of loss of water-retaining capacity of the MLK and OSK, resulting in substantially increased hydraulic loads for dykes in the hinterland is set on 1/30,000 per year and 1/10,000 per year respectively (Rijksoverheid, 2016). The norm is now explicitly based on the possible consequences of flooding behind flood defences. The norm unit has changed to the chance of flooding, which applies to dyke-sections. More information about the regulation change and the safety standard can be found in Section 3.2.4.

The MLK should be able to protect areas in Rotterdam with a safety standard of T=30,000. Some other areas in the RMD should meet the standard of 1/300 per year. To meet the prescribed safety standard, the MLK should prevent substantially increased hydraulic loads for the hinterland with a failure rate of 1/30,000 per year.

According to Table 6.6, the maximal water level in Rotterdam increases by 13 cm (+3.80 to +3.93 m NAP) after the changing the safety standard from T=10,000 to T=30,000. The hydraulic loads increase, but it is expected that the dyke sections meet the requirements for wave overtopping after small reinforcements. This is the same for the other areas, indicating that this regulation change does not affect the tipping point significantly. However, the combination with sea level rise affects the projected lifetime considerably which is addressed in the tipping point analysis.

The OSK should be able to prevent flooding of several areas in the hinterland with a maximum exceedance frequency of 1/10,000 per year. The maximum water levels in the Eastern Scheldt increase by 6-8 cm after changing the safety standard from T=4,000 to T=10,000. This change does not lead to a significant increase in the hydraulic loads.

To conclude, it is not entirely sure to what extent flood risk changes when the safety standard will be adjusted. The likelihood of a flood should be determined after including various failure mechanisms probabilistically. However, flood risk will not drastically increase because the hydraulic loads will not increase significantly according to the results of Hydra-NL.

If a future regulation change increases the hydraulic loads substantially for the hinterland, first a tradeoff should be made between dyke reinforcements and adapting the storm surge barrier. Therefore, it is advised to accept the risk of regulation changes for the lifetime of the storm surge barriers and to plan response strategies on beforehand to be able to implement effective adaptations plans.

### 7.1.9 Cost-benefit analysis

The construction of storm surge barriers was considered as cost-efficient measures compared to massive dyke reinforcements after the flood of 1953. The constructions of storm surge barriers are relatively expensive but shorten the effective coastline to a large extent. This strategy has frequently been chosen in the Netherlands to increase water safety in coastal areas. The problem is that the current storm surge barriers have not been designed for extremely accelerated sea level rise because the current insights in climate change and uncertainty were unknown a few decades ago.

The conducted risk analyzes above, assesses the ability of the MLK and OSK to perform also for more sea level rise than for which these barriers have been initially designed. However, it might also be the case that another strategy is financially more beneficial. The risk description of this uncertainty is:

*“The current storm surge barriers might not be financially effective to deal with climate change.”*

It should be emphasised that this study will not conduct a cost-benefit analysis. Therefore, it is advised to make a cost-benefit analysis of the proposed measures in Section 7.3. In the context of this study, it is assumed that it is cost-effective to postpone the operating lifetime of the storm surge barrier as long as possible with affordable measures. This is mainly due to the large investments in building both the MLK and OSK which are not sufficiently recovered in case of an early replacement. Therefore, the risk of a negative cost-benefit analysis of the proposed adjustments that can extend the lifespan is considered to be very small.

However, due to the large uncertainty in future climate change and sea level rise, it is recommended to design flood defences for a shorter lifespan. It is possible that a future replacement of the MLK and OSK will only be effective for a few decades because of the potential extreme sea level rise of several meters per century.

## 7.2 Tipping point analysis

This section will describe the tipping point of Maeslant Barrier (MLK) and the Eastern Scheldt Barrier (OSK). This analysis can be applied to the Netherlands as a basis for the Delta Decisions. The methodology and prescribed steps in the technical tipping point analysis are described in Section 2.3.2 (p. 10). First, the tipping point for the water storage capacity will be determined in Section 7.2.1. Subsequently, the tipping points of other factors will be calculated and the lowest tipping point is expected to be decisive for the barrier (Section 7.2.2). The tipping points will be calculated for the previous safety standard and the new standard after the regulation change in 2017. The safety standard is changed to  $T=30,000$  for the MLK and  $T=10,000$  for the OSK.

Climate change and potentially accelerated sea level rise is a risk for the remaining lifetime of the storm surge barriers. This section will analyze the remaining lifetime of both storm surge barriers by combining the analyzed risks described in the risk analysis. The focus will be on the technical aspects of the tipping point analysis. Financial and social tipping points are not part of this research and are recommended for future research. The technical tipping point of the storm surge barriers can be defined as the following:

*“The extent of sea level rise at which the storm surge barrier can no longer protect the water system at the agreed water level, resulting in substantially increased hydraulic loads on landward dyke trajectories.”*

In other words, if sea level rise in combination with a storm event exceeds the maximum threshold value of the storm surge barrier, the barrier no longer offers the desired safety against flooding. By combining the tipping point with a climate scenario, it is possible to derive the moment in the time that the tipping point will be exceeded. If this moment occurs earlier than anticipated, significant adjustments to the barrier or water system are required. An economic tradeoff can be made to improve or replace the storm surge barriers or the strengthen the dykes in the hinterland to a large extent.

Response strategies can potentially postpone the technical tipping point by several decades. If the new extended tipping point is reached and cannot be extended by additional measures, an adjustment of the entire water system might be required. This implies that the continuation of the current policy of the storm surge barriers becomes technically or physically impossible and should be changed (Jeuken & te Linde, 2011). In the case of the storm surge barriers, this technical tipping point can, therefore, persuade the transition from an open, lockable delta to another type of flood policy.

### 7.2.1 The tipping point of the water storage capacity

The storage capacity of both water systems is influenced by the failure rate and the closing procedure of the storm surge barrier. This section combines the storage capacity, failure rate and closing procedures to determine the technical tipping point of the storm surge barrier for the water storage capacity of the water system. The approach is to calculate the water storage capacity of the water system including the failure rate and the closing procedure (described in Section 7.1.2, 7.1.4 & 7.1.5). Consequently, the effects of various response measures to the peak water levels of the Rhine-Meuse Delta and the Eastern Scheldt are determined which could extend the technical lifetime of both the Maeslant Barrier and Eastern Scheldt Barrier. Ultimately, the tipping points of the storage capacity will be compared to the other tipping points to determine the critical tipping point of the storm surge barriers which will be done in Section 7.2.3.

#### 7.2.1.1 Maeslant Barrier and Rhine-Meuse Delta

In the risk analysis, it was supposed that two storm situations could be decisive in determining the technical tipping point of the MLK. These situations are:

1. high river discharge and a closed MLK;
2. extreme sea level (high-water) and modest river discharge.

These situations and the effects to the water storage capacity are explained in more detail in Section 7.1.2.1 pp. 81-87. That analysis of the storage capacity applies in case of a fully reliable barrier and did not include the risk of a closing failure of the MLK and the Hartel Barrier (HK). The failure rate is computed separately in Section 7.1.5.1 and has an adverse effect on the tipping point.

In this section, the effect of the failure rate of the Europoort Barrier (MLK+HK) is added to the calculation of the water level increase in the RMD during a closure. Furthermore, this analysis comprehends more sea level scenarios to calculate the tipping point more precisely. The technical tipping point of the MLK in terms of water storage will be reached at an exceedance of the predefined peak water levels in the RMD. This is +3.4 ( $\pm 0.1$ ) m NAP for T=10,000 and +3.6 ( $\pm 0.1$ ) m NAP for T=30,000 (Table 7.4). The clarification and motivation of these values can be found in Section 7.1.2.1 (pp. 82-83).

Table 7.24 and 7.25 represent the results for both situations including the peak water levels in the RMD for various sea level scenarios. Values which are close to the tipping point for the water storage are highlighted in orange. The exact tipping point for the water storage is given in Table 7.26 including an uncertainty range given the uncertainty around the maximum permissible peak level in the RMD.

*Table 7.24: Calculation of the water level increase in Rotterdam (RMD-5) for situation 1: high-river discharge. The results include the effect of the failure rate of the MLK and the HK. The total closure time of the storm surge barriers in the analysis is 10 hours. Orange: water level close to the tipping point. Red: exceedance of the storage capacity.*

Sea level rise [m] (yr. 2000)	Return period (T) [yr.]	Sea level [+m NAP]	Total River discharge [m <sup>3</sup> /s]	Leakage + overflow MLK & HK [m <sup>3</sup> /s]	Closure water level [+m NAP]	Effect failure rate to RMD [m]	Average peak water level RMD [+m NAP]
0.05	10,000	3.72	13,354	572	1.00	0.05	2.61
0.05	30,000	3.89	13,779	616	1.00	0.10	2.71
0.30	10,000	3.84	13,779	596	1.25	0.08	2.91
0.30	30,000	3.99	13,832	662	1.25	0.21	3.05
0.40	10,000	3.95	13,779	644	1.35	0.11	3.03
0.40	30,000	4.09	14,421	685	1.35	0.26	3.26
0.50	10,000	3.82	13,779	592	1.45	0.14	3.15
0.50	30,000	4.13	13,966	694	1.45	0.31	3.35
0.65	10,000	4.02	13,779	659	1.60	0.20	3.35
0.65	30,000	4.08	14,207	683	1.60	0.39	3.59
0.81	10,000	4.13	13,832	709	1.76	0.28	3.59
0.81	30,000	4.38	14,849	807	1.76	0.48	3.91

*Table 7.25: Calculation of the water level increase in Rotterdam (RMD-5) for situation 2: extreme sea level. The results include the effect of the failure rate of the MLK and the HK. The total closure time of the storm surge barriers in the analysis is 20 hours. Orange: water level close to the tipping point. Red: exceedance of the storage capacity.*

Sea level rise [m] (yr. 2000)	Return period (T) [yr.]	Sea level [+m NAP]	Total River discharge [m <sup>3</sup> /s]	Leakage + overflow MLK & HK [m <sup>3</sup> /s]	Closure water level [+m NAP]	Effect failure rate to RMD [m]	Average peak water level RMD [+m NAP]
0.05	10,000	5.70	3,582	1,478	2.00	0.05	3.12
0.05	30,000	6.07	4,134	1,894	2.00	0.10	3.38
0.30	10,000	5.90	3,582	1,728	2.00	0.08	3.20
0.30	30,000	6.27	4,134	2,064	2.00	0.21	3.52
0.40	10,000	6.00	3,582	1,828	2.00	0.11	3.26
0.40	30,000	6.37	4,134	2,168	2.00	0.26	3.59
0.50	10,000	6.09	3,582	1,898	2.00	0.14	3.30
0.50	30,000	6.46	4,134	2,248	2.15	0.31	3.81
0.65	10,000	6.20	3,582	2,013	2.00	0.20	3.38
0.65	30,000	6.58	4,134	2,380	2.20	0.39	3.96
0.81	10,000	6.36	3,582	2,136	2.10	0.28	3.59
0.81	30,000	6.74	4,134	2,520	2.25	0.48	4.12

The probability of a closing failure of the floodgates of the Maeslant Barrier is approximately 1/100 per closure. Sea level rise leads to more frequent closures which enhance the likelihood of a closing failure. Therefore, the effect of the failure rate to the peak water level at RMD-5 is larger at more SLR. The effect of the failure rate increases from 0.10 m in the current situation to 0.48 m at 0.81 m SLR (T=30,000).

The tipping points for the storage capacity are given in Table 7.26 for both situations. The tipping points prescribe a maximum amount of SLR including the uncertainty range. A high river discharge in combination with a closure

(situation 1) of the Maeslant Barrier result to slightly lower peak water levels in the Rhine-Meuse Delta than a closure during an extreme sea level (situation 2).

The maximum acceptable sea level rise is 0.67 m for T=10,000 and 0.40 m for T=30,000. The lower value for T=30,000 is caused by the larger effect of the failure rate which is valid in Rotterdam (RMD-5). For this very small exceedance frequency, it is acceptable that the other areas in the RMD will flood where a lower safety standard applies. The results of Table 7.24 and 7.25 show a slightly higher tipping point for situation 1 which is therefore not the normative situation according to this tipping point analysis. This is in contrast with the results of Hydra-NL, expecting that situation 1 results in critical water levels (Chapter 6).

Table 7.26: Tipping points of the MLK for the water storage in the RMD measured in sea level rise after the year 2000. The results include the uncertainty bandwidth. The critical tipping points are indicated in orange.

Situation	Return period [yr.]	Critical water level RMD (including uncertainty)	Tipping point of the storage capacity (including uncertainty)
1 (river)	T=10,000	+3.4 m NAP ( $\pm 0.1$ m)	0.68 m (0.61-0.75 m)
	T=30,000	+3.6 m NAP ( $\pm 0.1$ m)	0.65 m (0.59-0.71 m)
2 (sea)	T=10,000	+3.4 m NAP ( $\pm 0.1$ m)	0.67 m (0.50-0.74 m)
	T=30,000	+3.6 m NAP ( $\pm 0.1$ m)	0.40 m (0.28-0.45 m)

## Response measures

The tipping point of the Maeslant Barrier can be reached earlier than initially thought in case of accelerated sea level rise. It is expected that an extreme sea level combined with a modest river discharge affects the water storage to a greater extent than a closure during a high river discharge. Various response measures have been suggested which may improve the tipping point of the storage capacity in the RMD for situation 1 and 2.

### Situation 1: high river discharge

The risk analysis (Section 7.1) suggests the following two measures to extend the tipping point:

- A<sub>1</sub>: improving the closing procedure;
- B<sub>1</sub>: reduce the failure rate to 1/200 per closure.

The closing procedure can be improved by reducing the delay before the closure. This adjustment results in a reduced closing time which lowers the closing water level by 0.05 m in situation 1 (Section 7.1.4.1 p. 104).

Improving the failure rate of the MLK from 1/100 to 1/200 per closure will have a benefit of 3 cm to the storage capacity for T=10,000 and 6 cm for T=30,000 (p. 107). Sea level rise leads to more frequent closures which increase the effectivity of improving the failure rate of the barrier. The benefit increases to respectively 14 cm and 16 cm for T=10,000 and T=30,000 after 0.81 m SLR.

The peak water levels for Rotterdam (RMD-5) are presented in Table 7.27 after improving the closing procedure (A<sub>1</sub>) and in combination with improving the reliability of the MLK (A<sub>1</sub>+B<sub>1</sub>). The tipping point for situation 1 is given in Table 7.28 which is obtained after interpolation between the sea level scenarios and the peak water levels.

Table 7.27: Calculation of the water level increase at RMD-5 for situation 1: high-river discharge. The results include the effect of the failure rate of the MLK and the HK after implementing adjustments. The total closure time of the storm surge barriers in the analysis is 10 hours.

Measure	Sea level rise [m] (yr. 2000)	Return period (T) [yr.]	Sea level [+m NAP]	Total River discharge [m <sup>3</sup> /s]	Leakage + overflow MLK & HK [m <sup>3</sup> /s]	Closure water level [+m NAP]	Effect failure rate to RMD [m]	Peak water level RMD-5 [+m NAP]
Measure A <sub>1</sub>	0.65	10,000	4.02	13,779	659	1.55	0.20	3.31
	0.65	30,000	4.08	14,207	683	1.55	0.39	3.54
	0.81	10,000	4.13	13,832	709	1.71	0.28	3.55
	0.81	30,000	4.38	14,849	807	1.71	0.48	3.86
Measure A <sub>1</sub> +B <sub>1</sub>	0.65	10,000	4.02	13,779	659	1.55	0.08	3.19
	0.65	30,000	4.08	14,207	683	1.55	0.23	3.38
	0.81	10,000	4.13	13,832	709	1.71	0.14	3.41
	0.81	30,000	4.38	14,849	807	1.71	0.32	3.70

Table 7.28: Tipping point of the MLK for the water storage in the RMD for situation 1 (High river discharge) measured in sea level rise after the year 2000. The results show the tipping point after implementing adjustments to the MLK and include the uncertainty bandwidth. Orange: the critical tipping point for this high river discharge situation.

Measure	Return period [yr.]	Critical water level (including uncertainty)	Tipping point of the storage capacity (including uncertainty)	Improvement of the tipping point
A <sub>1</sub>	T=10,000	+3.4 m NAP (±0.1 m)	0.71 m (0.64-0.78 m)	0.03 m
	T=30,000	+3.6 m NAP (±0.1 m)	0.68 m (0.63-0.73 m)	0.03 m
A <sub>1</sub> +B <sub>1</sub>	T=10,000	+3.4 m NAP (±0.1 m)	0.80 m (0.73-0.88 m)	0.12 m
	T=30,000	+3.6 m NAP (±0.1 m)	0.76 m (0.71-0.81 m)	0.11 m

Table 7.28 shows that the tipping point can be extended by 11 cm which means that the MLK might resist 0.76 m SLR compared to 2000 after implementing response measures. It turns out that situation 2 (extreme sea level) is the decisive situation in case of T=30,000 (p. 119). However, situation 1 is considered critical if a lower annual exceedance frequency of 1/10,000 will be maintained.

### Situation 2: extreme sea level

The risk analysis (Section 7.1) suggested four measures which can be applied to extend the tipping point in case of a storm event with an extreme sea level. For situation 2, the effects of the following adjustments will be analyzed:

- A<sub>2</sub>: improving the closing procedure;
- B<sub>2</sub>: turnaround closure;
- C<sub>2</sub>: partially raising the floodgates of the MLK;
- D<sub>2</sub>: reduce the failure rate to 1/200 per closure.

Measure A<sub>2</sub> is similar to the described adjustment to the closing procedure for situation 1. However, in this situation, the closing level can be reduced by 10 cm because of a larger reduction of the incoming tidal wave (Section 7.1.4.1, p. 103).

The strength of the ball-shaped joint is the limiting factor of the Maeslant Barrier. It is required to limit the water level difference between both sides to 4 m during a closure (Section 7.1.3). Therefore, it is useful to extend the tipping point of both the storage capacity and the construction because both aspects are interdependent.

Closing at a higher water level is not an option because the maximum storage capacity can be exceeded more easily at a closing level of +2.25 m NAP (Section 7.1.2). However, it is possible to perform a turnaround closure (B<sub>2</sub>) at +1-2 m NAP and to raise (partially float) the doors by 1-2 m (C<sub>2</sub>) when the sea level peak exceeds +5 m NAP. Such a water level occurs approximately for 3 hours in case of an extreme high-water event (T=30,000; SLR=0.81 m).

Raising the floodgates of the MLK by 2 m for 3 hours result in a decrease of the remaining storage capacity of 16-18 cm (Section 7.1.3.1 "Response"). However, this measure is effective to postpone the technical tipping point due to the reduced load on the construction. Furthermore, it is possible to perform always a turnaround closure to increase the storage capacity. This type of closure is possible in combination with temporarily raising the floodgates. This adjustment to the procedure allows a significant lower closing level which results in a net increase of the storage capacity of the RMD. Partially raising the floodgates of the MLK can also be applied for more modest storm events.

Furthermore, the risk of vibrations in the construction caused by wave overtopping is also negligible in this case because of the increased height of the barriers during the peak sea level. However, it is advised to investigate the risk of vibrations when the floodgates are partly raised.

Improving the failure rate of the MLK from 1/100 to 1/200 per closure (D<sub>2</sub>) will have the same benefits to the storage capacity as described in situation 1 (pp. 117-118).

The peak water levels for Rotterdam (RMD-5) are presented in Table 7.29 after improving the closing procedure (A<sub>2</sub>), combined with measures B<sub>2</sub> and C<sub>2</sub>, and all four measures together (A<sub>1</sub>+B<sub>1</sub>+C<sub>2</sub>+D<sub>2</sub>). The tipping point for situation 2 is given in Table 7.30.

Table 7.29: Calculation of the water level increase at RMD-5 for situation 2: Extreme sea level. The results include the effect of the failure rate of the MLK and the HK after implementing adjustments. The total closure time of the storm surge barriers in the analysis is 20 hours.

Measure	Sea level rise [m] (yr. 2000)	Return period (T) [yr.]	Sea level [+m NAP]	Total River discharge [m <sup>3</sup> /s]	Leakage + overflow MLK & HK [m <sup>3</sup> /s]	Closure water level [+m NAP]	Effect raising floodgates to RMD [m]	Effect failure rate to RMD [m]	Average peak water level RMD [+m NAP]
Measure A <sub>2</sub>	0.40	30,000	6.37	4,134	2,168	1.90	x	0.26	3.50
	0.50	10,000	6.09	3,582	1,898	1.90	x	0.14	3.21
	0.50	30,000	6.46	4,134	2,248	2.05	x	0.31	3.71
	0.65	10,000	6.20	3,582	2,013	1.90	x	0.20	3.29
	0.65	30,000	6.58	4,134	2,380	2.10	x	0.39	3.87
	0.81	10,000	6.36	3,582	2,136	2.00	x	0.28	3.49
	0.81	30,000	6.74	4,134	2,520	2.15	x	0.48	4.03
Measure A <sub>2</sub> +B <sub>2</sub> +C <sub>2</sub>	0.50	10,000	6.09	3,582	1,898	1.65	0.17	0.14	3.14
	0.50	30,000	6.46	4,134	2,248	1.80	0.16	0.31	3.63
	0.65	10,000	6.20	3,582	2,013	1.65	0.17	0.20	3.23
	0.65	30,000	6.58	4,134	2,380	1.85	0.18	0.39	3.81
	0.81	10,000	6.36	3,582	2,136	1.75	0.16	0.28	3.42
	0.81	30,000	6.74	4,134	2,520	1.90	0.17	0.48	3.96
	Measure A <sub>2</sub> +B <sub>2</sub> +C <sub>2</sub> +D <sub>2</sub>	0.50	10,000	6.09	3,582	1,898	1.65	0.17	0.06
0.50		3,0000	6.46	4,134	2,248	1.80	0.16	0.16	3.48
0.65		10,000	6.20	3,582	2,013	1.65	0.17	0.08	3.11
0.65		30,000	6.58	4,134	2,380	1.85	0.18	0.23	3.65
0.81		10,000	6.36	3,582	2,136	1.75	0.16	0.14	3.28
0.81		30,000	6.74	4,134	2,520	1.90	0.17	0.32	3.80
1.00		10,000	6.52	3,582	2,314	1.85	0.16	0.23	3.50
1.00		30,000	6.92	4,134	2,730	2.10	0.16	0.42	4.13

Table 7.30: Tipping point of the MLK for the water storage in the RMD for situation 2 (Extreme sea level) measured in sea level rise after the year 2000. The results show the tipping point after implementing adjustments to the MLK and include the uncertainty bandwidth. Orange: the critical tipping point for this high-water situation.

Measure	Return period [yr.]	Critical water level (including uncertainty)	Tipping point of the storage capacity (including uncertainty)	Improvement of the tipping point
A <sub>2</sub>	T=10,000	+3.4 m NAP (±0.1 m)	0.74 m (0.66-0.82 m)	0.07 m
	T=30,000	+3.6 m NAP (±0.1 m)	0.45 m (0.40-0.50 m)	0.05 m
A <sub>2</sub> +B <sub>2</sub> +C <sub>2</sub>	T=10,000	+3.4 m NAP (±0.1 m)	0.79 m (0.71-0.87 m)	0.12 m
	T=30,000	+3.6 m NAP (±0.1 m)	0.48 m (0.41-0.56 m)	0.08 m
A <sub>2</sub> +B <sub>2</sub> +C <sub>2</sub> +D <sub>2</sub>	T=10,000	+3.4 m NAP (±0.1 m)	0.91 m (0.82-1.00 m)	0.24 m
	T=30,000	+3.6 m NAP (±0.1 m)	0.61 m (0.52-0.70 m)	0.21 m

Table 7.30 shows that the tipping point can be extended by 21 cm which means that the MLK could resist 0.61 m SLR compared to 2000 after implementing all four response measures. It turns out that situation 2 (extreme sea level) is the decisive situation in case of T=30,000 while situation 1 might be decisive if a lower annual exceedance frequency of 1/10,000 will be maintained. Both tipping points for the storage capacity will be related to the other risk factors which can affect the remaining lifetime of the Maeslant Barrier (Section 7.2.3: Tipping point analysis and expected remaining lifetime).

### 7.2.2.2 Eastern Scheldt Barrier and the Eastern Scheldt estuary

This section analyzes the technical tipping point of the Eastern Scheldt Barrier which is measured in sea level rise. The focus is on the water storage capacity in the Eastern Scheldt which is an important aspect of the tipping point analysis. Table 7.31 shows the peak water level in the Eastern Scheldt, averaged over all 12 test locations for various sea level scenarios. The test locations are described in Appendix K. The critical average peak level is +3.7 m NAP (±0.1 m) for T=10,000, described in Table 7.11 (p. 88). If this level will be exceeded during an extreme high-water event, it is supposed that the OSK fails to prevent substantially increased hydraulic loads for the dykes

around the Eastern Scheldt. This will not directly mean that a flooding occurs but it is expected that response measures are required to extend the remaining lifetime of the OSK.

Values which are close to the tipping point for the water storage are highlighted in orange and an exceedance of the storage capacity is emphasized in red. The exact tipping point for the water storage is given in Table 7.32 including an uncertainty range given the uncertainty around the maximum permissible peak level.

Table 7.31: Calculation of the water level increase in Eastern Scheldt. The results include the effect of the failure rate of the OSK. The total closure time of the storm surge barriers is 20 hours. Orange: water level close to the tipping point. Red: exceedance of the storage capacity.

Sea level rise [m] (yr. 2000)	Return period (T) [yr.]	Sea level [+m NAP]	Leakage [m <sup>3</sup> /s]	Average overflow [m <sup>3</sup> /s]	Closure water level [+m NAP]	Water level increase [m]	Effect failure rate of the OSK [m]	Average peak water level of the OS [m NAP]
0.05	4,000	5.18	6,025	1,318	0.50	1.54	0.00	2.04
0.05	10,000	5.44	6,200	1,782	0.50	1.68	0.00	2.18
0.81	4,000	5.94	6,025	3,628	1.26	2.03	0.02	3.31
0.81	10,000	6.20	6,200	4,293	1.26	2.20	0.04	3.50
0.90	4,000	6.03	6,025	3,785	1.35	2.06	0.03	3.44
0.90	10,000	6.29	6,200	4,514	1.35	2.25	0.05	3.65
1.00	4,000	6.13	6,025	3,970	1.45	2.10	0.04	3.59
1.00	10,000	6.39	6,200	4,761	1.45	2.30	0.08	3.83
1.28	4,000	6.41	6,025	4,651	1.73	2.24	0.09	4.06
1.28	10,000	6.67	6,200	5,600	1.73	2.48	0.19	4.40

Table 7.32: Tipping point of the OSK for the water storage measured in sea level rise after the year 2000. The results include the uncertainty bandwidth.

Return period [yr.]	Critical water level (including uncertainty)	Tipping point of the storage capacity (including uncertainty)
T=4,000	+3.6 m NAP ( $\pm 0.1$ m)	1.00 m (0.81-1.07 m)
T=10,000	+3.7 m NAP ( $\pm 0.1$ m)	0.93 m (0.87-0.98 m)

The maximum permissible water level in the Eastern Scheldt (OS) will be reached at 1 m SLR for T=4,000 and 0.93 m SLR for T=10,000 which is considerably higher than the initial design requirement of 40 cm relative sea level rise. The results include the risk of a potential emergency failure and failing floodgate(s). The effect of the failure rate is shown in Table 7.31 and calculated in Section 7.1.5.2 (pp. 109-110).

If SLR increases to a larger extent, it is expected that the hydraulic loads for the hinterland substantially increase. It should be addressed that leakage, wave overtopping and water overrun are the main contributors to the water level increase in the estuary during a closure.

### Response measures

The tipping point of the Eastern Scheldt Barrier might be higher than initially thought, but potentially accelerated SLR can lead to a significantly shorter remaining lifetime than the intended 200 years (1986-2186). This study examines the following two adjustments which may positively affect the tipping point of the storage capacity:

- A: reduce the leak opening to 600 m<sup>2</sup>;
- B: adjustment closing procedure.

Leakage is the dominant contributor to the increasing water level in the Eastern Scheldt during a closure. Reducing the leak opening from 1250 m<sup>2</sup> to 600 m<sup>2</sup> will decrease the total leak volume by approximately 60%. This measure is also considered in Rijkswaterstaat (2015b). The results are described in Table 7.33 (Measure A).

Furthermore, the reduced leak volume makes it possible to close 10 hours earlier in advance of a high-water event on a lower sea level. This is possible because of the lower leak volume so that a longer closure on a lower water level becomes effective. Without adjusting the leak opening, closing at a lower water level is not beneficial.

The result of the calculation of this tradeoff is shown in Table 7.16 (p. 97). The peak water level averaged in the Eastern Scheldt during a high-water event is given in Table 7.33 after implementing the described adjustments.

Table 7.33: Calculation of the water level increase in Eastern Scheldt after implementing adjustments. The results include the effect of the failure rate of the OSK.

Measure	Sea level rise [m] (yr. 2000)	Return period (T) [yr.]	Sea level [+m NAP]	Leakage [m <sup>3</sup> /s]	Average overflow [m <sup>3</sup> /s]	Closure water level [+m NAP]	Closure time [hr.]	Effect of the failure rate of the OSK [m]	Average peak water level of the OS [m NAP]
Measure A	0.05	4,000	5.18	2,574	1,318	0.50	20	0.00	1.32
	0.05	10,000	5.44	2,646	1,782	0.50	20	0.00	1.43
	0.81	4,000	5.94	2,574	3,628	1.26	20	0.02	2.58
	0.81	10,000	6.2	2,646	4,293	1.26	20	0.04	2.76
	1.28	4,000	6.41	2,574	4,651	1.73	20	0.09	3.34
	1.28	10,000	6.67	2,646	5,600	1.73	20	0.19	3.65
	1.40	4,000	6.53	2,574	4,978	1.85	20	0.14	3.58
	1.40	10,000	6.75	2,634	5,864	1.85	20	0.25	3.88
	1.50	4,000	6.63	2,574	5,287	1.95	20	0.19	3.79
1.50	10,000	6.89	2,646	6,319	1.95	20	0.31	4.14	
Measure A+B	1.60	4,000	6.73	2,862	3,739	0.95	30	0.24	3.27
	1.60	10,000	6.99	2,928	4,453	0.95	30	0.36	3.63
	1.70	4,000	6.83	2,862	3,963	1.05	30	0.30	3.50
	1.70	10,000	7.09	2,928	4,703	1.05	30	0.41	3.86

Reducing the leak opening (A) leads to a decrease of 74 cm of the maximal water level after a closure which lasts 20 hours (pp. 90-91). Consequently, the tipping point can be extended by 38 cm for T=10,000 (Table 7.34). After reducing the leak opening, it is beneficial to close 10 hours earlier during the previous tidal minima (ebb). After 1.6 m sea level rise, the closing level can be lowered to +0.95 m NAP instead of +2.05 m NAP because of the early closure (A+B). This adjustment reduces the water level in the Eastern Scheldt by 1.48 m (T=10,000) (p. 91). This results in extra storage capacity that can postpone the tipping point by 0.70 m which is 1.63 m SLR. It should be noted that the effect of the failure rate significantly increases for more than 1.3 m sea level rise.

The tipping points of the OSK for the water storage are given in Table 7.34 which are based on the analysis of Section 7.1 and 7.2.1. The critical tipping point which determines the remaining lifetime of the OSK is addressed in Section 7.2.2 and includes other essential aspects such as the construction, vertical land movement and the effects to the ecology.

Table 7.34: Tipping point of the OSK for the water storage measured in sea level rise after the year 2000. The results show the tipping point after implementing adjustments to the OSK and include the uncertainty bandwidth.

Measure	Return period [yr.]	Critical water level (including uncertainty)	Tipping point of the storage capacity (including uncertainty)	Improvement of the tipping point
A	T=4,000	+3.6 m NAP ( $\pm 0.1$ m)	1.41 m (1.36-1.46 m)	0.41 m
	T=10,000	+3.7 m NAP ( $\pm 0.1$ m)	1.31 m (1.25-1.36 m)	0.38 m
A+B	T=4,000	+3.6 m NAP ( $\pm 0.1$ m)	1.74 m (1.70-1.79 m)	0.74 m
	T=10,000	+3.7 m NAP ( $\pm 0.1$ m)	1.63 m (1.59-1.67 m)	0.70 m

## 7.2.2 Tipping point and expected remaining lifetime

The technical tipping point of the MLK and OSK determines the remaining lifetime of both storm surge barriers. The consequences of climate change and other risks to the storm surge barriers are prioritized and described in the risk analysis (Chapter 7).

According to the risk register (p. 78), most risks are caused or enhanced by sea level rise. Therefore, sea level rise is the predominant contributor to shortening the projected lifetime of the storm surge barriers. This section combines the tipping point of the water storage (Section 7.2.1) with other important factors to determine the critical tipping point of both storm surge barriers. Furthermore, an indication will be given how long the barriers could remain operational before and after implementing adjustments in case of accelerated SLR.

### 7.2.2.1 Maeslant Storm Surge Barrier

According to the design, the MLK should be able to provide sufficient flood safety for 50 cm sea level rise. However, research shows that changing the safety standard to an exceedance frequency 1/30.000 per year (T=30,000) can reduce the remained lifetime considerably (Chapter 7).

The following assumptions have been made:

- wave overtopping does not result in a failure of the arc-shaped doors of the MLK due to vibrations;
- current dykes will be reinforced before the year 2050 according to WBI-2017;
- the soil protection will not determine the technical tipping point.

#### Results

This section combines the factors that influence the remaining lifetime into the tipping point analysis. The tipping point is calculated for the highest safety standards (T=10,000 and T=30,000) which are related to Rotterdam (RMD-5). The tipping points are combined with sea level rise and shown in Table 7.35. The tipping points of the storage capacity are calculated in Section 7.2.1. (pp. 115-119). The tipping point of the construction is computed in Section 7.1.3 (p. 97) and the closing procedure is discussed in Section 7.1.4.1 p. 103. The economic tipping point and the effect of soil subsidence are discussed in Section 7.1.6.1 (pp. 110-111) and 7.1.7.1 (p. 112).

*Table 7.35: Tipping point MLK measured in SLR for Rotterdam (RMD-5) compared to the year 2000\*: in alignment with storage capacity and closing water level. Orange: critical tipping point. Yellow: tipping point when the current closing procedure will not be changed.*

Tipping points and risk factors	Tipping point measured in sea level rise	
	T=10,000	T=30,000
Storage capacity	0.67 m (0.51-0.74 m)	0.40 m (0.28-0.45 m)
Construction*	0.65 m	0.30 m
Closing procedure	0.0 m	0.0 m
Closing frequency (economic effect)	> 0.65 m	> 0.65 m
Vertical movement	n/a	n/a

The effects of sea level rise on the storage capacity in the RMD are calculated in Section 7.2.1 and includes the risk of a closing failure of the MLK and the Hartel Barrier (HK). The failure rate is computed separately in Section 7.1.5.1 and has an adverse effect on the tipping point. The analysis of the storage capacity shows that the maximum acceptable rate of sea level rise is 0.67 m for T=10,000 and 0.40 m for T=30,000 in case of an extreme sea level situation.

The water level difference during the situation of an extreme sea level peak exerts a large horizontal load on the closed MLK. The maximum acceptable water level difference between both sides of the floodgates is 4 m which occur at 0.65 m (T=10,000) and 0.30 m (T=30,000) sea level rise compared to the year 2000 (Section 7.1.3.1). This means that the strength of the construction (ball joint) is the determining risk factor for the MLK for both safety standards (T=10,000 and T=30,000). The tipping point of 0.30 m can be seen as the optimal balance between the construction, water storage and closing water level which is analyzed on p. 97.

The closing procedure is another critical factor for the MLK. The effect of the closing procedure to the hinterland is analyzed in Section 7.1.4.1. The incoming tidal wave can temporarily ( $\pm 1-2$  hours) exceed critical water levels in the RMD due to the delay in the closing procedure. The closing delay of 30 minutes should be reduced to limit the risk of flooding and to prevent a further shortening of the lifespan of the barrier. The closing delay can be reduced to a few minutes which will lower the tidal wave considerably which makes the closing procedure not a decisive tipping point (Section 7.1.4.1).

The closing frequency does not influence the technical tipping point which is described in Section 7.1.6. However, the closing frequency can have a significant effect on the economy of Rotterdam and might have an influence in the decision-making of the future of the Maeslant Barrier. The MLK should close on average once per year after 0.65 m SLR which should not be a significant economic issue for the harbour of Rotterdam. A solution might be to cancel the functional closure in that circumstance to minimize the adverse economic effects for the harbour.

The vertical movement of the foundation is estimated at 6 cm per century which should not affect the technical tipping point of the MLK. The water-retaining height of the storm surge barrier is determined by the threshold blocks which are not expected to sink below the design requirement. Despite, the threshold blocks can be raised to restore the water-retaining height in case of a large deviation. Vertical movement in relation to the MLK is discussed in more detail in Section 7.1.7.1.

After adjusting the closing procedure to prevent the large tidal wave in the harbour during a high-water event, the limited strength of the construction will be the critical tipping point. Particularly, the adjustment of the safety standard will lead to the relatively low margin of 0.30 m sea level rise compared to the year 2000. This is mainly because of the projected sea level peak of +6.27 m NAP which can exert a critical load on the floodgates. If the allowances in the construction are significantly larger than currently known, the tipping point for the water storage can be seen as the normative situation which is 0.40 m SLR.

### Expected lifetime

The tipping point can be combined with the sea level scenario for the Netherlands to determine the expected remaining lifetime. The results are shown in Figure 7.13. In the high-end situation (P95) of RCP8.5, a chance of 5% exists that the MLK does not meet the required safety standard in the year 2042 (1). However, RCP8.5 is not the most likely emission scenario. The average between both emission scenarios (avg. RCP8.5/4.5) is assumed to be expected which means that a 50% chance exists that the tipping point (T=30,000) will be reached after 2055 (2). The tipping point may extend to the year 2079 (P50 avg. RCP8.5/4.5) if the previous safety standard of T=10,000 will be applied (4). Another possibility is that the barrier reaches the initial planned lifetime for both T=30,000 and T=10,000 if sea level rise turns out to be significantly lower than expected (5). It is important to mention that significant uncertainties have been applied in the calculations that can change both the sea level rise and the maximal acceptable sea level rise for the MLK.

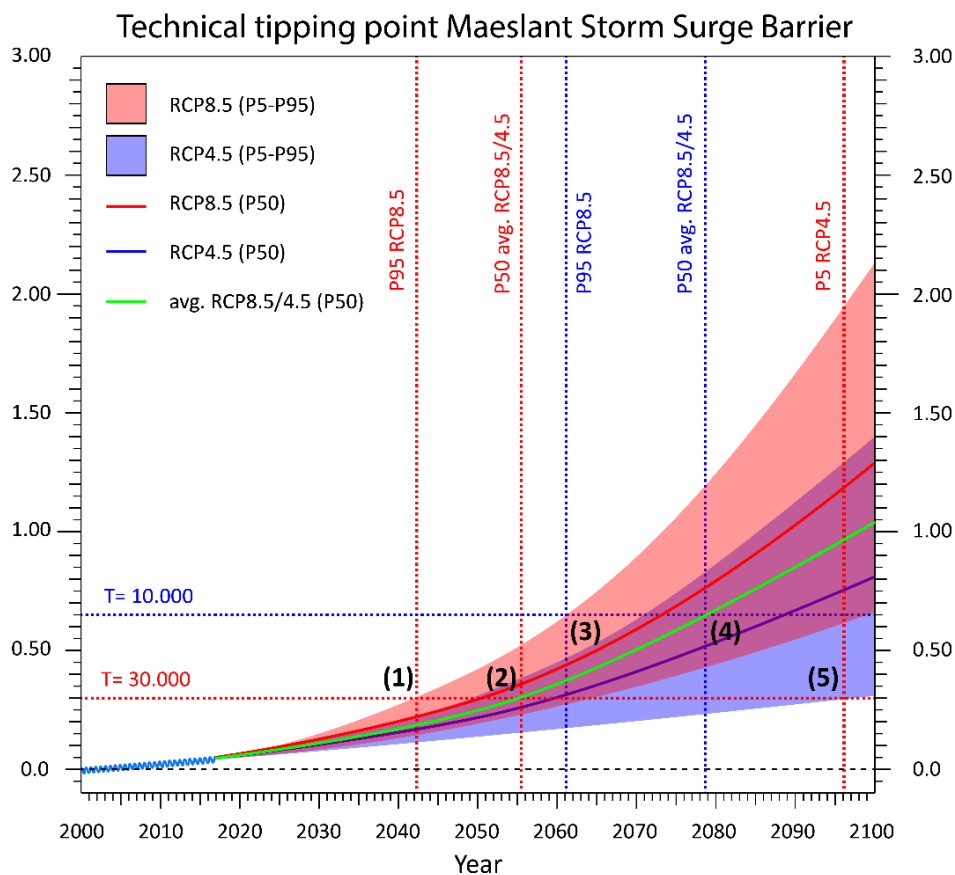


Figure 7.13: Technical tipping point for the MLK for T=10,000 and T=30,000 combined with sea level rise.

## Response measures

The expectation is that the initial planned lifetime of 100 years of the MLK (built in 1997) will not be reached if sea level rise accelerates. Nevertheless, it can be considered to be financially effective to postpone the tipping point by implementing different feasible adjustments instead of an entire replacement of the storm surge barrier.

The strength of the construction determines the tipping point in the current situation for  $T=30,000$ . According to Table 7.35, the margin for the storage capacity was slightly larger (40 cm SLR). Therefore, it is useful to extend the tipping point of both the storage capacity and the limiting strength.

Various measures have been analyzed in Section 7.2.1 in order to extend the tipping point for the water storage in case of a high-water event. It is noteworthy that some of these measures are also very effective to reduce the hydraulic loads exerted on the construction. In summary, the following measures can be implemented to extend the technical tipping point of the MLK:

- maximize the water level difference to 4 m for the MLK. The floodgates can be raised by maximal 2 m to reduce the horizontal force on the construction;
- always perform a turnaround closure to maximize the storage capacity of the RMD and to limit the tidal wave in the harbour;
- optimize the closing process by minimizing the delay before the closure.
- reduce the failure rate to 1/200 per closure;

The following measures are optional and recommended for future research:

- increase the water-retaining height of the HK;
- relocation of the threshold blocks.

The effect of the response measures to the tipping point of the MLK is given in Table 7.36.

Table 7.36: Tipping point MLK measured in sea level rise for Rotterdam (RMD-5) compared to the year 2000. Orange: critical tipping point after response measures.

Tipping points and risk factors	Tipping point measured in sea level rise	
	T=10,000	T=30,000
Storage capacity	0.80 m (0.73-0.88 m)	0.61 m (0.52-0.70 m)
Construction	1.20 m	0.80 m
Closing procedure	n/a	n/a
Closing frequency (economic effect)	> 0.65 m	> 0.65 m

It is required to limit the hydraulic head between both sides of the MLK to maximal 4 m during a closure. Therefore, it is advised to lay down this requirement in the closing procedure. Closing at a higher water level is not an option because the storage capacity can be exceeded more easily. A solution might be to raise the (partially float) the doors by 1-2 m when this condition ( $\Delta h > 4$  m) occurs. This is only required during an extreme high-end sea level peak of more than +5 m NAP which might only take place for roughly 3 hours. As a result, the load on the ball joint will remain within the permissible load of 60,000 tons and the construction will no longer be decisive for the tipping point. The tipping point of the construction can be postponed to 0.80 m sea level rise according to the analysis on p. 98.

In addition, it is possible to perform a turnaround closure at +1-2 m NAP, depending on the minimum sea level (ebb), to compensate for the loss of the storage capacity. The risk of exceeding critical water levels due to the delay in the closing procedure is negligible for this type of closure because the barrier closes well in advance of a high-water event. Subsequently, the tipping point for the water storage capacity includes also an optimized closing process and an improved failure rate of the Europort Barrier to 1/200 per closure. The effect of these measures is calculated in Section 7.2.1.

The closing frequency is not considered decisive for the new safety standard ( $T=30,000$ ) of the Maeslant Barrier because of the limited amount of expected closures per year. The closing frequency could be a relevant factor in the decision-making of the Maeslant Barrier if the critical tipping point is above 0.65 m SLR.

The results of Section 7.2.1 indicate that a high river discharge in combination with a closure is decisive in the tipping point analysis after implementing the response measures for  $T=10,000$ . The tipping point can be postponed to 0.80 m for  $T=10,000$  after implementing all four adjustments. On the other hand, an extreme high-water event is decisive with a tipping point of 0.61 m sea level rise for  $T=30,000$ .

### Expected lifetime after response measures

The response measures increase the tipping point significantly for the MLK and therefore also the expected remaining lifetime will be extended. This is visualized in Figure 7.14. In the high-end situation (P95) of RCP8.5, the lifetime extends from 2042 to 2060 (1). This tipping point will be reached in 2067 for the former safety standard ( $T=10,000$ ) for the similar high-end situation (2). The expected (P50) remaining lifetime based on the average of both emission scenarios is the year 2077 for  $T=30,000$ , which is an increase of 22 years (3). The MLK is expected to be operational for another 11 years if the safety standard will be maintained at  $T=10,000$  (4).

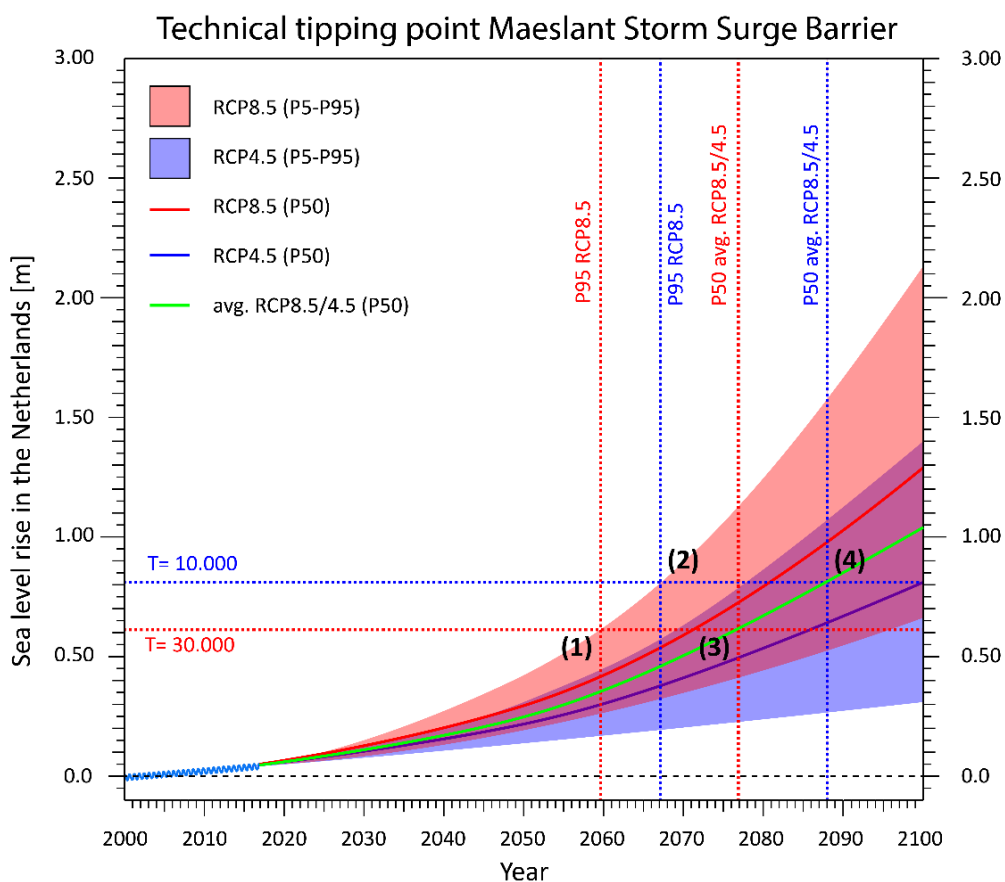


Figure 7.14: Technical tipping point for the MLK for  $T=10,000$  and  $T=30,000$  combined with sea level rise after implementation of response measures.

### 7.2.2.2 Eastern Scheldt Storm Surge Barrier

According to the design, the OSK should be able to deliver sufficient flood safety up to 40 cm relative sea level rise. At the time of the construction, it was expected that the barrier would be operational for 200 years. However, sea level rise can accelerate drastically, making it very unlikely to reach the planned lifetime.

The regulation change resulted in an increased safety standard of T=10,000. In comparison, the tipping points are calculated for T=4,000 and T=10,000. The following assumptions have been made:

- wave overtopping does not result in a failure of the construction components due to vibrations or fatigue damage;
- all dykes around the Eastern Scheldt will be reinforced before the year 2050 according to WBI-2017;
- all dykes can withstand the maximum hydraulic loads for a sea level < +3.00 m NAP with open floodgates;
- the soil protection will not determine the technical tipping point.

It is assumed that all dykes will be reinforced to the renewed safety standard and can withstand the hydraulic loads during a strategic non-closure of just below +3 m NAP. According to Chapter 6, the hydraulic loads for the dykes are determined by the water level in the Eastern Scheldt during a non-closure. The OSK closes in advance of a forecasted sea level of +3 m NAP, but water levels in the Eastern Scheldt can locally exceed +3.2 m NAP due to the additional storm surge in the estuary. It is expected that all dykes can withstand this load including a specific surcharge.

### Results

The contributing risks to the technical tipping point are described in Section 7.1. This section combines the factors that have an effect on the remaining lifetime in the tipping point analysis. The calculated tipping points should determine the maximum acceptable rate of sea level rise for the OSK. An extremely high sea level is the normative situation for the OSK because of the absence of river supply in the Eastern Scheldt.

The effect of sea level rise to the hydraulic loads in the Eastern Scheldt is relatively small according to results of Hydra-NL (Section 6.4). However, according to the risk analysis, approximately 0.9-1 m sea level rise will probably exceed the permissible water levels in the Eastern Scheldt when the barrier functions optimally. The dykes with an increased safety standard to T=10,000 will have to be reinforced to meet the wave overtopping requirement (Section 6.4.2.2). However, this will not determine the tipping point of the storm surge barrier.

The technical tipping point will be reached if the hydraulic loads substantially increase in the Eastern Scheldt or the increased hydraulic forces on the construction exceed the design requirements of the storm surge barrier. The tipping point of the OSK will be determined by assessment of three risk factors including:

- exceeding the storage capacity;
- exceeding of the maximal permissible load on the construction of the OSK;
- ecology.

Table 7.37: Tipping point OSK measured in sea level rise compared to the year 2000. Orange: critical tipping point.

Tipping points and risk factors	Tipping point measured in sea level rise	
	T=4,000	T=10,000
Storage capacity	1.00 m (0.81-1.07 m)	0.93 m (0.87-0.98 m)
Storage capacity (including land movement)	0.97 m (0.78-1.04 m)	0.90 m (0.84-0.95 m)
Construction (including land movement*)	1.52 m*	1.30 m*
Ecology	(1.00 m)	(1.00 m)

The maximum storage capacity of the Eastern Scheldt (OS) will be reached at 1 m SLR for T=4,000 and 0.93 m SLR for T=10,000. These results include the risk of a potential emergency failure or failing floodgate(s) which is calculated in Section 7.2.1.

Based on the knowledge about vertical land movement a decline of 5 cm should be taken into account during the expected remaining lifetime (Appendix B). This will increase the rate of overtopping slightly due to the reduced water-retaining height of the barrier. The effect on the water level of the Eastern Scheldt is an increase of approximately 3 cm due to extra overtopping during a closure (Section 7.1.7.2, p. 113).

It is expected that the strength of the construction will not determine the tipping point of the OSK without implementing adjustments (Section 7.1.3.2). The barrier is probably able to withstand a sea level of +6.70 m NAP due to the applied design surcharges. This corresponds to 1.52 m SLR for T=4,000 and 1.30 m SLR for T=10,000 including 5 cm vertical land movement. This assumption only applies to the condition that water overrun does not cause fatigue damage to the components of the construction.

It should be noted that the OSK should close at least 45 times a year if SLR exceeds 1.0 m compared to the year 2000 (Section 7.1.6.2). It is technically possible to close every day, but the effects of the diminishing tidal activity to flora and fauna in the Eastern Scheldt might be too devastating to accept. It is recommended to perform a Cost Benefit Analysis (CBA) which should show at what level of SLR the OSK should be replaced in terms of ecology and other financial aspects.

### Expected lifetime

The expected remaining operational lifetime is determined by interpolation of the projected sea level rise for the Netherlands. The results are shown in Figure 7.15. In the high-end situation (P95) of RCP8.5, a chance of 5% exists that the OSK does not meet the required standard in the year 2070 for T=10,000 (1). The remaining lifetime can be extended for 2 extra years (2072) for the lower safety standard (T=4,000) for the same high-end situation (2). It is expected (P50) that the tipping point (T=10,000) will be reached in the year 2093 for the average emission scenario (3). The lifetime can be extended until the year 2097 for safety standard T=4,000 when the average emission scenario (P50 avg. RCP8.5/4.5) is used (4). If sea level rise turns out to be lower than expected, there is also a possibility that the barrier can operate beyond 2100 but it is unlikely to reach the initial planned lifetime to 2186 in case of accelerated sea level rise. It is important to mention that significant uncertainties have been applied in the calculations that can change both the sea level rise and the maximal acceptable sea level rise for the OSK.

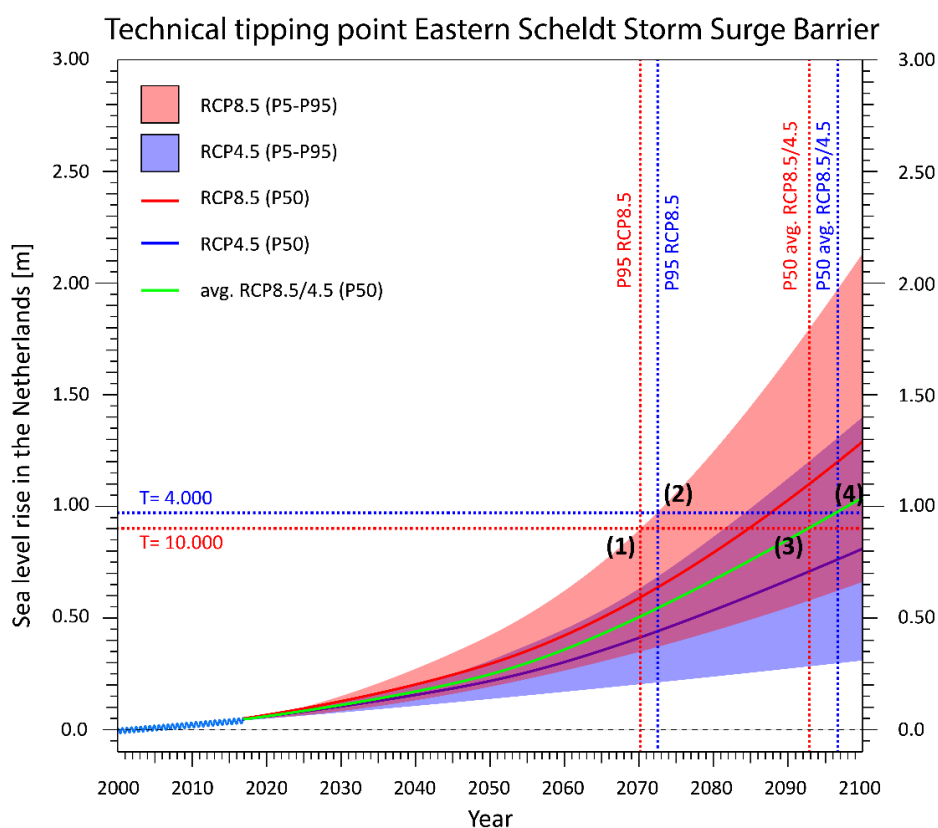


Figure 7.15: Technical tipping point for the OSK for T=4,000 and T=10,000 combined with sea level rise.

## Response measures

Based on the conducted analysis, it is not expected that the initial planned lifetime of 200 years of the OSK (built in 1986) will be reached in case of accelerated SLR. However, it is considered as financially attractive to extend the tipping point by implementing response measures.

The calculated tipping point for the OSK might be reached at 0.90 m sea level rise (T=10,000) which is projected to occur around the year 2093. According to the results, reducing the water supply from leakage is effective to decrease the risk of exceeding the storage capacity. In order to extend the lifetime of the OSK the following measures are proposed:

- reduce the leak opening to 600 m<sup>2</sup>;
- adjust the closing regime.

The adjustments are described in more detail in Section 7.2.1. The tipping points are shown in Table 7.38.

The following measures are optional and recommended for future research:

- increase the water-retaining height of the OSK by constructing a vertical wall (1 m) on top of the concrete beam.

*Table 7.38: Tipping point of the OSK measured in sea level rise compared to the year 2000. Orange: tipping point after response measures.*

Tipping points and risk factors	Tipping point measured in sea level rise	
	T=4,000	T=10,000
Storage capacity (leak opening 600 m <sup>2</sup> + adjusted closure)	1.74 m (1.70-1.79 m)	1.63 m (1.59-1.67 m)
Storage capacity (including land movement)	1.71 m (1.67-1.76 m)	1.60 m (1.56-1.64 m)
Construction (including land movement*)	1.52 m*	1.30 m*
Ecology	(1.00)	(1.00)

Reducing the leak opening from 1250 m<sup>2</sup> to 600 m<sup>2</sup> leads to a decrease of the peak water level in the Eastern Scheldt by 75 cm during a closure which takes 20 hours (pp. 90-91). The tipping point, in terms of sea level rise, can be extended by 38 cm, according to Table 7.33 (p. 121). Another benefit of the reduced leak opening is that an earlier closure at a lower water level can be very beneficial. By closing 10 hours in advance, it is possible to close at a considerable lower water level which results in extra storage capacity (Section 7.2.1). Both adjustments combined can postpone the tipping point further by 32 cm which is visualized in Figure 7.4 (p. 92). The tipping point for water storage can be increased to 1.60 m for T=10,000 including soil subsidence.

It is still unclear what amount of water overrun and wave overtopping will be acceptable. The maximum volume of overflow is roughly 5,500 l/s/m at the OSK during a high-water event (T=10,000) with 1.35 m sea level rise using Formula [6]. This is comparable to the design parameters according to the design Handbook which refers to a design water level of +5.5 m NAP and a wave height of 6.2 m (Rijkswaterstaat, 1991). Therefore, it is assumed that 1.30 m sea level rise including 5 cm subsidence is the decisive tipping point after implementing both adjustments to the barrier. If such a rate of overtopping turns out to be too much for the construction, a potential option is to increase the height of the OSK by 1 m. This will reduce the rate of wave overtopping to 3800 l/s/m. However, this measure will considerably increase the load on the construction.

It should be noted that the floodgates should remain closed all the time at 1.30 m sea level rise which implies that the tidal interaction with the Eastern Scheldt will disappear. Increasing the closing level will have only a small influence because of the high rate of sea level rise in that situation. Increasing the closing level also results in significant reinforcements of the dykes around the Eastern Scheldt. With more than 1.30 m SLR, the OSK will probably no longer function properly due to an exceedance of the design loads.

### Expected lifetime after response measures

The response measures increase the tipping point of the OSK to a large extent. The results of the projected timeframes of the tipping points are shown in Figure 7.16. In the high-end (P95) sea level scenario of RCP8.5, the lifetime extends from 2070 to 2081 for  $T=10,000$  (1). On the other hand, the tipping point can be reached in 2087 in case of a safety standard of  $T=4,000$  (2). It should be noted that the life-end can be reached in the year 2073 under the high-end scenario (P95) of Le Bars et al. (2016). The projected life-end for the 50<sup>th</sup> percentile (P50) of RCP8.5 is the year 2100. The expected remaining lifetime based on the average projected sea level rise (avg. RCP8.5/4.5) is until the year 2115-2120. However, another possibility is that the barrier can reach its initially planned lifetime after adjusting the leak opening and the closing procedure if the rate of sea level rise turns out to be lower as expected.

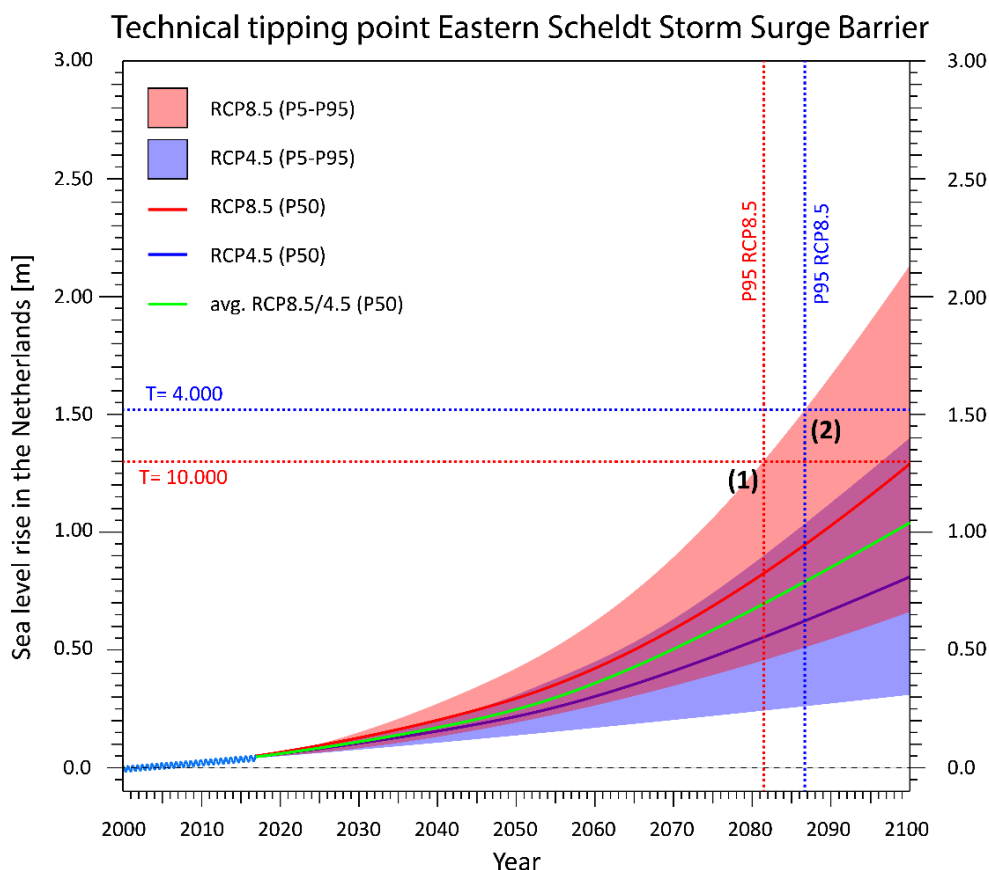


Figure 7.16: Technical tipping point for the OSK for  $T=4,000$  and  $T=10,000$  combined with sea level rise after implementation of response measures.

## 7.3 Strategies

This section advises how to implement the results into effective strategies for the water system of the Rhine-Meuse Delta and the Eastern Scheldt. Adaptive Delta Management is the implementation programme of the Delta Programme and is intended to develop effective strategies for uncertain forecasts of climate change and sea level rise. Sea level rise is the most dominant factor for the remaining lifetime of the storm surge barriers. Storm surge barriers often designed for a lifetime of 100-200 years are not very adaptive. Nevertheless, several measures can be taken to make the storm surge barriers resistant to a greater extent of sea level rise.

An important aspect of adaptive delta management is to implement measures to keep options open for the future and to monitor developments in climate change carefully. Plans should be made to be adequately prepared if accelerated sea level rise indeed occurs. It will probably take many years to replace the current storm surge barriers by new flood defences.

This chapter proposes optional strategies to extend the operating lifetime of the storm surge barriers. On the other hand, dunes and dykes are more adaptive and have a shorter intended lifespan. These types of flood defences are easier to improve in case of accelerated sea level rise. More information about Adaptive Delta Management can be found in Section 3.2.6.

Dyke improvements in both the Rhine-Meuse Delta and the Eastern Scheldt are required to comply with the stricter safety standards of the adapted flood risk assessment approach. The Delta Programme states that all flood defences must meet these new standards for the year 2050.

Stricter safety standards will not directly lead to the technical tipping point of the storm surge barriers but will reduce the expected remaining lifetime. Furthermore, the future rate of sea level rise is very uncertain and can potentially increase to a large extent after 2050. All risks described in Section 7.1 can influence the remaining lifetime of the storm surge barriers. This section describes the proposed strategies to minimize the risks that affect the tipping point to extend the lifetime of the Maeslant Barrier and Eastern Scheldt Barrier.

### 7.3.1 Maeslant Storm Surge Barrier

The tipping point analysis suggests that the MLK probably cannot reach its initially planned lifetime of 100 years due to the risk of accelerated sea level rise. The tipping point of the MLK can occur in 2042 for the highest sea level rise scenario without implementing noteworthy response measures. However, future sea level rise is still very uncertain making accurate prognoses impossible. The tipping point is expected to occur in the year 2055 for the average sea level scenario (P50 avg. RCP8.5/4.5). There is also a possibility that the MLK will reach the end of the planned lifespan if global carbon emissions and SLR turns out to be lower than expected according to the P5 of RCP4.5. Nonetheless, it is expected that the tipping point will occur sooner than the expected timeframe according to the preferred strategy (2070) of the Delta Programme based on the KNMI'14 scenarios. Therefore, it is desired to implement feasible measures to extend the lifetime of the MLK until at least 2070 in case of accelerated sea level rise.

The focus of this research is mainly on the determination of the tipping point of the current storm surge barriers including the measures to extend the remaining lifetime of the storm surge barriers. It can be financially efficient to postpone the tipping point of the MLK by implementing various response measures instead of a replacement of the barrier or to choose for an entirely new water system in the RMD including dams.

In the preferred strategy of the Delta Programme, the current Europoort barrier could be replaced around the period 2070-2100 by a new, improved barrier with failure probability 1/1000 per closure (Rijkswaterstaat, 2015b). This strategy is based on the climate scenarios, including sea level projections, of KNMI'14. Another option is to replace the MLK by constructing two dams in Rotterdam including shipping locks and large pumps to discharge the river supply. This plan (Dutch: "Plan Sluizen") results in a complete change of the water system of the Rhine-Meuse Delta. This means that the open-closable strategy will be changed to an entirely closed delta. This second plan is included as an alternative when the tipping point of the MLK is reached (Delta Programme 2018).

Before an entirely new strategy is required, various measures can be implemented to extend the operating lifetime of the MLK. The following response measures, including the recommended period (year) to implement, are advised:

- maximize the water level difference to 4 m during a closure. The floodgates can be raised temporarily by maximal 2 m to reduce the horizontal force on the construction (2018-2020);
- always perform a turnaround closure to maximize the storage capacity of the RMD and to limit the tidal wave in the harbour (2018-2020);
- optimize the closing process by minimizing the delay to close (2018-2025);
- reduce the failure rate to 1/200 per closure (2025-2035).

According to the design requirements of the MLK, the acceptable probability of a collapse is less than once per 1,000,000 years (Appendix H). However, the forces on the ball-shaped joint are considered to be too large during a hydraulic head of more than 4 m between both sides of the floodgates. This limitation of the construction is the determining factor in the technical tipping point analysis. To extend this tipping point, it is recommended to temporarily raise the floodgates by 2 m during extreme high-water events of more than +5 m NAP. The force on the barrier will decrease to an acceptable value and wave overtopping will no longer be a problem.

The temporary partial opening of the MLK will slightly reduce the storage capacity. On the other hand, this measure makes the relatively late closure from +2 m NAP irrelevant so that the closure can be started at a lower water level. It is advised to start the closure at the turnaround point during ebb. This increases the net storage capacity of the RMD, resulting in an extended tipping point.

It is essential to implement this procedural change in the short term because, otherwise, the MLK does not meet the safety standard upon 30 cm sea level rise. Changing the procedure can be realized quickly because the water levels are accurately measured, and it is possible to intervene during the automated closing process. An additional advantage is that impact of the tidal wave will be negligible by performing a turnaround closure. The incoming tidal wave during a storm can lead to a very high temporal water level if the storm surge barrier closes during upcoming tide (e.g. closure of Jan 2018). Therefore, it is also recommended to limit the delay in the closure by optimization of the automated operating system (BOS). This measure is explained in more detail on pp. 102-103.

Also, it is advised to investigate possibilities to improve the reliability of the MLK in the longer term, between the year 2025 and 2035. Improving the reliability to a failure rate of 1/200 per closure has a positive effect on the tipping point. Another reason to improve the reliability is the increasing number of required closures due to sea level rise. This will increase the likelihood of a failure during a high-water event. It should be investigated whether such reliability can be achieved by optimizing various contributing factors such as improvement of maintenance intervals, backup systems or operating teams. Furthermore, it is recommended to test the feasibility of improving the failure rate to 1/200 per closure.

The implementation of the above-mentioned measures can be seen as feasible and affordable options to extend the operating lifetime of the MLK. It is expected that these measures improve the lifetime until 0.61 m sea level rise which is expected to occur around the year 2077 (P50 avg. RCP8.5/4.5). Other larger adjustments will probably not result in a significant additional extension of the technical tipping point and are considered to be not financially feasible. After 2050, it is possible that sea level rise accelerates to a large extent, making relatively small measures ineffective.

### 7.3.2 Eastern Scheldt Barrier

The tipping point analysis suggests that the Eastern Scheldt Barrier is probably resistant to a larger extent of SLR than initially planned. However, it is not expected that the barrier will reach the end of its intended lifetime of 200 years in case of accelerated sea level rise without additional measures. According to the risk analysis, the tipping point of the OSK will be reached at 90 cm ( $T=10,000$ ) SLR which is expected around the year 2093 according to the 50<sup>th</sup> percentile of the average between RCP8.5 and 4.5.

It should be noted that the tipping point is caused by the limiting storage capacity and a closing procedure which is inadequate for significant sea level rise. On the other hand, unlike the MLK, the strength of the construction of the OSK is not the decisive limiting factor.

The OSK should remain operational for as long as possible according to the preferred strategy of the Delta Programme, including small modifications to maintain the ecosystem. This implies that an alternative to replace the OSK is not yet available when the ultimate tipping point is reached. A logical consequence is that implementation of measures to extend the technical lifetime of the OSK will be within the preferred decision of the government.

It is proposed to implement the following measures to be able to extend the technical lifetime of the OSK:

- reduce the leak opening to 600 m<sup>2</sup> (2030-2040);
- adjust the closing regime (2030-2040).

Sea level rise will increase the hydraulic loads for the dykes around the Eastern Scheldt due to leakage and a higher closing level during high-water events. Therefore, it is proposed to reduce the leak opening through the floodgates. This measure will reduce the maximum water level in the Eastern Scheldt significantly during a closure under high-end conditions. Furthermore, the slower rate of the water level increase in the Eastern Scheldt during the closure due to the reduced leakage allows an adjusted closing regime. Currently, the protocol is to close in advance of a high-water at 0.5 m NAP (turnaround point ebb). Sea level rise linearly increases this turnaround point of the tidal minimum. Because of the reduced volume of leakage, it is beneficial to close one tide in advance to achieve a lower water level in the Eastern Scheldt during the storm event. This will reduce the risk of exceeding the storage capacity even further. This feature is explained in section 7.1.2.2 and 7.2.1 in more detail.

Both measures extend the technical tipping point significantly. The technical tipping point will be reached at 1.30 m ( $T=10,000$ ) due to exceeding the design load for the construction. It should be noted that the ecological tipping point might be reached at 1 m sea level rise because the floodgates have to close 45 times per year. The effect of more frequent closures to the flora and fauna in the Eastern Scheldt needs to be determined by expert judgment of ecologists. At 1.30 m SLR, the floodgates will have to be permanently closed.

The critical tipping point of the OSK after implementing the prescribed measures can be reached in the year 2081 in case of incredibly accelerating sea level rise but is expected to occur between 2115 and 2120 (avg. RCP8.5/4.5).

Thereafter, attention should be paid to the needs for flood risk management and ecology of the Eastern Scheldt which are unknown yet. At that time, the current flora and fauna including sand plates can only be enforced by large-scale sand replenishments. There is a possibility that a complete closure of the Eastern Scheldt is unavoidable after the year 2100 due to the potential rate of sea level rise of 2-4 m per century.

# 8. Conclusions, Discussion and Recommendations

This last chapter presents the conclusions, discussion and recommendations of this report. Section 8.1 will describe the answers to the research questions. Then, section 8.2 discusses the validity of the results. Finally, the most important recommendations will be provided in section 8.3.

## 8.1 Conclusions

This section presents the conclusions of the report by answering the research questions. First, the answers to the sub-questions will be given to steer towards the solutions which will be answered in the main research question.

### 8.1.1 Sub-question 1

*What is the impact of climate change on sea level rise projections for the 21<sup>st</sup> century?*

In 2016, the global average temperature has risen by 1.1 °C compared to the pre-industrial period in the year 1750. It might be the case that Earth's atmosphere is already committed to 1.3 °C of global warming, by current CO<sub>2</sub> concentration, because of various climate feedback mechanisms. In 2013, the IPCC concluded that it is incredibly likely that the human influence was dominant in causing the temperature rise over the last century due to increasing carbon emissions. Earlier studies argued that the "business as usual" emission scenario RCP8.5 is likely to be expected by proceeding the current global emission trend, but recent technological innovations and the reducing dependency on fossil energy indicate that a slightly lower emission scenario between RCP4.5 and RCP8.5 is more likely to occur. Nevertheless, it can be concluded that limiting global warming within the Paris Agreement (1.5-2.0 °C) is almost out of reach.

Recent global warming resulted in an accelerated rate of global SLR and is currently increasing to 3.3±0.2 mm per year with an extra acceleration of 0.08 mm every year. The long-term global average was 1.2±0.2 mm per year (1900-1990). The expectation is that this increase will accelerate further due to accelerated mass loss of ice sheets and glaciers but also by steric expansion and land water changes. The accelerated trend is not observed yet in the Netherlands. The regional sea level rise in the Netherlands is currently lower than the global average due to significant variations in wind patterns in the North Sea and gravitational effects of the Greenland ice sheet.

DeConto & Pollard (2016) argue that future sea level rise is much more uncertain than previously thought because of the instability of the West-Antarctic ice sheet. Several dynamic processes such as hydrofracturing, grounding line retreat and ice-cliff failure could increase Antarctic contribution to global sea level rise to a large extent. The condition for this is that the floating ice shelves that provide a buttressing effect to land ice must first disappear in order to start massive ice sheet instability. Ice shelves have lost mass over the past decades and it is expected that floating ice shelves will be largely disappeared around 2050, leading to large-scale crumbling and ice-cliff collapse of land ice. This could be the case in the high carbon emission scenario (RCP8.5) because ice shelves are relatively sensitive to atmospheric and oceanic warming. The Antarctic contribution to global sea level rise might be more than 1 m in the year 2100 for the RCP8.5 emission scenario. The study indicates that large-scale mass loss of the Antarctic ice sheet can be postponed or even prevented by an aggressive reduction in global carbon emissions. It is worth mentioning that the risk of rapid ice sheet dynamics has been included only to a very small extent in the KNMI'14 scenarios. The results are prone to limitations, but the risk of accelerating sea level rise originating from Antarctica cannot be ignored.

Sea level projections for the Netherlands were made during this study based on the current global scenarios and the latest insights around sea level rise. Projected regional sea level rise in the Netherlands is different compared to the global average due to processes such as gravitational effects, vertical land movement and ocean dynamics. Absolute sea level rise in the Netherlands in the long-term perspective could be even more than the global average due to the gravitational effect of ice sheets. The Antarctic ice sheet is expected to become the dominant contributor to sea level rise and have more impact on sea level rise for regions that are relatively far away.

For RCP8.5, the average sea level rise is 1.28 m in the year 2100 compared to 2000. This is 81 cm for the modest emission scenario RCP4.5. The sea level scenarios have a significantly increased uncertainty range. The high-end estimate suggests a rate of 25 mm to 40 mm per year for RCP4.5 and RCP8.5 respectively. It is impossible to forecast the future emission scenario with certainty because of the unknown future climate policies. However, it is assumed that the average between RCP4.5 and RCP8.5 is the most likely to occur during this century based on the trend of the carbon intensity. Therefore, 1.04 m sea level rise is expected at the end of this century.

The essential conclusions are that the impact of climate change on sea level rise could be very large and sea level projections are much more uncertain than previously thought. Two meters of sea level rise or more in the year 2100 cannot be ruled out. The degree of correlation between ice sheet dynamics and temperature change is essential for determining high-end sea level projections. Uncertainty in ice sheet dynamics dominates the high-end percentiles of sea level projections. Focusing only on the median sea level rise with symmetric probability distribution underestimates the flooding risk.

This research advises to include the full bandwidth of the distribution function of sea level rise projections into the other sea level statistics. This method allows making more accurate sea level projections by combining probabilistic sea level rise scenarios. Extra attention should be paid to the potential high-end sea level rise which poses an increased risk for the storm surge barriers. Nevertheless, from 2050 an extra acceleration is expected in all sea level scenarios which can be relevant for the design of new flood defences.

### 8.1.2 Sub-question 2

*What are the hydraulic loads for the Maeslant Barrier and the Eastern Scheldt Barrier and the dykes in the hinterland using the latest sea level rise scenarios?*

The storm surge barriers are of primary importance because these are the first line of defence for the dykes in the hinterland. The storm surge barriers will be assessed on the same heaviest safety standard which will be applied to a dyke within the water system. The required safety standards that will be applied to a specific dyke section, after the regulation change in 2017, depend on the chance of a failure and the risk of flooding. This implies that the storm surge barrier or a dyke does not necessarily fail if a certain water level is exceeded. Nevertheless, it is necessary to determine the hydraulic loads to assess the risk of flooding in detail. The definition of the required safety standard of storm surge barriers is the following:

*The probability of the loss of the water-retaining capacity of a storm surge barrier, resulting in a substantially increased hydraulic load on a backward dyke trajectory.*

The required failure probability for the Maeslant Barrier is increased from 1/10,000 to 1/30,000 per year after the regulation change. Also, the safety standard for the Eastern Scheldt Barrier is changed from 1/4,000 to 1/10,000 per year. These storm surge barriers protect the dykes in the hinterland against aggregated hydraulic loads. Different safety standards between 1/300 and 1/30,000 apply for the dykes in the Rhine-Meuse Delta and the Eastern Scheldt. The hydraulic loads are calculated for both storm surge barriers and several dyke-sections which are part of both water systems.

The hydraulic loads for the storm surge barriers are influenced mainly by sea level projections. Currently, coastal flood defences are usually designed with a fixed sea level rise of 0.85-1 m in the year 2100. Research has shown that the uncertainty in SLR has increased significantly which should be incorporated in the risk analysis.

It can be stated that for the applicable safety standard for the MLK, a significant volume of wave overtopping occurs. This is similar to the OSK where roughly 1,700 l/s/m wave overtopping could occur during a high-water event with a yearly exceedance frequency of 1/10,000. The expected peak sea levels in front of the barriers are

+6.07 m NAP for the MLK and +5.44 m NAP for the OSK. The water-retaining height of the closed arc-shaped doors of the MLK is +5.0 m NAP which means that a significant volume of water overrun can occur in addition to wave overtopping. Water overrun is considered acceptable, because of the large storage capacity of the water system. Nevertheless, increasing hydraulic loads introduces risks to the construction of the storm surge barrier. Sea level rise significantly increase the sea level and rate of wave overtopping.

The consequences of SLR to the inherent water system of both storm surge barriers are analyzed for seven dyke-sections located in the Rhine-Meuse Delta and for twelve dyke sections in the Eastern Scheldt. It can be concluded that the effect of SLR is much smaller in the hinterland due to the storm surge barriers. The effect of SLR to the maximum water levels is transferred for 35% to the Rhine-Meuse Delta and only for 15% to the Eastern Scheldt. It should be noted the effects of sea level rise to the hydraulic loads for backward dykes are underestimated. This is because the model assumes a functioning storm surge barrier and a maintained closing water level in all conditions. In reality, the storm surge barrier can also fail due to a construction failure.

Sea level rise results in more frequent closures and an increased likelihood of a closing failure which increases the maximum hydraulic loads for dykes in the hinterland. Various dyke sections in both water systems should be reinforced to meet the requirements for wave-overtopping despite the underestimation of the effects of SLR.

In the end, it can be concluded that the model cannot give a definitive answer about the technical tipping point of the storm surge barriers due to the limitations of assessment programme Hydra-NL. This will require a risk analysis which includes all effects of sea level rise.

### 8.1.3 Sub-question 3

*What is the remaining lifetime of the Maeslant Barrier and the Eastern Scheldt Barrier and how many years of extension can be achieved by implementing adjustments?*

The Maeslant Barrier and Eastern Scheldt Barrier were built in a period in which seriously accelerated sea level rise was not expected. For the MLK, no explicit prescribed design requirement for sea level rise was given, but specialists indicate that 50 cm sea level rise at the end of the 100-year operating lifetime has been implemented in the design. On the other hand, the OSK should be operational for 200 years, but only 40 cm relative sea level rise was considered in the design.

It is clear that the designers have underestimated the uncertainty of sea level rise. However, it appears that margins have been implemented in the design which results that the barriers might be able to endure more SLR. The ability of the barriers to deal with sea level rise primarily depend on the effect of sea level rise to the hydraulic loads in the hinterland.

As result of the risk analysis, the technical tipping point of the MLK is 0.30 m sea level rise for exceedance frequency 1/30,000 per year. However, the barrier should be able to withstand 0.65 m SLR for the previous safety standard of T=10,000. It should be noted that a high-water event with an extreme sea level in combination with a modest river supply is a decisive situation for the construction of the MLK. This implies that the large water level difference between both sides of the floodgates have the potential to exceed the maximum acceptable load on the ball-shaped joint of the barrier. Moreover, the current closing procedure induces a risk of temporarily exceeding critical water levels in Rotterdam due to the relatively late closure. Implementing adjustments to the procedure and the closing reliability can extend the technical tipping point of the MLK to 0.61 m SLR for T=30,000.

The technical tipping point of the OSK will be reached at 0.90 m sea level rise which is considerably more than according to the design. The leak volume during a closure poses the largest risk for exceeding the maximum water storage capacity of the Eastern Scheldt. Adjustments to the leak opening and the closing procedure can extend the tipping point to 1.30 m SLR.

The remaining lifetime of the storm surge barriers depends on the rate of future SLR, which is very uncertain. Before implementing adjustments, the expected remaining lifetime of the MLK is 37 years (2055) and 75 years for the OSK (2093). However, a 5% chance exists that the remaining lifetime of the MLK is only 24 years (2042) and 52 years for the OSK (2070) for the high-end situation of the highest emission scenario.

Significant extension of the remaining lifetime can be obtained by implementing the described adjustments. The remaining lifetime of the MLK can be extended by 22 years (2077) for the expected sea level scenario which is the average between RCP8.5 and RCP 4.5. An extension of 18 years (2060) can be achieved in case of using the high-end scenario of RCP 8.5. For the OSK, the remaining lifetime can be extended by 22-27 years (2115-2120) for the median sea level scenario and by 11 years (2081) for the high-end scenario of RCP 8.5.

### 8.1.4 Main research question

*How can the Dutch storm surge barriers be adapted to extend the remaining lifetime to deal with the risk of accelerated sea level rise due to climate change?*

Climate change and future sea level rise have a significant impact on water safety and the remaining lifetime of the Maeslant Barrier and Eastern Scheldt Barrier. The remaining lifetime of both barriers is expected to be considerably shorter than initially planned in case of accelerated sea level rise. It is important to identify the degree of uncertainty of climate change and sea level rise in order to develop effective strategies for the storm surge barriers.

The risk analysis showed that the MLK is relatively vulnerable to sea level rise. The construction may not be sufficiently resistant to the horizontal load exerted on the doors during a high-water event. Furthermore, the current procedure has the potential to let in a tidal wave which can temporarily exceed the critical water levels for the primary dykes in Rotterdam.

The technical tipping point of the MLK will be reached at 30 cm sea level rise which is expected to occur sooner than the expected timeframe according to the preferred strategy (2070) of the Delta Programme. Therefore, it is recommended to implement the following adjustments to the Maeslant Barrier to extend the remaining lifetime:

- maximize the water level difference to 4 m during a closure. The floodgates can be raised temporarily by maximal 2 m to reduce the horizontal force on the construction (2018-2020);
- always perform a turnaround closure to maximize the storage capacity of the RMD and to limit the tidal wave in the harbour (2018-2020);
- optimize the closing process by minimizing the delay to close (2018-2025);
- reduce the failure rate to 1/200 per closure (2025-2035).

The implementation of the above-mentioned measures can be seen as feasible and affordable options to reduce the risk of flooding and extend the operating lifetime of the MLK. It is expected that these measures will extend the lifetime until approximately the year 2077, which corresponds to 61 cm sea level rise. This expectation lies within the timeframe of the preferred strategy of the Delta Programme to replace the MLK around 2070-2100. At that time, the change of the open-closable strategy to an entire closed delta may be one of the alternatives.

On the other hand, the robustness of the Eastern Scheldt Barrier and the implemented surcharges in the design makes this barrier resistant to a larger extent of SLR than previously thought. Nevertheless, it is not expected that the barrier will reach the end of its intended lifespan of 200 years. According to the risk analysis, the tipping point of the OSK will be reached at 90 cm (T=10,000) sea level rise which is expected to occur in 2093.

The OSK should remain operational for as long as possible according to the preferred strategy of the Delta Programme. Therefore, it is proposed to perform the following measures to extend the lifetime of the OSK:

- reduce the leak opening to 600 m<sup>2</sup> (2030-2040);
- adjust the closing regime (2030-2040).

Both measures will significantly extend the technical tipping point and are feasible within the strategy of the Delta Programme. After implementing the adjustments, the technical tipping point will be reached at 1.30 m SLR (T=10,000) which probably extend the remaining lifetime beyond 2100. At that point, a considerable chance exists that a permanent closure of the Eastern Scheldt cannot be avoided without significantly changing the closing strategy.

## 8.2 Discussion

This subsection reflects on the validity of the research including the methodology and assumptions.

### 8.2.1 Climate change and sea level rise

The IPCC presented 4 carbon emission scenarios, RCP2.6, RCP4.5, RCP6.0 and RCP8.5 including sea level projections. These sea level projections are based on outdated studies that only cover the ice dynamics of the Antarctic ice sheet to a very small extent. Furthermore, the SLR projections of the IPCC did not include the full bandwidth of the probability distribution function because of limitations in ice sheet modelling. The risk of ice sheet dynamics to the SLR scenarios is incorporated by other studies, discussed in Section 5.3.5.

Recent studies suggest that both the mean (P50) as the high end (P95) of the distribution function should shift towards higher values. The recent insights of Deconto & Pollard (2016) indicate that the contribution of the ice sheet dynamics in Antarctica can potentially become the dominant factor in sea level rise, starting around the year 2050. This research has modelled ice sheet dynamics quantitatively for the first time, so these results should not be underrated. The ice hydrofracturing and ice-cliff collapse mechanisms in DP16 lead to a significant upward shift in sea level projections for scenarios RCP8.5 and RCP4.5. Despite the uncertainties in the used model, which can either under- or overestimate the outcomes, the results are audited and are considered to be potentially realistic. That is why it was decided to include the results of DP16 for 50% in the analysis. The remaining 50% consists of a combination of several studies which are based on the IPCC AR5 projections which partly include the risk of ice sheet dynamics. This is explained in Section 5.7.2 in more detail. The ratio between the used reference studies is kept the same but might change when new information will be available. Nevertheless, there is still no clear indication to use a different ratio. It is advised to use the latest upcoming new studies to validate the given scenario more specifically.

It should be noted that the scenario for the Netherlands is based on the global projections using a factor based on the regionalization methods of de Vries et al. (2014) and Grindsted et al. (2015). This means that the regional scenario is based on the same regionalization factors as used in the two reference studies. It is not expected that the results will differ significantly when a regionalization model is used, but it is advised to redo the analysis according to methods of both studies.

This thesis used emission scenario RCP4.5 and RCP8.5 as lower- and upper bound of the range of the potential future carbon concentration. This assumption is based on the recent study conducted by Raftery et al. (2017). According to their results, emission scenario RCP8.5 which is often used for SLR projections is not very probable to occur (<10%). On the other hand, an ambitious scenario such as RCP2.6 is even more unlikely. RCP6.0 should be reasonable, but only a few SLR studies are based on RCP6.0. Ultimately, the average between SLR scenario for RCP8.5 and RCP4.5 during this century is used as basis. However, the future sea level pathway is very uncertain and dependent on global future carbon emission policies. This uncertainty is addressed in the tipping point analysis of the storm surge barriers which is presented in Section 7.2.

The results provide physically meaningful projections that can lead to more than 2 m sea level rise with RCP8.5 and more than 1.4 m with RCP4.5 in the year 2100 in case of high-end SLR. Policymakers should use these results as an expanding understanding of the potential range of sea level rise, rather than using the numbers.

### 8.2.2 Hydraulic loads and Hydra-NL

The hydraulic loads for the flood defences for various safety standards are computed using Hydra-NL according to the WBI-2017 standards. Important to note is that the focus of this thesis is primarily on the storm surge barriers. However, the effects on dykes in the hinterland are excessive, so these also have to be considered. This research is limited only to failure mechanism wave overtopping. It is assumed that dykes will be strengthened in such way that the other failure mechanisms such as macro instability and piping will not apply.

It is not yet possible to calculate the uncertainty in the SLR scenarios probabilistically in combination with other sea level statistics using Hydra-NL. Therefore, the hydraulic loads are determined by using fixed values for median SLR and high-end SLR for emission scenarios RCP4.5 and RCP8.5.

Furthermore, Hydra-NL is prone to various limitations underestimate the effects of sea level rise. For example; the model assumes that the closing level does not change for significant SLR. However, SLR results in an increased sea level during ebb which leads to a higher closing water level which reduces the remaining storage capacity to a large extent. This effect of SLR is included in the risk analysis.

Sea level rise has been included in the model until the year 2023. The SLR projections are given from 2000 until 2100, requiring 5 cm reduction of the SLR projection to avoid double counting in Hydra-NL.

The failure rate of the Europoort Barrier is set on 1/100 per closure which is in accordance with the user guideline of Hydra-NL. This value is obtained from the current failure rate of the MLK. It has been determined that the failure rate of the HK which is 1/10 per closure only has a very limited effect. As a result, the combined failure probability is not adjusted. However, a slightly higher failure rate could also be chosen.

Test location 2 (MLK-2) has been used to determine the hydraulic loads on the MLK. This location is about one km in front of the storm surge barrier (Appendix K). The results showed that for MLK-1, which is closer to the MLK, no representative calculation could be made due to the inconsistent geometry of the bottom. Therefore, the results of MLK-2 are retained in the further analysis.

It should be noted that the used geometry of various dyke-sections can slightly differ from the actual situation. This means that the maximum volume of wave overtopping can deviate slightly from the actual situation. It is not expected that this deviation is large because only the slope of the dyke profiles is not always accurate. The hydraulic loads in Rotterdam RMD-5 are obtained by using an accurate dyke profile.

The water levels on location RMD-6 are too low at low return periods and limited SLR. This dyke section is located in a floodplain, which will not inundate at lower water levels. Still, it is clearly visible that the limited height of this dyke leads to an increased risk of flooding. It is expected that this dyke will be strengthened in the short-term to the adapted safety standard.

For the assessed dykes around the Eastern Scheldt, a simplified profile has been chosen in which the geometry almost corresponds to the reality, but without including a foreland. According to the results, the height of many dykes turned out to be insufficient, in terms of wave overtopping, so that the rejected dykes were assessed with accurate profiles, including the actual foreland. It can be stated with certainty that the dykes that meet the requirements for the simplified profile will also be sufficiently assessed when adding a foreland. Unfortunately, no further information was available about the soil and foreland in front of the Oesterdam (OS-4) and Philipsdam (OS-9) which will have a relatively high rate of wave overtopping. This will not be an immediate problem due to the presence of a backward water storage basin. The main reason for the minor deviations in the dyke profiles that have not been adjusted for each test location is caused by the restricted availability of the data and the long calculation time in Hydra-NL (including model uncertainties).

### 8.2.3 Risk analysis

In the risk analysis, the remaining lifetime of the Maeslant Barrier (MLK) and the Eastern Scheldt Barrier (OSK) is determined. It should be emphasized that the risk analysis needs to be used as an addition to the full assessment method of the WBI-2017.

The risk analysis can be seen as a validity test of the results from Hydra-NL. According to the results of Hydra-NL, the hydraulic loads for the dykes behind the storm surge barriers do only slightly increase at accelerated sea level rise. This is based on the assumption that the storm surge barriers continue to function according to the current protocol during a storm closure with significant SLR. However, the actual influence of SLR on the maximum hydraulic loads during a high-water event might be more significant. The closing water level will increase considerably due to the increased minimum water level during low tide. Also, the volume of wave overtopping will increase with SLR. These consequences are only included to a limited extent in Hydra-NL.

The risk analysis contains various assumptions which will be discussed in more detail. First, it should be noted that the risk factors are not probabilistically combined which can slightly under- or overestimate the results.

Second, it is expected that the dykes in the Rhine-Meuse Delta and around the Eastern Scheldt will be reinforced to the new safety standard if required. The risk analysis focuses primarily on the storm surge barriers and it is not expected that a small exceedance of some previous critical water levels (MHW) in the hinterland will lead to the technical tipping point of the barrier.

Third, the water levels in front of the MLK calculated by using Hydra-NL include the effect of seiches. Combined with an additional impoundment of seawater due to the closed barrier, this results in a considerably higher peak water level than the water-retaining height of the MLK for (T=10,000 and T=30,000). However, this water level is not entirely representative for determining the horizontal load on the floodgates, because this water level reduces considerably due to the large volume of water overrun and leakage. This could potentially lower the horizontal loads on the closed floodgates. The calculated horizontal loads (Section 7.1.3.1) indicate that the MLK could potentially resist, a greater water difference than 4 m between both sides. However, it is recommended to prevent exceeding this requirement. This leads to the conclusion that the limitation in the construction may be decisive in the tipping point analysis without the implementation of the recommended adjustments.

Furthermore, partly raising the floodgates of the MLK during a temporarily sea level above +5 m NAP introduces a secondary risk. The top layer of the stone grading behind the floodgates can be damaged during peak water levels. Nevertheless, it is assumed that small damage is acceptable during T=10,000 storm events. If the soil protection appears to be inadequate, it can be decided to reinforce the bed protection behind the floodgates.

Fourth, according to the design calculations, the OSK should be able to handle a water level difference of 6.2 m, which means that there is virtually no risk for the construction. This design requirement has been applied in the risk analysis. However, significant sea level rise can result to a large volume of water overrun over the top of the construction. The risk of fatigue damage or horizontal displacement of the OSK for such accelerated sea level rise should be investigated in more detail.

Fifth, the leak volume and the rate of wave overtopping (>2,000 l/s/m) are calculated by various hydraulic formulas. These calculations are based on assumptions such as average water level difference to determine the flow velocity and the dominant wave angle that influences the volume of overflow. Furthermore, the hydraulic loads are computed for one location in front of the MLK and for the three sections of the OSK.

Sixth, the total duration of the closure and the average water level in the hinterland at the start of the closure are both very important in the calculation of the risk of exceeding the storage capacity. Values are based on the analysis of model storms and actual data of past storms in the Netherlands. The values used are determined by own judgment and compared with Hydra-NL. The risk analysis does not include (model) uncertainties. However, model uncertainties according to the WBI-2017 are used for the hydraulic loads computed by Hydra-NL.

Seventh, the impact of the failure rate of both barriers to the storage capacity is calculated using Hydra-NL and is added to the maximum water levels under an ideal functioning barrier. This approach can be discussed but is an appropriate way to quantitatively include the failure rate into the risk analysis.

Eight, the number of required closures per year might deviate for more than 1 m sea level rise from reality due to model limitations of Hydra-NL. This model calculates the required number of closures during a period of 180 days (winter) per year. This will underestimate the closing frequency for high sea level rise (>1 m) because a closure can also take place in summer.

The proposed adjustments to extend the tipping point are considered as adequate, which are also feasible to execute. More rigorous measures such as increasing the height of the floodgates of the Hartel Barrier or the relocation of the threshold blocks can extend the technical lifetime further but are considered as less effective. The same applies to the OSK where raising the water-retaining height of the barrier with a wall (1 m) placed on the concrete beam is less effective than reducing the leakage opening.

To conclude, the performed risk analysis is a tool to generally recognize the factors that can influence the tipping point of the storm surge barriers. This analysis should be seen as a useful enhancement for the understanding of the effects of SLR on the storm surge barriers. For validation, it is advised to perform a customised assessment using the WBI-Software Ringtoets.

## 8.3 Recommendations

This section provides recommendations for future research.

- Recent studies show that the uncertainty of future sea level rise depends mainly on the future emission scenario (DeConato & Pollard, 2016). Most studies analyzed the effect of SLR for the highest emission scenario RCP8.5, while it is not very likely that this scenario will occur (Raftery et al., 2017). Therefore, the emphasis should be more on examining the likelihood of the various global emission scenarios by assessing the latest insights of the carbon intensity to project the future emission scenario. This can reduce the uncertainty of future SLR significantly which helps to design water policy strategies to deal effectively with future SLR.
- A major limitation of the results of DP16 is the lack of observations on the Antarctic ice sheet. Primarily, the available data of ice properties, ocean temperature and the bathymetry of the bedrock is limited (Griggs et al., 2017). The results of DP16 may have consequences for global coastal reinforcement and adaptation plans, which will cost a lot of money despite the considerable uncertainty in the sea level projections. For this reason, it is recommended to first invest in monitoring the Antarctic ice sheet to reduce the uncertainty in the sea level scenarios before implementing expensive measures.
- The time when the large-scale Antarctic contribution to future SLR will start is still profoundly uncertain, Deconato & Pollard (2016) (DP16) project that this contribution starts around 2050 for RCP8.5 and RCP4.5. However, various uncertainties in the processes that can influence the Antarctic contribution can both over- or underestimate the rate of SLR. This thesis includes the results of DP16 for 50% in the sea level projections while the other 50% is based on studies that refer to IPCC projections. It is recommended to make an updated sea level scenario when more studies about the Antarctic contribution are published in the next years.
- This thesis only analyzes the effect of climate change on sea level rise. Water safety is influenced by more factors that are caused by climate change. Increasing river supply to the Rhine-Meuse Delta is included in the analysis. However, it is expected that the wave height increases due to the rising water levels and higher wind velocities in the future. Furthermore, climate change might cause additional storm surge which potentially increases the peak sea level. These uncertainties are discussed in the report but are not included in the calculations. It is recommended to investigate the effects of these potential consequences of climate change.
- Latest studies show that the actual uncertainty around future SLR is significantly larger than initially thought in the IPCC AR5 and KNMI'14 scenarios. Currently, a fixed high-end value of SLR is included in the design of flood defences. However, due to this increased uncertainty, it is advised to include the total uncertainty range into the probabilistic assessment models. According to the results of this thesis, the expected average rate (P50) of sea level rise can be compared to the current high-end projections. The difference here is that the upper range of the new SLR projections should also be considered in the risk analysis. Another recommendation would be to investigate the feasibility of constructing flood defences with a relatively short lifespan due to the considerable climate uncertainty.
- The risk analysis assesses various factors that influence the remaining lifetime of the storm surge barriers. The primary purpose of this analysis is to gain insight into which factors can have a significant influence on the tipping point of the storm surge barriers. Furthermore, it can help to clarify the limitations of the assessment model Hydra-NL. Therefore, it is being required to deviate from the assessment method of WBI-2017 because it is impossible to determine all failure mechanisms of the flood defences in the Rhine-Meuse Delta and the Eastern Scheldt. Redoing the analyses according to the assessment methodology of WBI-2017 might partly change the conclusions.
- It is recommended to further analyze the effects of SLR on the other components and connecting constructions of the storm surge barriers. The emphasis of this study is mainly on the main elements such as the arc-shaped floodgates and foundation of the MLK and the three sections of the OSK.
- The focus of this thesis is mainly on determining the technical tipping point of the storm surge barriers using the latest insights into climate change. Accelerated SLR will make water safety increasingly important, but the effects of climate change on the economy, ecology and society are not examined in detail. It is not expected that the Maeslant Barrier and the Eastern Scheldt Barrier will be removed or

replaced in favour of economics, ecology or society in the area before the technical tipping point is reached. However, it is recommended to include these aspects in more detail in a Cost-Benefit Analysis in a subsequent study.

- It is recommended to focus also on the effect of another type of adjustments described in Section 7.2.2 such as increasing the height of the floodgates of the Hartel Barrier and increase the water-retaining height of the Eastern Scheldt Barrier.
- Reinforcing flood defences take a long period of time. It might take too long to upgrade flood defences and especially the fixed storm surge barriers when accelerated sea level rise will begin. It is advisable to analyze how quickly the current storm surge barriers can be replaced, if necessary, and how much this replacement will cost.
- This research focuses mainly on the effects of SLR within this century, in which the tipping points of the storm surge barriers are expected to be reached. However, if SLR starts to accelerate in the Netherlands, the consequences will be much more significant in the 22<sup>nd</sup> century and thereafter. SLR can potentially become the main threat to the habitability of the low-lying parts of the Netherlands. There is still a significant shortage of studies and literature that extensively discusses this risk including long-term strategies. It is, therefore, recommended to investigate the effects of SLR to the Netherlands in the very long-term.

## List of references

- Alexander, P. (2013, July). *Glacier d'Argentière*. Retrieved from Randos Mont Blanc: <http://www.randos-montblanc.com/en/intermediate-hikes/glacier-argenterie.html>
- Arnell, N., Brown, S., & Gosling, S. (2016). *Global-scale climate impact functions: the relationship between climate forcing and impact*. *Climate Change* 134 475-87.
- Arrhenius, S. (1896). *On the influence of carbonic acid in the air upon the temperature of the ground*. London, Edinburgh: Dublin Philosophical Magazine and Journal of Science.
- Aton, A. (2017). *Earth almost certain to warm by 2 degrees*. Retrieved from Scientific America: <https://www.scientificamerican.com/article/earth-almost-certain-to-warm-by-2-degrees-celsius/>
- Bamber, J., & Aspinall, W. (2013). *An expert judgement assessment of future sea level rise from the ice sheets*. *Nature Climate Change*. DOI: 10.1038/NCLIMATE1778.
- Banwell, A., Caballero, M., Arnold, N., Glasser, N., Cathles, L., & Macayeal, D. (2014). *Supraglacial lakes on the Larsen B ice shelf, Antarctica, and at Paakitsoq, West Greenland: a comparative study*. *Annals of Glaciology* 55(66) DOI: 10.3189/2014AoG66A049.
- Boardman, A., Greenberg, D., & Vining, A. (2012). *Cost Benefit Analysis: Concepts and Practice*. New Jersey: Pearson.
- Bortman, M., Brimblecombe, P., Freedman, W., & Cunningham, M. (2003). *Environmental Encyclopedia*. Farmington Hills, USA: Thomson Gale.
- BWW. (1995). *Handleiding voor het ontwerpen van granulaire bodemverdedigingen achter tweedimensionale uitstromingsconstructies. doc nr: BOD-R-95002*. Bouwdienst Weg en Waterbouwkunde; Rijkswaterstaat.
- Church, J., Clark, P., Cazenave, A., Gregory, J., Jevrejeva, S., Levermann, A., . . . Unnikrishnan, A. (2013). *Sea Level Change*. In: *Climate Change 2013: The Physical Science Basis. Contribution of Working Group I to the Fifth Assessment Report of the Intergovernmental Panel on Climate Change*. Cambridge: Cambridge University Press.
- Climate Analytics. (2016). *Global warming reaches 1°C above preindustrial, warmest in more than 11,000 years*. Retrieved from Climate Analytics: <http://climateanalytics.org/hot-topics/global-warming-reaches-1c-above-preindustrial-warmest-in-more-than-11000-years.html>
- Council, National Research. (2012). *Climate Change: Evidence, Impacts and Choices*. Washington D.C.: The National Academies Press.
- Cubasch, U., Wuebbles, D., Chen, D., Facchini, M., Frame, D., Mahowald, N., & Winther, J. (2013). *Introduction*. In: *Climate Change 2013: The Physical Science Basis. Contribution of Working Group I to the Fifth Assessment Report of the Intergovernmental Panel on Climate Change*. Cambridge, United Kingdom and New York: Cambridge University Press.
- Curtis, T. (2015). *CO2 lags temperature - what does it mean?* Retrieved from Skeptical Science: <https://skepticalscience.com/argument.php?a=7&p=11>
- D. Le Bars, H. d. (2016). *Probabilistic projection of sea level along the Dutch coast*. De Bilt: KNMI.
- de Boer, B., Van de Wal, B., Lourens, L., & Tuetter, E. (2010). *Cenozoic global ice-volume and temperature simulations with 1-D ice-sheet models forced by benthic  $\delta^{18}O$  records*. *Ann. Glaciol.* 51, 23–33. DOI:10.3189/172756410791392736.
- de Jong, M. (2004). *Origin and prediction of seiches in Rotterdam harbour basins*. TU Delft.
- de Ronde, J., Baart, F., Katsman, C., & Vuik, V. (2014). *Zeespiegelmonitor*. Delft: Deltares.
- de Vries, H., Katsman, C., & Drijfhout, S. (2014). *Constructing scenarios of regional sea level change using global temperature pathways*. *Environmental Research Letters*.

- de Winter, R. T., de Winter, R., Reerink, T., Slangen, A., de Vries, H., Edwards, T., & van der Wal, R. (2017). *Impact of asymmetric uncertainties in ice sheet dynamics on regional sea level projections*. *Natural Hazard and Earth System Sciences*.
- DeConto, R., & Pollard, D. (2016). Contribution of Antarctica to past and future sea-level rise. *Macmillan Publishers Limited: Nature*, 531 591-7.
- Delta Programme 2015*. The Hague: Ministry of infrastructure and environment.
- Delta Programme 2016*. The Hague: Ministry of infrastructure and environment.
- Delta Programme 2017*. The Hague: Ministry of infrastructure and environment.
- Delta Programme 2018*. The Hague: Ministry of infrastructure and environment.
- Deltares. (2014). *Delta programme and Adaptive Delta Management*. Retrieved from [https://www.deltares.nl/en/projects/deltaprogram/?return\\_id=2978](https://www.deltares.nl/en/projects/deltaprogram/?return_id=2978)
- Deltares. (2015a). *WTI 2017 Kunstwerken*.
- Deltares. (2015b). *Handreiking Dijkbekledingen Deel 4: Breuksteenbekledingen*.
- Deltares. (2017a). *Hydraulic loads Oosterschelde; WBI 2017*.
- Deltares. (2017b). *Hydraulische Belastingen Rijntakken en Maas; WBI-2017. 1230087-003*.
- Deltares. (2017c). *Basisstochasten WTI-2017. Statistiek en statistische onzekerheid*.
- Deltares. (2018). *Average sea level in 2017 the highest ever recorded along Dutch coast*. Retrieved from <https://www.deltares.nl/nl/nieuws/zeespiegel-nederlandse-kust-2017-hoogste-ooit-gemetten/>
- Deltawerken. (2004). *De Deltawerken*. Retrieved from Deltawerken online: <http://www.deltawerken.com/De-Deltawerken/1548.html>
- Deugd, H. D. (2007). *Waterloopkundige berekeningen TMR2006 Benedenrivierengebied*. RWS RIZA rapport 2007.017. Lelystad 2010.
- Dieng, H., Cazenave, A., Meyssignac, B., & Ablain, M. (2017). *New estimate of the current rate of sea level rise from a sea level budget approach*. *Geophysical Research Letters*, 44, 3744-3751, DOI:10.1002/2017GL073308.
- Dutton, A., Carlson, E., Long, A. J., Milne, G. A., Clark, P. U., DeConto, R., . . . Raymo, M. E. (2015). *Sea-level rise due to polar ice-sheet mass loss during past warm periods*. *New York: Science* p. 349 DOI: 10.1126/science.aaa4019.
- Earth Observatory. (2001). *The Impact of Climate Change on Natural Disasters*. Retrieved from Earth Observatory: [https://earthobservatory.nasa.gov/Features/RisingCost/rising\\_cost5.php](https://earthobservatory.nasa.gov/Features/RisingCost/rising_cost5.php)
- ENW. (2016). *Grondslagen voor hoogwaterbescherming*. Ministry of Infrastructure and Environment.
- Favier, L. G.-C. (2014). *Retreat of Pine Island glacier controlled by Marine Ice Sheet Instability*. *Nature Climate Change*.
- Flood Protection Programme. (2017). *New safety norm*. Retrieved from Dutch Flood Protection Programme: <http://www.hoogwaterbeschermingsprogramma.nl/Nieuwe+normering/default.aspx>
- Fretwell, P., Pritchard, H., Vaughan, D., Bamber, J., Barrand, N., & Bell, R. (2012). *Bedmap2: improved ice bed, surface and thickness datasets for Antarctica*. *Antarctica. Cryosphere* 7:375–393.
- Gardner, A., Moholdt, G., Cogley, J., Wouters, B., Arendt, A., Wahr, J., . . . Paul, F. (2013). *Reconciled estimate of glacier contributions to sea level rise: 2003 to 2009*. *Science*, 340, 852–857.
- Gerritsen, H. (2005). *What happened in 1953? The Big Flood in the Netherlands in retrospect*. Delft: Philosophical transactions.

- Gomez, N. D. (2015). *Sea-level feedback lowers projections of future Antarctic ice-sheet mass loss*. Nature Communications 8798 DOI: 10.1038/ncomms9798.
- Google. (2018). *Google Earth*. Retrieved from <https://www.google.nl/earth>
- Gouretski, V., & Koltermann, K. (2007). *How much is the ocean really warming?* Geophys. Res. Lett., 34, L01610.
- Griggs, G., Árvai, J., Cayan, D., DeConto, R., Fox, J., Fricker, H. A., . . . Group), (. O. (2017). *Rising seas in California; An update on sea-level rise science*.
- Grindsted, A., Jevrejava, S., Riva, R., & Dahl-Jensen, D. (2015). *Sea level projections for northern Europe under RCP8.5*. Climate Research Vol.64 15-23 DOI: 10.3354/cr01309.
- Haasnoot, M. J. (2013). *Dynamic Adaptive Policy Pathways: A method of crafting robust decisions for a deeply uncertain world*. Global Environment Change 23(2) 485-498 DOI: 10.1016/j.gloenvcha.2012.12.006.
- Haasnoot, M., & Middelkoop, H. (2012). *A history of futures: A review of scenario use in water policy studies in the Netherlands*. Delft, The Netherlands: Elsevier Ltd.
- Hanna, E., Navarro, F., Pattyn, F., Domingues, C., Fettweis, X., Ivins, E., . . . Zwally, H. (2013). *Ice-sheet mass balance and climate change*. Macmillan Publishers Limited Vol 498; DOI:10.1038/nature12238.
- Hansen, J., Sato, M., Russel, G., & Kharecha, P. (2013). *Climate sensitivity, sea level and atmospheric carbon dioxide*. New York, USA: Philosophical Transactions of the Royal Society.
- Hartmann, D., Klein Tank, A., Rusticucci, M., Alexander, L., Brönnimann, S., Charabi, Y., . . . Zhai, P. (2013). *Observations: Atmosphere and Surface*. In: *Climate Change 2013: The Physical Science Basis. Contribution of Working Group I to the Fifth Assessment Report of the Intergovernmental Panel on Climate Change*. Cambridge, United Kingdom and New York: Cambridge University Press.
- Hawkins, E., Ortega, P., Suckling, E., Schurer, A., Hegerl, G., Jones, P., . . . van Oldenborgh, G. (2017). *Estimating changes in global temperature since the pre-industrial period*. Bull. Amer. Meteor. Soc. DOI:10.1175/BAMS-D-16-0007.1, in press.
- Hay, C., Morrow, E., Kopp, R., & Mitrovica, J. (2015). *Probabilistic re-analysis of twentieth-century sea-level rise*. Nature 517 p481-481 DOI:10.1038/nature14093.
- Hijma, M., Kooi, H., & Erkens, G. (2017). *Bodemdaling van het kustfundament en de getijdenbekkens*. Deltares.
- HKV. (2012). *Onderzoek naar de verbetering van de veiligheid die de Maeslantkering biedt*.
- HKV. (2015). *Achtergrondrapportage varianten voor afsluiting Rijnmond*.
- Hoogland, T., van den Akker, J., & Brus, D. (2012). *Modeling the subsidence of peat soils in the Dutch coastal area*. Wageningen, The Netherlands.
- Horton, B., Rahmstorf, S., Engelhart, S., & Kemp, A. (2013). *Expert assessment of sea-level rise by AD 2100 and AD 2300*. Elsevier.
- HSK. (2015). *Feiten en fabels over dijken in Nederland*. Opgehaald van Waterschappen: <https://www.waterschappen.nl/feiten-en-fabels-over-dijken-in-nederland/>
- IMBIE Team. (2018). *Mass balance of the Antarctic ice sheet from 1992 to 2017*. Nature volume 558, pages 219–222 (2018).
- Ingenieur. (2016). *De Oosterschelde bracht het keerpunt*. Retrieved from De Ingenieur: <https://www.deingenieur.nl/artikel/de-oosterschelde-bracht-het-keerpunt>
- IPCC. (1990). *Climate Change 1990: First Assessment report*. UK: Cambridge University Press.
- IPCC. (2013). *Climate Change 2013: The Physical Science Basis. Contribution of working group I to the Fifth Assessment Report of the Intergovernmental Panel on Climate Change*. Cambridge, United Kingdom and New York: Cambridge University Press.

- IPCC. (2014). *Climate Change 2014: Synthesis Report. Contribution of Working Groups I, II and III to the Fifth Assessment Report of the Intergovernmental Panel on Climate Change*. Geneva, Switzerland: IPCC.
- Jackson, L., & Jevrejeva, S. (2016). *A probabilistic approach to 21st century regional sea-level projections using RCP and High-end scenarios*. Elsevier.
- Jeuken, A., & te Linde, A. (2011). *Werken met knikpunten en adaptatiepaden*. Deltares.
- Jevrejeva, S., Grindsted, A., & Moore, J. (2014). *Upper limit for sea level projections by 2100*. Environmental Research Letters.
- Johansson, M., Pellikka, H., Kahma, K., & Ruosteenoja, K. (2012). *Global sea level rise scenarios adapted to the Finnish coast*. Elsevier.
- Jorissen, R., Kraaij, E., & Tromp, E. (2016). *Dutch flood protection policy and measures based on risk assessment*. Lyon: European Conference on Flood Risk Management.
- Joughin, I. B. (2014). *Marine ice sheet collapse potentially under way for the Thwaites glacier basin, West Antarctica*. Science.
- Joughin, I., Smith, B., Howat, I., Floricioiu, D., Alley, R., Truffer, M., & Fahnestock, M. (2012). *Seasonal to decadal scale variations in the surface velocity of Jakobshavn Isbrae, Greenland: Observation and model-based analysis*. Journal of Geophysical Research: VOL. 117, F02030, DOI:10.1029/2011JF002110.
- Keringshuis. (2017). *Europoortkering*. Retrieved from Keringshuis: <http://www.keringshuis.nl/index.php?id=14>
- KNMI. (2006). *KNMI Climate Change Scenarios 2006 for the Netherlands*. De Bilt, The Netherlands: KNMI.
- KNMI. (2014). *KNMI'14-klimaatscenario's voor Nederland; Leidraad voor professionals in klimaatadaptatie*. de Bilt: KNMI.
- KNMI. (2017). *Changes in the Atlantic Meridional Overturning Circulation*. Retrieved from KNMI: <https://www.knmi.nl/kennis-en-datacentrum/achtergrond/changes-in-the-atlantic-meridional-overturning-circulation>
- KNMI. (2017). *Stormvloed*. Retrieved from KNMI: <https://www.knmi.nl/kennis-en-datacentrum/uitleg/stormvloed>
- KNMI, R. a. (1961). *Verslag over de stormvloed van 1953 (Report on the 1953 Flood)*. 's-Gravenhage: Staatsdrukkerij en Uitgeverijbedrijf, 714 pp.
- Kooi, H., Johnston, P., Lambeck, K., Smither, S., & Molendijk, R. (1998). *Geological causes of recent (~100yr) vertical land movement in the Netherlands*. Tectonophysics 299:297–316.
- Kopp, R. R., Kopp, R., Horton, R., Little, C., Mitrovica, J., Oppenheimer, M., . . . Tebaldi, C. (2014). *Probabilistic 21st and 22nd century sea-level projections at a global network of tide-gauge sites*. Earth's Future, 2, 383–406, DOI:10.1002/2014EF000239.
- Kopp, R., DeConto, R., Bader, D., Hay, C., Horton, R., Kulp, S., . . . Strauss, B. (2017). *Evolving Understanding of Antarctic Ice-Sheet Physics and Ambiguity in Probabilistic Sea-Level Projections*. Earth's Future, 5, 1217–1233, <https://doi.org/10.1002/2017EF000663>.
- Kroos, J. (1999). *Nauwkeurigheid waterstandsverwachtingen SVSD voor Hoek van Holland*. RIKZ.
- Kroos, J. (2006). *Evaluatie van 50 jaar stormvloedverwachtingen. De nauwkeurigheid van stormvloedverwachtingen en de juistheid van de berichtgeving van de SVSD onderzocht over de periode 1954 t/m 2004*. RIKZ Rapport 2006.010. Rijkswaterstaat RIKZ.
- Lancaster, G. (2005). *Research Methods in Management*. Oxford: Elsevier.
- Landerer, F., Jungclaus, J., & Marotzke, J. (2006). *Regional dynamic and steric sea level change in response to the IPCC-A1B scenario*. J Phys Oceanogr 37: 296–312.

- Le Bars, D., Drijfhout, S., & de Vries, H. (2017). *A high-end sea level rise probabilistic projection including rapid Antarctic ice sheet mass loss*. Environmental Research Letters.
- Leeuwddrent, W. (2012). Verwijderen Oosterscheldekering niet kosteneffectief. *Land+Water*.
- Levermann, A., Clark, P., Marzeion, B., Milne, G., Pollard, D., Radic, V., & Robinson, A. (2013). *The multimillennial sea-level commitment of global warming*. PNAS, <http://www.pnas.org/content/110/34/13745.full.pdf>.
- Lindsey, R. (2017). *Climate Change: Global Sea Level*. Retrieved from Climate.gov: <https://www.climate.gov/news-features/understanding-climate/climate-change-global-sea-level>
- Little, C., Urban, N., & Oppenheimer, M. (2013). *Probabilistic framework for assessing the ice sheet contribution to sea level change*. United States Of America: Proceedings of the National Academy of Sciences.
- Lowe, J., Howard, T., Pardaens, A., Tinker, J., Holt, J., Wakelin, S., . . . Bradley, S. (2009). *UK Climate Projections science report: Marine and coastal projections*. Exeter, UK: Met Office Hadley Centre,.
- Marinov, I., & Sarmiento, J. (2004). *The Role of the Oceans in the Global Carbon Cycle: An Overview*. DOI: 10.1007/978-1-4020-2087-2\_8.
- Martin, P., Archer, D., & Lea, D. (2005). *Role of deep sea temperature in the carbon cycle during the last glacial*. Paleogeography, 20, PA2015, DOI:10.1029/2003PA000914.
- Mcguire, B. (2012). *Waking the Giant: How a changing climate triggers earthquakes, tsunamis and volcanoes*. Oxford University Press.
- Meehl, G. T., Meehl, G., Stocker, T., Collins, W., Friedlingstein, P., Gaye, A., . . . Raper, S. (2007). *Global Climate Projections*. In: *Climate Change 2007: The Physical Science Basis. Contribution of Working Group I to the Fourth Assessment Report of the Intergovernmental Panel on Climate Change*. Cambridge: Cambridge University Press.
- Meer, v. d. (2002). *Technisch Rapport Golfploop en Golfoverslag bij Dijken*. Technische Adviescommissie voor de Waterkeringen.
- Met Office. (2016). *Is UKCP09 still an appropriate tool for adaptation planning?* Devon, United Kingdom.
- Met Office. (2016). *UK Climate Projections*. Retrieved from Met Office: <https://www.metoffice.gov.uk/services/climate-services/uk/ukcp>
- Miller, K. (2009). *Sea level change, last 250 million years*.
- Miller, R. (2001). Understanding and managing risks in large engineering projects. *International Journal of Project Management* , 437-443.
- Milne, G., & Mitrovica, J. (1998). *Postglacial sea-level change on a rotating Earth*. Geophysical Journal International, 133: 1–19. DOI:10.1046/j.1365-246X.1998.1331455.x.
- Myhre, G., Shindell, D., Bréon, F., Collins, W., Fuglestedt, J., Huang, J., . . . Zhang, H. (2013). *Anthropogenic and Natural Radiative Forcing*. In: *Climate Change 2013: The Physical Science Basis. Contribution of Working Group I to the Fifth Assessment Report of the Intergovernmental Panel on Climate Change*. Cambridge, United Kingdom and New York: Cambridge University Press.
- Nerem, R., Beckley, B., Fasullo, J., Hamlington, B., Masters, D., & Mitchum, G. (2018). *Sea level rise accelerating: acceleration in 25-year satellite sea level record*. The University of Colorado.
- Nicholas, J. M. (2012). *Project Management for Engineering, Business and Technology*. Chicago: Routledge.
- NOAA. (2017). *Monthly CO2*. Retrieved from CO2 Earth: <https://www.co2.earth/monthly-co2>
- NSIDC. (2017, July 6). *All About Sea Ice: Thermodynamics: Albedo*. Retrieved from National Snow & Ice Datacenter: <https://nsidc.org/cryosphere/seaice/processes/albedo.html>
- Paolo, F., Fricker, H., & Padman, L. (2015). *Volume loss from Antarctic ice shelves is accelerating*. New York: Science 348. . 10.1126/science.aaa0940.

- PBL. (2007). *Correctie formulering over overstromingsrisico Nederland in IPCC-rapport*. Retrieved from <http://www.pbl.nl/dossiers/klimaatverandering/content/correctie-formulering-over-overstromomgsrisico>
- Peltier, W. (2004). *Global glacial isostasy and the surface of the ice age earth: The ICE-5G (VM2) model and Grace*. Toronto, Ontario, Canada: Annu. Rev. Earth Planet. Sci. 2004. 32:111–49 DOI: 10.1146/annurev.earth.32.082503.144359.
- Planton, S. (2013). *IPCC Annex III: Glossary. Climate Change 2013: The Physical Science Basis. Contribution of Working Group I to the Fifth Assessment Report of the Intergovernmental Panel on Climate Change*. Cambridge, United Kingdom and New York: Cambridge University Press.
- Port of Rotterdam. (2018). Operational flow velocity model Rotterdam (OSR). Retrieved from: <http://mx-systems.nl/osr/>
- POST. (2017). *Rising Sea Levels*. London: Houses of Parliament; Parliamentary Office of Science & Technology.
- Raftery, A., Zimmer, A., Frierson, D., Startz, R., & Liu, P. (2017). *Less than 2 C warming by 2100 unlikely*. Nature Climate Change: 7, 637-641 DOI:10.1038/nclimate3352.
- Ranger, N. T. (2013). *Addressing 'deep' uncertainty over long-term climate in major infrastructure projects: four innovations of the Thames Estuary 2100 Project*. Springer-Verlag Berlin Heidelberg and EURO.
- Rignot, E., Mouginot, J., Morlighem, M., Seroussi, H., & Scheuchl, B. (2014). *Widespread, rapid grounding line retreat of Pine Island, Thwaites, Smith, and Kohler glaciers, West Antarctica, from 1992 to 2011*. Geophys. Res. Lett., 41, 3502–3509, DOI:10.1002/2014GL060140.
- Rijksoverheid. (2016). *Regeling veiligheid primaire waterkeringen 2017*. Ministerie van Infrastructuur en Milieu. Water act: IENM/BSK-2016/283517.
- Rijksoverheid. (2016). *Stand zeespiegel langs de Nederlandse kust en mondiaal, 1890-2014*. Retrieved from Compendium voor de Leefomgeving : <http://www.clo.nl/indicatoren/nl0229-zeespiegelstand-nederland-en-mondiaal>
- Rijksoverheid. (2016). *Wet van 2 november 2016 tot wijziging van de Waterwet en enkele andere wetten (nieuwe normering primaire waterkeringen)*. 's Gravenhage: Staatsblad 2016-431 ISSN 0920-2064.
- Rijksoverheid. (2017). *WBI*. Retrieved from Helpdesk Water: <https://www.helpdeskwater.nl/onderwerpen/waterveiligheid/primaire/beoordelen-wbi/>
- Rijkswaterstaat. (1991). *Ontwerpnota Stormvloedkering Oosterschelde, Boek 2: De waterbouwkundige werken*.
- Rijkswaterstaat. (1991). *Ontwerpnota Stormvloedkering Oosterschelde, Boek 3: De betonwerken*.
- Rijkswaterstaat. (2006). *TMR2006 bodemhoogtegrid*.
- Rijkswaterstaat. (2007). *Hydraulische randvoorwaarden primare keringen [HR2006]*. Ministerie of Verkeer en Waterstaat.
- Rijkswaterstaat. (2015a). *Waterkeringen*. Retrieved from [https://staticresources.rijkswaterstaat.nl/binaries/Factsheet%20onze%20waterkeringen\\_tcm21-70612.pdf](https://staticresources.rijkswaterstaat.nl/binaries/Factsheet%20onze%20waterkeringen_tcm21-70612.pdf)
- Rijkswaterstaat. (2015b). *Motie Geurts, Deltaprogramma: Onderzoek naar de effecten van sluizen in de Nieuwe Maas en Oude Maas op waterveiligheid en zoetwatervoorziening*.
- Rijkswaterstaat. (2017a). *Maeslantkering*. Retrieved from Rijkswaterstaat: <https://www.rijkswaterstaat.nl/water/waterbeheer/bescherming-tegen-het-water/waterkeringen/deltawerken/maeslantkering.aspx>
- Rijkswaterstaat. (2017b). *Water safety*. Retrieved from Helpdeskwater: <https://www.helpdeskwater.nl/onderwerpen/waterveiligheid/>
- Rijkswaterstaat. (2017c). *Beoordingsproces*. Retrieved from Helpdesk Water: <https://www.helpdeskwater.nl/onderwerpen/waterveiligheid/primaire/beoordelen-wbi/beoordelingsproces/>

- Rijkswaterstaat. (2017d). *Schematiseringshandleiding betrouwbaarheid sluiting kunstwerk*. Ministerie van Infrastructuur en Milieu.
- Rijkswaterstaat. (2017e). *Nationaal Basisbestand Primaire Waterkeringen*. Retrieved from Waterveiligheidsportaal: <https://waterveiligheidsportaal.nl/#/nss/nss/norm>
- Rijkswaterstaat. (2017f). *Schematiseringshandleiding hoogte kunstwerk*. Ministerie van Infrastructuur en Milieu.
- Rijkswaterstaat. (2018). Retrieved from Waterinfo: <https://waterinfo.rws.nl>.
- Rohling, E., Grant, K., Bolshaw, M., Roberts, A., Siddall, M., Hemleben, C., & Kucera, M. (2009). *Antarctic temperature and global sea level closely coupled over the past five glacial cycles*. *Nat. Geosci.* 2, 500–504. (DOI:10.1038/ngeo557).
- Rohling, E., Haigh, I., Foster, G., Roberts, A., & Grant, K. (2013). *A geological perspective on potential future sea-level rise*. *SCIENTIFIC REPORTS* | 3 : 3461 | DOI: 10.1038/srep03461.
- Rondvaart Europapoort. (2016). *De Maeslantkering*. Retrieved from Rondvaart Europapoort: <http://www.rondvaarteuropoort.nl/index.php?page=Maeslantkering>
- RWS. (1953). *De watersnoodramp 1953*. Retrieved from Beeldbank Rijkswaterstaat: <https://beeldbank.rws.nl/MediaObject/Details/274912>
- Sanderson, B., O'Neill, B., & Tebaldi, C. (2016). *What would it take to achieve the Paris temperature targets*. *Geophys. Res. Lett.*, 43, 7133–7142, DOI:10.1002/2016GL069563.
- Schaeffer, M., Hare, W., Rahmstorf, S., & Vermeer, M. (2012). *Long-term sea-level rise implied by 1.5 C and 2.0 C warming levels*. *NATURE CLIMATE CHANGE* DOI: 10.1038/NCLIMATE1584.
- Schär, C. (2004). *The role of increasing temperature variability in European summer heatwaves*. Zurich: Nature.
- SHC. (2007). *Pannerdensch kanaal 300 jaar geleden geopend*. Retrieved from De Studiekring Historische Cartografie: <https://www.historischecartografie.nl/nieuws/2007/07/pannerdensch-kanaal-300-jaar-geleden-geopend/>
- Skeptical Science. (2016). *CO2 lags temperature - what does it mean?* Retrieved from <https://skepticalscience.com/argument.php?a=7&p=11>
- Slangen, A., Carson, M., Katsman, C., van de Wal, R., Köhl, A., Vermeersen, L., & Stammer, D. (2014). *Projecting twenty-first century regional sea-level changes*. *Clim. Change* 124 317–32. DOI: 10.1007/s10584-014-1080-9.
- Slomp, R., Geerse, C., & de Deugd, H. (2005). *Onderbouwing Hydraulische Randvoorwaarden 2001 voor het benedenrivierengebied*. Rijkswaterstaat.
- Steenepoorte, K. (2014). *Storm surge barrier in the Eastern Scheldt*. Rijkswaterstaat Zee en Delta.
- Sterl, A., van den Brink, H., de Vries, H., Haarsma, R., & van Meijgaard, E. (2009). *An ensemble study of extreme North Sea storm surges in a changing climate*. KNMI.
- STOWA. (2017). *Water veiligheid begrippen*. Ministry of infrastructure and environment.
- Sweet, W., Kopp, R., Weaver, C., Obeysekera, J., Horton, R., Thieler, E., & Zervas, C. (2017). *NOAA Technical Report NOS CO-OPS 083: GLOBAL AND REGIONAL SEA LEVEL RISE SCENARIOS FOR THE UNITED STATES*. Maryland: Silver Spring.
- SWOV. (2017). *Verkeersdoden in Nederland*. Retrieved from SWOV: <https://www.swov.nl/feiten-cijfers/factsheet/verkeersdoden-nederland>
- TNO. *Bodemdaling*. Retrieved from Natuurinformatie: <http://www.natuurinformatie.nl/ndb.mcp/natuurdatabase.nl/i000331.html>
- Toggweiler, J. (1991). *Variation of atmospheric CO2 by ventilation of the oceans deepest water*. *Paleoceanography* Vol 14, no: 5, pages 71-58.

- Tsimopoulou, V. (2015). *Economic optimisation of flood risk management projects*. Delft: TU Delft.
- TU Delft. (2017). *CT4310 Bed Bank & Shore Protection. Flow/stability chapter 3*.
- United Nations, Department of Economic and Social Affairs. (2015). *World Population Prospects: The 2015 Revision*. New York: United Nations.
- Vaughan, D., Comiso, J., Allison, I., Carrasco, J., Kaser, G., Kwok, R., . . . Zhang, T. (2013). *Observations: Cryosphere*. In: *Climate Change 2013: The Physical Science Basis. Contribution of Working Group I to the Fifth Assessment Report of the Intergovernmental Panel on Climate Change*. Cambridge, United Kingdom and New York: Cambridge University Press.
- Veerman, C., & Stive, M. (2008). *Working together with water: a living land builds for its nature*. the Hague: Ministerie van Verkeer en Waterstaat.
- Vellinga, P., Katsman, C., Sterl, A., Beersma, J., Church, J., Hazeleger, W., . . . Vaughan, D. (2008). *Exploring high-end climate change scenarios for flood protection of the Netherlands. International scientific assessment carried out at request of the delta committee. Technical Report Scientific Report WR-2009-05*. The Netherlands: KNMI & Alterra.
- Verschuren, P., & Doorewaard, H. (2010). *Designing a Research Project*. The Hague: Eleven International Publishing.
- von Schuckmann, K., Palmer, D., Trenberth, K., Cazenave, A., Chambers, D., Champollion, N., . . . Wild, M. (2016). *An imperative to monitor Earth's energy imbalance*. *Nature Climate Change* 6, 138-144  
DOI:10.1038/nclimate2876.
- Wada, Y. L., Wada, Y., van Beek, L., Sperna, F., Chao, B., Wu, Y., & Bierkens, M. (2012). *Past and future contribution of global groundwater depletion to sea-level rise*. *GEOPHYSICAL RESEARCH LETTERS*, VOL. 39.
- Water Informatiehuis. (2017). *Landelijk veiligheidsbeeld*. Retrieved from Waterveiligheidportaal: <https://waterveiligheidsportaal.nl/#/home>
- Watson, C., White, J., Church, J., King, M., Burgette, R., & Legresy, B. (2015). *Unabated global mean sea level over the satellite altimeter era*. *Nat. Clim. Change*, DOI:10.1038/NCLIMATE2635.
- White, J., Alley, R., Archer, D., Barnosky, A., Foley, J., Fu, R., . . . Wofsy, S. (2013). *Abrupt impacts of climate change: Anticipating surprises*. Washington: THE NATIONAL ACADEMIES PRESS.
- Wild, M. (2016). *Radiation and Climate Change: Earth radiation balance under present day conditions*. Retrieved from ETH Zurich: [https://www.ethz.ch/content/dam/ethz/special-interest/usys/iac/iac-dam/documents/edu/courses/radiation\\_and\\_climate\\_change/Lecture8\\_6\\_may2016.pdf](https://www.ethz.ch/content/dam/ethz/special-interest/usys/iac/iac-dam/documents/edu/courses/radiation_and_climate_change/Lecture8_6_may2016.pdf)
- Witteveen+Bos. (2017). *Integrale Veiligheid Oosterschelde; MIRT onderzoek, knikpunten, oplossingsrichtingen en effecten*. Rijkswaterstaat Zee en Delta.
- World Meteorological Organization. (2017, January). *WMO confirms 2016 as hottest year on record, about 1.1°C above pre-industrial era*. Retrieved from World Meteorological Organization: <https://public.wmo.int/en/media/press-release/wmo-confirms-2016-hottest-year-record-about-11%C2%B0c-above-pre-industrial-era>
- Yi, S., Sun, W., Heki, K., & Qian, A. (2015). *An increase in the rate of global mean sea level rise since 2010*. *Geophysical Research Letters*, 42, 3998-4006.
- Yin, J., Griffies, S., & Stouffer, R. (2010). *Spatial variability of sea-level rise in 21st century projections*. *J Clim* 23: 4585-4607.

# Appendix

## Appendix A: Global sea level rise components

Appendix A will describe the contributing components to sea level rise. All components except land water changes are reliant on global temperature rise (Le Bars et al., 2017). Due to global warming ice sheets and glaciers melt which increases the amount of water. Furthermore, the warming atmosphere will slowly increase the temperature of upper part of the oceans. One of the physical properties of water is that it is expanding at higher temperatures that affect the global and regional sea level. Global sea level ice loss affects global ocean circulation and marine ecosystems. The main contributors to global sea level rise are explained below. The components that have an impact on regional sea level will be described in Appendix B.

### ***Mass component 1: Antarctic ice sheet changes***

The Antarctic ice sheet (AIS) is an enormous ice mass that covers 8.3% of the global land surface (Vaughan et al., 2013). The AIS has the potential to contribute to a large extent to future sea level rise by adding mass to the oceans. The average global sea level rises 58.3 m if all Antarctic land ice would melt (Vaughan et al., 2013).

The average rate of ice loss from the Antarctic ice sheet to the sea level equivalent was according to the IPCC 2013;  $0.08 \pm 0.19$  mm per year over the period 1992–2001 and is increased to  $0.41 \pm 0.20$  mm per over the period 2002–2011 (Vaughan et al., 2013). Dieng et al. (2017) used other datasets and periods and estimated  $0.29 \pm 0.04$  mm per year (1993–2004) and  $0.33 \pm 0.06$  mm per year (2004–2015). The IMBIE team used the latest datasets and estimates a contribution of  $7.6 \pm 3.9$  mm between 1992 and 2017 of which 3 mm has occurred during the last 5 years. This results in a current estimated contribution of  $0.60 \pm 0.31$  mm per year (IMBIE Team, 2018).

The described references observe an accelerated rate of the Antarctic ice sheet melt. Several parts of West-Antarctica could become unstable which could enhance calving, due to the decreasing buttressing effect of floating ice shelves. This process might lead to much more Antarctic ice sheet loss than currently observed. More information can be found in Section 5.4 and Appendix E & F.

### ***Mass component 2: Greenland ice sheet changes***

The Greenland ice sheet (GIS) is much smaller than the AIS and covers 1.2% of the global land surface. Nevertheless, the GIS could potentially add 7.32 m sea level rise (Vaughan et al., 2013). The rate of ice loss from the Greenland ice sheet has accelerated since 1992. The average rate is increased from  $0.09 \pm 0.11$  mm per year (1992–2001) to  $0.59 \pm 0.16$  mm per year (2002–2011). This contribution was  $0.63 \pm 0.17$  mm per year between 2005 and 2010, but this timeframe is relatively short to confirm trends (Vaughan et al., 2013). Dieng et al. (2017) also estimate a large increase from  $0.32 \pm 0.04$  mm/yr (1993–2004) to  $0.82 \pm 0.06$  mm/yr (2004–2015). The atmospheric temperature at Greenland is considerably higher than in Antarctica with many melting days per year. The average atmospheric temperature difference is the main distinction between both ice sheets. The prediction is that this rise will continue. Dynamic effects that can potentially increase Antarctic ice sheet loss will probably not be the case for the Greenland ice sheet (GrIS). This is because most part of the GrIS is grounded on bedrock above sea level and is therefore not affected by rising ocean temperature. More information in Appendix E.

### ***Mass component 3: glaciers***

Glacier melt refers to mountain glaciers in particular and glaciers nearby Antarctica. Mountain glaciers respond more rapidly to climate change compared to the Antarctic- and Greenland ice sheets. This is because their mass is much smaller in comparison and the local atmospheric temperature is higher than at the poles of the Earth. Nonetheless, there are large areas with glaciers. IPCC identifies in total 168,331 glaciers around the world. For example; Alaska covers 12.3% of all glaciers while North Canada covers 14.3% of all glacier areas around the world. Their impact on sea level rise if all ice would melt is only 5.5 mm and 8.4 mm respectively. In contrast, the Alps in Europe only covers 0.3% of all glaciers and could only contribute 0.3 mm to sea level rise (Vaughan et al., 2013). Melting glaciers probably have a significant contribution to sea level rise in the short term. The potential

total sea level rise is approximately 31-53 cm if all glaciers melt (de Vries et al., 2014). The IPCC calculated a potential maximal sea level rise by glacier melt of 41 cm (Vaughan et al., 2013). The mass balance of a glacier is determined by the sum of accumulation and ablation. Accumulation is the result of precipitation (snowfall) and of refreezing water. Ablation occurs due to surface melting, runoff and calving. More information about the mass balance of ice can be found in Appendix E.

Several methods have been used in the past to determine current glacier mass change, but it is complicated to calculate glacier loss precisely. Gardner et al. (2013) estimate a glacier mass loss between 2003 and 2009 of  $259 \pm 28$  Gton per year which is also reviewed by the IPCC. This ice mass loss contributes  $0.71 \pm 0.08$  mm per year to sea level rise. This accounts currently for approximately 29% of the total rate of sea level rise per year. It is important to avoid double counting with glaciers on ice sheets. Excluding the glaciers in the Sub-Antarctic and Arctic glacier mass loss is  $215 \pm 26$  Gton per year and sea level rise  $0.59 \pm 0.07$  mm per year (Gardner et al., 2013). Dieng et al. (2017) took the average of three datasets and estimated  $0.71 \pm 0.10$  mm/yr (1993-2004) and  $0.78 \pm 0.07$  mm/yr (2004-2015).



Figure A.1: Glacier d'Argentière (Chamonix, France) (Alexander, 2013).

#### **Mass component 4: land water storage**

This component is about the amount of water stored in lakes and rivers, wetlands, and snow at high altitudes. The contribution to sea level change is partially related to human activities such as groundwater mining, changes in land-use and the construction of dams and reservoirs (Wada et al., 2012). Dieng et al. (2017) estimates  $0.23 \pm 0.10$  mm/yr (1993-2004) and  $0.25 \pm 0.08$  mm/yr (2004-2015). Roughly half ( $0.12 \pm 0.04$  mm/yr) of this contribution is caused by anthropogenic land water changes (Dieng et al., 2017). Wada et al. (2012) showed that the contribution of groundwater depletion to sea level rise increased from 0.035 mm per year in 1900 to 0.57 mm per year in the year 2000.

Significant permafrost degradation has occurred in northern Russia and Europe due to increasing local temperatures. It is very uncertain what the contribution would be to the sea level equivalent, but Vaughan et al. (2013) expect that permafrost degradation has the potential to add 0.02-0.10 m sea level rise in the future. The estimations for snow are ignored because of lacking data, but it is expected to be insignificant (Dieng et al., 2017).

### **Mass component 5: water vapour**

The atmospheric water vapour content (expressed in equivalent sea level) is shown in Figure A.2. An apparent increase in water vapour and a decrease in the sea level equivalent can be noted between 1993 and 2015 (Dieng et al., 2017). Dieng et al. (2017) estimate a contribution to sea level of -0.03 mm per year (1993-2004) and -0.05 mm per year (2004-2015). This implies that this component has a minimal negative contribution to sea level rise.

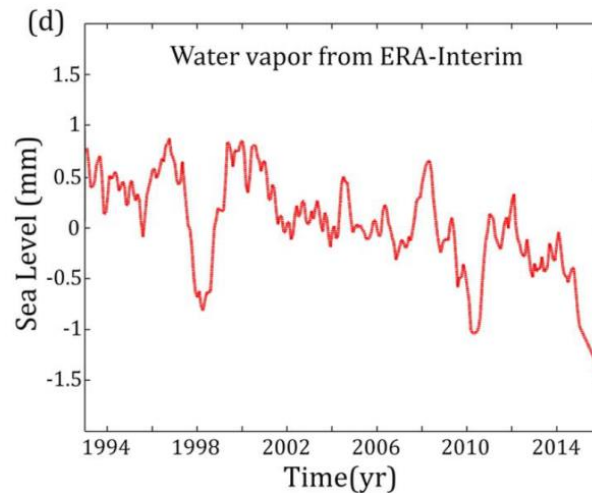


Figure A.2: water vapour contribution expressed in equivalent sea level (data from ERA-interim) (Dieng et al., 2017).

### **Steric component: Seawater expansion**

The expansion of the global ocean is driven by increasing ocean temperature and correlated with atmospheric temperature (Le Bars et al., 2017). Dieng et al. (2017) used three data sets from previous research, and after 2005, the data sets from Argo were used. The data from Argo has a spatial resolution of 1° between 65°S and 65°N and range from the surface to about 2,000 m in depth (Dieng et al., 2017). Dieng et al. (2017) estimate a contribution to sea level rise of  $0.94 \pm 0.27$  mm per year (1993-2004) and  $1.14 \pm 0.09$  mm per year (2004-2015) from steric effects. It is not expected that global climate change affects ocean temperature at larger depths (>2000 m). However, this lack of data can be relevant if the sea level budget calculation deviates from altimetry records.

The IPCC also used datasets from Argo, but these are combined with other older calculations. The ocean temperature was recorded after 1970. This was done by lowering temperature recorders to a depth of 700 m with a cable attached to a (moving) ship. These measurements were not very accurate due to some malfunctions in the recordings before reaching 250 m depth (Gouretski & Koltermann, 2007). After 2005, Argo datasets became available with higher accuracy. The IPCC estimated a contribution of  $0.8 \pm 0.3$  mm per year to sea level rise by thermal expansion between 1971 and 2010 ( $0.6 \pm 0.2$  mm/yr 0-700 m depth). Over the altimetry period (1993–2010), the rate for the 0 to 700 m depth range is  $0.8 \pm 0.3$  mm/yr and  $1.1 \pm 0.3$  mm/yr when accounting for the deep ocean (Church et al., 2013).

Steric expansion can lead to mass distribution changes over the oceans. Steric expansion of the oceans is the largest in the deep ocean where the water column is very deep. This non-uniform expansion will induce a redistribution of water from the open ocean to coastal regions (Landerer, Jungclaus, & Marotzke, 2006) (Grindsted et al., 2015).

## Appendix B: Local sea level rise components

Appendix B describes the contributing components to relative sea level rise. Figure A.3 presents numerous climate-sensitive processes and components that can influence local and global sea level change. Elastic deformation of the Earth's crust and gravitational changes can diverge the rate of regional sea level change from the global mean. Relative sea level is the sea level related to the level of the continental crust. Relative sea level rise is measured by combining absolute changes of global sea level rise (Appendix A) and regional sea level rise with local motions in the Earth's crust and soil. Appendix B explains the relevant processes that contribute to relative sea level change in the Netherlands.

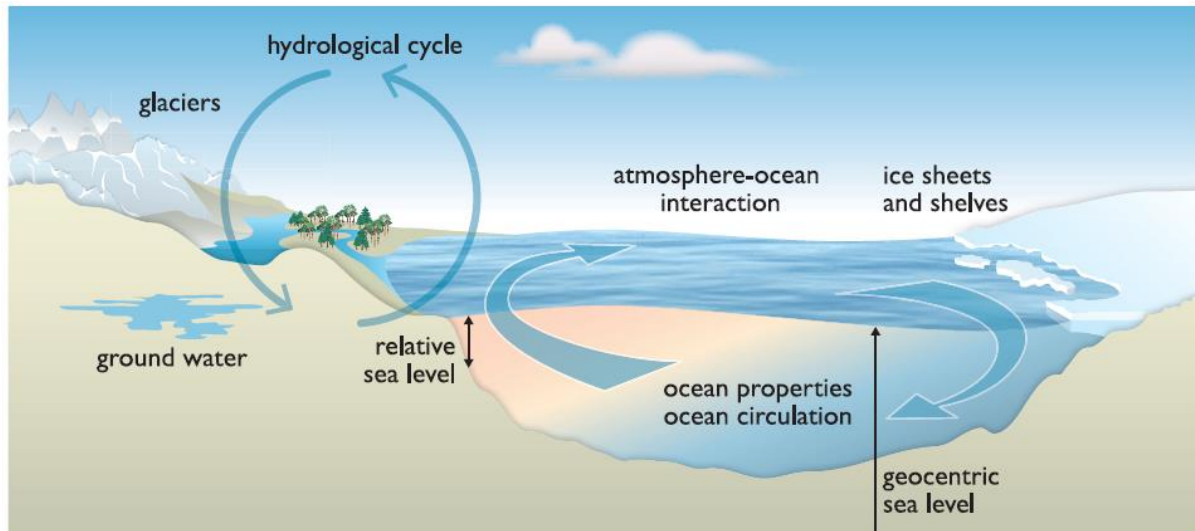


Figure A.3: Climate-sensitive processes and components that can influence global and regional sea level (Church et al., 2013).

### Gravitational effects

All masses, such as ice sheets, gravitationally attract the ocean around them and distorts sea level globally (POST, 2017). Ice sheet mass loss reduce this gravitationally pull and causes sea level to drop locally nearby the melting ice sheet. On the other hand, further away from the ice sheet, the total sea level rises. This is visualized in Figure A.4. Regional sea level estimates consider the gravitational effects of ice sheets which point out that the contribution of ice sheet melt to sea level rise is not evenly distributed over the oceans. The Antarctic ice sheet has a significantly higher impact on sea level rise in the Netherlands than the Greenland ice sheet (GrIS) due to its relatively large distance (Figure A.5).

Water mass exchange between land and the ocean results in patterns of sea level change called “*sea level fingerprints*”. Sea level fingerprint shows the fraction of the world average sea level rise at a specific location on earth. Hay et al. 2015 computed a global map with the distribution of water mass during melting ice sheets. The Antarctic fingerprint for the Netherlands is approximately 1.1-1.2 should be interpreted as having 1 m global sea level rise caused by only Antarctic melt will raise regional sea level in the Netherlands with 1.1-1.2 m. The sea level fingerprint in the Netherlands for GrIS melt is 0.2, indicating a 0.2 m sea level rise in the Netherlands for 1 m global sea level rise caused by GrIS. All gravitational sea level fingerprints induced by ice sheet mass loss are shown in Figure A.5.

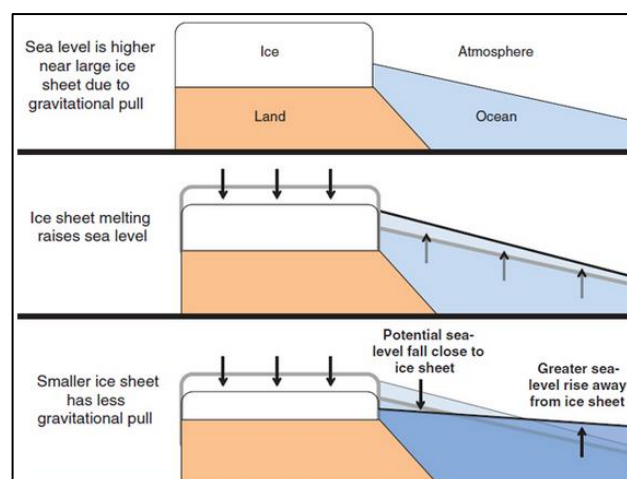


Figure A.4: Effect of “self-gravitation” of ice sheets on sea level rise during ice-sheet melting. Melting of ice raises the global average sea level, and reduces the gravitational attraction from the ice, which allows the sea level near the ice to fall while sea level far from the ice rises more than the global average (White et al., 2013).

Massive changes in the mass distribution also affect the Earth's inertia tensor and therefore rotation, which produces an additional sea level response (Milne & Mitrovića, 1998). This response is not fully understood yet, and future research is advised to indicate the impact on Earth's rotation and sea level response.

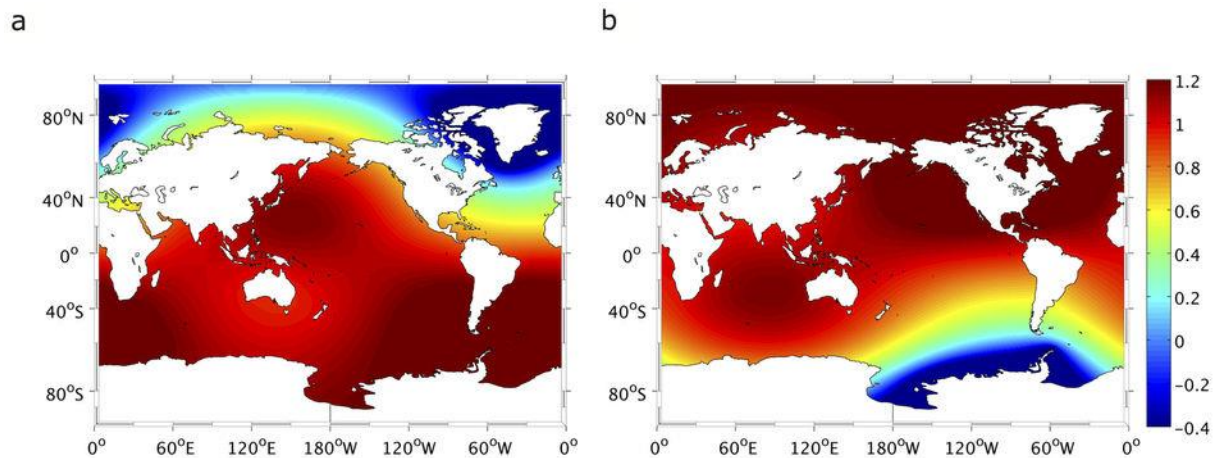


Figure A.5: Normalized sea level change due to rapid melting (a) GrIS and (b) AIS. The colours indicate sea level fingerprints for a specific place. This may be interpreted as having the unit of meters of sea level change per meter of the equivalent GMSL change associated with the melt event (Hay, Morrow, Kopp, & Mitrovića, 2015).

## Vertical land movement

Relative sea level (RSL) defined as the sea level relative to the Earth's crust is required for projection regional sea level rise (POST, 2017). Vertical land movement includes long-term subsidence of the crust due to soil compaction, redistribution of mass in the oceans and ice sheets during last glacial cycle, changing ocean volumes and tectonic motion (Kooi et al., 1998). The natural geological processes that lead to vertical movement are isostasy, tectonics and compaction of deep soil layers.

In addition, there are several anthropogenic processes that can cause local vertical land movement. The anthropogenic components of vertical land movement in the Netherlands are oil/gas extraction, salt extraction, groundwater extraction, water drainage and settlement.

### **Vertical land movement due to natural geological processes.**

Natural vertical land movement is caused by natural, geological processes that are not influenced by human activity. There are in total three components that contribute to natural vertical land movement. The main geological processes are described below.

#### **Glacial isostatic adjustment**

Isostasy refers to the floating balance of Earth's lithosphere (crust) plates. These tectonic plates float on liquid (viscous) rocks of the Earth's mantle. Locally changing masses such as growing ice sheets (last ice age) causes deformations in the relatively elastic lithosphere. The European crust is on average 70-100km thick. When ice sheets melt, the solid Earth deforms to reach a new equilibrium. This process takes thousands of years due to the high viscosity of the rocks and fluid in the Earth mantle. A large part of Europe's geology is still re-adjusting as a response to the disappearing massive ice sheets of the last glacial period. This glacial isostatic adjustment (GIA) is a viscoelastic rebound of the solid earth after (ice) mass loss. The response in the Earth's crust to mass changes will be far from uniform. For example; southern England is subsiding by about 1-2 mm per year, whereas Scotland is rising at 1-2 mm per year. Also, local vertical motion in Sweden rise can be 10 mm per year due to the disappeared ice sheet. The Netherlands is subsiding with 0.1-0.4 mm/year in Zeeland and with 0.3-0.8 mm/year in the Waddenzee due to GIA effects (Hijma et al., 2017).

The main reason that the Netherlands is subsiding is because it was located on a crustal glacial forebulge. The lithosphere was deformed upwards due to the mass of the ice sheet. When the mass is disappeared, the crust declines very slowly to restore isostatic balance. This process is visualized in Figure A.6.

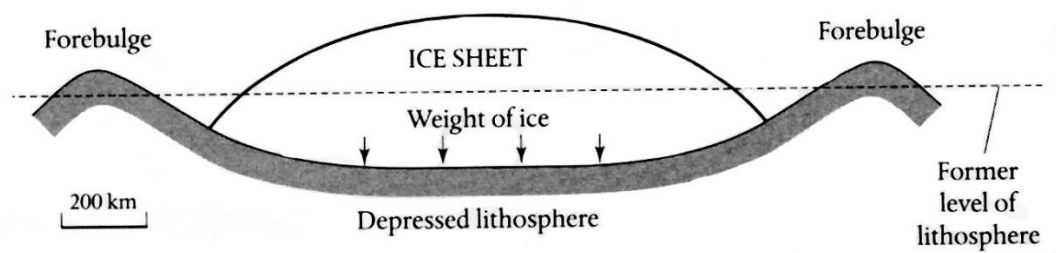


Figure A.6: Deformation of the Lithosphere by an ice sheet. After removal of the ice sheet, the depressed lithosphere including the forebulge will deform back to the original level: a process that takes thousands of years (McGuire, 2012).

Also, sea level change and sediment transportation over the last thousands of years is not uniformly distributed over the earth's surface. This mass distribution also affects isostatic adjustment. Kooi et al. (1998) estimated an isostatic adjustment due to ice, sediment and water loads of  $-0.3 \pm 0.5$  mm per year for the Dutch coast. Peltier (2004) estimated a glacial isostatic adjustment between  $-0.02$  and  $+0.4$  mm per year along the Dutch coast (Peltier, 2004). These values are slightly lower than Hijma et al. (2017) which is referring to the British research: British-Chrono project.

### Tectonic activity

Tectonics relate to movements and deformations of Earth's tectonic plates. Tectonic activity has the ability to cause vertical movement of the Earth's lithosphere due to the forces that the plates exert on each other (Hijma et al., 2017). This process usually operates on very long time-scales and therefore it is difficult to estimate past and future tectonic activity. Kooi et al. (1998) concluded that is impossible to estimate past and future tectonic activity precisely but assumed changes of  $0.0 \pm 0.7$  mm per year to the surface of the Netherlands. Important to note is that future tectonic activity can differ completely. Reconstructions of the last 2.5 million years show reduced tectonic activity in the south-west of the Netherlands (location of Maeslant Barrier and Eastern Scheldt Barrier). This is shown in Figure A.7.

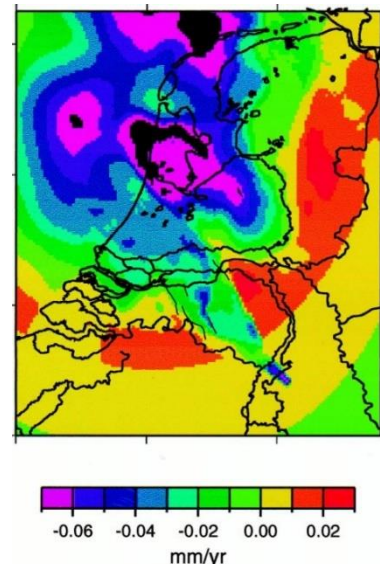


Figure A.7: Reconstruction of tectonic activity over last 2.5 m years (Kooi, Johnston, Lambeck, Smither, & Molendijk, 1998).

### Subsidence due to (auto)compaction

Auto-compaction is caused by (natural) compression of deep soil layers. This process covers a large subsurface of many kilometres of depth. The compaction of thick, poorly permeable layers that occur at large depth is a prolonged process. To compact soil layers, pore water must be expelled out of the grain skeleton to compress (in geotechnics this process is called consolidation). This process can take thousands of years for thick, poorly permeable layers at large depth under high pressure. It is expected that auto-compaction is very limited in the coastal area with circa  $0.1 \pm 0.05$  mm/yr (Hijma et al., 2017) (Kooi et al., 1998).

### Subsidence due to anthropogenic processes

Vertical land movement can also be caused by anthropogenic processes which are related to human activities. The anthropogenic components of vertical land movement in the Netherlands are oil/gas extraction, salt extraction, groundwater extraction, water drainage and settlement of added mass. These activities take place at different locations in the Netherlands, and this research examines the impact of the Maeslant Barrier (MLK) and Eastern Scheldt Barrier (OSK).

### Oil and gas extraction

Oil and gas extraction causes a local pressure reduction in oil or gas fields which result in compression of the relevant soil layers at considerable depth (1000 m). The largest gas fields are located in Groningen and the Waddenzee and cause significant vertical land movement. There are some gas extraction points near the MLK, but these locations are expected to close in 2018-2020 (Hijma et al., 2017). The expected contribution to vertical land movement at the MLK is estimated at 1-1.5 cm (2017-2050). It is unclear if more gas fields will be explored in this area in the future which makes it challenging to provide long-term projections. This research will include 2-2.5 cm for the timespan 2000-2100.

### Salt extraction

Salt extraction takes place only in a few places in the Netherlands. Soil decline can be significant at these locations, but the only the salt extraction location that influences coastal land movement is near Harlingen. Soil decline due to salt extraction is caused by the low pressure in the caverns (hollow caves at a depth of more than thousand meters) initiated by winning salt. The caverns will be compressed and lead to subsidence of the superposed deep layers in the subsoil. This is out of the scope of this study as the MLK and OSK are located in Zeeland and South Holland.

### Groundwater extraction

Soil decline due to groundwater extraction is caused by water pressure drops that compress soil layers. Groundwater extraction takes place at limited depths which have a relatively large impact on local compaction and subsidence. In the Netherlands, almost no research has been done into subsidence due to groundwater abstraction, also because soil subsidence is not or hardly measured. The amount of soil subsidence that can occur due to groundwater extraction depends on the rate of pressure head decrease (a pressure reduction) and on the properties of the subsoil (Hijma et al., 2017). Most major water extraction points are at higher ground and are not located near the OSK. The small extraction points near the MLK are not expected to have any effect on vertical land movement in that area. Nonetheless, it is important to accurately determine the impact on soil subsidence when new extraction wells are created.

### Water drainage

Water drainage is the periodical adjustment (with respect to NAP) of the water level in canals and watercourses to maintain the desired drainage depth for land use changes (agricultural purposes in particular). The drainage depth is the difference between ground surface level and (ground)water level. Water level adjustments are required in peatlands because these soils are in low-lying areas. Peat soils are the predominant type of soil in large parts of the low-lying parts of the Netherlands (Hoogland et al., 2012). Soil decline in the upper layers of peat is enhanced by the settling, compaction, oxidation and decomposition of the peat soils, caused by groundwater level reductions. During the draining process, peat above the groundwater level is oxidizing and shrinks. The water level reductions ensure that ground level decline continues through peat oxidation. In addition, water drainage also ensures water pressure reduction in clay and peat layers under the groundwater level which is therefore slightly compressed (Hijma et al., 2017).

The decline of peat soil can have a substantial impact on flood risk management because peatlands only occur in already low-lying areas. Hoogland et al. (2012) calculated that soils composed of peat layers decline up to a rate of 8 mm per year due to peat oxidation. These peatlands are located inland and usually not in the coastal area. It is essential to estimate future soil decline in peatlands behind flood defences because this process increases the potential flooding depth and therefore the damage in case of flooding. The MLK and OSK are not built on peat soils. However, some areas near Rotterdam are at risk of further subsidence due to peat oxidation.

### Settlement

Settlement is a vertical land decline after placing extra weight on the soil. This additional weight compresses subsoil layers. Both the MLK and OSK are located on stable soil layers (sand) which are compact and stable and are therefore not expected to decline significantly in the coming decades. Nevertheless, it is important to assess whether an eventual weight increase, due to adjustments, results in an additional settlement.

## Vertical land movement in the Netherlands

Land subsidence in the west of the Netherlands strengthens the relative sea level rise due to the increasing height difference between the rising sea level and the falling land. It is essential to include vertical land movement into the design of coastal flood defences. Furthermore, it is required to include land subsidence to examine whether the MLK and OSK are up to improvements.

The observed vertical land decline in the Netherlands is 0.2-1.5 mm per year due to GIA, auto-compaction, and tectonic activity (Kooi et al., 1998)(Hoogland et al., 2012). This number does not include anthropogenic contributions that can locally increase vertical land movement to a much greater extent. Anthropogenic factors that contribute to vertical land movement are peat oxidation in polders and subsidence due to drainage and gas/oil/salt/groundwater extraction (Vellinga et al., 2008).

Due to the three natural processes, the land is tilting in the direction of the North Sea around the southwest-oriented axis, causing the west and north to fall slightly and the east and south rise to a small extent. Kooi et al. (1998) concluded that this tilt slightly accelerates over the last thousands of years.

Figure A.8 shows the estimated vertical land movement in the Netherlands in the year 2050 compared to the year 2000. Most peat soils are drained for agricultural use, resulting in decomposition and consolidation of these soils. Particularly areas in the low-lying western part of the Netherlands, which compose of peat, could decline by 40-60 cm in 2050 (TNO). Furthermore, gas extraction in Groningen causes soil subsidence in the northern area of the Netherlands. The expected soil subsidence in 2050 is shown in Figure A.8, which combines both geological processes and human factors.

Already 40% of the Netherlands is situated at below-average sea level ( $\approx 0$  m NAP), and some low-lying “polders” are more than 6 m below NAP. Vertical land movement has a relatively large impact on these low-lying areas because this increases the impact of a potential flood considerably.

Important to note is that soil decline of 8 mm per year only occurs in drained areas, including peat soils and not on the locations of primary flood defences such as the MLK and OSK. Some coastal flood defences are situated in areas prone to subsidence due to anthropogenic factors such as oil/gas extraction (Hijma et al., 2017). However, the focus of this study is on the MLK and OSK only.

Based on the results of Hijma et al. (2017), the total vertical land decline, including all contributions, at the MLK is estimated at  $6 \pm 8$  cm (2000-2100). Approximately 2 cm subsidence is included in this period due to lag effect of gas extraction which is located near the barrier. The OSK is located in an area with limited contributors to vertical land decline and is expected to decline with  $3 \pm 6$  cm (2000-2100).

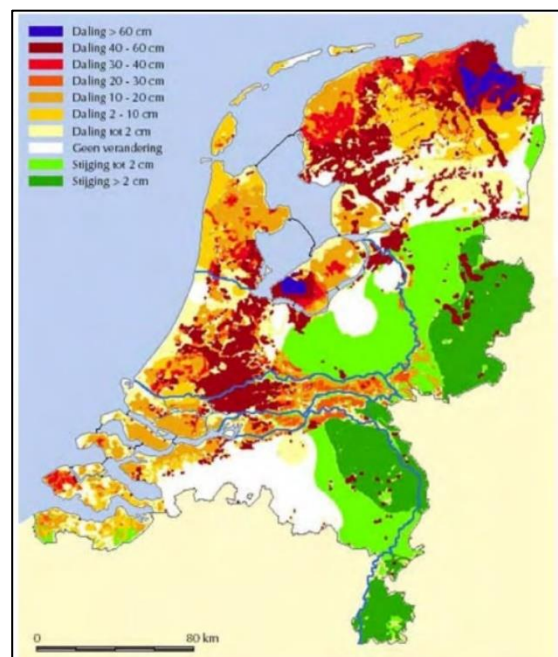


Figure A.8: Expected soil subsidence in 2050, including geological processes and human processes (TNO-NITG).

## Dynamic local sea level response

Global warming of the oceans can result in many responses that have an impact on local sea level. For example; global warming can change ocean circulation patterns. Freshwater fluxes originating from melting Greenland ice sheet are able to perturb the Atlantic meridional overturning circulation (MOC). As a result of accelerating melt rates, most climate models project a decrease of the MOC between 0 and 50% for the next century (KNMI, 2017). This dynamic response of the ocean to the freshwater forcing is still very uncertain. (Church et al., 2013). These effects are not yet included in sea level change models (Grindsted et al., 2015).

One important aspect of dynamic ocean responses is temperature change. Steric expansion of the oceans is the largest in the deep ocean. The rate of steric sea level expansion is different over the global ocean basins caused by heating and salinity changes of various ocean layers (Yin et al., 2010). As a result, ocean water will redistribute from the deep ocean to the coastal regions in particular. Yin et al. (2010) argue that, in London, the dynamic response of the ocean to steric expansion is similar to the global mean. Despite, local sea level change, affected by steric effects can be very different compared to the global mean. London is relatively close to the Dutch coast thus it can be assumed that the dynamic response of steric effects is similar to global mean in the Netherlands.

## Atmosphere-ocean interaction

Regional climate models are required to determine regional sea levels. These models include the atmosphere-ocean interaction in their climate projections. Wind displaces water and wind patterns could change due to climate change. The KNMI expect that future climate change does not affect the strength of storms but are not very confident in their projections (KNMI, 2014). Storms can result in significant storm surge, depending on wind direction, that can increase the sea level temporarily by several meters. Wind and storm surge significantly affects the hydraulic loads for the MLK and OSK. More information can be found in Chapter 6.

### *Atmospheric loading*

The atmosphere exerts pressure on the ocean surface. Changes in the atmospheric pressure immediately affect the local sea level. It can be revealed that the impact on sea level is minimal. A surface pressure decreases (increase) of 1 millibar yields a sea level rise (drop) of approximately 0.01 m (the inverse barometer effect). This has no effect on global mean sea level, but locally it can temporarily contribute to sea level change (de Vries et al., 2014). Future global warming can increase the average atmospheric moisture content, and if this moisture originates from the ocean, this will yield a net decrease in sea level. Models indicate that the change in regional sea levels accounts for a small drop in average sea level of -0.004 m (RCP4.5) and -0.009 m (RCP8.5). Compared to the other contributions is atmospheric loading negligible (Slangen et al., 2014).

## Appendix C: Millennial sea-level commitment

It is known that Earth's climate system is not in balance and that both the atmosphere and oceans are warming due to human-made greenhouse gases in particular (Church et al., 2013). Earth's response to climate forcings is slowed down by the inertia of the global oceans and the massive ice sheets (Hansen et al., 2013). This means that, nowadays, the ice sheets barely start to respond to the atmospheric temperature rise of the last decades. Although current sea level rise is dominated by ocean warming and glacier melt, historic sea levels suggest that the ice sheets are also sensitive to climate change (Levermann et al., 2013). Based on historical climate change proxy recordings, we can expect substantial sea level rise with current CO<sub>2</sub> levels in the long-term.

On very long timescales of 10,000 years or more, there is medium confidence that near-complete Greenland ice sheet loss can be expected between 0.8 and 2.2 °C temperature increase above pre-industrial levels. Global average warming is currently exceeding 1 °C and even further warming could be expected due to the inertia of both the atmosphere and the oceans. However, it is expected that this loss is a very slow process which takes millennia (Levermann et al., 2013). The IPCC confirms the theory of long-term sea level commitment but argue that they were unable to quantify this precisely.

Based on studies about the historic sea level rise (Section 5.1), the current commitment to sea level rise in the long-term (multiple millennia) is probably 2-10 m sea level rise according to the IPCC (Church et al., 2013). This is confirmed by Dutton et al. (2015), who project a sea level commitment of 6 m per degree global warming (Dutton et al., 2015).

Accelerated warming according to RCP8.5 may start large-scale ice sheet shrinkage on the Antarctic ice sheet (Deconto & Pollard, 2016). This depends entirely on the rate of diminishing ice shelves which provide a buttressing effect for land-ice. If floating ice shelves disappear, an irreversible ice cliff collapse may give several meters of additional sea level rise for the higher temperature scenarios. The figures of (Deconto & Pollard, 2016) are not included in Figure A.9. This may imply that the sea level commitment on multi-millennia timescales is even more.

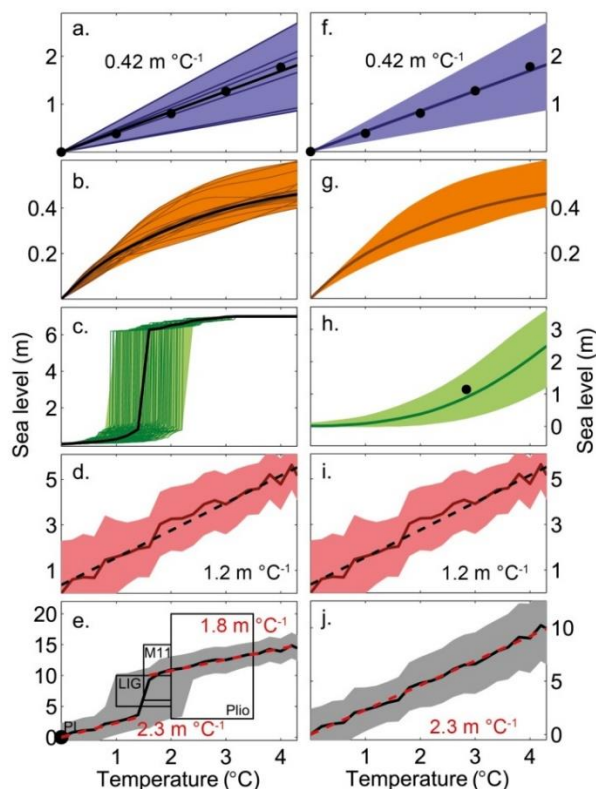


Figure A.9: Sea level commitment per degree of warming obtained from (Levermann et al., 2013) of (A) ocean warming, (B) mountain glaciers and ice caps, (C) the Greenland and (D) the Antarctic Ice Sheets. (E) The corresponding total sea level commitment, which is consistent with paleo estimates from past warm periods. Right figures (F-J) refer to sea level commitment in the first 2000 years.

## Appendix D: Sea level Projections

This appendix describes the sea level projections of the NOAA and the UK.

### NOAA

National Oceanic and Atmospheric Administration (NOAA) of the U.S. Department of Commerce projects global sea level rise scenarios and specifically for the United States. The latest sea level projections date from January 2017 in the report: *NOAA Technical Report NOS CO-OPS 083* (Sweet et al., 2017). This report will give input for the new project of the U.S. Global Change Research Program and upcoming Fourth National Climate Assessment (NCA4). The focus of the NOAA report is on high-end sea level rise in particular.

Several studies argue for a physically plausible worst-case GMSL rise in the range of 2.0–2.7 m and recent results regarding Antarctic ice-sheet instability indicate that such outcomes may be more likely than previously thought. Sweet et al. (2017) recommend a potential range of GMSL rise of 0.3–2.5 m during the 21<sup>st</sup> century (Figure A.10). Important to note is the small exceedance probability of 0.01% for 2.5 m sea level rise (Sweet et al., 2017). Sweet et al. (2017) emphasize that these high-end projections are outside the upper bound of the 95% confidence interval of the IPCC projections. These extreme sea level rise projections differ from the IPCC methodology which only quantifies more likely scenarios. The high-end probability approach favour risk-averse decision-makers, because some people are interested in extreme high-end scenarios with very small probability to occur to manage their risks robustly. For example, it could be interesting to quantify the 99,9<sup>th</sup> percentile in order to assess the robustness of expensive infrastructure with long operating lifetime such as the MLK. It is not advised to design flood defences on the requirements of the extreme high-end scenario (99,9%) since this scenario is extremely unlikely. However, combining the full probabilistic density function (PDF) of a sea level rise scenario and other weather- and water level statistics can provide a more accurate view of the current water safety.

The report of the NOAA uses various peer-reviewed literature about sea level rise published after the AR5 of the IPCC and combines this in several scenarios. The results are mainly based on a full probabilistic study including high-end tails of the IPCC AR5 made by (Kopp et al., 2014). The results are shown in Table A.1. Based on the information about sea level rise according to various scientists, NOAA concluded that future sea level rise projections are very uncertain. Therefore, six potential sea level pathways are presented in Figure A.10.

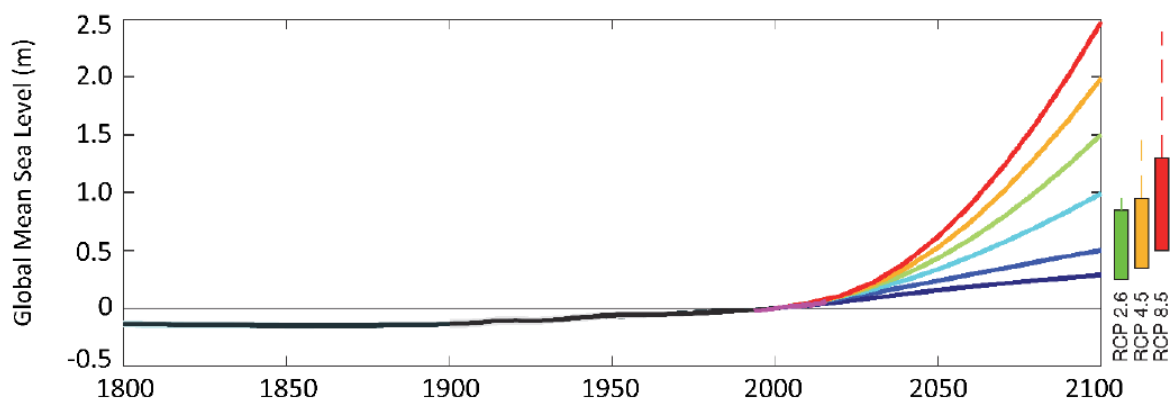


Figure A.10: Six GMSL rise scenarios of the NOAA for 2100 (6 coloured lines) combined with tide gauge and satellite altimeter GMSL reconstructions from 1800–2015 (black). RCP-based GMSL projections of recent studies (Sweet et al., 2017).

Table A.1: Probability of exceeding GMSL (median value) scenarios in 2100 based on (Kopp et al., 2014) & (Sweet et al., 2017).

GMSL rise scenario	RCP2.6	RCP4.5	RCP8.5
Low (0.3 m)	94%	98%	100%
Intermediate-Low (0.5 m)	49%	73%	96%
Intermediate (1.0 m)	2%	3%	17%
Intermediate-High (1.5 m)	0.4%	0.5%	1.3%
High (2.0 m)	0.1%	0.1%	0.3%
Extreme (2.5 m)	0.05%	0.05%	0.1%

According to Kopp et al. (2014), the projected results of sea level rise for 2100 are the following:

Table A.2: Projected sea level rise for different RCP's between the year 2000 and 2100 (Kopp et al., 2014). TE: thermal expansion, LWS: land water storage.

cm	RCP 8.5					RCP 4.5					RCP 2.6				
	50	17-83	5-95	0.5-99.5	99.9	50	17-83	5-95	0.5-99.5	99.9	50	17-83	5-95	0.5-99.5	99.9
2100—Components															
GIC	18	14-21	11-24	7-29	<30	13	10-17	7-19	3-23	<25	12	9-15	7-17	3-20	<25
GIS	14	8-25	5-39	3-70	<95	9	4-15	2-23	0-40	<55	6	4-12	3-17	2-31	<45
AIS	4	-8 to 15	-11 to 33	-14 to 91	<155	5	-5 to 16	-9 to 33	-11 to 88	<150	6	-4 to 17	-8 to 35	-10 to 93	<155
TE	37	28-46	22-52	12-62	<65	26	18-34	13-40	4-48	<55	19	13-26	8-31	1-38	<40
LWS	5	3-7	2-8	-0 to 11	<11	5	3-7	2-8	-0 to 11	<11	5	3-7	2-8	-0 to 11	<11
Total	79	62-100	52-121	39-176	<245	59	45-77	36-93	24-147	<215	50	37-65	29-82	19-141	<210

Kopp et al. (2014) revised the IPCC scenarios with a full probability range in Table A.2. It is interesting to see that the tails refer to extreme sea level rise due to uncertainty. Another conclusion is that the differences in terms of SLR between scenarios are considerably smaller than in the IPCC projection. For RCP8.5, the projected of SLR is 121 cm for the 95<sup>th</sup> percentile and 245 cm for the 99.9<sup>th</sup> percentile. For the low emission scenario (RCP2.6) sea level rise is estimated at 82 cm for the 95<sup>th</sup> percentile and 210 cm for the 99.9<sup>th</sup> percentile.

## UK Climate Projections

UK Climate Projections is a climate analysis tool designed to help decision-makers to assess the risk exposure to climate change (Met Office, 2016). UK Climate Projections is funded by the UK government Department for Environment, Food & Rural Affairs (Defra). The UKCP09 project shows the latest official climate projection from the UK. A new project UKCP18 is in progress with new information about sea level rise. This report will be published from 2018 to 2022. This study addresses the UKCP09 projections which were based on the results of the IPCC AR4 and the Phase 3 Coupled Model Intercomparison Project CMIP 3.

Met Office (2016) advice to avoid using this information and to wait for the updated UKCP18 projections to become available if possible (Met Office, 2016). This because of the missing of the latest insights about climate change and sea level rise. Nonetheless, the UKCP09 report is still interesting because of its High++ scenario.

The UKCP09 provided sea level projections for the UK in specific. Table A.3 shows the results global sea level rise of the IPCC AR4 (2007) and the projections for the UK are summarized in Table A.4. The expected sea level rise for the UK is slightly higher due to the improved understanding of melting ice sheets. The results for the High++ scenario are also provided in both tables but are explained later in this appendix. The other results are based on three different emission scenarios which roughly represent RCP8.5, RCP4.5 and RCP2.6. The results of the UKCP09 are intended for the UK and are shown in table A.4:

Table A.3: GMSL change according to IPCC AR4 (\*: High++ based on UKCP09) (Lowe et al., 2009).

Absolute GMSL rise in the year 2100 in cm (global) (IPCC AR4)	5 <sup>th</sup> percentile (P5)	Mean estimate (P50)	95 <sup>th</sup> percentile (P95)
High++ scenario (global)	93.0-250.0*		
High emission scenario	26.0	42.5	59.0
Medium emission scenario	21.0	34.5	48.0
Low emission scenario	18.0	28.0	38.0

Table A.4: Absolute sea level rise projections for the UK according to UKCP09 (Lowe et al., 2009).

Absolute sea level rise in the year 2100 in cm (UK) (UKCP09)	5 <sup>th</sup> percentile (P5)	Mean estimate (P50)	95 <sup>th</sup> percentile (P95)
High++ scenario (UK)	93.0-190.0		
High emission scenario	15.4	45.6	75.8
Medium emission scenario	13.1	36.9	60.7
Low emission scenario	11.6	29.8	48.0

The focus of the UKCP09 is on the high-end scenarios (High++) for both sea level rise and storm surge. UKCP09 also made a high++ scenario to project the effect of climate change to storm surge. Storm surge is essential in determining the hydraulic requirements for the storm surge barriers. Temporarily sea level during storms could be considerably higher when additional storm surge and sea level rise of the H++ scenario is included. More information can be found in Chapter 6.

Scenario High++ is developed to test the vulnerability of the flood defences in the UK (Lowe et al., 2009). In 2009, this high-end sea level scenario of 190 cm in 2100 was considered as an improbable scenario, but cannot be completely ruled out (Lowe et al., 2009). According to the latest insights, the High++ scenario might become a reality due to the potentially accelerated contribution to SLR of the Antarctic ice sheet (Section 5.4).

This high-end scenario (High++) is based on past sea level rise and expert knowledge and judgement. Proxy data of ice cores and sea sediment is analysed and combined with the known limitations in the physics of ice sheet models. The UKCP09 report projects a maximum global sea level rise of 2.5 m in the year 2100 based on the maximum known historical rate of sea level rise during the last Interglacial period. Important to note is that this projection is based on the historic sea level rise and not on climate models and ice sheet models. For the UK specific, the maximum sea level rise in the High++ scenario is lower due to the gravitational effects of the Greenland ice sheet. In 2009, it was expected that the ice sheet of Greenland would contribute to a more significant extent than the ice sheet of Antarctica. The projected maximum sea level rise for the UK is 1.9 m in the year 2100 for the highest emission scenario. The lower bound of the High++ is 93 cm based on UKCP09 which include 17 cm contribution from ice sheets (Lowe et al., 2009). Potential changes in ice sheet dynamics are only incorporated into the H++ scenario. These estimations remain very uncertain due to the complexity of the climate system. More information about the ice sheet dynamics of Antarctica can be found in Section 5.4 and Appendix F.

## Appendix E: Ice sheet contribution to sea level rise

The Antarctic ice sheet (AIS) and the Greenland ice sheet (GrIS) contain enough water to raise global mean sea level (GMSL) with 58 m and 7 m respectively (Fretwell et al., 2012). The current rate of contribution to SLR of both the AIS and GrIS is increasing due to climate change. However, this process develops relatively slowly due to the inertia of the global oceans and the ice sheets (Hansen et al., 2013). This means that the ice sheets barely start to respond to the recent atmospheric temperature rise. It can be expected that the full response will come in the next centuries.

It is evident that the focus is on ice which is supported by land because that mass can contribute to sea level rise. Figure A.11 shows the dimensions of both ice sheets. The GrIS is maximal 3000 m thick, and the ice is located mainly above GMSL. This implies that the GrIS is prone to atmospheric warming rather than oceanic warming. The AIS is much larger and nearly half of the ice sheet is supported on bedrock that is hundreds of meters below sea level (Fretwell et al., 2012). Therefore, the AIS is prone to both atmospheric and oceanic warming.

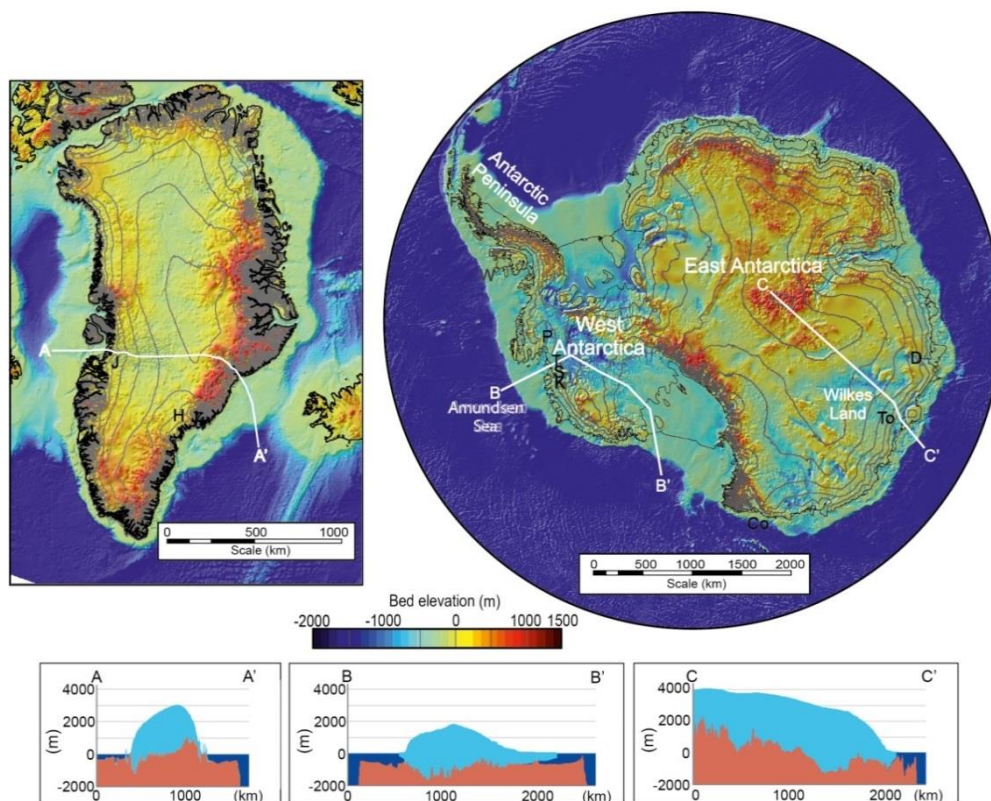


Figure A.11: Dimensions of the AIS and GrIS including a cross-section of supporting bedrock (Vaughan et al., 2013).

Ice sheets lose mass in various ways. First, large ice sheets will respond to climate change in the Surface Mass Balance (SMB), which is the sum of snowfall, run-off and melt which is predominantly controlled by the atmospheric temperature. Second, the grounding line retreat and cliff failure are dynamic processes triggered by climate change which were not fully understood yet. These ice sheet dynamics are influenced by changes in ocean temperature, circulation, and atmospheric changes (Bamber & Aspinall, 2013). DeConto and Pollard (2016) are the first that captured dynamic responses into ice sheet models (Section 5.4 and Appendix F). Dynamic responses are changes in iceberg calving and tidewater glaciers due to the warming ocean water which could have a significant impact on the mass balance of ice sheets. Both SMB and the dynamic responses are explained below. The mass change of an ice sheet is as follows:

Mass change = Surface Mass Balance - Ice Discharge = Precipitation – Runoff – Sublimation – Calving – Marine melt.

In 2013, the IPCC estimated that the contribution of ice sheet melt is  $0.63 \pm 0.17$  mm per year for the Greenland ice sheet and  $0.41 \pm 0.20$  mm for Antarctica. The total contribution is estimated at  $1.04 \pm 0.37$  mm for ice sheet melt of both the Antarctica and Greenland ice sheet (2005-2010) (Vaughan et al., 2013).

Bamber et al. (2013) were one of the first that quantified the uncertainty of ice sheet contribution to sea level rise. Floating ice shelves around the WAIS are weakening which reduces the buttressing effect to grounded ice. Ice shelves are critical for ice sheet stability. Without these ice shelves, significant shrinkage of the WAIS is to be expected. Ice sheet contribution to sea level rise for both AIS and GIS is 84 cm (P95) in the high-end estimate (Bamber & Aspinall, 2013). More information about the uncertainty of the sea level contribution of Antarctica is provided Appendix F.

Global warming can trigger various feedback mechanisms that might increase ice mass loss. Changes in floating sea ice content can affect local temperature (decreased albedo effect) but do not contribute to sea level rise. However, sea ice can provide a buttressing effect that prevents sliding ice mass towards the sea.

## Surface Mass Balance

The Antarctic and Greenland ice sheet surface mass balance (SMB) is the difference between the ice accumulation from precipitation and loss from melting and sublimation. Iceberg calving and snowdrift should also be included in the SMB. The Surface Mass Balance is as follows:

Surface Mass Balance (SMB) = Accumulation – Ablation = Precipitation – Runoff – Sublimation – Snowdrift.

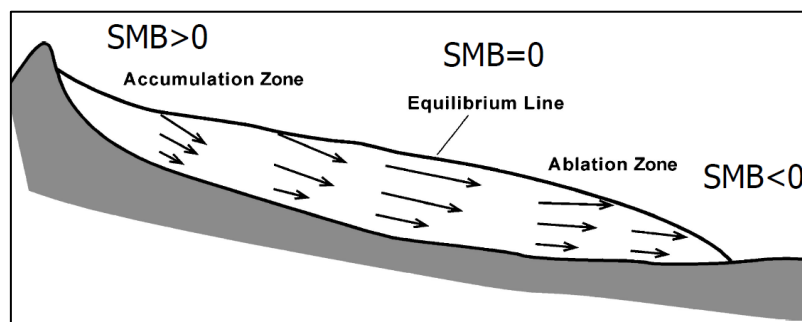


Figure A.12: Surface Mass Balance (CIE4510 Climate Change, TU Delft).

Glaciers and ice sheets gain mass through snowfall. At the surface, ice mass will reduce due to surface melt, runoff, and sublimation. In the places where land ice reaches the ocean, ice melt can also occur due to ocean heat.

Climate change might result in more snowfall what leads to a positive SMB. According to (Church et al., 2013), precipitation may increase by  $5.1 \pm 1.5\%$  per degree temperature rise. Important to note is that this only is the case for East-Antarctica and many scientists expect that dynamic effects outweigh a slightly positive SMB (Bamber & Aspinall, 2013), (DeConto & Pollard, 2016). The SMB contribute 0.04 m (-0.06 to 0.14 m) to sea level rise in 2100 according to the IPCC AR5 (Church et al., 2013).

A recent study shows that the current SMB is negative caused by ice loss in West-Antarctica and in particular the Pine Island glacier. This melting is mainly due to the warming seawater which affect the marine terminating glaciers. It is noteworthy that current global warming does not lead to more snowfall in East-Antarctica (IMBIE Team, 2018).

## Dynamic responses

The Antarctic ice sheet (AIS) will lose mass due to dynamic responses to climate change. Dynamic responses such as hydrofracturing, grounding line retreat and cliff failure (calving) are dynamic responses that are the result of the combination of atmospheric warming and oceanic warming. The IPCC estimated a global sea level contribution of 0.12 m (-0.01 to 0.16 m) for ice sheet dynamics but did not rule out a more significant contribution (Church et al., 2013).

### Hydrofracturing

Rain and meltwater influence crevassing and calving rates which already occurred on the Antarctic Peninsula's Larson B ice shelf, which was lost in 2002 (Banwell et al., 2014). Hydrofracturing of ice percolates the ice shelves and reduces its strength. Similar dynamics could have affected ice sheets during past warm intervals between the Ice Ages.

### Grounding line retreat

Grounding line retreat is a process driven by oceanic warming which melts ice below sea level that triggers ice sheet instability. The grounding line separates land- and floating ice and is below the ocean surface. Nearly half the AIS is supported by bedrock that is hundreds of meters below sea level which is essential for the grounding line retreat mechanism (Fretwell et al., 2012). The reverse sloped bed of the supporting rock accelerates grounding line retreat and increases marine terminating cliff height.

It is expected that grounding line retreat will accelerate by global warming. On the other hand, the migration speed of grounding line retreat can slow down at increased water depth where the melting point of ice is lower (Griggs et al., 2017). However, the ocean temperature change in Antarctica is relatively limited at increasing depth, so the impact of this negative feedback is minimal.

### Ice-cliff collapse

When floating ice disappears due to surface and ocean melt, the buttressing effect of these ice shelves reduces. This will trigger increased flow of land ice towards the ocean.

The AIS is at risk of losing an immense amount of ice mass as a result of marine instability and ice-cliff instability. Marine instability results from a bedrock that is deeper inland (reverse slope). Hydrofracturing results to high unstable ice-cliffs which can collapse due to the reduced buttressing effect of sea ice. More in-depth information about the dynamic effects of the AIS can be found in Appendix F.

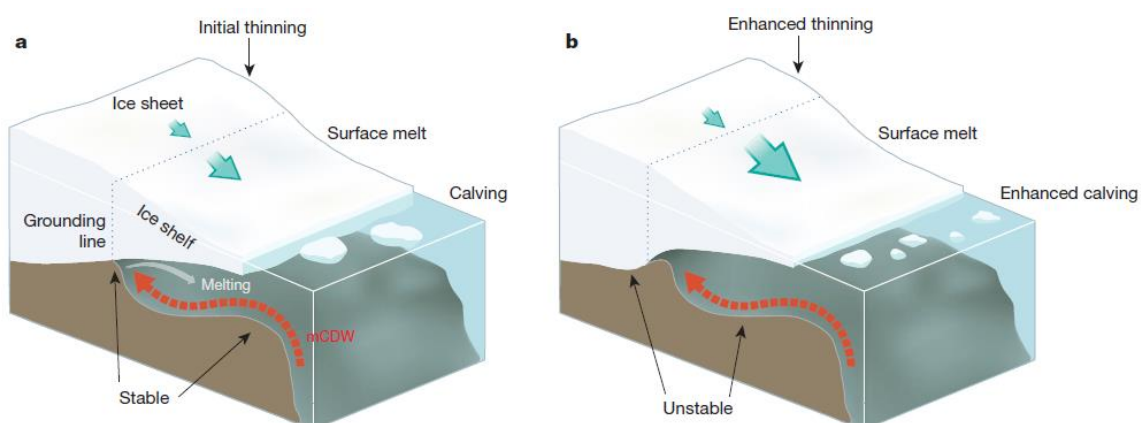


Figure A.13: Dynamic responses to climate change (Hanna et al., 2013).

## Appendix F: Future Antarctic contribution to sea level rise

The Antarctic ice sheet could be the largest contributor to future sea level rise but is also the most uncertain (Meehl et al., 2007).

DeConto and Pollard (2016) (DP16) argue that global sea level rise can accelerate to a much greater extent than was predicted earlier. This argument is based on recently acquired knowledge about the stability of ice cliffs and ice shelves in Antarctica. The total size of floating ice shelves could reduce drastically in the next decades if global carbon emissions continue unabated. According to the results of DP16, most sea ice may be disappeared around West-Antarctica in 2050, leading to large-scale ice flow towards the sea in combination with ice cliff collapse.

The new ice model includes both Marine Ice Sheet Instability (MISI) and Marine Ice Cliff Instability (MICI) (dynamic) processes (Deconto & Pollard, 2016). MISI processes were already computed before, but primarily MICI has the potential to contribute to SLR to a large extent. Both processes are visualized in Figure A.14.

Figure A.14 (a) shows a stable marine terminating ice sheet with a buttressing ice shelf. The seaward ice flux is essential in determining the thickness of land ice on the grounding line. The oceanic melt of the ice shelves allows more relatively warm water to flow towards the grounded ice mass. This will increase the grounding line retreat. Thinning ice shelves and reduced buttressing increase the seaward ice flux and the total Antarctic contribution (b). More ice will flow into the ocean when the bed slope changes (c).

MICI (d) increases the dynamic ice loss processes due to hydrofracturing of ice shelves. Hydrofracturing is possible when the atmospheric temperature is high enough to create surface meltwater that cracks into the ice shelf. Hydrofracturing reduces the strength of the ice shelves which will break up much earlier (calving). This process might accelerate the ice flux more than in MISI. Rapid disappearing ice shelves also result in tall vertical cliffs. These cliffs are structurally unstable leading to large-scale ice-cliff collapse. Together MISI and MICI might increase the Antarctic contribution to SLR significantly (Deconto & Pollard, 2016).

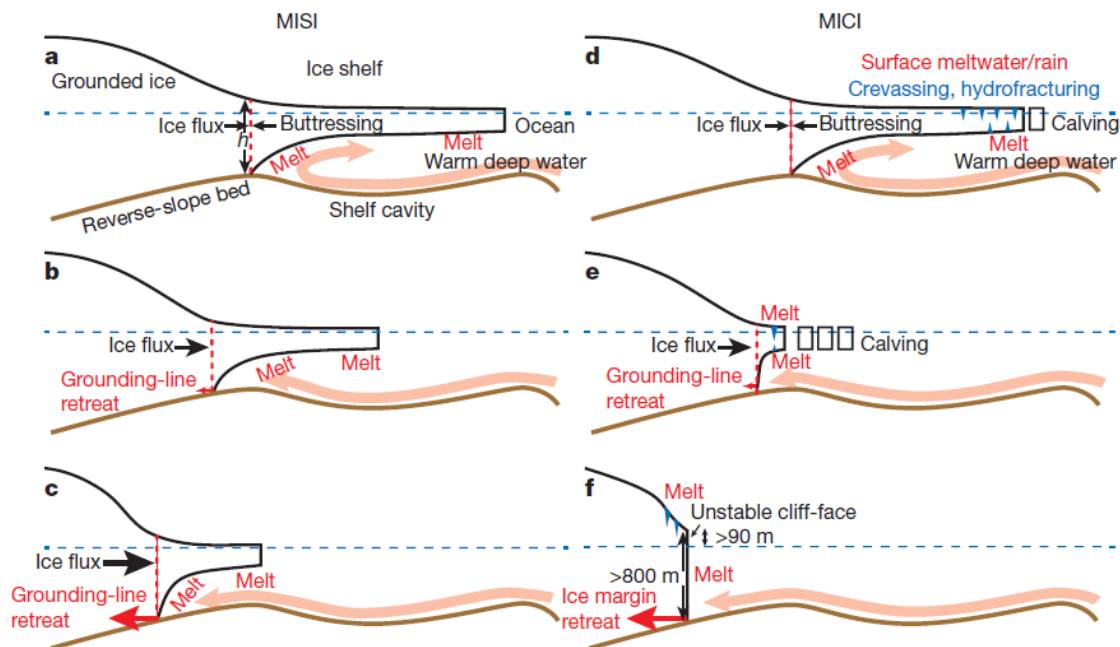


Figure A.14: (a-c) show MISI and the melting ice shelf. (d-f) show MICI with accelerated ice shelf retreat and cliff collapse. Both processes are triggered by oceanic and atmospheric warming (Deconto & Pollard, 2016).

The model is calibrated on proxy records of past sea level rise in the Last Interglacial (LIG) and the Pliocene period and is the first model that shows comparable results that match past sea level fluctuations (Deconto & Pollard, 2016). This might imply that the previous sea level projections were not equivalent to past sea level rise without

incorporating hydrofracturing and ice-cliff failure (Griggs et al., 2017). Estimations of past sea level rise in the Pliocene are relatively uncertain because that high-sea level period was roughly 3 million years ago.

For this reason, DP16 has made calculations for two Pliocene targets (5-15 m) and (10-20 m). Furthermore, DP16 included an ocean bias correction of the Amundsen and Bellingshausen seas (+3 °C) because it is expected that these seas are gaining more heat than surrounding oceans. The calculation is made for three RCP scenarios.

Table A.5 shows the results of DP16 for the year 2100. The results for longer timescales (e.g. 2500) are shown in Figure A.15. The difference between RCP2.6 and RCP8.5 is significant. The results of DP16 indicate that it is very beneficial to reduce SLR by investing in global climate mitigation policies to reduce carbon emissions. Major Antarctic contribution is expected to start about the year 2050 for both RCP4.5 and RCP8.5. This is because ice shelves should first disappear in order to start the large-scale ice sheet retreat.

There are some uncertainties and limitations in the simulations of the report of DP16 which can either underestimate or overestimate ice sheet retreat. These are summarized in Section 5.4.2.

Table A.5: Results of DP16 for the year 2100 including 1σ standard deviation.

Antarctic contribution to sea level rise in m for the year 2100	Ocean temperature correction of Amundsen and Bellingshausen seas (+3 °C)	RCP2.6	RCP4.5	RCP8.5
LIG: 3.6-7.4 m, Pliocene: 5-15 m	No	0.02±0.13	0.26±0.28	0.64±0.49
	Yes	0.14±0.19	0.41±0.30	0.79±0.46
LIG: 3.6-7.4 m, Pliocene: 10-20 m	No	0.11±0.11	0.49±0.20	1.05±0.30
	Yes	0.16±0.16	0.58±0.28	1.14±0.36

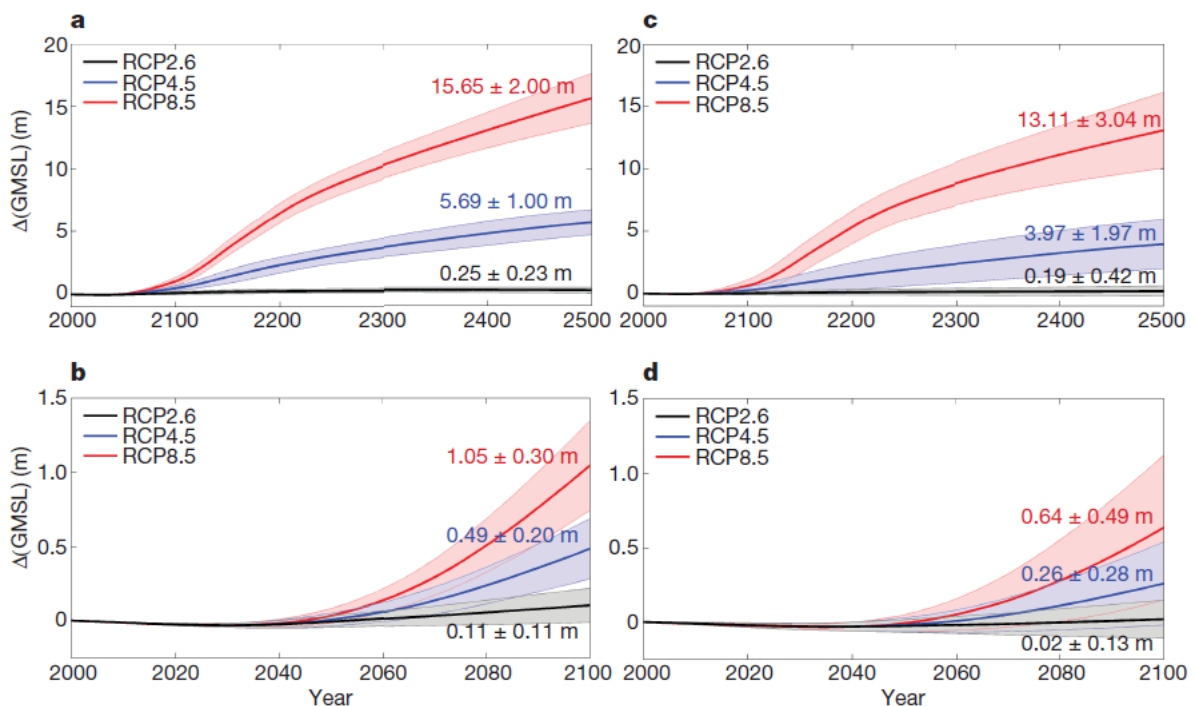


Figure A.15: a) RCP ensembles to the year 2500. b) results for the year 2100. Similar to (a, b) but for the lower Pliocene target of 5-15 m.

DP16 showed that diminishing ice shelves are essential to start significant retreat of land-ice. Latest studies show that increasing retreat of ice shelves is already started (Paolo et al., 2015). Paolo et al. (2015) argue that ice volume losses of floating ice shelves increased 70% in the last decade around the West-Antarctic ice sheet (WAIS). Almost all ice shelves at the WAIS that provide buttressing effect are losing mass (Figure A.16). This indicates that the processes described by DeConto & Pollard (2016) might become a reality.

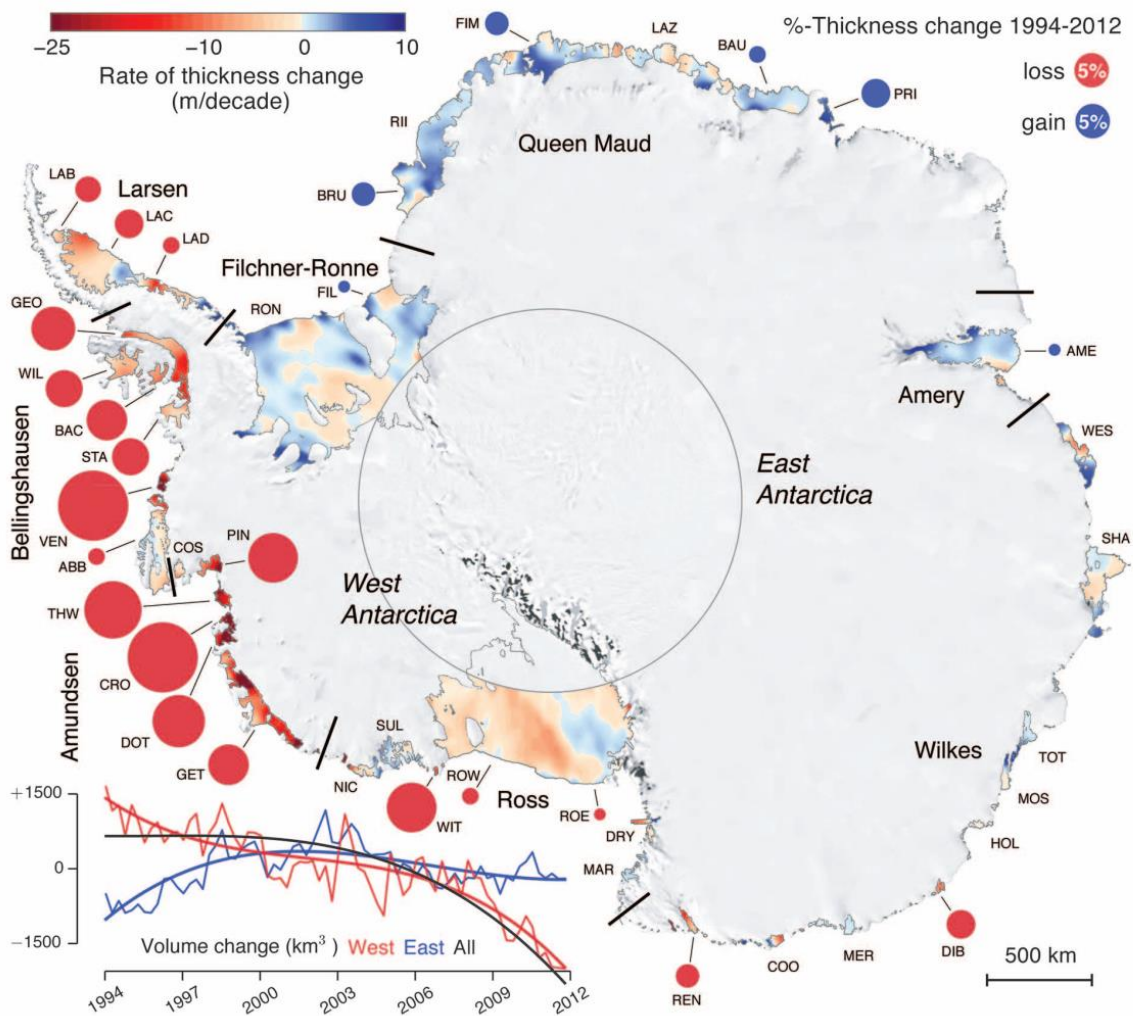


Figure A.16: Change in thickness and volume of Antarctic ice shelves over the last 18 years (Paolo et al., 2015).

## Appendix G: An overview of levee systems in the Netherlands (2017)



**Figure 2.3**  
Levee segments in  
the Netherlands.



Figure A.18: Levee segments in the Netherland (2017) (ENW, 2016)

## Appendix H: Storm surge barriers

This appendix describes the technical aspects and current performance of the Maeslant Barrier (MLK) and the Eastern Scheldt Barrier (OSK). This appendix in combination with Chapter 5 and 6 deliver informative input for the risk analysis to be able to determine the technical tipping points of both storm surge barriers. This section contributes to the assessment of the remaining lifetime of the MLK and OSK for the mentioned climate and sea level rise scenarios.

The technical information of the MLK is gathered from the design handbooks of Rijkswaterstaat and by asking questions to specialists. The technical information of the OSK is also obtained from design books and using various sources on the internet.

### Technical analysis of the Maeslant Storm Surge Barrier

The MLK and the Hartel Barrier (HK), together with connecting dykes also called Europoort Barrier, are part of the Delta Plan. It was a challenge to design a storm surge barrier that only close during extreme high-water. The Rotterdam Waterway (NWW) had to remain open during daily circumstances for economic purposes of the port of Rotterdam.

In April 1987, the Minister of Transport, Public Works and Water Management commissioned an investigation to build a storm surge barrier in the Nieuwe Waterweg. In October of that year, six different designs were submitted by different contractor combinations.

The MLK is primarily designed to protect the hinterland against high-water events. The arc-shaped doors close-off the NWW to reduce the water level in the backward Rhine-Meuse Delta (RMD) during storms and extremely high-water events. The effect of the storm surge barrier is the greatest for regions close to the sea such as Rotterdam and reduces further inland because of the influence of the rivers. The barrier is designed to reduce the water level of at least 1.6 meters at Rotterdam and 0.4 m in Dordrecht.

The MLK is an economically efficient alternative compared to further dyke raising, which has significant negative consequences in urban areas.

The MLK is designed for a lifespan of 100 years, including 50 cm sea level rise. This was the high-end projection of sea level rise at that time. The main components such as the floodgates, trusses, ball-shaped joint and foundation should last 100 years. Smaller components will be replaced in time during the maintenance intervals.

It is not clear whether the MLK can continue to function efficiently for more sea level rise. Sea level rise leads to more frequent closures when the closing level is maintained. It is, therefore, possible that this barrier is no longer economically attractive in the future because of the increased delays in shipping. The strength, stability and loads are decisive in determining the robustness of the storm surge barrier for climate change, but other changes can also be decisive. The requirements for storm surge barriers might change after regulation changes or the economic development in the hinterland might change substantially. Chapter 7 analyzes these aspects in more detail to determine the remaining lifetime of the MLK for different climate scenarios.

### **Technical information**

This section is about the technical details of the MLK who influence the performance during a closure. The HK is described in less detail because of the limited influence on the performance of the MLK. Wave overtopping and water overrun over the top of the HK are included in the analysis of the effects to the water level in the Rhine-Meuse Delta. Other effects of sea level rise for the Hartel Barrier are left out of the analysis.

### **Design requirements**

The preconditions and design requirements have been drawn up by Rijkswaterstaat. The main aim was to lower the maximal high-water levels in the RMD and especially in Rotterdam and Dordrecht. The design requirements at that time were:

- reduce the maximum water level in Rotterdam and Dordrecht under design storm conditions;
- chance of collapse of the barrier should be less than once per 1,000,000 years;

- the maximum failure rate to close should be 1/1000 per year;
- the passage width should be at least 360 m;
- the unobstructed depth of the water must be -17 m NAP;
- shipping may not be hindered during the construction;
- the maximum closing time is 2.5 hours;
- the maximum opening time is 2.5 hours;
- non-replaceable parts must have a lifespan of at least 100 years;
- the barrier must be able to discharge water from the river.

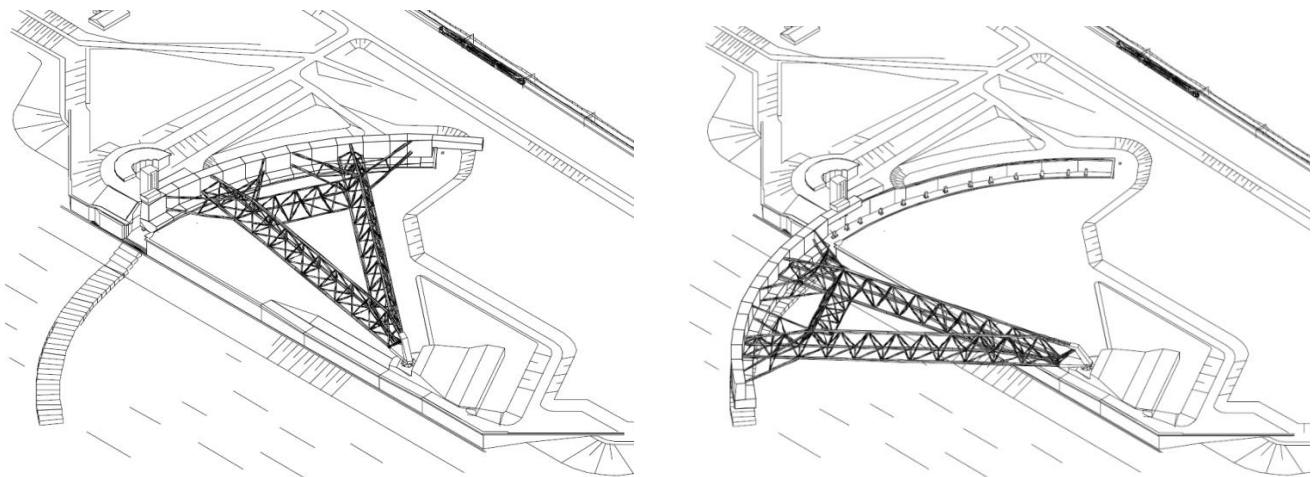


Figure A.19: Schematic design of the MLK.

### Floodgates and Trusses

The water-retaining floodgates and trusses are the largest moving elements of the MLK (Figure A.20). Both arch-shaped doors have a total length of 248 m, whereof 216 m is used to close the 360 m wide waterway (NWW). The total height of the doors (floodgates) is 22 meters. The height of the barrier is +5.0 m NAP when the floodgates are sunk on the threshold blocks at a depth of -17 m NAP. The retaining walls can operate in two separate ways:

- the horizontal movement using the hydraulic movement works on top of the doors (Dutch: “locomobiles”);
- vertical movement using the ballast system within the floodgates.

The primary functions of the water-retaining doors are:

- minimizing the flow opening in the NWW during a closure;
- transmitting the immense forces, exerted on the gates, to one single joint at the rear of each gate;
- to be in control to float and sink by means of a ballast system.

The steel floodgates compose of 15 compartments whereof 13 sections can be filled with water. Each compartment contains two valves to fill the (ballast)tanks to allow the doors to sink to the bottom. With the use of two pumps per compartment, the ballast tanks can be dry-pumped in order to re-float the floodgates. The significant number of compartments contribute to minimize the failure probability. Therefore, several pumps or valves may fail without disturbing the operation. The outer sections have trim tanks which can be used to regulate the trim angle of the doors. This will be managed automatically by BOS with the use of sinking matrices.

The upper sections of the doors are resistant to significant wave loads. Furthermore, many components of the barrier have been duplicated to minimize the chance of failure. Both floodgates can still operate during failures in several compartments (e.g. leakage or failing pumps).

The floodgates are connected to 238 m long steel trusses weighing 6.800 tons each. Both the doors and trusses are painted in white to minimize the expansion of the steel structure in case of temperature differences. Otherwise, the floodgates might not fit into the drydock.

The doors do not close completely to prevent a potential collision between the doors. Therefore, there is a gap of 80 cm between the doors. Also, the construction does not provide a complete connection to the quays. The total opening is 100 m<sup>2</sup>, which leads to a considerable amount of leakage (Slomp et al., 2005). The effects of this leak are considered in the study of the remaining storage capacity in the hinterland.

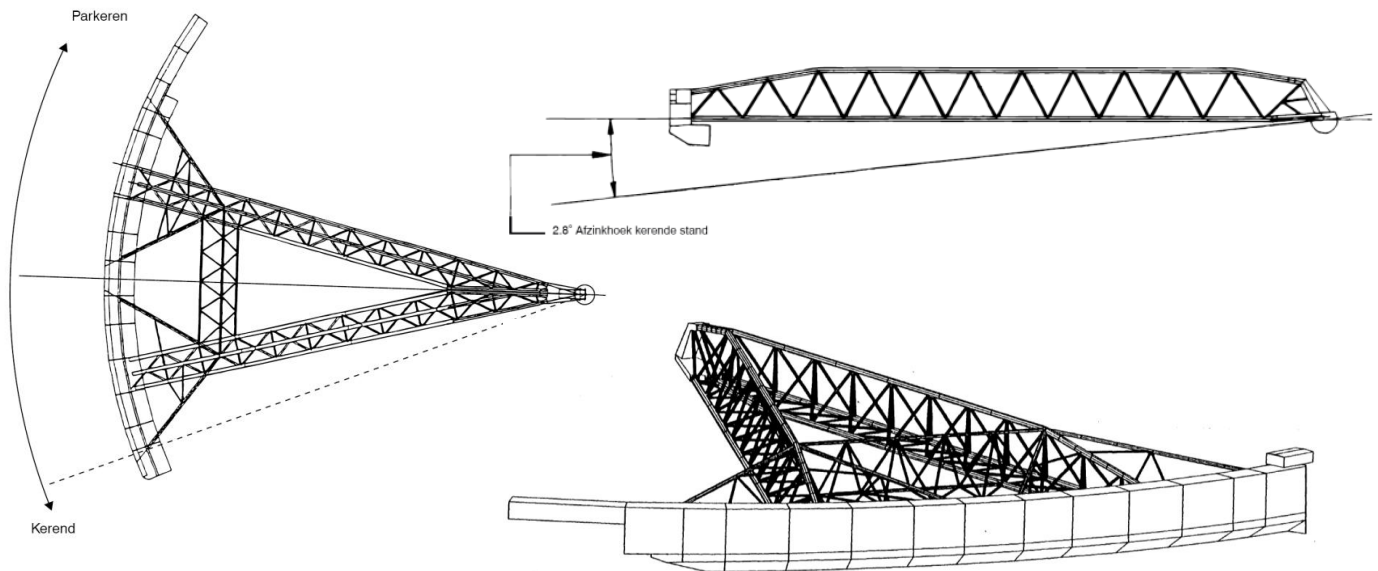


Figure A.20: Arc-shaped doors (floodgates) of the MLK.

### Ball-shaped joint

The ball-shaped joint (Dutch: “bolscharnier”) is an essential part of the MLK. The design of the ball-shaped joint is presented in Figure A.21. First, the joint can rotate in three directions, which is necessary to follow all movements of the doors. Second, the water pressure exerted to the doors will be transferred via the trusses to the foundation.

The ball joint weighs 680 tons and has a diameter of 10 m and is made with an accuracy of 2 mm.

The construction is designed for 35,000 tons of horizontal water pressure which will be absorbed by the fixed bearing part (Dutch: “achterstoel”). This corresponds to a water level difference of more than 4 m. The ball joint is not designed for a huge negative force, exerted by a higher river level. This pulling force (negative water level difference) is absorbed by the bowl at the front of the joint (Dutch: “voorstoel”), which is much smaller. The maximal acceptable positive pressure is 6,500 tons, translated to a difference in water level of 1.5 m.

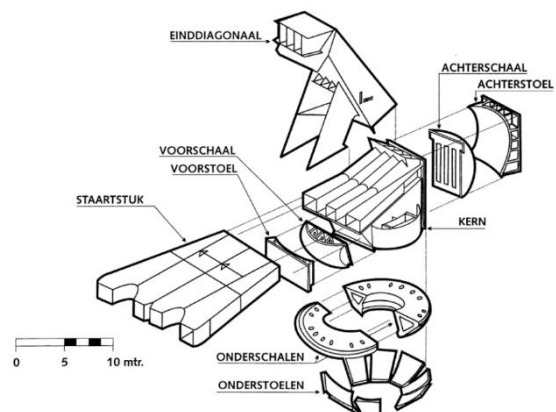


Figure A.21: Components of the ball-shaped joint.

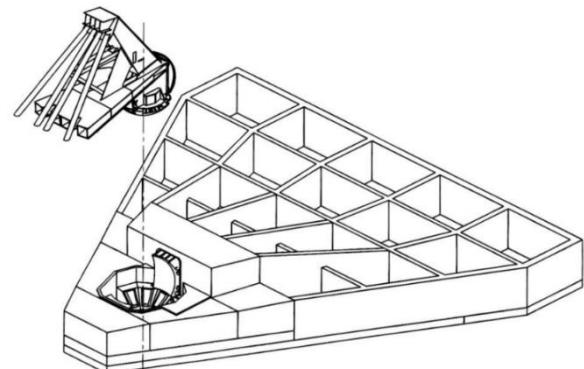


Figure A.22: Foundation of the MLK.

## Foundation

The forces on the floodgates are transferred to the concrete foundation. The foundation is a pre-stressed concrete tub with a weight of 52.000 ton each (Figure A.22). Both constructions can handle a total load of 70,000 tons. The construction is supported on compacted sand and is not reinforced by piles. However, there is sufficient shear resistance due to the friction between the concrete and the subsoil. The foundation can move and stretch 20 cm backwards in the event of an extreme water level difference but will return afterwards because of the elasticity. The construction is designed for a small permanent movement during the first heavy-duty operation. The second and subsequent closures will be considerably more elastic be included because of the increasing compaction of the sand body.

## Threshold blocks and soil protection

If the doors are sunk in the river, the arc-shaped doors are supported on concrete threshold blocks on the bottom of the river. Large fenders on the underside of the doors ensure that the water leakage underneath the floodgates is limited. The bed was deepened and reinforced with a granular filter before the blocks were placed (Figure A.23).

The 65 threshold blocks, with dimensions of 15 by 5.6 meters and a height of 3.2 meters have a weight of 630 tons per unit. The threshold blocks are placed with considerable accuracy at a depth of -17 m NAP. This was one of the design requirements of the MLK, including the guarantee for sufficient depth for shipping. The current depth of the soil bed of the Rotterdam Waterway is -14.5 m NAP, but it can be dredged to allow access for larger ships in the future. The result is that the threshold blocks are placed with significant accuracy. The maximum allowable deviation is 7 cm.

It was calculated that the blocks could decline 0.1-0.2 m after multiple loadings of the massive doors. The current altitude of the threshold blocks determines the retaining water height of the MLK and should therefore not move. That is the main reason why the doors are not completely filled with water to minimize the load on the threshold blocks during a closure. It is intended to transfer all loads of closure to the ball-shaped joint without via the shear stress on the threshold blocks. It also turned out that the construction height of the blocks was slightly higher than according to the design, resulting in a current barrier height of +5.0 m NAP.

The soil protection (granular filter) is installed in a dredged bed on the bottom of the river. The primary function of the soil protection is to ensure the stability of all construction components behind the storm surge barrier. The soil protection is applied according to Figure A.23.

The upper layer of the soil protection should resist a high flow velocity during closure and opening of the storm surge barrier. The soil protection consists of a 2.4 m top layer of stone blocks (3000-6000kg) at the riverside. At the seaside, the layer is 1.2 m thick with smaller stones (300-1000kg). The soil protection around the threshold blocks is about 60 to 75 m wide. The required stone grading of the top layer is calculated in Appendix P.

The strength of the soil protection decreases further away from the barrier, as the flow velocities reduce significantly. The total length of the soil protection is approximately 400 m, of which the majority is on the river side of the barrier.

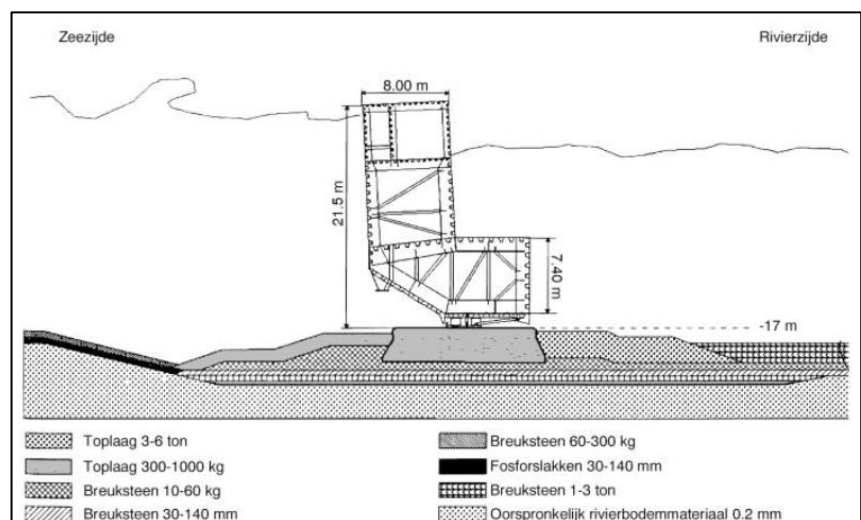


Figure A.23: Cross-section of the floodgates of the MLK including the soil protection and threshold blocks.

Excavation pits might occur after a storm closure on the transition from the soil protection and the original bottom. If the excavation pits exceed the prescribed condition, the stability of the soil protection is at risk, with the possible consequence that the adjacent structures lose their stability. The protocol is to refill existing pits with a deviation of more than one meter from the design which is part of the routine maintenance.

### Drydock

The function of the drydock is to park the arc-shaped doors in a controlled environment outside the shipping lane. The depth of the dock ranges from -8.0 m NAP at the land side to -8.9 m NAP at the riverside. The doors begin to float from -2 m NAP and have a draught of approximately 6 m. However, due to safety margins, the barrier may only close or open at a water level exceeding +0.3 m NAP.

### Failure rate

The reliability of closing the MLK is an essential aspect of the determination of the risk of flooding. The failure rate of the MLK and HK affect the hydraulic loads mainly for the dykes around the Rhine-Meuse Delta (RMD).

The link between the failure probability to close/open, the requirements for operation and maintenance is done by a comprehensive risk analysis. The quality and performance of all components, systems, operations and maintenance, including human errors, are laid down in a Fault Tree Analysis (FTA). The FTA includes the failure behaviour and assumptions of technical quality, management and maintenance.

In 2003, the calculated failure probability was 10% and did not meet the standard of 1/100 per closure. Since then, the reliability is significantly increased after implementing series of improvement in technology, components, organization and staffing (protocols). Since 2009, the failure rate per closure is 1/100. It is being investigated whether an additional reduction of this failure rate to 1/200 per year could be achieved by implementing various optimization measures. This can result in a significant improvement of flood risk throughout the RMD. The probability of failure per closure has a substantial impact on the water levels and the hydraulic load on dykes in the hinterland. This will be calculated using the probabilistic model Hydra-NL in Chapter 7 (Risk analysis).

### Operating process

The storm surge barrier is initially designed to be controlled entirely automatically by a computer system (BOS) which is the Decision and Support System. This system decides whether a closure is needed and operates, in principle, entirely automatically which reduces the chance of human errors. Based on experiences, it turned out that the software is not entirely reliable (is also human work). In 2006, an adjustment was made to the operating protocol. BOS is still the centre of the decision process to decide if a closure is required. However, the process is always being monitored by the operational team. If there is a signal of a (potential) failure, the operational team is trained to manage the BOS operation correctly and can close the barrier manually.

BOS uses various information and statistics of current and expected water levels, wind data and the river discharges to decide if the MLK and HK should close. Also, this system commands the operating systems of both storm surge barriers to perform a full automatic closure.

The storm surge barrier closes at an expected water level of +3.00 m NAP at Rotterdam or +2.90 m NAP at Dordrecht. If one of the levels is exceeded, the BOS system comes into action. The entire closure is intentionally controlled by the Decisions Supporting System (BOS). The standard closing procedure is explained in Table A.6.

Table A.6: The closing procedure of the MLK.

<b>Normal closing procedure</b>	
-20/-16 hours	The Operational Team is alarmed to go to the operating building if the water level expectations exceed +2.60 m NAP at Rotterdam
-8 hours	Notification to restrict shipping
-4 hours	Levelling of the docks and the opening of the dock doors
-2 hours	Set shipping restriction; no shipping is allowed
0 hours	Start horizontal departure of the arc-shaped doors (begin closure)
+0.5 hours	Floodgates are in place to start sinking process

+2 hours	The sinking of the floodgates is completed, MLK is closed
	MLK remains closed during positive water level difference between seaside and riverside.
0 hours	The decision to start un-ballasting the floodgates (arc-shaped doors). This moment can be considered as the beginning of the opening procedure.
+1.5 hours	The doors float. The decision to re-open depends on predicted water levels. The opening procedure starts if flood danger is passed. Also, the opening can only start if the gap between the barrier and bottom of the dock is sufficient to enter the docks. Start moving back to the drydocks. Another option is to close again for the next high tide. Flushing occurs at the moment that a next high-water peak is still expected.
+2 hours	The floodgates are restored in the docks. Start closing the dock doors and dock gates. Rotterdam Waterway is available for shipping.

Before the high-water event, the water level in the docks will be raised to be in align with the water level in the river. As a result of levelling the water level in the docks, the arc-shaped doors start to float at a water level of approximately -1.3 m NAP. The time of the departure depends on the type of closure. Due to safety margins, the barrier can only move if the water level in the river exceeds +0.3 m NAP. The doors move in place with the use of "locomobiles", who push the doors via a guide rail to the middle of the river in thirty minutes. Important to note is that the doors and guide rail moves instead of the locomobiles, which are fixated on the guide towers.

The vertical movement (sinking) of the floodgates lasts more than one hour. Each compartment within the floodgates has two valves which will be opened to fill the compartments with water, allowing to sink the doors to the bottom. Before the bottom is reached, the sinking process stops for several minutes to flush the threshold to remove sludge and sediment. A layer of sediment may have formed on the thresholds with a thickness of 1 m, which should be removed before the closure. When the risk of flooding has passed, the doors will be drained (dry-pumped) so that they float again. This process takes about 90 minutes. It is possible to drain water between the high waters by partially raising the doors. This may be necessary if the water level behind the barrier rises rapidly and is temporarily higher than the sea water level. The doors should return to the docks, which takes another 30 min before shipping is allowed.

### ***Closing process and criteria***

The storm surge barrier closes at an expected water level of +3.00 m NAP at Rotterdam or +2.90 m NAP at Dordrecht. Table A.6 indicates that the total time to close (departure and sinking) is approximately 2 hours. It is, therefore, necessary to start the closure considerably earlier to avoid exceeding the maximum water levels in Rotterdam or Dordrecht.

The condition is that the barrier must be closed in time so that these water levels do not occur. However, different safety margins have been implemented including the storage of incoming water supply from rivers and leakage through the MLK during the closure. The maximum water level in Rotterdam has been set at +3.60 m NAP although the critical water levels vary among the RMD.

Because the margin for water storage is relatively limited for a relatively long closure, it is required to close at a lower sea level to increase the storage capacity in the RMD. On the other hand, it is recommended to minimize the water difference between both sides to prevent potential damage to components of the storm surge barrier.

In order to make a consistent judgement, two criteria have been established in the protocol:

- *Water level closure* (Dutch: "Peilsluïting"); closure starts at a water level +2.0 m NAP during a river discharge of <6,000 m<sup>3</sup>/s.
- *Turnaround closure* (Dutch: "Kenteringsluïting"); closure starts at the turning point from ebb to flood. The closure starts at roughly +0.5-1 m NAP during a river discharge of >6,000 m<sup>3</sup>/s.

Usually, the river discharge is below 6,000 m<sup>3</sup>/s whereby the barrier closes at a water level of +2.0 m NAP. This closure provides a relatively low load on the barrier, but the water levels in the hinterland rise. It takes a while before the barrier is completely closed, resulting in a significant flow of seawater into the RMD. This type of

closure has recently been implemented on 3-1-2018. This process is further analyzed in Section 7.1.4.1 and Appendix Q.

If the discharge of the Rhine exceeds 6,000 m<sup>3</sup>/s, measured at Lobith, the MLK will close at an earlier time. In that case, the closure should start at the turning point of the flow direction of the current between ebb and the high-water. This is called a turnaround closure. The advantage of this closure is that the incoming high-water, originating from the sea, is stopped as much as possible. The storage capacity of the sub-river area (RMD) is fully available for the large incoming volume of water of the rivers. A turnaround closure was executed in November 2007, during a lower river discharge of roughly 1500 m<sup>3</sup>/s (Rijkswaterstaat, 2018).

To be able to start the horizontal departure, the floodgates must have enough space to prevent a collision with the threshold bars in the dock. The closing process only starts if a sufficient gap height (Dutch: “spleethoogte”) has been reached. Due to safety margins, it is not allowed to move the doors at a water level below +0.3 m NAP.

### ***Operational team***

The MLK and the HK can in principle close fully automatic by the BOS computer system. However, the operational team should be standby during every closure. This team consists of:

- Operating Manager (Dutch: “leader keringproces”)
- Leader Technical Specialists
- Leader Hydrological Specialists
- HCC guard of the Port Authority
- Process supervisor
- Monitor
- Technical Specialists
- Hydrological Specialists

The operational team monitors the progress of the closure and has an obligation to intervene or to carry out recovery actions if this is necessary. Hydrological specialists focus primarily on the functioning of the BOS system and other operating systems. All technical components are controlled by the Technical Specialists. All potential errors that might contribute to the failure probability have been analyzed in advance. Recovery actions have been prepared that can be executed by the operational team. A lot of attention is paid to the training of the members of the operational team because an emergency closure is relatively rare.

### ***Translation wave***

A translational wave is created when the current (incoming high-tide) is stopped by the closing storm surge barrier. This long-wave affect the local water level for roughly one hour. In general, the water level increases in front of the barrier and decreases at the riverside. This effect will diminish later on through reflection via the harbour basins. The sinking process of the doors is also tuned to minimize the effect of this translation wave in the harbour. This translation wave is visible in the data of the two previous closures (Appendix Q). The decline behind the barrier is caused by the inertia effect of the flowing water. This inclination results in a relatively low water level close to the barrier at the riverside.

### ***Seiche***

Seiches are waves with a length of several kilometres and occur primarily in harbours. Seiches are mainly caused by convection cells in the atmosphere at sea. Atmospheric pressure drops (inverted barometer effect) can slightly increase the water level on the sea. On the North Sea, the wave period of this phenomena is between 5 and 90 minutes. These cells originate almost exclusively during a northwestern wind. The amplitude of the seiche can increase significantly in the harbour of Rotterdam. The waves start to oscillate in the harbour and can strengthen each other, causing a significant increase in water level, especially in front of a closed storm surge barrier. A seiche with the amplitude of 0.9 m has occasionally been observed in the Rotterdam harbour (de Jong, 2004). The size of a seiche at the MLK is a function of the layout of the harbour basin. The influence of the shape of the harbour on seiches was extensively tested in the design of Maasvlakte 2 (Dutch: “Tweede Maasvlakte”). This will also be done before making future adjustments to the geometry of the harbour.

## **Hartel Barrier and Europoort Barrier**

The Hartel Barrier (HK), Maeslant Barrier (MLK) and dykes between both storm surge barriers are together called as the Europoort Barrier. As well as the MLK, the HK operates fully automatically according to the BOS operating system. The HK closes and opens simultaneously with the MLK to avoid unwanted currents in the harbour of Rotterdam. Nevertheless, the operational team is always present during the closure to monitor the automatic process and are standby to intervene manually if necessary.

The construction of the HK was necessary after the decision to build the MLK. With the MLK alone, the hinterland is not sufficiently protected against flooding because the seawater can then flow around to Rotterdam and Dordrecht. The HK uses two oval-shaped floodgates between four towers to close when predicted water levels exceed +3.00 m NAP in Rotterdam or +2.90 m NAP in Dordrecht. The width of the gates is 98 m and 49 m with a water-retaining height of +3.00 m NAP.

The barrier is designed for substantial water overflow because of the limited height of the barrier. The elliptical gates are robust and efficient for overflow of water. The consequence is that the water levels in the delta can rise during a high-water event, but this influence is relatively small due to the size of the Rhine-Meuse Delta. The leak opening is 47 m<sup>2</sup> (Slomp et al., 2005). The impact of leakage and overflow to the storage capacity will be examined in Section 7.1.2.1.

The water-retaining height of the HK is limited to +3 m NAP by purpose to prevent an increase of flood risk in the harbour (Europoort) and at the Brielse Maas.

The Europoort Barrier is not a continuous dyke and includes high areas which are officially part of the flood defence trajectory. Unlike most other flood defences, the Europoort Barrier does not have to be a high and robust dyke. A certain amount of water may flow over it due to the buffer in the Rhine-Meuse Delta (Keringshuis, 2017). The dykes have a height of +5.70-6.90 m NAP.

The effects of sea level rise to the Hartel Barrier and the dykes of the Europoort Barrier are outside the scope of this research. Water overflow is the only parameter that influences the performance of the MLK and is therefore included in the analysis.

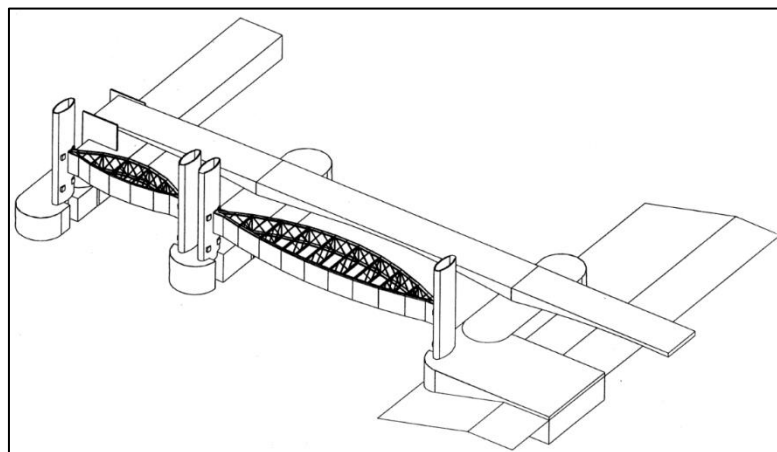


Figure A.24: Schematization of the Hartel Barrier.

## Eastern Scheldt Barrier

The Eastern Scheldt Barrier (OSK) has been built between 1976 and 1986 and is located between Schouwen-Duiveland and Noord-Beveland. It is the largest storm surge barrier in the world with a total length of 8.5 km of which 3 km can be closed. The construction of the OSK was part of the Delta Act, which was established after the Flood of 1953. It concerns a half-open structure that can be shut off by floodgates in the event of a high-water. The overview of the storm surge barrier is shown in Figure A.25.

The primary purpose of this storm surge barrier is to reduce the hydraulic loads for the dykes around the Eastern Scheldt during extreme high-water events. The OSK was considered as a cost-effective measure compared to reinforcing 150 kilometres of dykes.

The decision was made to build an open structure instead of a dam to maintain the tidal activity and sand plates in the Eastern Scheldt. The three sections (enable water passage) are constructed in the deep trenches to prevent disturbing the current channel system in the Eastern Scheldt (Steeneporte, 2014).

The construction consists of 65 pillars and 62 movable steel doors distributed over sections Hammen, Schaar and Roompot.

The floodgates close in advance of high expected sea levels to reduce the hydraulic loads on the dykes around the Eastern Scheldt. This approach should provide sufficient flood safety in large part of the Province of Zeeland. During regular days, the floodgates are raised to enable 75% of the tidal activity in the Eastern Scheldt. The unique saltwater environment, the mussel and oyster cultivation and the tidal activity should be preserved by this design.

### Exceedance frequency and design water level

The OSK was designed to guarantee water safety in Zeeland for 200 years. The barrier has been designed for a sea level from +5.2 m NAP, corresponding to a high-water situation that occurs statistically once in the 4000 years (Rijkswaterstaat, 2007). The height of the barrier is +5.8 m NAP at segments Roompot and Schaar and +5.6 m NAP at Hammen providing space for 40 cm relative sea level rise (sea level + vertical land decline). Latest calculations show peak levels of +5.09-5.14 m NAP for  $T=4,000$ . Chapter 7 analyzes whether the OSK can continue to function at more SLR. Sea level rise leads to more frequent closures when the current closing level of +3.00 m NAP will be maintained. After changing regulations in 2017, the failure probability of the OSK should be maximal 1/10,000 per year (Deltares, 2017a).

### Construction

First, the seabed was improved by dredging the sludge. The sludge was replaced with sand. To ensure that the pillars could stand on a relatively flat seabed another firm surface was needed. A mattress of 200 m wide, filled with sand and gravel, was installed to avoid sand grains from washing away.

The 65 concrete pillars have a height of 30 to 40 meters with a dry-weight up to 18,000 tons. The construction of one pillar lasted roughly 1.5 years. The construction of a new pillar started every two weeks.

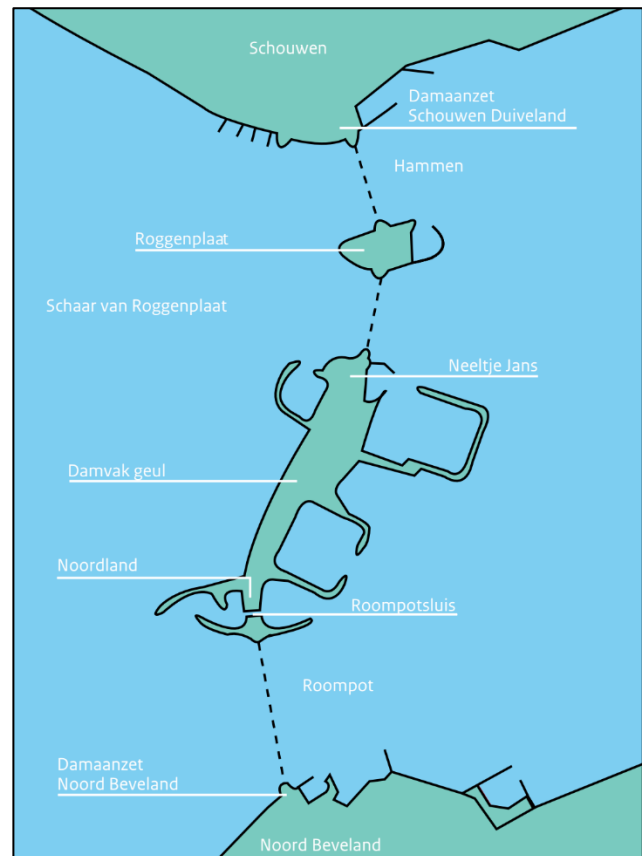


Figure A.25: Storm surge barrier in the Eastern Scheldt (Steeneporte, 2014).

After placement of the pillars on site, the stability was increased by adding sand to the hollow pillars. In addition, the stability was increased even further by adding rocks up to 6,000-10,000kg to protect the threshold bars. These stones are also resistant to maximum flow velocities under the failure of one floodgate.

The 62 floodgates are about 42 m wide and weigh 260-480 metric tons. The height of the floodgates varies between 8 and 12 meters.

Soil protection was applied up to 600 m from the barrier to prevent excavation occurring close to the foundation of the OSK. The soil protection consists of plastic mattresses and concrete blocks. These pits can reach depths of 40 m or more and can undermine the barrier without the emplacement of soil protection on the sea floor. It has been decided to remove excavation pits with a depth of 40 m or more to prevent further undermining of the soil protection (Witteveen+Bos, 2017).

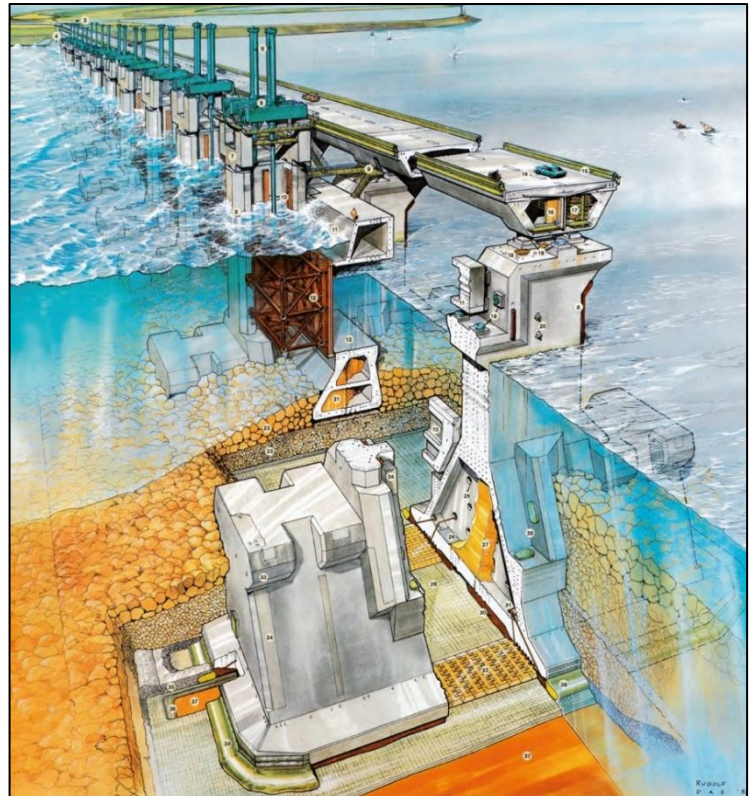


Figure A.26: Overview of the components of the OSK (Steeneporte, 2014).

## Operation

When sea level exceeds +2.75 m NAP, the operation team discusses if a closure is needed. This meeting takes place in the control building located on the barrier (Neeltje Jans). If the sea level forecast on the North Sea exceeds +3.00 m NAP, the team is obligated to close the gates. The total time to close takes 82 minutes, so it is essential to investigate the sea level forecasts in the last hours before a storm. An emergency locking system is operational if other operations fail. When this happens, the doors close automatically when currently measured sea level exceeds +3.00 m NAP (Steeneporte, 2014).

On average once per year it is required to close the floodgates of the OSK. The aim is to achieve a water level of +1 m NAP on the Eastern Scheldt during a closure. This water level will be maintained for approximately 10 hours, as the barrier cannot be reopened until the next low tide. If it is predicted that the next high-water will also be higher than +3 m NAP, the aim is to limit the water level on the Eastern Scheldt to +2 m NAP after the second closure of the barrier. An eventual third closure should limit the water level again at +1 m NAP.

In total, the OSK was closed 27 times (stand 1 February 2018) due to high water levels. The highest sea level during the current operating lifetime of the barrier was on 27 February 1990 (+3.69 m NAP). As a reference, the Flood of 1953 resulted in a water level of +4.55 m NAP at Vlissingen.

## Other dams in the Eastern Scheldt

With the decision to build the storm surge barrier, it was also decided to construct the Philipsdam and the Oesterdam in the Eastern Scheldt. The dams are located on the east side of the Eastern Scheldt and were completed simultaneously with the OSK (Steeneporte, 2014).

Both dams have been constructed for two purposes:

- reducing the size of the tidal basin and tidal difference in the Eastern Scheldt;
- create a shipping lane between Antwerp and the Rhine free of tidal activity.

The hydraulic loads of these dams are computed in Chapter 6.

## Appendix I: Hydra-NL

The water levels, waves and required height of the flood defences are calculated with Hydra-NL. Hydra-NL is part of the Legal Assessment Instrumentation 2017 (WBI-2017). The Test Mode of Hydra-NL will be used in order to include the specific sea level rise scenarios, described in Chapter 5.

The first step is to choose specific locations from the different datasets. More information about the locations and calculation points can be found in Appendix K. Figure A.27 shows the location in Rotterdam (yellow) which is used in the analysis.

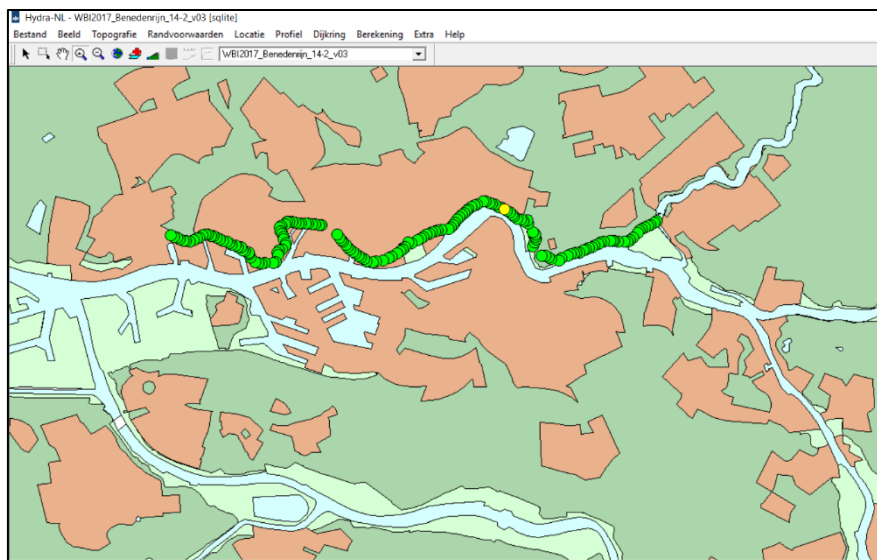


Figure A.27: Calculation points of dyke section 14-2 (Location nr. 5: Rotterdam) Hydra-NL.

It is required to generate a dyke profile before the assessment of the hydraulic loads can be made. A dyke profile contains a cross-section including heights, slopes and roughness of the covering. Relevant datasets of dyke profiles are requested at Rijkswaterstaat and the waterboards to achieve realistic results. Figure A.28 shows the used dyke profile for a primary dyke in Rotterdam (RMD-5).

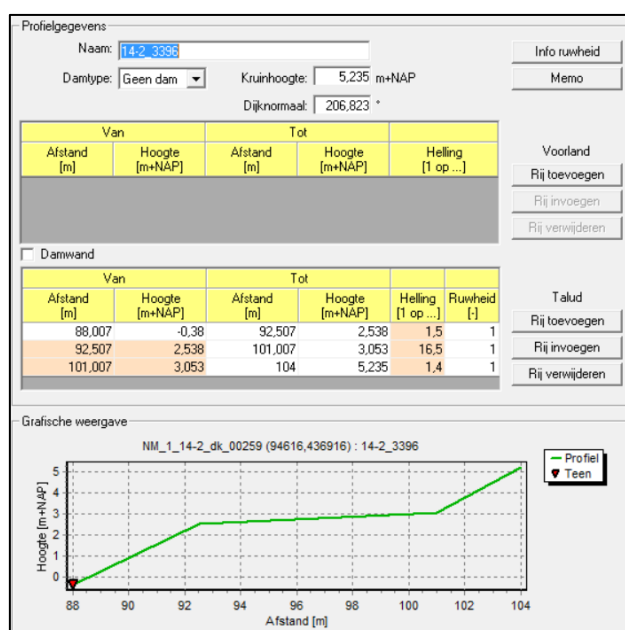


Figure A.28: Dyke profile of dyke section 14-2 (Rotterdam) Hydra-NL.

## General

The “General” tab of Hydra-NL can be used to specify boundaries for integration of the used datasets (e.g. river discharge, sea levels and wind statistics). Furthermore, it is allowed to include SLR on the input screen. Also, the appearance of this tab is depending on the type of water system for which it is being calculated. The used water system for the MLK is “River to sea with storm surge barriers” (Figure A.29). The displayed tab refers to the discharge of the Rhine at Lobith. For calculations with the discharge of the Meuse, a different database is needed.

The variant for the OSK is water system type 'Estuary with barrier'. This tab is slightly different and includes two options:

- increase water level for sensitivity analysis;
- increase water level for maintenance (Dutch: “beheerruimte”).

The increase in water level is an integral increase in the water level at the location used for the sensitivity analysis. The standard increase is 0.1 m which will be used in the calculations. The “beheerruimte” is a water level surcharge that offers space to a variable failure probability of the OSK by a varying the condition of maintenance and repairs.

The screenshot shows the 'Algemeen' (General) tab of the Hydra-NL software. The window title is 'Hydra-NL - Parameters - Dijkvakberekening'. The tabs at the top are 'Algemeen', 'Criterium', 'Gegevensblokken', 'Uitsluitingen', 'Modelonzekerheid', and 'Kettingen'. The main area contains several input fields and checkboxes:

- Laagste piek-waarde afvoertapasie: 750 m<sup>3</sup>/s
- Hoogste piek-waarde afvoertapasie: 25000 m<sup>3</sup>/s
- Stapgrootte piek-waarde afvoertapasie: 250 m<sup>3</sup>/s
- Altoppen afvoertapasie
- Laagste zee-waterstand: 0.8 m+NAP
- Hoogste zee-waterstand: 10 m+NAP
- Stapgrootte zee-waterstand: 0.1 m
- Discretisatiestap afvoertapasie: 12 uur
- Bovengrens windsnelheid: 50 m/s
- Waterstanden en andere belastingniveaus indien nodig repareren lang:
  - Afvoer
  - Zee-waterstand
- Rekenen met klimaatscenario zee-waterstand
  - Zeespiegelrijging: 1.23 m
  - Verhoging waterstand: 0 m
- Berekenen illustratiepunten
- Wegschrijven tussenrijde uitvoer naar bestanden

At the bottom, there are buttons for 'Parameters uit berekening', 'Memo', 'OK', and 'Annuleren'.

Figure A.29: General tab; River to sea with storm surge barriers. Used for the analysis of the MLK.

The screenshot shows the 'Algemeen' (General) tab of the Hydra-NL software. The window title is 'Hydra-NL - Parameters - Dijkvakberekening'. The tabs at the top are 'Algemeen', 'Criterium', 'Statistiek', 'Aanvullingen', and 'Modelonzekerheid'. The main area contains several input fields and checkboxes:

- Hoogste zee-waterstand: 10 m+NAP
- Stapgrootte zee-waterstand: 0.1 m
- Zeespiegelrijging: 0.76 m
- Bovengrens windsnelheid: 55 m/s
- Stapgrootte windsnelheid: 1 m/s
- Verhoging waterstand: 0.1 m
- Waterstanden oplopen met beheerruimte uit database
- Waterstanden en belastingen alleen in windsnelheidsrichting repareren
- Waterstanden en belastingen in windsnelheids- en zee-waterstandrichting repareren
- Wegschrijven tussenrijde uitvoer naar bestanden

At the bottom, there are buttons for 'Parameters uit berekening', 'Memo', 'OK', and 'Annuleren'.

Figure A.30: General tab; Estuary with barrier'. Used for the analysis of the OSK.

## Criteria

The criteria tab offers the choice to select the type of the required calculation. In this study, the water level, significant wave height, hydraulic load level and the rate of overtopping are computed. Water levels and waves are calculated with the use of the models IMPLIC and SWAN. Each criterion has been calculated for many return periods, varying from 10 to 100,000 years and various sea level scenarios.

The hydraulic load level is the minimally required dyke height at a given maximum amount of wave overtopping. This amount is usually 1 to 5 litres per second per meter dyke, depending on the applied coverings and slope. The bandwidth in which wave overtopping can be calculated is between 0.1 l/s/m and 2,000 l/s/m. A larger value cannot be calculated by the model and is calculated with Formula [6].

## Data and statistics

The statistics tab is about the data sets used in the probabilistic model. The datasets agree with WBI-2017. The datasets include statistical uncertainty in order to estimate conditions and hydraulic loads for very long return periods. Statistical uncertainty is explained in more detail in “Uncertainty.” It is often assumed that design conditions only occur in the winter half-year. The datasets are also based on the winter period and different datasets are needed for the summer. Therefore, the sum of the data blocks is 180 days per year.

In the calculation of the closing frequency of the storm surge barriers with sea level rise, the results can deviate from reality. This calculation (Section 7.1.6) is only accurate until a SLR scenario of 1 m. Storm surge barriers should also close during the summer period by more than 1 m sea level rise, which is not included in the analysis yet. With more than 1.5 m SLR, the barrier must even close during all tides if the closing criteria are not adjusted. Therefore, it is not relevant to determine the closing frequency for a sea level rise scenario of more than 1 m.

### Storm surge barriers

Storm surge barriers are extremely important in determining the hydraulic loads for the dykes behind. Hydra-NL includes the effects of storm surge barriers into the probabilistic model. Therefore, it is required to use the option: “dependent on the failure of storm surge barriers” to compute the hydraulic loads for dykes around the RMD. The failure rate of the Europort Barrier is set on 1/100 per year according to the current reliability of the MLK.

Figure A.31 shows the input screen of Hydra-NL for the dependency of the Maeslant Barrier (MLK) and the Hartel Barrier (HK). The predicted sea water level is determined using the normal distribution function. The projected high-water events are based on an analysis of the water statistics between 1990 and 2004. It was determined that the average deviation in the water level projections at Hoek van Holland was  $\mu = -0.067$  m with a standard deviation of  $\sigma = 0.12$  m (Kroos, 2006). Hydra-NL assumes a deviation of  $\mu = -0.09$  m and  $\sigma = 0.18$  m which are based on a previous dataset (Kroos, 1999). It is advised to use the prevailing deviation for the sea level at Hoek van Holland (Deltares, 2017c). This implies that the water level predictions at the MLK are on average 9 cm lower than the actual maximal high-water levels during extreme storms. The option to select the dependency of the storm surge barriers is not possible for the Eastern Scheldt Barrier (OSK).

The failure rate of the floodgates of the OSK is calculated by changing the datasets of the scenarios. For the calculation of a 100% reliable OSK, the possibility of 0 failing floodgates is set on 1 and all other scenarios on zero. The likelihood of 62 failing floodgates is set on 1 and all other scenarios on zero to assess the effect to the water levels on the Eastern Scheldt during a non-closure.

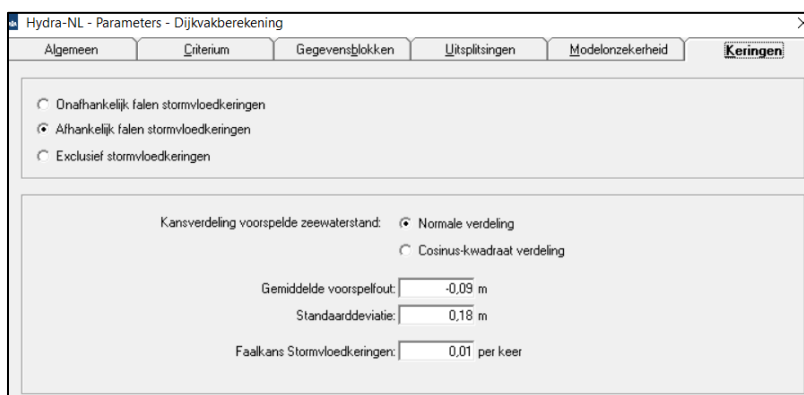


Figure A.31: Barrier tab of the Europort Barrier in Hydra-NL.

### Uncertainties

There are two types of uncertainties which are natural variability and knowledge uncertainty. The natural variability is the chance of occurrence of a particular hydraulic load. Natural variability is included in Hydra-NL. Knowledge uncertainty is not included in previous assessment rounds but is very important.

The knowledge uncertainties are explicitly included in WBI and can be subdivided into statistical uncertainties and in model uncertainties.

Statistical uncertainties are related to the statistical reliability of the estimate and choice of probability distributions that must describe the threats, including the distribution parameters. This type of uncertainty is the result of a limited data and measurements. The probability distributions fitted to this data are extrapolated to make estimations of the water levels and loads for events with return periods of 10,000 years or more ( $T=10,000$ ). Hydra-NL uses extrapolations of statistics of sea levels, river discharges and wind speeds and this has been incorporated into the statistics. It is evident that this extrapolation has a considerable amount of uncertainty.

Model uncertainties concern the uncertainties in model results generated by mathematical formulas of certain physical phenomena, such as flow patterns and wave generation (Witteveen+Bos, 2017). Specifically, this concerns the results of the production calculations with IMPLIC for water levels and SWAN for wave conditions. It is required to use model uncertainties in Hydra-NL to be in accordance with the Statutory Assessment Instrumentation of 2017 (WBI-2017).

Model uncertainties are included in calculating water levels, wave heights and/or wave periods depending on the type of calculation. Calculation of the hydraulic load level uses all three model uncertainties. Figure A.32 shows an output screen with the model uncertainties in Hydra-NL. Calculating with model uncertainty is possible with SQLite databases in the Basic and Test mode. Calculations with model uncertainty and MDB databases are only possible in the Test Mode of Hydra-NL.

The calculations of the MLK and influence will be computed using the standardized model uncertainties of the parameters in the SQLite database. For the OSK and Eastern Scheldt only MDB databases are available, so the model uncertainties have to be added manually. This has been done for all calculations and in accordance with the manual (version 2.3.5) of Hydra-NL.

The model uncertainty of seiches is included for databases on the seaward side of the MLK and HK. The amplitude of a seiche is hard to predict because of the significant uncertainties in the atmospheric and wave parameters. A seiche can cause a considerable increase in the temporary water level which has to be calculated in Hydra-NL.

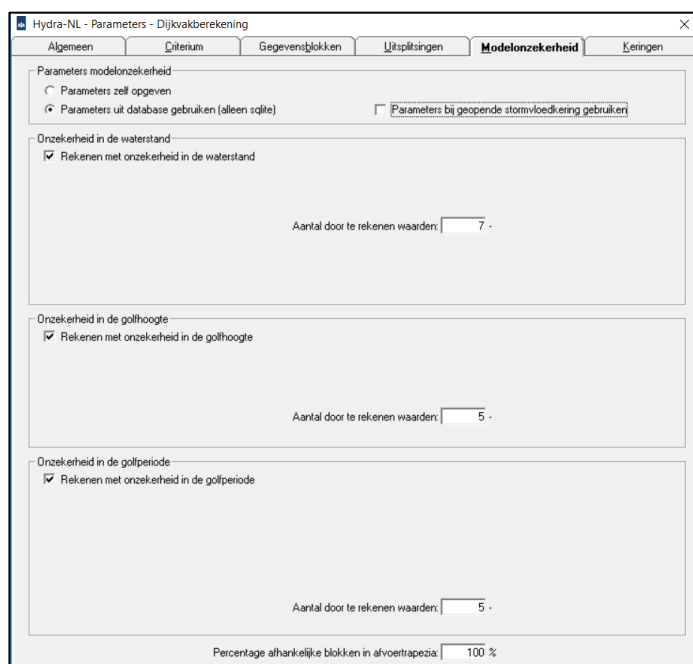
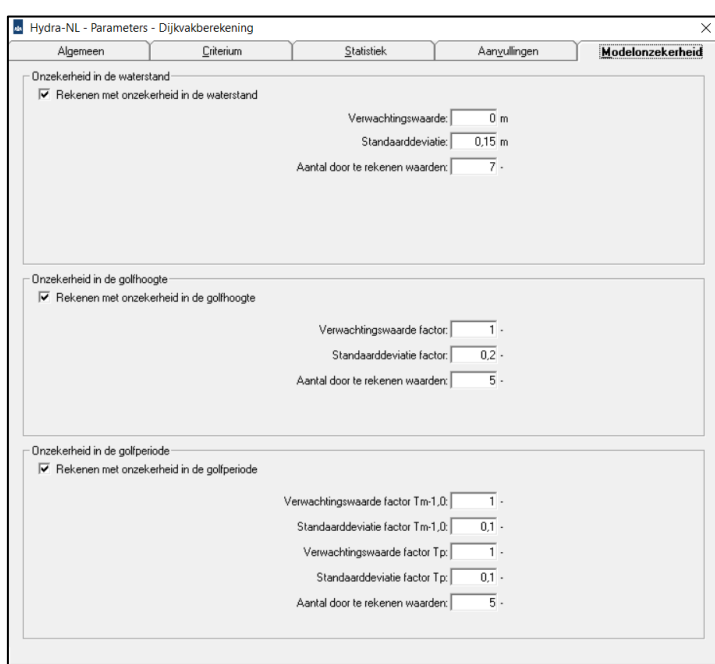



Figure A.32: Model uncertainty tab of the Europort Barrier in Hydra-NL. Figure A.33: Model uncertainty tab of the OSK in Hydra-NL.

## Appendix J: Storm surge, tides and waves

This appendix briefly describes the impact of storm surge, tides, and waves to the hydraulic loads.

### **Storm surge**

Storm surge is a short increase of the local water level above the tide. Storm surge is driven by atmospheric pressure gradients and winds in shallow seas. The water body increases near the shore due to the wind-driven current.

The 1953 flood resulted in a water level of 4.55 m (Vlissingen) originating from 3.05 m storm surge combined with high tide (KNMI, 2017). The coast of the Netherlands is vulnerable to storm surge, because of the bathymetry of the shallow sea floor and the dominant north-western wind direction aimed towards the shore. Despite, it is not projected that future climate change will significantly increase storm surge in the North Sea (KNMI, 2014). Also, according to the KNMI, the expectation is that the number of storms will not change much for the Netherlands. Furthermore, it is considered unlikely that the storm formation for the Dutch coast will increase substantially over the course of this century (Ministry of Housing, 2009). Sterl et al. expect increasing wind speeds from the southwest, but this has no consequence storm surge for the Dutch coast (Sterl, van den Brink, de Vries, Haarsma, & van Meijgaard, 2009).

These conclusions are the main reason why WBI-2017 did not change storm surge estimates in the long-term perspective.

Still, there are measurable changes in wind velocity at a larger area. The wind velocity increased between 1950 and 1990 in the Northern hemisphere (IPCC, 2014). However, this increase has mostly been overridden by recent decreases. According to the Intergovernmental Panel on Climate Change (IPCC), an increase of greenhouse gases in the atmosphere will probably boost temperatures over most land surfaces. The warming surfaces might increase the intensity of storms, with higher wind speeds (IPCC, 2014). This uncertainty might increase the estimates of extreme sea levels in the future, but this is currently not included in the WBI-2017 analysis. On the other hand, sea level rise may possibly have a negative contribution to storm surge because the local water depth may increase.

Lowe et al. (2009) suggested that extreme sea levels have changed over the past in England. However, there is no observational evidence for regional trends in storm surge frequency or magnitudes over last decades (Lowe et al., 2009). Nevertheless, it may be expected that the wind speed of storms increases to a small extent which could increase storm surge. UK climate projection UKCP09 tried to observe a change in storm surge height. They found a maximal annual increase of less than 0.9 mm/year in storm surge for 2, 10, 20 and 50-yr storms. It is complicated to estimate future storm surge, but it is not projected to increase by more than 9 cm around the coast in England in the year 2100 (Lowe et al., 2009). However, using global climate models combined with high-end estimates of the increase of storminess around the UK might lead to an increase of 0.2-0.95 m storm surge for Thames estuary (Lowe et al., 2009). Important to note is that this value is only applicable in the H++ scenario for storm surge.

To conclude, there is significant uncertainty in the future storm surge since it is uncertain if climate change increases the intensity of storms in the North Sea. Lowe et al. (2009) project a small increase in storm surge with a large uncertainty range for the coast around England. The KNMI does not expect significant storm surge changes in the Netherlands by climate change and sea level rise. For this reason, probabilistic model software (Hydra-NL) does not include an increase in the storm surge in the year 2100.

### **Tides**

Tides are temporarily sea level changes caused by the gravitational forces exerted by the Moon and the Sun and the rotation of Earth. The amplitude, location and time of the tide are also influenced by the pattern of tides in the deep ocean, amphidromic points, the bathymetry of the shore and the shape of the coastline (Reddy & Affholder, 2002). In the Netherlands, one tide-cycles is 12 hours and 25 minutes.

If the sun and the moon are on the same side of the earth in line with each other, the attraction they exert on the earth increases. This happens during full and new moon. In the Netherlands, approximately 2 days later, spring tide occurs. During spring tide, the high water is extra high and the low water very low.

The amplitude of the tide is essential for determining the hydraulic load for the storm surge barriers because tides can increase extreme water levels during storms. Especially the combination of springtide and storm surge can result in peak water levels. Hydra-NL uses extrapolations of datasets of the interaction of storm surge and tides to compute peak water levels that for instance, statistically occur once in the 10,000 years.

Tidal activity varies considerably over time due to gravitational forces. In addition, the amplitude of the tide is different along the coast of the Netherlands due to the shape of the coastline and the bathymetry of the shore. Table A.7 shows the amplitudes of the tide at the MLK and the OSK in the year 2017.

Table A.7: Tides and average sea level at Hoek van Holland and the Eastern Scheldt. Values retrieved from Rijkswaterstaat (2018).

Tide station	Hoek van Holland	Eastern Scheldt 4
Flood defence	MLK	OSK
Average sea level (year 2000)	+0.10 m NAP	+0.0 m NAP
High tide (year 2017)	+0.82-1.45 m NAP	+1.12-1.87 m NAP
Low tide (year 2017)	[-81] - [-41] m NAP	[-161] - [-120] m NAP
Max springtide (year 2017)	+1.53 m NAP	+2.05 m NAP

Table A.7 shows that the tidal amplitude at the OSK is significantly higher than at the MLK. It can be concluded that the tidal waves are higher for the OSK than for the MLK. This does not imply that the water levels are higher for the OSK because the water levels are also influenced by storm surge, seiches and gravitational effects. For instance, observations show that the average sea level is 10 cm higher at the MLK (Kwaad, 2013).

Important to note is that storm surge and the tide interacts non-linearly, with the tide having a reducing effect on the total water level. According to Sterl et al. an increasing water depth due to sea level rise does not have an effect on the tidal activity. Only the propagation speed might slightly increase of both storm surge and the tidal wave (Sterl et al., 2009).

## Waves

Waves contribute significantly to the hydraulic loads for storm surge barriers. The height of sea waves can increase if the water depth increases during storm conditions. The precondition where waves break and lose energy is the following:

$$\frac{H}{h} = 0.6 \text{ a } 0.8 \text{ (depth criterium)}$$

H: wave height [m]

h: depth [m]

It is expected that the seabed will also change when the sea level rises, but to a less extent as sea level rise. As a result, the potential maximal wave height increase resulting in an increased load on the barrier during extreme storm events. This is also included in the Hydra-NL model. In this probabilistic model, the wave height increases with a heavier storm, but also with sea level rise. Furthermore, climate change may influence the wind speed and direction. In general, there is low confidence in projections of future storm conditions and the in predictions of ocean waves (Church et al., 2013). The expectations of waves at the Dutch shore are similar to storm surge, where no significant change is expected (Sterl et al., 2009).

## Appendix K: Test locations and safety standards

This appendix gives a description of the locations which are calculated by Hydra-NL. Furthermore, this appendix describes the applicable safety standard for each location according to the WBI-2017 standards. The hydraulic loads at all locations are presented in Chapter 6.

### Test locations

The focus of this study is on the remaining lifetime of the MLK, OSK for different sea level scenarios. In addition to the assessment of the storm surge barriers, the hydraulic loads for dykes in both estuaries should also be determined. After all, these both storm surge barriers have the function to protect the hinterland against high water levels from the sea, resulting in reduced hydraulic loads for the dykes in the temporarily closed estuary. The entire scope can be divided into four areas:

- Maeslant Barrier
- Rhine-Meuse Delta (influenced by MLK)
- Eastern Scheldt Barrier
- Eastern Scheldt (influenced by OSK)

#### **Maeslant Barrier**

Different locations will be assessed on the seaward side of the MLK in order to determine the hydraulic loads and effects for this storm surge barrier. The locations of the used calculation points are visualized in Figure A.34. The locations are labelled as MLK-1 to MLK-4, depending on location number in the figure. It is important to understand the used model and statistics in terms of water level and waves. The sea level can be different over the locations during extreme storm events ( $T=30,000$ ). Waves will be lower in the port of Rotterdam. On the other hand, the shape of the harbour of Rotterdam triggers the occurrence of seiches. A seiche can increase the peak water level in front of the closed barrier as result of the reflecting waves in the port.



Figure A.34: Test locations (MLK-1 to MLK-4) to determine hydraulic loads for the MLK (Hydra-NL).

#### **Rhine- Meuse Delta**

The Rhine-Meuse Delta (RMD) is a large estuary in Rotterdam and Dordrecht. Water levels fluctuate continuously in this estuary due to the tidal activity and the supply of water from the rivers. If the MLK and the Hartel Barrier (HK) close during storm events with an expected water level of 3.0 m NAP in Rotterdam or 2.9 m NAP in Dordrecht, the estuary will change into a closed basin. This basin will be filled by river water and by leakage through both the MLK and the HK. The dykes within the RMD are designed for this situation but climate change, e.g. sea level rise and more precipitation, may result in increased hydraulic loads for these dykes. In addition, the safety standards have been changed during recent legislative changes. As a result, all dykes have to be re-assessed according to WBI-2017. The hydraulic loads and required crest height are calculated for 7 locations in

the total area. The locations are labelled as RMD-1 to RMD-7. The locations have been carefully chosen, based on flood risk and required safety standard, to make an impression of the total Rhine-Meuse Delta.

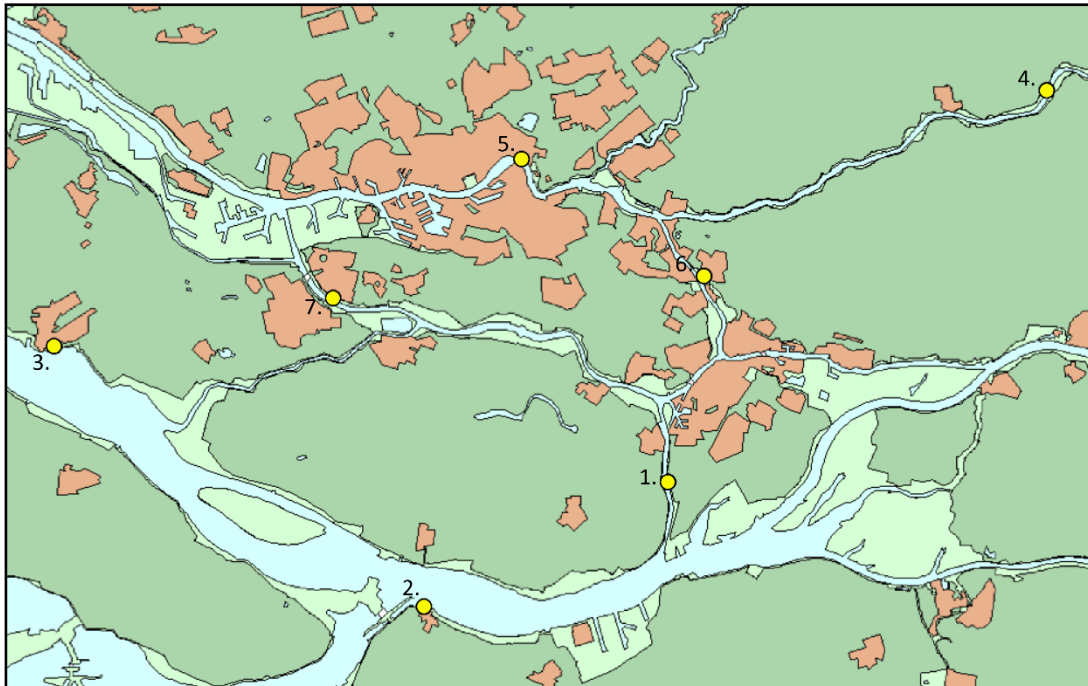


Figure A.35: Test locations (RMD-1 to RMD-7) to determine hydraulic loads for several dyke sections in the Rhine-Meuse Delta (Hydra-NL).

### Eastern Scheldt Barrier

The OSK is an 8km long storm surge barrier whereof 3 segments can be closed with floodgates. The test locations are labelled as OSK-1 to OSK-4. OSK-1 will be used to determine maximum wave height during extreme storm events. The other three locations are located in front of the 3 closable segments of the storm surge barrier. Each location has unique characteristics in bathymetry, wave angle and storm surge. Also, the height of the barrier is varying between +5.6-5.8 m NAP. All parameters are important in calculating the hydraulic loads and eventual water overrun during extreme storm conditions. The volume of water overrun and leakage determines combined the rate of water level increase in the Eastern Scheldt which then determines the required height of the dykes around the Eastern Scheldt estuary.

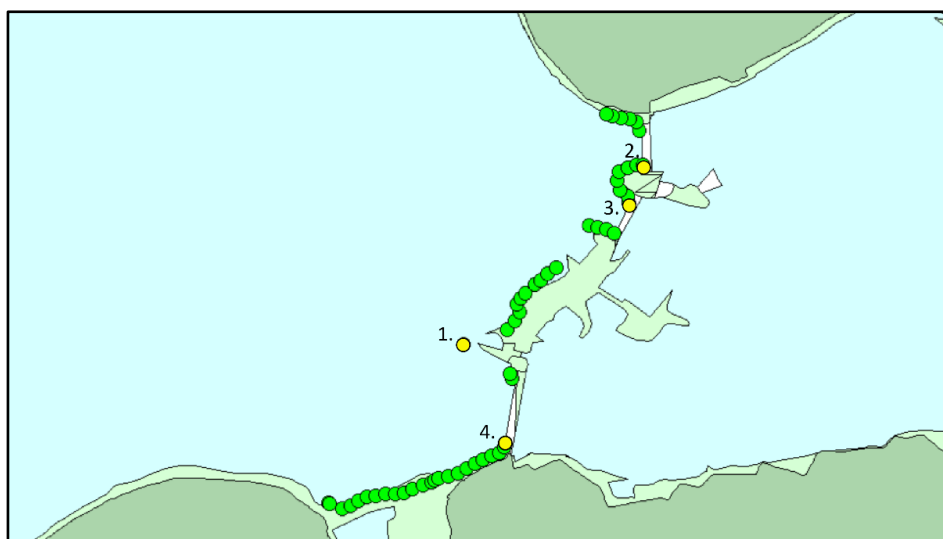


Figure A.36: Test locations (OSK-1 to OSK-4) to determine hydraulic loads for the OSK (Hydra-NL).

### Eastern Scheldt estuary

Twelve locations will be used to test the robustness of the dykes around the Eastern Scheldt to the increasing demands for climate change. The test locations, labelled as OS-1 to OS-12, are distributed over the Eastern Scheldt and include most dyke sections. Also, the safety standards are changed from a failure frequency of 1/4,000 per year to a more tailored approach depending on the chance of flooding and damage.



Figure A.37: Test locations (OS-1 to OS-12) to determine hydraulic loads for most dyke sections in estuary of the Eastern Scheldt (Hydra-NL).

### Limit values and signalling values

As explained in Section 3.2.4.1, each dyke section has a limit value and a signalling value. The signalling value is stricter than the required minimum safety (limit value) and is meant to warn the dyke operator that the flood defence will probably no longer meet the minimum required protection level in the foreseeable future. The focus of this study is primarily on the identification of the current strength of a flood defence compared to the prescribed limit value. If the calculated hydraulic load is too high for a dyke section, the dyke is likely to be rejected in the next assessment round.

The required safety standard for the MLK is increased from 1/10,000 to 1/30,000 per year. The main consequence is that the barrier must withstand an increased hydraulic load. Because of the unique design, the assessment of this storm surge barrier should be determined by probabilistic calculations in combination with expert elicitation.

The MLK is part of the Europort Barrier where today a safety standard applies of  $T=30,000$ . The Europort Barrier also consists of dyke sections 208 and 209. This is shown in Figure A.38. The MLK has a unique function of substantially reducing the hydraulic loads of backward dyke trajectories. The applicable exceedance frequency for the test locations in the Rhine-Meuse Delta is given in Table A.8.

Table A.8: Exceedance frequencies of limit safety values and signalling values for test locations in Rhine-Meuse Delta (Rijksoverheid, 2016)

Location number	Trajectory	Signaling value (T) [year]	Limit value (T) [year]
MLK	208 (MLK)	1:100,000	1:30,000
RMD-1	22-1 (Dordtsche Kil)	1:3,000	1:1,000
RMD-2	34-2 (Willemstad)	1:1,000	1:300
RMD-3	10-4 (Hellevoetsluis)	1:1,000	1:300
RMD-4	15-1 (Lek)	1:30,000	1:10,000
RMD-5	14-2 (Rotterdam)	1:100,000	1:30,000
RMD-6	16-2 (Alblasserdam)	1:30,000	1:10,000
RMD-7	17-2 (Hoogvliet)	1:3,000	1:1,000

Figure A.38 shows the limit safety values of all dyke sections in the Rhine-Meuse Delta.

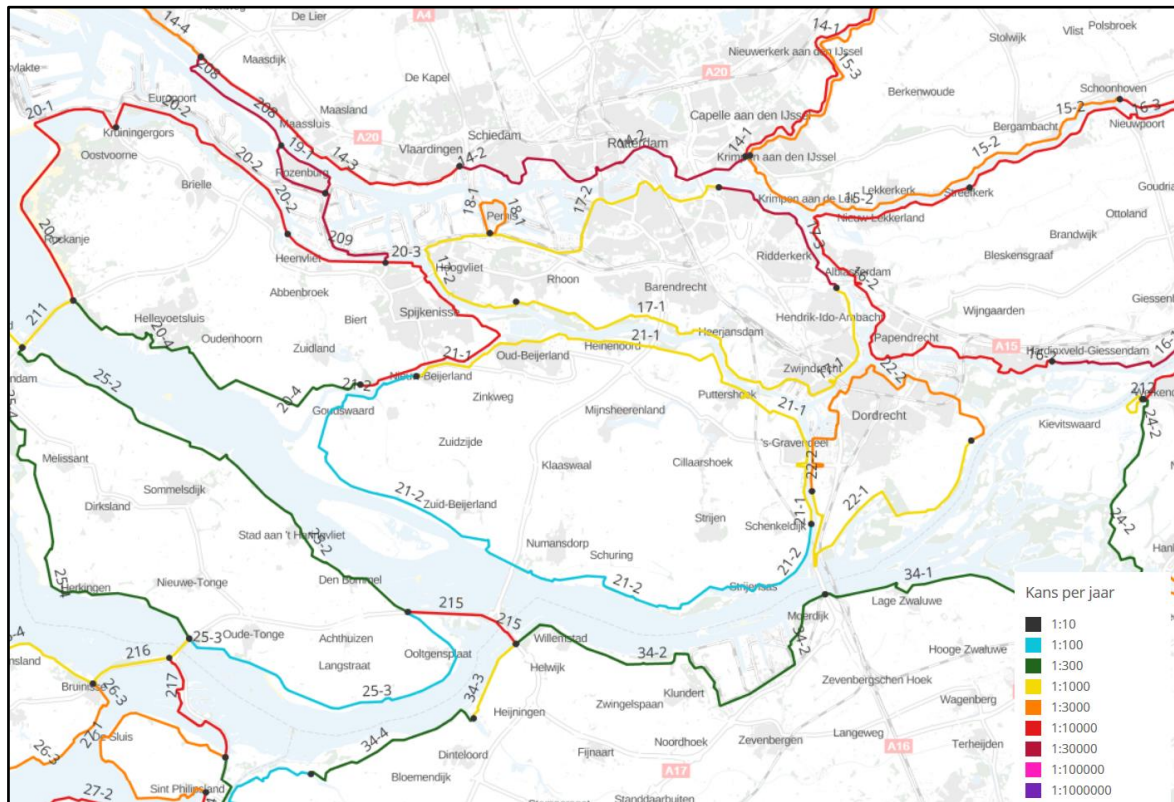


Figure A.38: Safety standards for flood defences in the Rhine-Meuse Delta (Rijkswaterstaat, 2017e).

The required safety standard for the OSK is increased from 1/4,000 to 1/10,000 per year. Also, the maximum exceedance frequencies for the dykes around the Eastern Scheldt have been changed expressively. The old prevailing standard frequency was 1/4,000 per year for the entire area including the OSK. The new safety standard depends on the chance of flooding and the estimated damage. The results are that all dyke sections have an own safety standard varying between  $T=300$  and  $T=10,000$ . Figure A.39 shows the limit safety values of all dyke sections in the Eastern Scheldt. The applicable exceedance frequency for the test locations are given in Table A.9.



Figure A.39: Safety standards for flood defences in the Eastern Scheldt estuary (Rijkswaterstaat, 2017e).

Table A.9: Exceedance frequencies of limit safety values and signalling values for test locations in Eastern Scheldt (Rijksoverheid, 2016).

Location number	Trajectory	Signaling value (T) [year]	Limit value (T) [year]
OS-1, 2	28-1	1:1,000	1:300
OS-3	31-2	1:10,000	1:3,000
OS-4	219 (Oesterdam)	1:30,000	1:10,000
OS-5, 6, 7	27-2	1:10,000	1:10,000
OS-8	27-1	1:3,000	1:3,000
OS-9	217 (Philipsdam)	1:30,000	1:10,000
OS-10, 11	26-3	1:10,000	1:3,000
OS-12	26-2	1:3,000	1:1,000

## Appendix L: Storage capacity and storm duration

The storage capacity is determined by the characteristics of the water system of the delta behind the closed storm surge barriers during a high-water event. This concerns the permissible water level increase rise within the water system multiplied by the surface area. River discharge, leakage and wave overtopping contribute to the incoming water volume in the delta. If the incoming volume of water exceeds the total storage capacity, severe consequences may occur in the hinterland, such as dyke breaches and floods. Both the Maeslant Barrier and Eastern Scheldt Barrier close-off a large water system during a high-water event.

It can be assumed that the risk is too high when the storage capacity in the hinterland is exceeded (Rijkswaterstaat, 2017f).

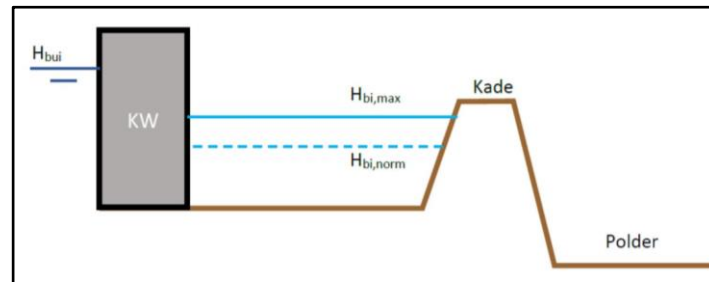


Figure A.40: Schematic representation of the water system and storage capacity (Rijkswaterstaat, 2017f).

The following formula applies to the storage capacity of a water system located within in a temporarily closed water basin:

$$S_c = A * \Delta h_{\text{delta}} \quad [3]$$

$S_c$ : storage capacity [m<sup>3</sup>];

$A$ : the surface area of the open inland water that is connected to the storm surge barrier [m<sup>2</sup>];

$\Delta h_{\text{delta}}$ : permissible water level increase of the inland water [m].

The surface area is the surface of the open water which is affected by closing the storm surge barrier(s). Also, the surface area can change depending on the initial water level in the delta. The water level in the Rhine-Meuse delta changes significantly at various water levels. This principle is schematized in Figure A.41.

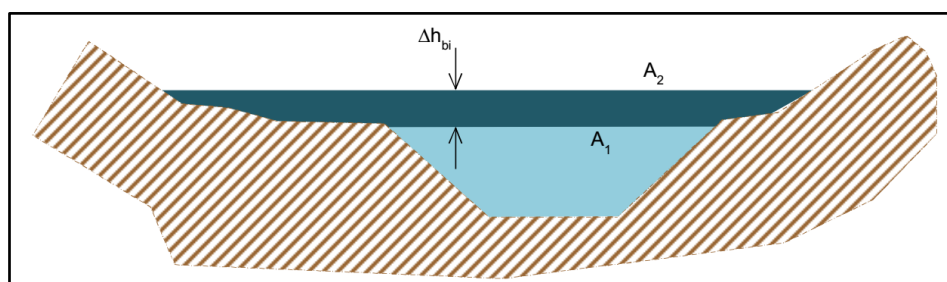


Figure A.41: Changing water surface for different water levels (Deltares, 2015a).

In addition to the storage surface, the maximum permissible water level rise should also be determined to calculate the water storage capacity. This water level increase is directly related to the critical level and the target level in the area. The used formula is:

$$\Delta h_{\text{delta}} = h_{\text{critical}} - h_{\text{average}} \quad [4]$$

$h_{\text{critical}}$ : critical water level (MHW) [m NAP];

$h_{\text{average}}$ : average water level at the start of closing the floodgates [m NAP].

The critical water level is different for various locations within the water system which are addressed in the section below. If the water level exceeds the critical water level, various failure mechanisms to the dykes might occur. The actual water levels in the hinterland are calculated using Hydra-NL in Chapter 6. In addition, several dykes are tested against failure mechanism wave overtopping. However, if the water level exceeds the critical water level, other failure mechanisms such as macro-instability and piping could occur. This section and Chapter 6 identify vulnerable locations during a high-water closure including the effects of sea level rise.

The closing procedure has a crucial role because it determines the average water level at the start of the closure. The average water level in the hinterland before the closure determines the storage capacity. The remaining storage capacity can be calculated according to the following formula:

$$S_{c;r} = A * \Delta h_{\text{delta}} - V_r - V_{wo} - V_l \quad [5]$$

- $S_{c;r}$ : remaining storage capacity [m<sup>3</sup>];
- $V_r$ : incoming volume of river water from the hinterland [m<sup>3</sup>];
- $V_{wo}$ : incoming volume of water overrun and wave overtopping over the storm surge barrier [m<sup>3</sup>];
- $V_l$ : incoming volume of water leakage through the floodgates [m<sup>3</sup>].

A substantial rate of wave overtopping will increase the water level in the delta during a high-water closure. As a result, the load on the dykes in the hinterland will increase, which may cause a failure in specific dyke sections. However, the contribution of overtopping water to the water system of the Rhine-Meuse Delta and Eastern Scheldt is relatively small. However, in combination with leakage and river discharge, exceeding the storage capacity is a critical factor that contributes to the occurrence of various failure mechanisms. If the water system of dykes and storm surge barriers does not meet the boundary conditions, it can be expected that the risk of the occurrence of one or more failure mechanism(s) is significant. Subsequently, it can be considered whether the dykes need to be reinforced or whether the storm surge barriers need to be adjusted.

In addition to the mentioned factors, the following other aspects can also affect the water level and therefore the storage capacity behind a storm surge barrier:

- storm surge in the delta; the local water level in the delta can be influenced by wind variations, which may cause that the critical water level is reached earlier or later than expected;
- impoundment of river water; in case of significantly high river discharge, the water level can increase locally depending on the shape or the storage basin (Deltares, 2015a);
- tidal wave and translation wave; the timing and the closing speed of the storm surge barrier is decisive to the extent the tidal wave temporarily influences the water levels in the delta. Also, closing the floodgates result to a translation wave (backwater effect) which propagates through the basin.

As a result of the influencing factors above, it can be calculated in which situations the storage capacity will be exceeded during high-water events. The water level in combination with waves determine the hydraulic loads for the dykes in the hinterland. The hydraulic loads are calculated in Chapter 6 for various dykes during a closed storm surge barrier, using program Hydra-NL.

This program includes extreme sea level, sea level rise, river discharge, the failure rate of the storm surge barrier, closing procedure, leakage and wave overtopping of the barriers. The outcome indicates that the effects of increased wave overtopping over the top of the storm surge barrier due to sea level rise will be relatively limited. However, this will be validated in Chapter 7 using the specified Formulas [3,4,5] above.

## Duration of storm and closure

It is essential to estimate the duration of a high-water event to be able to project the water level increase in the closed delta. An extreme storm ( $T=10,000$ ) result probably in a closure of the storm surge barriers during two tidal maxima. Figure A.42 shows an example of one storm event of 35 hours, whereof the extreme high-water event last roughly 20 hours. Furthermore, the closure in 2007 (Appendix Q), which lasted 18 hours can be taken as a modest storm example (estimated return period of 10 years).

The course of the high-water wave and the volume of overtopping is greatly simplified in the model of Hydra-NL. The model uses a maximum high-water block with a duration of 12 hours (Figure A.43). However, an extreme high-water event last probably around 20 hours, with peak water levels which last 3 hours. This calculation will consider a closure of 10 till 30 hours, depending on the high-water situation. A situation with high river discharge and a relatively modest sea level (+3.50-4.50 m NAP) result in a total closure of the MLK of 10 hours. One closure of 20 hours is required for both storm surge barriers during an extreme high-water situation at sea. In this case, the river discharge of the Rhine and Meuse is relatively low. Various situations have been analyzed in Chapter 7.

Sea level rise can significantly extend the closing time leading to the situation that the floodgates cannot close on the low tide (ebb) before the forecasted high-water. In case of more than 1 m sea level rise, the required closing level may not be achieved with a turnaround closure. In order to prevent exceeding the storage capacity, the floodgates should be closed during a previous low tide situation, or a high-water level closure should be maintained. In the case of an early closure, the total closure can be extended to 30 hours. The results are shown in Section 7.1.2.

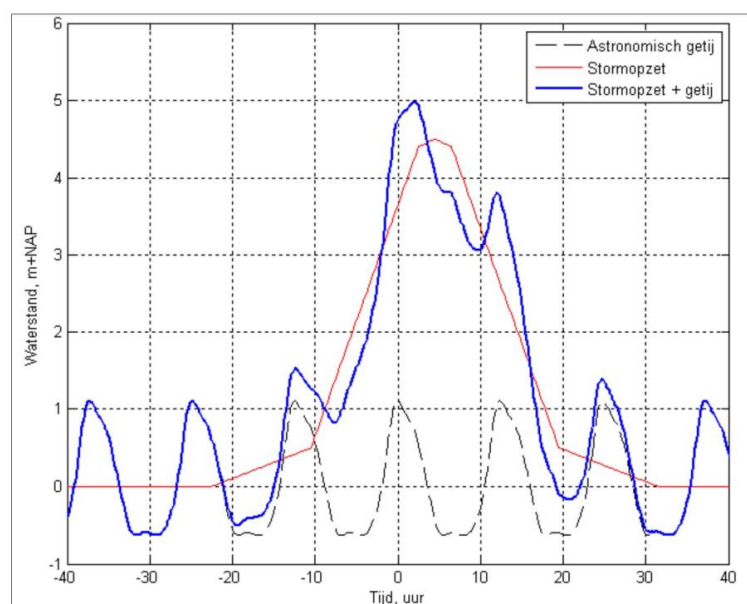


Figure A.42: Example of water level during extreme storm in the NWW (Rijkswaterstaat, 2017d).

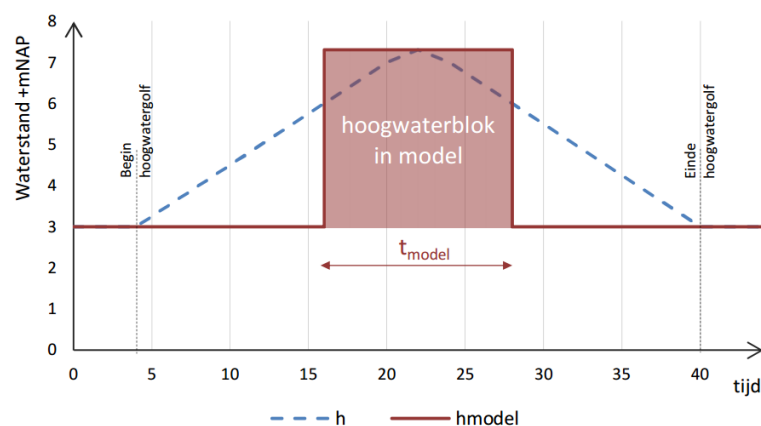


Figure A.43: High-water block in Hydra-NL (Rijkswaterstaat, 2017d).

## Appendix M: Wave overtopping and water overrun

Water overrun can occur over the top of the storm surge barrier during extreme high-water events. This volume of water increases the water level behind the storm surge barriers. In addition, the energy of the overflowing water should be absorbed by the soil protection closely behind the barrier. This is schematized in Figure A.44.

The critical rate of overrun is determined for various sea level situations in front of the MLK and OSK. In reality, the rate of water overrun is not constant due to wave effects. The combination of overrun and wave-overtopping is calculated with the use of Hydra-NL for storm surge barriers and dykes. The limitation of this model is that the volume of overflow above 2 m<sup>3</sup>/s cannot be calculated. However, sea level rise can result in higher values. Therefore, the following empirical formula is used in the analysis:

$$q_c = m_{ol} * 0.55 * \sqrt{-g * (h_{kh} - h)^3} + m_{os} * \sqrt{g * (H_s)^3}; \quad [6]$$

- q<sub>c</sub>: critical rate of overflow per meter width [m<sup>3</sup>/s/m];
- m<sub>ol</sub>: model factor water overrun (generally applies 1.1) [-];
- m<sub>os</sub>: model factor wave overtopping (For deterministic calculations applies 0.13) [-];
- g: gravitational acceleration [m/s<sup>2</sup>];
- h: local water level [+m NAP];
- h<sub>kh</sub>: water-retaining height storm surge barrier [+m NAP];
- H<sub>s</sub>: significant wave height [m].

Important to note is that this formula also encompasses wave overtopping. The calculation of wave overtopping is very complicated and depend on various factors (Meer, 2002). In this simplified calculation, the wave height is computed in a deterministic order (Deltares, 2015a). The used method largely corresponds to the approach of Hydra-NL.

When the rate of overflow is known, it is recommended to calculate the impact on the soil protection. Overflow might affect the granular filter close behind the storm surge barrier (Figure A.44). Formula [7] can be used for vertical barriers such as the MLK and OSK. Both storm surge barriers have a robust soil protection in place behind the floodgates to prevent undermining of the foundation at high flow velocities. The erosion depth as a result of the rate of overflow can be determined by the following empirical formula:

$$y_s = 0.4 * q_c^{0.6} * H^{0.4} * d_{50}^{-0.3} - 0.5 * h \quad [7]$$

Whereof:

- y<sub>s</sub>: erosion depth (>0) [m];
- q<sub>c</sub>: critical rate of overflow per meter width [m<sup>3</sup>/s/m];
- H: hydraulic head [m];
- h: water depth landward side [m];
- d<sub>50</sub>: diameter of grains or stones [m].

Formula [7] is obtained from the schematization manual of WBI-2017 (Rijkswaterstaat, 2017d). The results are presented in the next section.

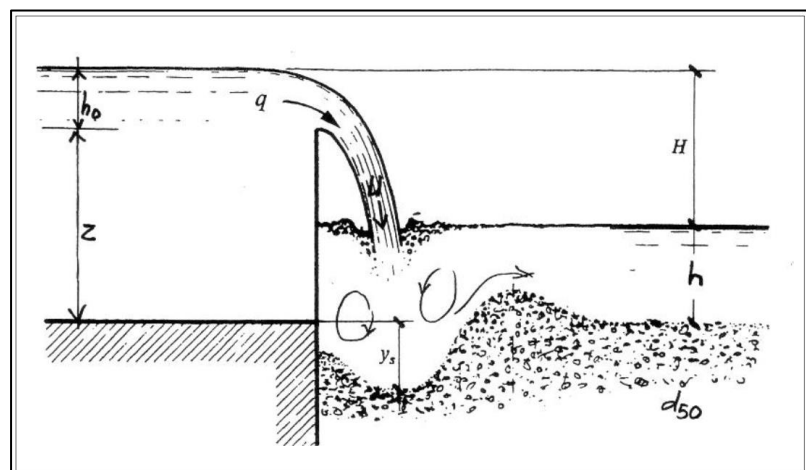


Figure A.44: Schematic representation of overflowing water with excavation pit behind the structure (Rijkswaterstaat, 2017d).

## Results

This section estimates the rate of overflow for extreme high-water events in front of the MLK and OSK based on formula [6]. The rate of overflow is also calculated for all locations (Chapter 6) using Hydra-NL. The limitation of this program is that the upper limit for overtopping is 2,000 l/s/m. The actual overtopping can be much higher during extreme high-water conditions. Therefore, estimations are made based on formula [6]. The calculated values are used to estimate the risk of exceeding the storage capacity and help to determine the erosion depth behind the barrier. These are the two primary failure mechanisms relating to the height of the barrier. The results are used in Chapter 6 and in the Risk Analysis (Chapter 7).

Table A.10: Results of water overrun for the MLK for different sea level scenarios. Values <2 m<sup>3</sup>/s/m are computed with Hydra-NL. Values >2 m<sup>3</sup>/s/m are computed deterministically using formula [6].

Maeslant Storm Surge Barrier								
Test location	MLK-2 crest height: +5.0 m NAP							
Sea level scenario (2100)	Criteria	1/10	1/100	1/300	1/1,000	1/3,000	1/10,000	1/30,000
<b>0.05 m</b> (2023)	Sea level [m NAP]	3.87	4.44	4.65	4.95	5.30	5.70	6.07
	Overflow [m <sup>3</sup> /s/m]	<0.001	<0.001	0.019	0.062	0.478	1.344	≈2.73
<b>0.81 m</b> RCP4.5 (P50)	Sea level [m NAP]	4.50	4.99	5.30	5.66	5.98	6.36	6.74
	Overflow [m <sup>3</sup> /s/m]	<0.001	68.67	0.455	1.225	≈2.36	≈3.62	≈5.05
<b>1.28 m</b> RCP8.5 (P50)	Sea level [m NAP]	4.83	5.43	5.73	6.07	6.39	6.79	7.20
	Overflow [m <sup>3</sup> /s/m]	0.003	680.6	1.377	≈2.58	≈3.66	≈5.19	≈6.92
<b>1.40 m</b> RCP4.5 High-end (P95)	Sea level [m NAP]	4.94	5.54	5.84	6.17	6.49	6.90	7.32
	Overflow [m <sup>3</sup> /s/m]	0.026	900.73	1.650	≈2.89	≈4.02	≈5.62	≈7.45
<b>2.14 m</b> RCP8.5 High-end (P95)	Sea level [m NAP]	5.63	6.19	6.48	6.84	7.20	7.62	8.04
	Overflow [m <sup>3</sup> /s/m]	1.059	≈2.85	≈3.88	≈5.28	≈6.81	≈8.76	≈10.88

Table A.11: Results of water overrun for the OSK for different sea level scenarios. Values <2 m<sup>3</sup>/s/m are computed with Hydra-NL. Values >2 m<sup>3</sup>/s/m are computed deterministically using formula [6].

Eastern Scheldt Storm surge barrier								
Test location	OSK-4 Roompot (crest height: +5.8 m NAP)							
Sea level scenario (2100)	Criteria	1/10	1/300	1/1,000	1/3,000	1/4,000	1/10,000	1/30,000
<b>0.05 m</b> (2023)	Sea level [m NAP]	3.60	4.48	4.80	5.10	5.18	5.44	5.77
	Overflow [m <sup>3</sup> /s/m]	0.08	0.484	0.770	1.134	1.251	1.692	≈3.63
<b>0.81 m</b> RCP4.5 (P50)	Sea level [m NAP]	4.36	5.24	5.59	5.86	5.94	6.20	6.53
	Overflow [m <sup>3</sup> /s/m]	0.262	1.084	1.637	≈3.30	≈3.44	≈4.07	≈5.09
<b>1.28 m</b> RCP8.5 (P50)	Sea level [m NAP]	4.83	5.71	6.03	6.33	6.41	6.67	7.00
	Overflow [m <sup>3</sup> /s/m]	0.475	1.743	≈3.35	≈4.16	≈4.41	≈5.31	≈6.57
<b>1.40 m</b> RCP4.5 High-end (P95)	Sea level [m NAP]	4.95	5.78	6.10	6.41	6.53	6.75	7.08
	Overflow [m <sup>3</sup> /s/m]	0.548	1.956	≈3.48	≈4.37	≈4.72	≈5.56	≈6.88
<b>2.14 m</b> RCP8.5 High-end (P95)	Sea level [m NAP]	5.69	6.57	6.89	7.19	7.27	7.53	7.86
	Overflow [m <sup>3</sup> /s/m] (SLR = 2 m)	1.216	≈4.36	≈5.55	≈6.80	≈7.15	≈8.36	≈9.99

The erosion depth behind the storm surge barrier is calculated by using formula [7]. The erosion depth should be smaller than 0.50 m to meet the requirement for failure mechanism erosion. The outcome of the formula should be positive (>0) to start erosion of the applied stone grading. The critical rate ( $q_c$ ) of overflow is calculated with formula [6] which corresponds to a most extreme situation (2.14 m sea level rise). The maximal water level difference (H) is 4 m for the MLK and 6.2 m for the OSK, corresponding to the maximal acceptable water level according to the design requirements. Three situations are schematized for the required stone size ( $d_{50}$ ) of the soil protection.

The top layer of the soil protection consists of a stone grading of 3,000-6,000kg for the MLK and 6,000-10,000kg for the OSK. This is heavier than the standard gradings according to the NEN-EN-13383 (Deltares, 2015b). Therefore, the nominal diameter can be estimated using the following formula:

$$D_n = \sqrt[3]{M/\rho} \quad [8] \text{ (TU Delft, 2017)}$$

M: mass of the stones [kg];

$\rho$ : specific weight [kg/m<sup>3</sup>].

The median stone diameter ( $d_{n50}$ ) of the top layer is 1.18 m behind the floodgates of the MLK and 1.44 m behind the OSK. Erosion due to water overrun does not occur for extreme rates of overflow of 10 m<sup>3</sup>/s/m for both storm surge barriers. This is because the soil protection must remain intact in case of a failing floodgate, where generally a higher maximum flow rate occurs. The load on the soil protection during a failing floodgate is much higher than the turbulence caused by water overrun which is calculated for the MLK in Appendix P. Erosion caused by overtopping will only occur for smaller grain sizes which are presented in Table A.12.

To conclude, a massive amount of wave overtopping does not affect the soil protection behind the storm surge barriers. The risk of failing soil protection due to overrun and wave overtopping is negligible.

Table A.12: Results erosion depth caused by wave overtopping using formula [7].

Situation	Maeslant Barrier			Eastern Scheldt Barrier		
	I	II	III	I	II	III
$y_s$ : erosion depth (>0) [m]	0	0	3.11	0	0	1.19
$q_c$ : critical rate of overflow [m <sup>3</sup> /s/m]	10.88	10.88	10.88	8	9.99	9.99
H: water level difference (hydraulic head) [m]	4	4	4	6.2	6.2	6.2
h: water depth landward side [m]	17	17	17	6	6	6
$h_0$ : water level above the crest of the barrier [m]	3.04	3.04	3.04	1.73	2.06	2.06
$d_{50}$ : diameter of grains or stones [m]	1.18	0.2	0.01	1.44	1.44	0.45

## Appendix N: Flow through the leak opening of the Eastern Scheldt Barrier

This section calculates the flow velocity through the leak opening of the OSK. The flow rate depends primarily on the water level difference ( $\approx \Delta H$ : energy height difference) between the sea level and the water level of the Eastern Scheldt. The variables that influence the flow rate are summarized in Table A.13. The formulas are obtained from TU Delft (2015) and are also applicable to determine friction through pipelines. It is advised to use Formula [9] because of the energy loss due to the narrow gap between the closed floodgate and the structure.

Table A.13: Technical Information of the OSK.

Energy height loss ( $\Delta H$ )	1-6	m	
Gravitational acceleration	9.82	m/s <sup>2</sup>	
Viscosity sea water	1.354*10 <sup>-6</sup>	m <sup>2</sup> /s	
Total leak opening	1,250	m <sup>2</sup>	
Floodgates	62	-	
Floodgate surface (A)	420	m <sup>2</sup>	
Average gap (D)	0.194	m	Hydraulic diameter
Width floodgates (l)	1.5	m	
Concrete roughness (k)	0.005	m	
contraction coefficient ( $\mu$ )	$\mu=0.6$	[-]	
Nod loss (knik verlies) $\xi_k$	1.1	[-]	2x 60°

The water level difference between the sea level and the water level of the Eastern Scheldt controls the flow velocity through the leak opening. The flow velocity is slowed down due to contraction ( $\xi_c$ ), wall friction ( $\xi_w$ ), bending loss ( $\xi_k$ ) and the energy loss of the outflow ( $\xi_u$ ). The appropriate formula for the energy level loss ( $\Delta H$ ) is Formula [9]. The  $\Delta H$  is known and can be rewritten to determine the flow velocity through the leak opening.

$$\Delta H = (\xi_c + \xi_w + \xi_k + \xi_u) * \frac{U^2}{2g} \text{ [m]} \quad [9] \quad U = \sqrt{\frac{\Delta H}{(\xi_c + \xi_w + \xi_k + \xi_u) * 2g}} \text{ [m/s]} \quad [9a]$$

The contraction coefficient is determined by the shape of the inflow opening. The contraction coefficient is used for sharp edges that reduce the effective inflow opening. The contraction can be calculated using Formula [10]. The water flows through two bends in order to flow around the floodgates into the Eastern Scheldt. The friction coefficient corresponds to 2 bends of 60 degrees. The loss of outflow should also be calculated, which is caused by the slowing down the flow to zero in the Eastern Scheldt lake. This loss is determined by Formula [11] and is equal to one.

$$\xi_c = (1/\mu - 1)^2 \quad [-] \quad [10] \quad \xi_u = (1 - \frac{u_{gap}}{u_{ES}})^2 = 1 \quad [-] \quad [11]$$

The determination of the wall friction requires combinations of different formulas which are [12], [13] and [14].

$$\xi_w = \lambda * \frac{L}{D} \quad [-] \quad [12] \quad \frac{1}{\sqrt{\lambda}} = -2 \log \left( \frac{k/D}{3.7} + \frac{2.51}{Re * \sqrt{\lambda}} \right) \quad [13] \quad \text{(Darcy Weisbach)}$$

$$Re = \frac{uD}{\nu} \quad [-] \quad [14]$$

The results are shown in Table A.14 for a leak opening of 600 m<sup>2</sup> and 1250 m<sup>2</sup>. The outcome is validated by comparison between the leakage of the MLK and the flow velocity for various water level differences.

Table A.14: Flow velocities through the leak opening in the OSK.  $\xi_c=0.44$ ,  $\xi_k=1.1$   $\xi_w=0.42$  and  $\xi_u=1$ . <sup>1</sup>Leak opening 1250 m<sup>2</sup>, <sup>2</sup>Leak opening 600 m<sup>2</sup>.

Water level difference $\Delta H$ [m]	1	2	3	4	5	6
Flow rate [m/s] <sup>1</sup>	2.57	3.64	4.46	5.14	5.76	6.31
Flow rate [m/s] <sup>2</sup>	2.29	3.24	3.97	4.58	5.12	5.61

## Appendix O: Forces on the floodgates and ball-shaped joint of the Maeslant Barrier

This appendix gives an indication of the horizontal forces on the floodgates during a high water closure. The vertical forces on the doors have been neglected because they have no influence on the force on the ball joint. Vertical forces on the doors and during wave overtopping can have an effect on the shear stress on the threshold blocks. However, specialists from the operational team have indicated that the vertical pressure on the threshold blocks is negligible.

Table A.15: Input information for calculation of the horizontal forces on floodgates of the MLK.

Design load ball-shaped joint	30,000 ton
Height floodgates	+5.00 m NAP
Depth	-17.00 m NAP
Length (per floodgate)	216 m
Water pressure (p)	$P = \rho gh$
Water force	$\frac{1}{2} \rho gh^2$
Gravitational acceleration	$9.81 \text{ m/s}^2$
$\rho_{\text{sea water}}$	$1025 \text{ kg/m}^3$
$\rho_{\text{fresh water}}$	$1000 \text{ kg/m}^3$
Uncertainty factor [ $\gamma$ ]	$\gamma = 1.2-1.5$ (20-50%)

The total length (432 m) of the water-retaining part of the floodgates is considerably more than the width of the river (360 m) because of arc-shaped doors. Saltwater with a density of  $1025 \text{ kg/m}^3$  is assumed on the outside of the floodgates and freshwater on the inside. This is a conservative approach. The difference in density will be significantly smaller because of the exchange of water between both sides.

An additional surcharge of 50% is added for the uncertainty in the hydraulic loads and the strength. Waves can increase the hydrostatic pressure and are part of the uncertainty factor. Furthermore, it is not sure whether the ball joint actually can withstand the design load of 30,000 tons. A total surcharge of 20% should be sufficient if it appears that an uncertainty factor has already been included in the design of the joint.

Figure A.45 and A.46 show a schematization of the horizontal forces exerted on the doors. It is stated in the design handbooks that the barrier is designed to withstand a water level difference of 4 m which is presented in Figure A.45. Figure A.46 features a higher sea level that might occur after significant SLR. Water overrun increase the hydrostatic pressure on the floodgates which is visualised in Figure A.46.

The water level in front of the barrier reduces during large volume of water overrun, which reduces the hydraulic load of the floodgates. However, this is not included in the calculation.

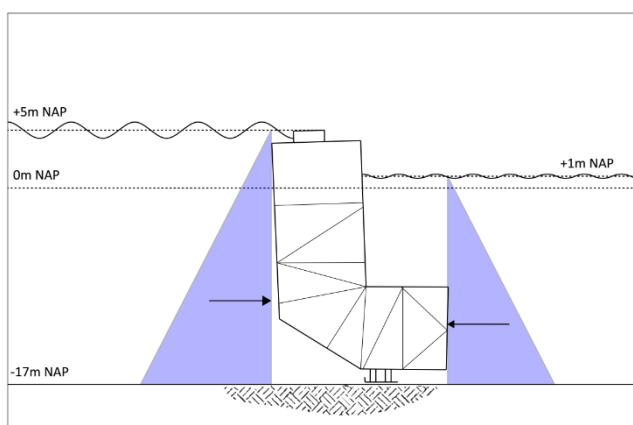


Figure A.45: Schematic view of the horizontal forces on the floodgates without water overrun.

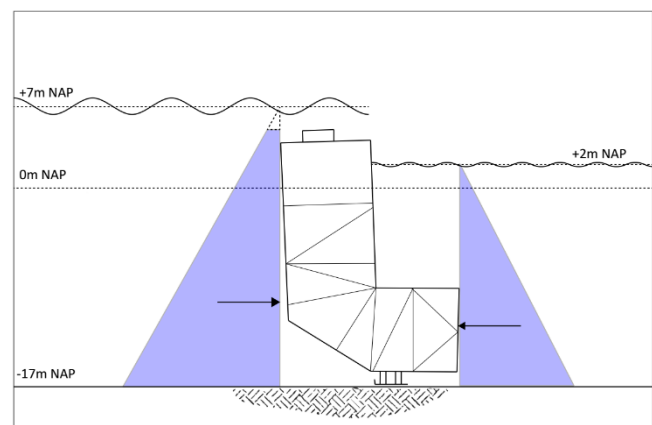


Figure A.46: Schematic view of the horizontal forces on the floodgates including water overrun.

## Results

The net horizontal loads on the ball-shaped joint are shown in Table A.16 for various water level situations.

Table A.16: Horizontal load on the floodgates of the MLK for different water levels. The safety margin (%) and uncertainty factors  $\gamma=1.2-1.5$  are applied to include uncertainty factors.

Sea level [m NAP]	Inland water level [m NAP]	Difference [m]	Total load on joint [ton]			Acceptable?
			$\gamma = 1.2$	$\gamma = 1.5$	Margin	
3.0	0.0	3.0	31,654	39,567	56.04%	Yes
4.0	0.0	4.0	42,647	53,309	40.77%	Yes
5.0	1.0	4.0	45,022	56,277	37.47%	Yes
5.0	0.0	5.0	54,178	67,722	24.75%	Probably
5.5	1.0	4.5	50,921	63,651	29.28%	Probably
5.5	1.5	4.0	38,455	57,683	35.91%	Yes
6.0	2.0	4.0	47,141	58,926	34.53%	Yes
6.0	1.5	4.5	52,045	65,057	27.72%	Probably
6.5	1.5	5.0	57,944	72,431	19.52%	Probably
6.5	2.0	4.5	53,040	66,300	33.33%	Probably
6.5	2.5	4.0	48,004	60,005	26.33%	Yes
7.0	1.5	5.5	63,844	79,805	11.33%	No
7.0	2.0	5.0	58,938	73,673	18.14%	Probably
7.0	2.5	4.5	53,903	67,379	25.14%	Probably
7.0	3.0	4.0	48,736	60,920	32.31%	Probably
7.5	2.5	5.0	59,802	74,753	16.94%	Probably
7.5	2.0	5.5	64,837	81,047	9.95%	No

## Appendix P: Calculation flow velocity and stone grading of the Maeslant Barrier

The floodgates of the MLK and OSK can partially close during a high-water event. This results in a high flow velocity which exerts a peak load on the soil protection close behind the floodgates. This is visualized in Figure A.47. The top layer of the soil protection behind the Maeslant Barrier consists of a stone grading of 3000-6000kg.

Future sea level rise increases the peak sea level during a storm event, which results in higher flow velocities and increased loads on the soil protection. This appendix assesses the current stone grading for the increased hydraulic loads.

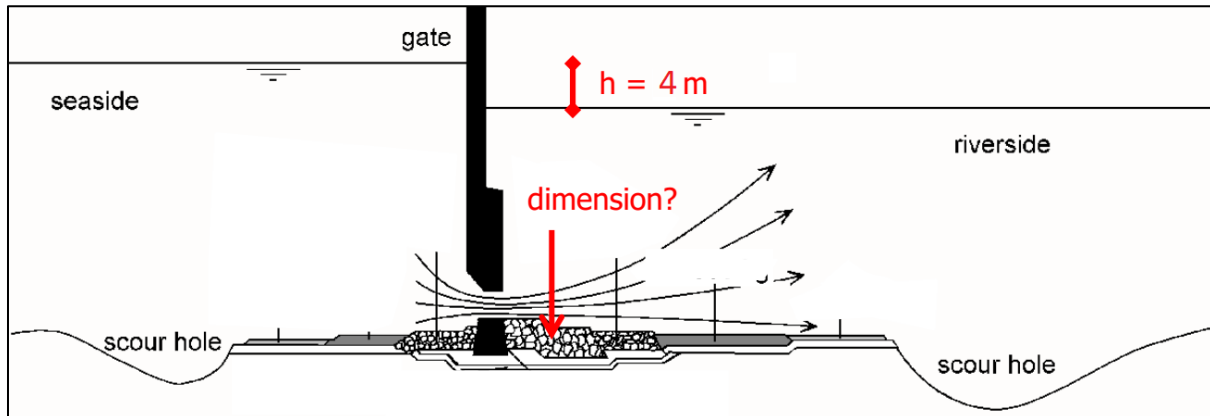


Figure A.47: Example of the flow stream under a partially closed floodgate during a high-water event (TU Delft, 2017).

First, a first-order calculation will be made using the Izbash Formula [15]. This formula is a conservative method and misses elements such as water depth and does not include the definition of the opening gap and the required stone grading. However, Izbash explicitly looks to individual large rocks (TU Delft, 2017). These aspects are discussed later. The Izbash formula is the following:

$$\Delta D_n = 0.7 * \frac{u_c^2}{2g} \quad [\text{m}] \quad [15]$$

- $\Delta$ : relative density of stones and rock ( $\rho_s - \rho_w$ ) [1.65 is used];
- $D_n$ : required nominal diameter of the stones [m];
- $u_c$ : critical flow velocity [m/s].

The flow velocity through the opening gap can be calculated by the following formula:

$$U = \sqrt{\Delta H * 2g} \quad [\text{m/s}] \quad [16]$$

- $\Delta H$ : energy loss (water level difference) [m].

The hydraulic head is the water level difference between both sides of the floodgates under the assumption of a negligible velocity head in the current. The results including the required stone grading are given in Table A.17.

Table A.17: required stone grading for potential situations of the MLK.

	$\Delta H=2.5 \text{ m}$	$\Delta H=3.0 \text{ m}$	$\Delta H=3.5 \text{ m}$	$\Delta H=4.0 \text{ m}$	$\Delta H=4.5 \text{ m}$
$u_c$	7.00	7.67	8.29	8.86	9.40
$D_n$	1.06	1.27	1.48	1.70	1.91
stone weight [kg]	3162	5463	8675	12950	18439
Stone grading [kg]	3,000-6,000	3,000-6,000	6,000-10,000	n/a	n/a

The results show that the maximal acceptable water level difference is 3 m according to Formula [15]. However, the formula of Izbash can be considered as too conservative. It is advised to calculate the stone grading behind hydraulic structures using the manual of Rijkswaterstaat (BWW, 1995).

This manual includes various processes according to the theory of Shields. Furthermore, the required stone size of the top layer can be determined as a function of the distance to the construction. The incorporated processes are visualized in Figure A.48.

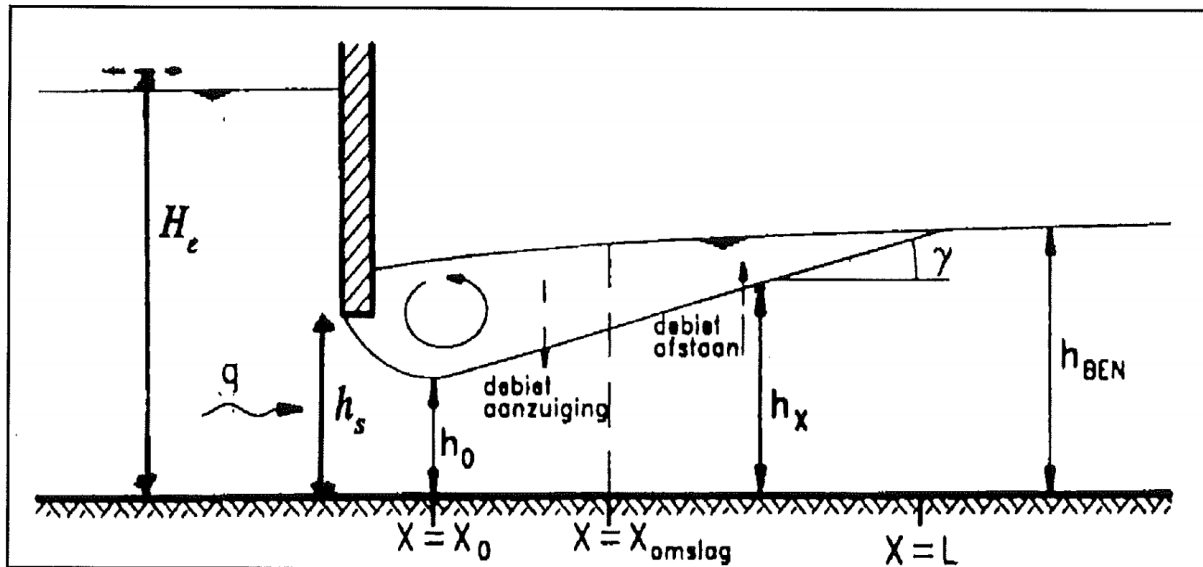


Figure A.48: Flow theory under a weir of a storm surge barrier (BWW, 1995).

Contraction occurs underneath the partially opened floodgates. The contraction coefficient ( $\mu$ ) for the MLK is 0.9 and 0.8 for the OSK. The manual describes 9 steps which help to determine the discharge of water under the floodgates and help to design the required stone size at each point behind the storm surge barrier (BWW, 1995). The highest load on the top layer of the soil protection occurs 4-8 m behind the centre of the floodgate. This point is precisely behind the floodgates where a stone grading of 3000-6000kg is applied. The cross-section of the MLK and the soil protection is shown in Figure A.23 (Appendix H). The primary condition to use the formulas is that  $\frac{h_0}{h_{ben}} < 0.25$  which is the case in the situation of the MLK. Furthermore, the formulas only apply for relatively deep water  $\frac{h_{ben}}{D_n} > 5$ . A correction should be made for the Shields parameter ( $\Psi$ ) for shallow water according to the theory of Ashida (TU Delft, 2017).

The specific discharge ( $q$ ) can be determined using the following formula:

$$q = \mu h_s \sqrt{2g(H_e - h_{ben})} \quad [\text{m}^2/\text{s}] \quad [17]$$

- $\mu$ : contraction coefficient [-];
- $h_s$ : opening gap under the floodgates [m];
- $H_e$ : energy head ( $h_{sea} + \frac{u^2}{2g} \approx 0$ ) (Law of Bernoulli) [m];
- $h_{ben}$ : water level behind the barrier [m].

The velocity head of the upstream water column is assumed to be negligible due to the slow flow velocity caused by the closed barrier. The velocity head is roughly 0,20 m during an open barrier ( $u_{tide} \approx 2$  m/s). Therefore, the formula can be rewritten using:

$$\Delta H = H_e - h_{ben} \quad [\text{m}] \quad [18]$$

The required diameter of the stones ( $D_n$ ) can be calculated by using a derived formula of Shields:

$$D_{nx} = \frac{K^3 u_x^3}{\Delta^{1.5} 25^3 h_x^{0.5} \psi^{1.5}} \text{ [m] [19] (BWW, 1995).}$$

K: constant stability factor of the construction geometry [m]  
 $\Psi$ : critical shield parameter [-]

The results are given in Table A.18 for an opening gap of 2 m between the floodgates and the threshold blocks of the MLK. These results will be used to assess the robustness of the current soil grading during partially raising the floodgates during peak water levels.

Table A.18: Flow velocity and required stone grading of the MLK for different water levels.

MLK	$\Delta H=2.5$ m	$\Delta H=3.0$ m	$\Delta H=3.5$ m	$\Delta H=4.0$ m	$\Delta H=4.5$ m
Sea level [m NAP]	4.5	5.0	5.5	6.0	6.5
q [m <sup>2</sup> /s]	12.61	13.81	14.92	15.95	16.91
$u_c$ [m/s]	7.00	7.67	8.29	8.86	9.40
$D_n$ $\Psi=0.032$ ( $\Psi=0.040$ )	0.71 (0.51)	0.93 (0.67)	1.18 (0.84)	1.44 (1.03)	1.72 (1.23)
stone weight [kg]	948 (352)	2,132 (797)	4,354 (1571)	7,913 (2896)	13,484 (4931)
Stone grading [kg]	1,000-3,000 (300-1,000)	1,000-3,000 (300-1,000)	3,000-6,000 (1,000-3,000)	6,000-10,000 (3,000-6,000)	>10,000 (3,000-6,000)

The specific discharge (q) should be multiplied by the width of the (raised) floodgates to determine the total additional volume of water supply to the remaining storage capacity of the hinterland. The results show that a peak sea level of +5.5 m NAP exerts the maximal permissible load on the top layer (3,000-6,000kg) of the soil protection. However, this is under the condition that some movements and distortion of the rocks is prohibited ( $\Psi=0.032$ ).

A water level difference of more than 3.5 m should only occur during extreme situations (T=10,000 or more). This makes it possible to discuss which shields parameter can be used. Some stones will disappear if a value of  $\Psi=0.04$  is used, but it is improbable that the entire soil protection fails during a short-term exceedance. It is allowed to use this shield parameter to assess the chance to collapse of the soil protection (BWW, 1995). Transport will only occur for values for  $\Psi<0.055$  which is not the case in these situations. This modification results that the current soil grading just meets the minimal requirement for a water level difference of 4.5 m.

## Appendix Q: Analysis of historical storms

Appendix Q describes the analysis of the four storm events with the highest measured water levels after the year 1900. First, the closure of the Maeslant Barrier and Eastern Scheldt Barrier will be analyzed during the recent storm in January 2018. This storm resulted to the closure of all five closure of all storm surge barrier in the Netherlands for the first time. Second, analyzing the effects to the water levels during the storm of December 2013 is useful because the MLK did not close. Furthermore, the closures during the storm of 2007 are included in the analysis. Finally, the storm of 1953 is included in the analysis, which resulted in a catastrophe with many casualties and the establishment of the Delta Act. The storm of 1953 had the highest water level ever recorded in Hoek van Holland of +3.85 m NAP. The used data is derived from <https://waterinfo.rws.nl>.

### Closure of the Maeslant Barrier in January 2018

On 3 January 2018, the MLK was closed for the second time in storm conditions. It has been decided to close the storm surge barrier at an expected water level of +2.60 m NAP, similar to the closure in 2007.

It was recommended to test the MLK during storm conditions and to lower the required closing criteria. This reduction increases the likelihood of a closure, which makes it possible to investigate how the barrier functions during storm conditions. Usually, the barrier closes at a predicted water level of +3.00 m NAP at Rotterdam.

The closure started at 14:40 with the horizontal departure of the floodgates and the barrier completely was closed at 16:13. After two hours, it was required to re-open the arc-shaped floodgates. The full scheme of the closure procedure is shown in Table A.19.

Table A.19: Scheme of the closures on 3 January 2018.

<u>Scheme</u>	<u>Proces</u>	<u>realization</u>	<u>Scheme</u>	<u>Proces</u>	<u>realization</u>
	<b>Maeslant Barrier</b>			<b>Hartel Barrier</b>	
T <sub>cl</sub> -8:00	Pre-warning	06:20	T <sub>cl</sub> -6:00	Pre-warning	08:10
T <sub>cl</sub> -4:00	Request stop shipping	10:10	T <sub>cl</sub> -3:10	Request stop shipping	11:00
T <sub>cl</sub> -4:00	Leveling docks	10:10	T <sub>cl</sub> -2:30	Prepare barrier	11:40
T <sub>cl</sub> -3:50	Opening dock doors	10:20	T <sub>cl</sub> -2:20	Prohibition on shipping	11:50
T <sub>cl</sub> -2:00	Prohibition of shipping	12:10	T <sub>cl</sub> -2:10	Close to safe position	12:06
<b>T<sub>cl</sub>+0:00</b>	<b>Closing time (start horizontal departure)</b>	<b>14:40</b>	<b>T<sub>cl</sub>+0:00</b>	<b>Closing time (start closure)</b>	<b>14:40</b>
T <sub>cl</sub> +0:30	Sinking floodgates	15:09			
<b>T<sub>cl</sub> +0:30+1:40</b>	<b>Complete closure</b>	<b>16:13</b>	<b>T<sub>cl</sub>+1:00</b>	<b>Complete closure</b>	<b>15:41</b>
T <sub>fl</sub>	Floating floodgates	18:13	T <sub>sp</sub>	Opening to a safe position	18:00
T <sub>fl</sub> +1:50	Floating completed	19:49	T <sub>sp</sub> +0:30	Safe position	18:27
T <sub>op</sub>	Start opening	19:51	T <sub>op</sub>	Start opening	19:50
<b>T<sub>op</sub> +0:30</b>	<b>Opening completed</b>	<b>20:20</b>	<b>T<sub>op</sub> +0:20</b>	<b>Opening completed</b>	<b>20:20</b>
T <sub>op</sub> +0:50	Allow shipping	20:40	T <sub>op</sub> +0:30	Allow shipping	20:20
T <sub>op</sub> +1:00	Closing dock doors	20:50			
T <sub>op</sub> +1:40	Cancel pre-warning	21:30	T <sub>op</sub> +0:50	Cancel pre-warning	20:40

Figure A.49 shows the water levels at eight locations in RMD during the closure of the MLK and the HK. The most important observations are the following:

- maximal sea level was +2.66 m NAP at the MLK (3-1-2018; 16:00);
- the MLK started to close at a water level of +2.32 m NAP and was fully closed at +2.54 m NAP;
- the maximal water level in the delta was +2.45 m NAP at Rotterdam (3-1-2018; 15:40);

- the high tide wave was largely passed before the barrier has closed. The high-water peak was lower than expected due to a small overestimate of the sea water level forecast. The reduction in maximum water level due to the closing MLK is 5 cm in Rotterdam;
- the high tide reaches Vlaardingen (40 min) and Rotterdam around 50 minutes later than at Hoek van Holland which is similar to a regular tide without storm surge;
- water levels drop significantly after the complete closure of the RMD due to the blocked supply of seawater. The water system was balanced at roughly +1.70 m NAP. Subsequently, the water level rose at a slow rate due to the supply of water from the rivers;
- the river discharge on 3-1-2018 was approximately 2,500 m<sup>3</sup>/s (Waal), 750 m<sup>3</sup>/s (Lek) and 1,150 m<sup>3</sup>/s (Meuse). The calculated water level increase in the delta is 5.1 cm/hour or 10 cm in total. This can be seen at locations Krimpen a/d Lek, Krimpen a/d IJssel and Dordrecht;
- the water levels will drop immediately after the opening at 18:10. The graph also indicates that MLK opens when the sea water level declines below the water level in Maassluis.

Table A.20 shows the peak water levels and the time-lag of the tidal activity during the storm on 3 January 2018.

Table A.20: Peak water levels and the time-lag of the tidal wave during the storm in January 2018.

Location	Closing MLK (3-1-2018)		"Normal" tide (4-1-2018)	
	Water level [+m NAP]	Time	Water level [+m NAP]	Time
Hoek van Holland	2.50	14:50 +0:00	1.97	16:00 +0:00
MLK	2.38 (2.66 after closure due to blocked flow)	15:10 (16:00) +0:20	1.82	16:00 +0:00
Maassluis	2.24	15:40 +0:50	1.84	16:40 +0:40
Vlaardingen	2.44	15:40 +0:50	1.97	16:40 +0:40
Rotterdam	2.45	15:40 +0:50	2.00	17:00 +1:00
Krimpen a/d IJssel	2.33	16:10 +1:20	1.91	17:40 +1:40
Krimpen a/d Lek	2.23	16:20 +1:30	1.85	17:40 +1:40
Dordrecht	1.90	16:30 +1:40	1.66	17:30 +1:30

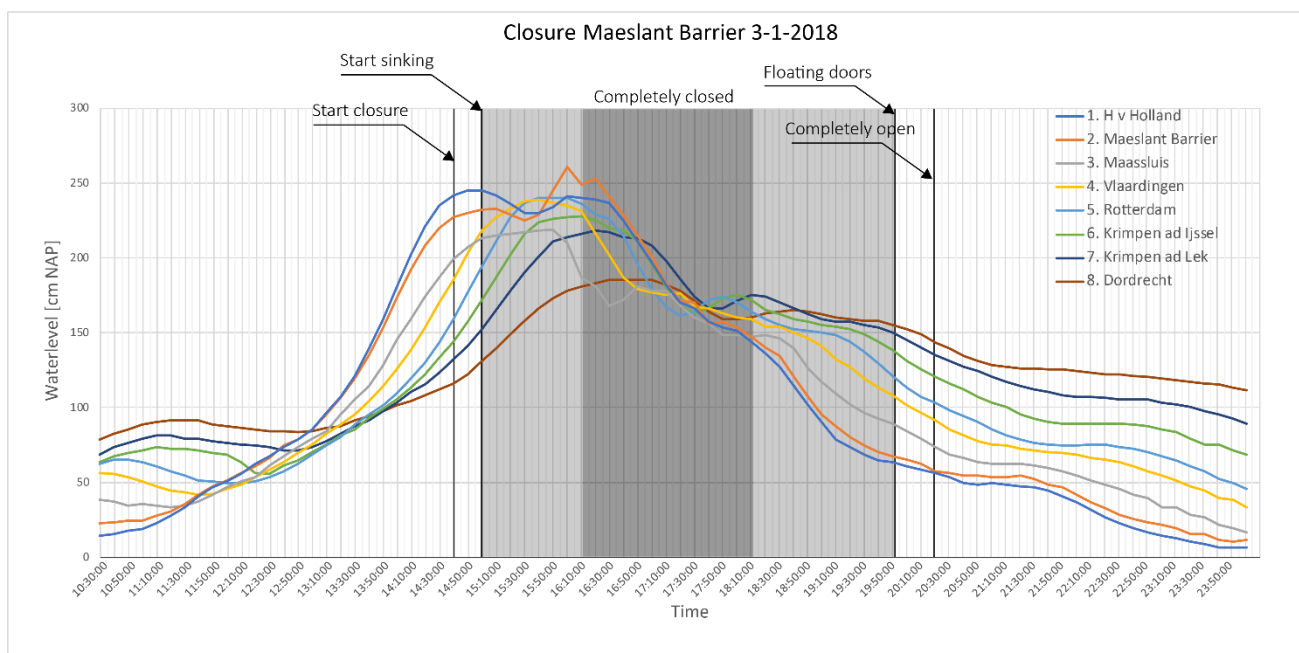


Figure A.49: Progression of water levels in the Rhine-Meuse Delta during the high-water event of January 2018 including the effect of the closure of the MLK.

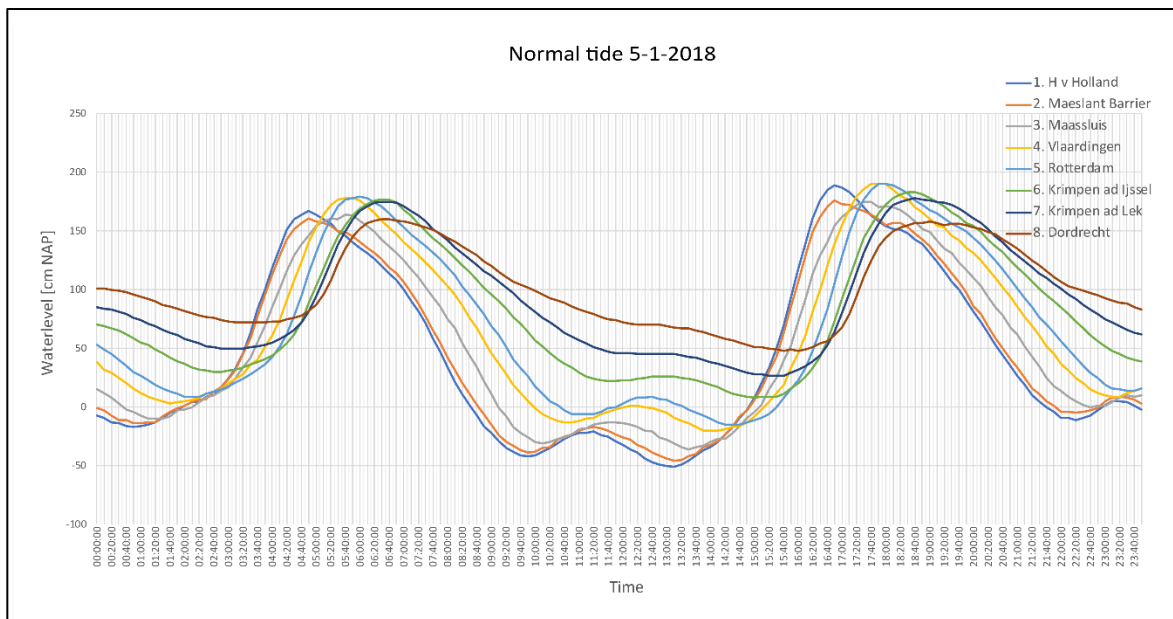


Figure A.50: Progression of water levels in the Rhine-Meuse Delta during normal tide.

Based on the analysis of the results, it can be concluded that the Maeslant Barrier was closed too late for the optimal performance. The high-water almost reached Rotterdam despite the closure of the storm surge barriers. Nevertheless, the closed barrier has blocked a substantial volume of seawater from reaching Dordrecht. Furthermore, the occurred water levels at Hoek van Holland were lower than the water level forecasts. In the end, the peak water level in Rotterdam was slightly lower than +2.60 m NAP.

The barrier should start to close at a water level of +2.00 m NAP according to the closing protocol for these conditions. This follows from the closing criteria described in Appendix H. The criterium is the following:

- *Water level closure* (Dutch: “Peilsluiting”); closure starts at a water level +2.0 m NAP during a river discharge of <math><6,000\text{ m}^3/\text{s}</math>.

According to the criteria, the floodgates had to close at 14:00 due to the exceedance of +2 m NAP measured at the MLK. The delayed closure is further discussed in the risk analysis (Chapter 7).

The delay was in this situation not a problem for water safety but the consequences may be higher if the water level is extremely high. The storm event in January 2007 showed that the water level could rise 2.4 m in just two hours through the tide (Figure A.55).

If a storm results in a water level slightly below +2 m NAP during ebb, the MLK closes not automatically according to the protocol. The closing process takes at least 100 minutes. As a result, the maximum water level of +3.00 m NAP in Rotterdam cannot be prevented under these potential conditions. It might happen that a water level of more than +4 m NAP temporarily occurs at the peak of the tide. Such situations can occur more frequently during accelerated sea level rise. This temporarily peak water levels in the delta cause severe damage to the urban areas in Rotterdam which are not protected by dykes. Furthermore, dykes can also fail due to temporarily exceeding the critical water levels.

The next paragraph determines the loss of the water storage capacity due to the relative late closure of the MLK.

### The flow velocity and of the tide and effect to the Rhine-Meuse Delta

The closure on 3-1-2018 was not very effective in reducing the height of the peak water levels in the Rhine-Meuse Delta. Figure A.51 shows that a large part of the incoming tidal wave reached Rotterdam due to the delayed closure. The water levels in the RMD drop significantly after the complete closure of the Europoort Barrier. This implies that the storm surge barriers still function despite the relatively late closure.

It is also relevant to analyze the volume of seawater that flowed into the RMD before the start of the closure. The flow velocity is much lower than the migration speed of the tidal wave. Subsequently, the loss of storage capacity of the RMD can be calculated due to the delayed closure.

Figure A.51 and A.52 show the modelled flow velocities at the MLK and HK during the storm of January 2018. These results are used to estimate the loss of water storage of the RMD during the closure.

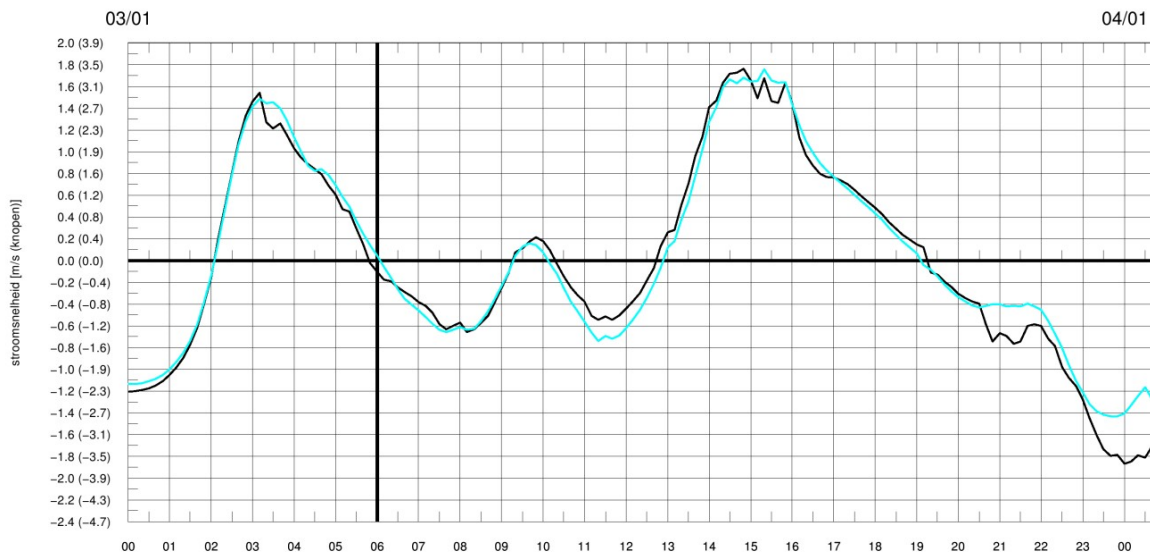


Figure A.51: Flow velocity [m/s] projections at the MLK on 3-1-2018. Closure is not included in the results. Black line: average flow velocity upper 5 m. Blue line: average flow velocity upper 15 m (Port of Rotterdam, 2018).

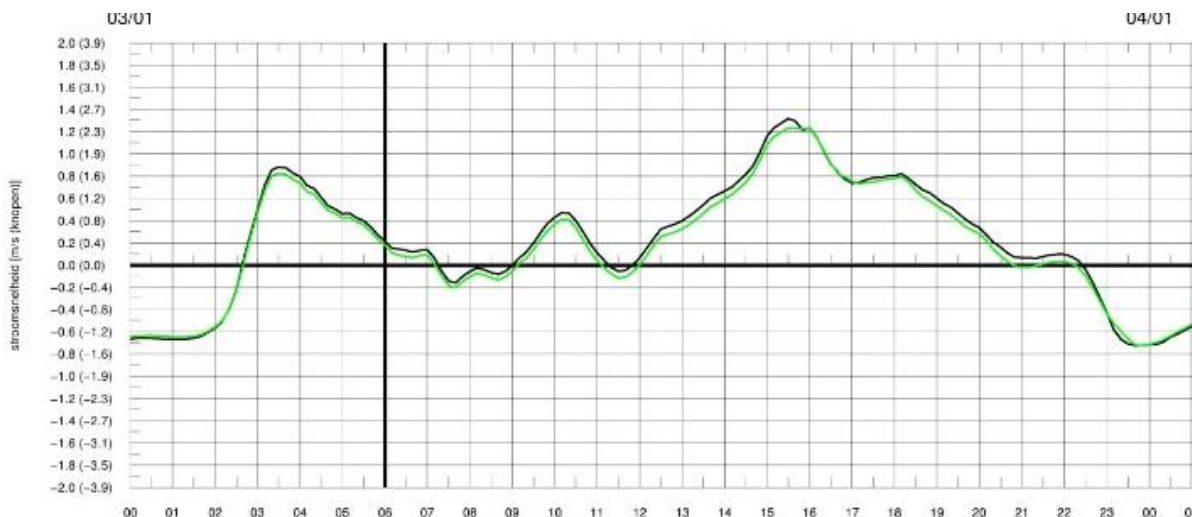


Figure A.52: Flow velocity [m/s] projections at the Hartel Barrier on 3-1-2018. Closure is not included in the results. Black line: average flow velocity upper 5 m. Green line: average flow velocity over total water column depth (Port of Rotterdam, 2018).

The graph shows that the flow velocity was roughly 1.6 m/s in the NWW during the closure of the MLK. The flow velocity at the Hartel Barrier was 1.2 m/s during the closure. The loss of remaining storage capacity in the RMD will be calculated according to the following formula:

$$\Delta h_{RMD} = \frac{((A_{MLK} * U_{MLK}) + (A_{HK} * U_{HK})) * t_{closure} * f_{closed}}{A_{RMD}} \quad [20]$$

$\Delta h_{\text{delta}}$ :	average water level increase in the total Rhine-Meuse Delta [m];
$A_{\text{MLK}}$ :	water flow area of the MLK [m <sup>2</sup> ] (6693 m <sup>2</sup> at +2 m NAP);
$A_{\text{HK}}$ :	water flow area of the HK [m <sup>2</sup> ] (816 m <sup>2</sup> at +2 m NAP);
$U$ :	flow velocity [m/s];
$t_{\text{closure}}$ :	total time to close [s] (140 min on 3-1-2018);
$f_{\text{closed}}$ :	factor of partly obstructing the waterflow during the closure (80%);
$A_{\text{RMD}}$ :	surface area of the Rhine-Meuse Delta [m <sup>2</sup> ] (276-327 km <sup>2</sup> at +1-2 m NAP).

The discharge through the NWW is the primary contributor to the increased water levels in the Rhine-Meuse Delta. The total water level increase caused by the tide before the closure 0.24 m averaged over the total delta. For extreme high-water events, this value is assumed to be 0.30-0.35 m. The results are much lower than the measured water levels in the delta, which are the remainders of the tidal wave. The tidal amplitude occurs temporary and will spread out in the delta.

According to the measured water levels, the closure should have started at 14:10. However, the closure started at 14:40 due to various delays. This resulted in a considerable volume of seawater to flow in the RMD which is not included in the current water storage models. In this period of 30 minutes, 17.7 million m<sup>3</sup> of water flowed into the RMD in addition to the tidal wave. This resulted in a water level increase of 0.05 m within this timeframe. The delayed closure might result in a water level increase of 0.1 m due to the higher flow rate during an extreme storm.

### Closure of the Eastern Scheldt Barrier in January 2018

On 3 January 2018, the OSK was closed due to an exceedance of the closing criteria of a projected water level of +3.0 m NAP. The water levels during this storm were measured at five locations presented in Figure A.53. The maximal water level at sea in front of the storm surge barrier was +3.01 m NAP, measured at 14:00. The floodgates of the OSK closes approximately one hour in advance to limit the water level in the Eastern Scheldt to +1.00 m NAP. The floodgates opened at 18:30 because the sea level at that time was lower than the water level in the Eastern Scheldt. According to the results, closing of the floodgates leads to a considerable translation wave in the closed estuary. Also, the water level in the basin rose by 20-30 cm due to wave overtopping and leakage during the closure of 4.5 hours.

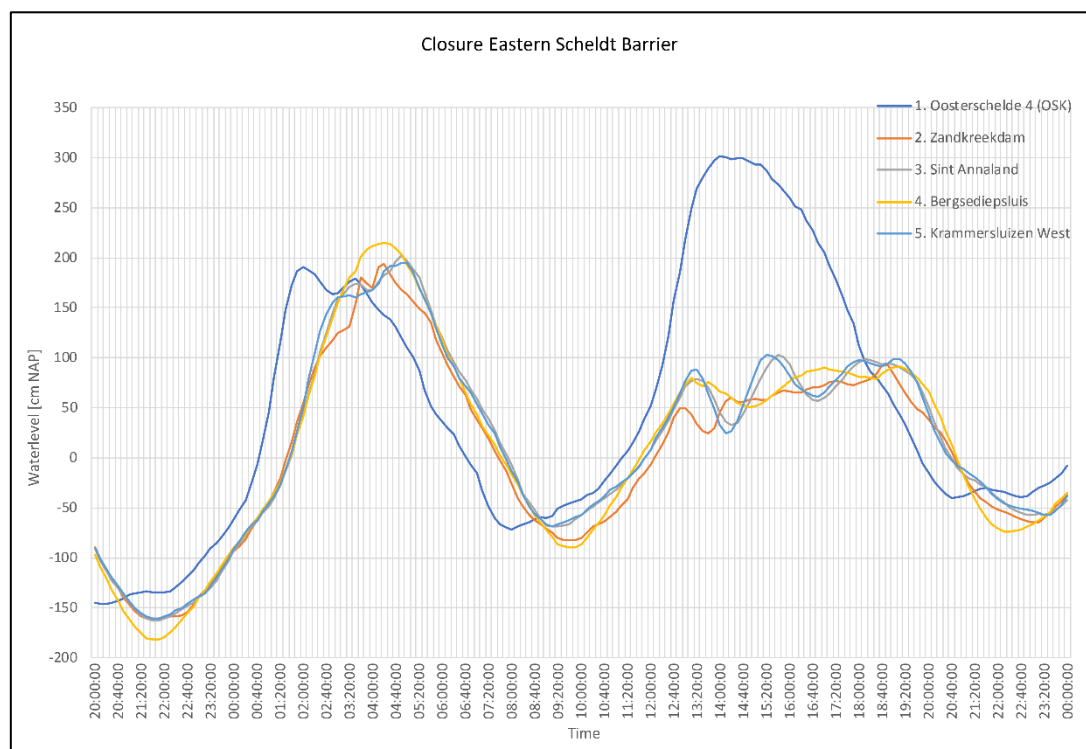


Figure A.53: Progression of water levels in the Eastern Scheldt during the high-water event of January 2018 including the effect of the closure of the OSK.

### Storm event on 6 December 2013

On 6 December 2013, a western storm caused to a high sea level in Northern Europe. In contrast to the Eastern Scheldt Barrier, the Maeslant Barrier was not closed during the storm. The closing requirements for a predicted water level of +3.00 m NAP in Rotterdam and/or +2.90 m NAP in Dordrecht were just not met according to the sea level forecasts.

The water levels are shown in Figure A.54 at eight different locations. This data is derived from (Rijkswaterstaat, 2018). The most important observations are the following:

- the peak sea water level was +3.07 m NAP measured at the MLK (6-12-2013; 05:00);
- the maximal water level in the delta was +2.90 m NAP in Rotterdam (6-12-2013; 05:40),
- the high water peak would have been much higher under persistent storm surge;
- the high-water effects are still noticeable several days after the end of the storm;
- during average tide, higher water level peak in Rotterdam than at sea;
- reduced tidal activity further inland (Dordrecht).

In retrospect, it turned out that the actual water levels in Rotterdam did not exceed the closing criterium of +3.00 m NAP. However, the analysis of the water levels shows that the storm surge decreased by more than 50 cm during the rising tide. It seems unlikely that the weakening of the storm could be predicted that accurately. If the storm surge of approximately 2 m was continued for one extra hour, the peak water level was approximately +3.6 m NAP at Hoek van Holland and +3.5 m NAP in Rotterdam. This is visible in Figure A.54. Before the peak water levels, the difference between ebb and flood is reduced due to the diminishing storm surge. These values are close to the maximum acceptable water level in Rotterdam. It would not have been possible to close the MLK in that timeframe.

The graph clearly shows the delay in tidal activity between the different locations. The flood reaches Rotterdam usually 50 min later than Hoek van Holland. The measured delay in Dordrecht is roughly 2 hours. An inherent consequence of the delayed tidal activity further in-land is a reducing amplitude between the tides. This is visible in the difference between the water levels in Dordrecht and Hoek van Holland.

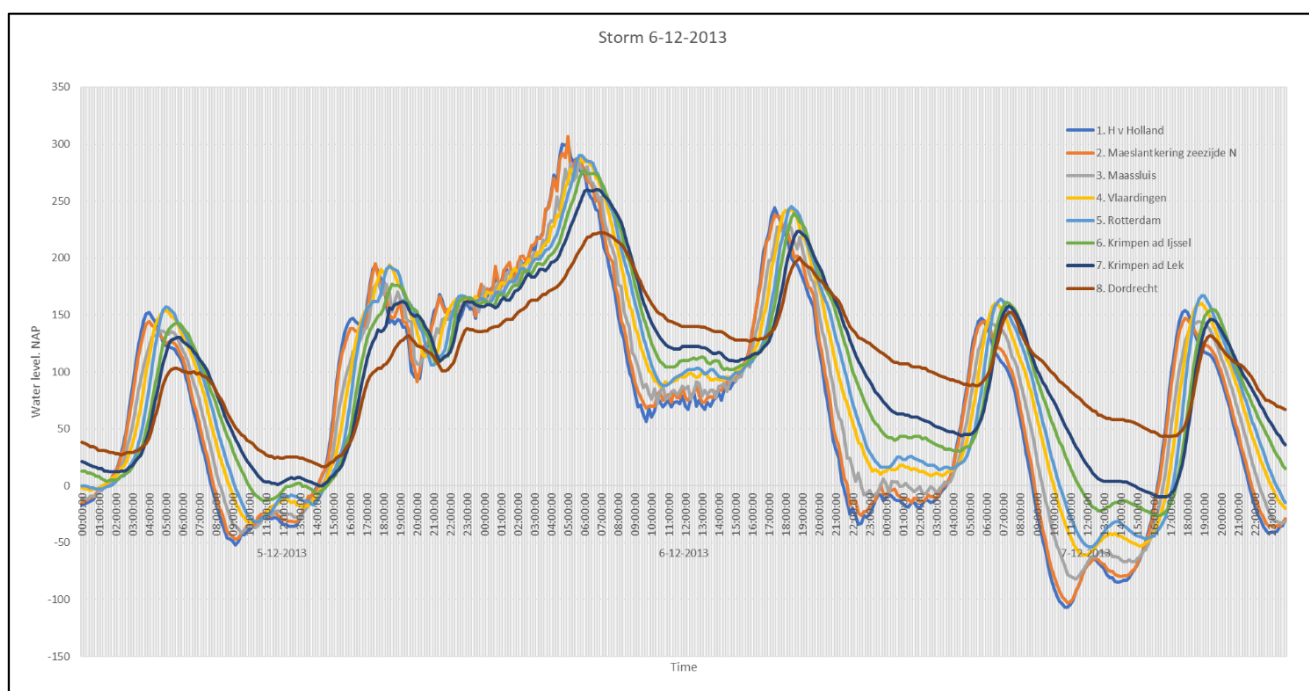


Figure A.54: Progression of water levels in the Rhine-Meuse Delta during the high-water event of December 2013 while the MLK was not closed.

## Closure Storm surge barriers November 2007

On November 2007, a storm event caused a closure of the Maeslant Barrier and the Eastern Scheldt Barrier.

### **Closure of the Maeslant Barrier**

On 8 November 2007, the Maeslant Barrier (MLK) was closed for the first time in storm conditions since the construction. The high-water level caused by a north-western storm was the first actual test to evaluate whether the MLK would really work.

The probability of a closure is relatively small (average once in 7-10 years). It was recommended to test the MLK under storm conditions and to lower the required water level to increase the likelihood of a closure. It was decided to temporarily lower the closing level to +2.60 m NAP to make it possible to investigate whether the barrier continues to function well under storm conditions. The BOS system continually calculates the expected water level in the "Nieuwe Waterweg" (NWW). The system automatically enters the preparatory work for a closure if a water level of more than 2.60 meters above NAP is expected in Rotterdam. Short after this adjustment, the storm surge barrier closed because of a predicted level in Rotterdam of +2.84 m NAP.

The closure began on 8 November at 23:05. The next day, the barrier started to open again at 17:45. After pumping water out the floodgates, the barrier was returned to the docks at 20:00. At 20:20 the passage was free for shipping. The Hartel Barrier was also closed at the same time as the MLK and opened at 19:25. The flood defences have both been closed during two high waters (high tide). The reason for this was that the conditions for the opening were only met after the second tide. The sea level should be lower than the water level at the riverside in order to open the storm surge barriers. The water levels at eight different locations are shown in Figure A.55. The most important observations are the following:

- the peak sea level was +3.24 m NAP measured at the MLK (9-11-2007; 02:50);
- the maximal water level in the delta was +1.35 m NAP in Rotterdam (9-11-2007 01:10), just before the occurrence of the translation wave;
- the turnaround closure of the MLK starting at +0.60 m NAP (8-11-2007; 23:05)
- the MLK was closed for more than 16 hours (two high-waters), leading to a small increase of the water level from +0.8 to +1.1 m NAP in the RMD due to the supply of river water;
- the barrier opens immediately at a higher river water level (9-11-2007; 17:45);
- influence of sea level relatively small further inland (Dordrecht) resulting in reduced tidal activity.

The closure started at a water level of +0.60 m NAP at the MLK. This process takes roughly 30 minutes before the doors can sink to the threshold blocks on the bottom of the waterway. Important to note is that the barrier also reduces the incoming current from the sea during the closure procedure by partly obstructing the incoming water. The barrier was entirely closed on 9 November at 1:00 am. The total closure took more than 16 hours before the barrier opened again.

The peak water level in front of the MLK was +3.24 m NAP and +3.16 m NAP at Hoek van Holland at 2:50 am. This is remarkable because the projected water level in Rotterdam was only +2.84 m NAP. Based on datasets from other storms, it appears that the water level in Rotterdam can exceed the sea level in Hoek van Holland on some occasions. The higher water levels in Rotterdam can be caused by the following:

- extra storm surge in the harbour basin;
- possible appearance of seiches;
- supply of river water and river water impoundment.

Based on data from other high-water situations, the probability that the water levels in Rotterdam exceed +3.0 m NAP instead of the predicted +2.84 m NAP is noteworthy. Therefore, it is questionable whether the predictions are accurate enough.

The maximum water level in Rotterdam was +1.35 m NAP at 01:10. This was at the time that the barrier was fully closed and sunk to the bottom. After closure, water levels behind the barrier drop sharply to +0.70 m NAP causing a translation wave in the harbour of Rotterdam. After 1.5 hours the water level in the delta stabilizes at +0.80 m NAP due to the diminishing supply of seawater. From 02:30, the water levels increase slightly at all locations in

the delta due to the supply of water from the rivers. In the following period of 15 hours, the water level rises to +1.10 m NAP in the total river basin. This increase of 2 cm per hour is caused by a total river discharge of 1,500 m<sup>3</sup>/s and a leakage by the MLK and HK of approximately 500 m<sup>3</sup>/s. The second high-water results in a peak water level of +2.50 m NAP in front of the MLK. It was not required to close during high-water, but the barrier was not yet opened due to the high low tide. At the opening of the doors, the sea water level was +1.0 m NAP and was declining to 0.0 m NAP.

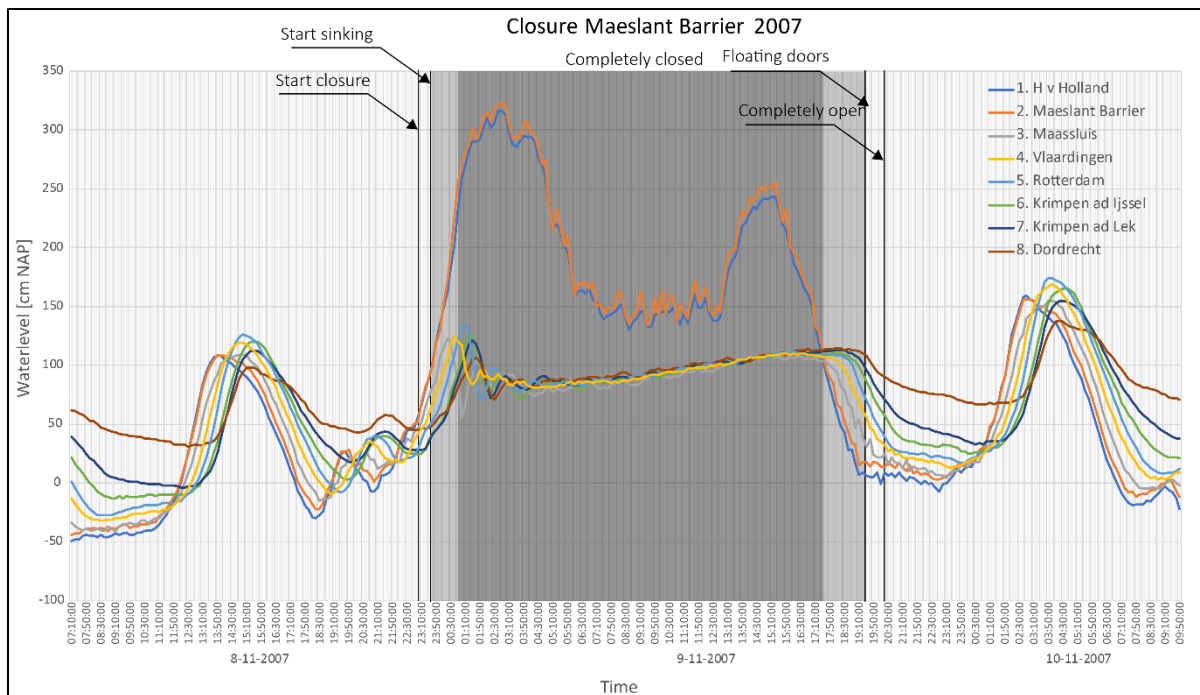


Figure A.55: Progression of water levels in the Rhine-Meuse Delta during the high-water event of November 2007 including the effect of the closure of the MLK.

In the end, this closure was successful because the MLK significantly reduced the water level at all observed locations. It is unclear if the +3.0 m NAP threshold value (Rotterdam) would be exceeded if the barrier did not close without changing the closing procedure. This storm event shows that it is important to close early before the tide arrives because this will increase the margin to store the river supply in the RMD.

#### Potential scenario

The river discharge on 8 November 2007 was relatively low which means that a turn-around closure was not required. A storm combined with a river discharge of 10,000 m<sup>3</sup>/s could have led to a high-end scenario. In that figurative situation, the arc-shaped doors had to float again after 7 hours because otherwise, a higher water level could have taken place inland than at sea. In that situation, the barrier has the specific function of draining water by floating the doors. The barrier can eventually sink again for the second high-water. In that situation, the water level would potentially have become about +2.00 m NAP. Due to the turnaround closure, this river discharge gives no cause for dangerous situations.

However, a heavier storm with considerably more storm surge could potentially lead to water levels above 5.00 m NAP at Hoek van Holland. In combination with a high river discharge of 10,000 m<sup>3</sup>/s, even a turnaround closure could lead to high water levels in the delta.

### Closure of the Eastern Scheldt Barrier

On 8 November 2007, the OSK closed due to the storm conditions. The barrier closes whether computer models project a water level of at least +3.00 m NAP in the Eastern Scheldt estuary. Figure A.56 shows that the barrier closed at 23:00 due to the reduced water levels in the Eastern Scheldt. The total closing time was 7 hours, and the water level of the basin rose 50 cm in that timeframe due to leakage and wave overtopping. The peak sea level was +3.39 m NAP measured at 01:10 am. The barrier opened after the first high-water and a second closure was not performed. The second peak with a height +2.82 m NAP reached the barrier at 13:40. Initially, it was thought that no closure was needed, but a peak water level of +3.12 m NAP was measured at the Bergse Diepsluis. This is because of extra storm surge in the Eastern Scheldt.

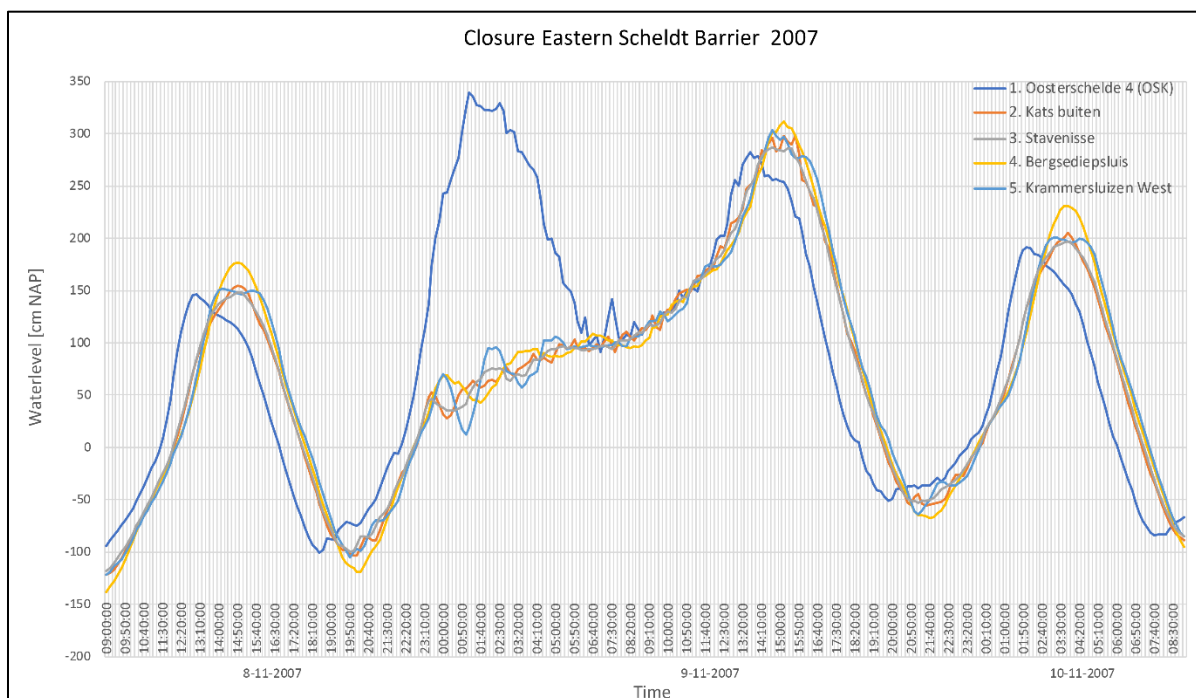


Figure A.56: Progression of water levels in the Eastern Scheldt during the high-water event of November 2007 including the effect of the closure of the OSK.

## Storm of 1953

The north-western storm in the evening of 31 January 1953 reached the highest water levels ever recorded at the coast of the Netherlands. More information about the impact of this disaster can be found in Section 3.1.

In Zeeland, the peak of the storm reached the coast at 10.00 pm. The strong north-westerly storm caused massive storm surge which came simultaneously with a spring tide. The maximum sea level at Vlissingen was +4.55 m NAP and +3.85 m NAP at Hoek van Holland. Without the storm surge barriers of the Delta Plan in place, these sea levels were hazardous for the densely populated areas in South Holland and Zeeland. As a result, the storm caused a widespread of dyke failures, particularly in Zeeland. Many dykes were not designed for such sea levels and resulted in a flooding disaster.

Rijkswaterstaat has an extensive historical database of water levels at various locations. Water level measurements at Hoek van Holland, Rotterdam, Hellevoetsluis and Dordrecht, were recorded at that time. These locations provide useful information with respect to the Rhine-Meuse Delta. This data is derived from <https://waterinfo.rws.nl> and is shown in Figure A.57.

Important to note is that the water levels and the locations are measured every 1-4 hours. The reason for this is that the measurements had to be carried out by hand at that time. This implies that the graph is less accurate and peak water levels might be missing. The most important observations are the following:

- a peak sea level of +3.85 m NAP at Hoek van Holland (1-2-1953; 04:40);
- a peak sea level of +4.02 m NAP at Hellevoetsluis (1-2-1953; 05:40).

The most extensive available dataset is Hoek van Holland, containing water level recordings of each hour. The maximal measured water level was +3.85 m NAP at 1-2-1953 04:40am. Even at low tide, the water level was +1.85 m NAP due to the enormous storm surge. The peak water level in Rotterdam was +3.20 m NAP at 02:40 am. This water level is comparable to the water level in Hoek van Holland at that same time. The upcoming recording was 6 hours later and missed the peak water level at Rotterdam. It can be assumed that the water level in Rotterdam does not deviate significantly from Hoek van Holland, resulting in a comparable water level.

The water levels at Hellevoetsluis were usually higher than at Hoek van Holland. The peak water level at this location was +4.02 m NAP. At that time, this area was not protected by the Haringvlietdam located in the Haringvliet. As a result, the water levels in Dordrecht were also significantly higher (+3.70 m NAP). Nowadays, the influence of the sea has become considerably smaller in Dordrecht due to the presence of the Haringvlietdam.

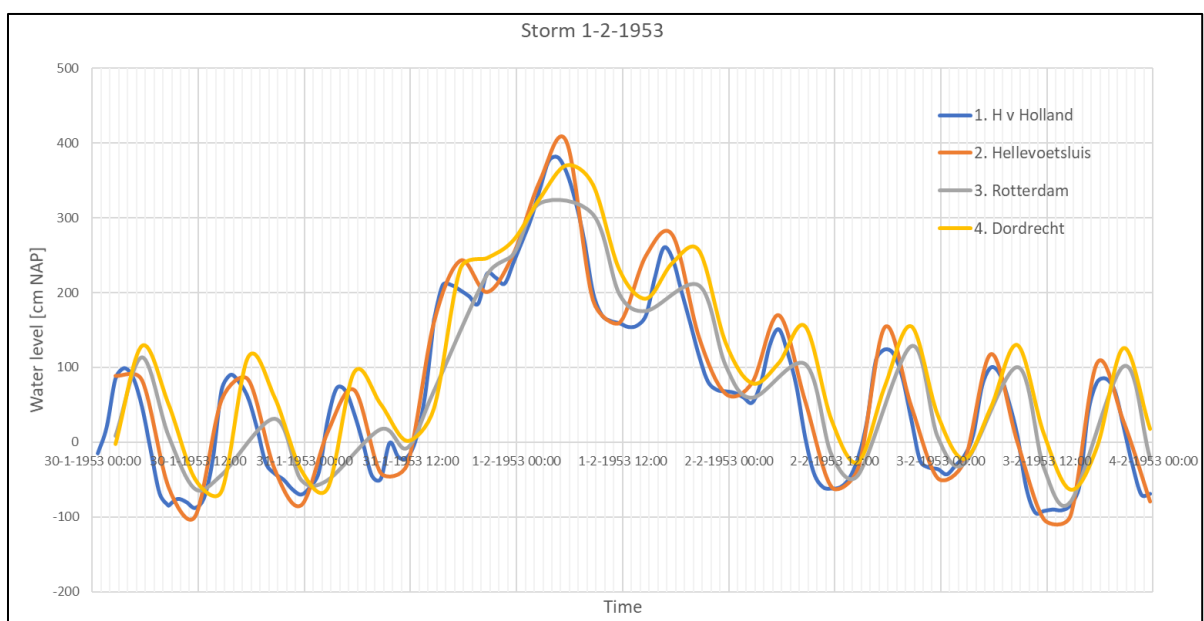


Figure A.57: Progression of water levels in the Rhine-Meuse Delta during the Flood of 1953.

## Appendix R: Failure rate Eastern Scheldt Barrier

The OSK is a unique storm surge barrier with 62 floodgates that can operate independently. The consequences of a failure depend on the number of floodgates that fail to close during a high-water event. Also, the position of the failing gates within the barrier influences the impact of the failure. Despite the complexity, the failure rate of one or more of the floodgates is relatively low. Table A.21 shows the estimations of the failure rate based on the current performance of the OSK for a regular closure (manned operation) and an emergency closure (unmanned operation). These estimations of the failure rate of one or more floodgates are used in the determination of the water levels in the Eastern Scheldt.

Table A.21: Probability of failure of the floodgates within the OSK (Deltares, 2014) & (Hydra-NL).

# Failing floodgates	Failure rate (Manned operation)	Failure rate (Unmanned operation)
0	0.98647 (reliability)	0.93951 (reliability)
1	0.01180	0.05410
2	0.00038	0.00183
5	0.00019	0.00200
10	0.00062	0.00100
16	0.00038	0.00060
31	0.00017	0.00023
62	0.00002	0.00075

Table A.21 shows that the reliability of the OSK for the manned operation is circa 98.6%. The effects of various reliability situations are presented in Table A.22 for all twelve test locations in the Eastern Scheldt. The results indicate that benefit of a 100% reliable storm surge barrier is negligible for the water levels in the Eastern Scheldt. However, accelerated sea level rise has a considerable influence on the effect of the failure rate. The effect of 0.81 m SLR is 0-4 cm to the water levels in the Eastern Scheldt for the maximal applicable safety standard. This effect increases to 1-27 cm for 1.40 m SLR depending on the location. The main reason is the drastically increasing frequency of required closures of the OSK for high sea level scenarios, which increases the likelihood of failing floodgates. This result will affect the technical tipping point and the remaining lifetime of the Eastern Scheldt Barrier significantly which will be discussed in Section 7.2.

Table A.22: Effect of the reliability of the OSK to the maximum water levels of test locations OS-1 to OS-12 in the Eastern Scheldt for the applicable safety standard. [1]: Water levels for the current reliability of the OSK. [2]: Water levels for 100% reliability of the OSK. [3]: Effect to the water levels in the Eastern Scheldt during a complete failed closure of the OSK.

Eastern Scheldt Estuary														
Sea level scenario (2100)	Test location	OS-1	OS-2	OS-3	OS-4	OS-5	OS-6	OS-7	OS-8	OS-9	OS-10	OS-11	OS-12	
	Standard (WBI-2017)	1/300	1/300	1/3,000	1/10,000	1/10,000	1/10,000	1/10,000	1/10,000	1/3,000	1/10,000	1/3,000	1/3,000	1/1,000
	Crest height [m NAP]	7.00	6.60	7.10	6.00	6.40	6.40	6.60	6.30	6.60	6.09	7.25	6.77	
<b>0.05 m</b> (Year 2023) Mean value	Water level [m NAP] [1]	3.29	3.44	3.86	4.17	3.9	3.84	4.14	3.88	3.95	3.74	3.57	3.41	
	Water level 100% reliability OSK [2]	3.29	3.44	3.86	4.17	3.90	3.84	4.14	3.88	3.95	3.74	3.57	3.41	
	No closure [3]	4.33	4.32	4.98	5.75	5.37	5.41	5.55	5.14	5.45	5.05	4.93	4.76	
	Difference [m] ([2]-[1])	0.00	0.00	0.00	0.00	0.00	0.00	0.00	0.00	0.00	0.00	0.00	0.00	
	Difference [m] ([3]-[1])	1.04	0.88	1.12	1.58	1.47	1.57	1.41	1.26	1.50	1.31	1.36	1.35	
<b>0.81 m</b> RCP4.5 Mean value (50%)	Water level [m NAP]	3.43	3.51	3.88	4.20	3.93	3.92	4.24	3.93	4.02	3.78	3.62	3.56	
	Water level 100% reliability OSK [2]	3.42	3.51	3.87	4.18	3.91	3.88	4.23	3.92	4.00	3.77	3.61	3.55	
	No closure [3]	5.09	4.96	5.52	6.38	5.96	6.05	6.19	5.78	6.10	5.70	5.58	5.54	
	Difference [m] ([2]-[1])	-0.01	0.00	-0.01	-0.02	-0.02	-0.04	-0.01	-0.01	-0.02	-0.01	-0.01	-0.01	
	Difference [m] ([3]-[1])	1.66	1.45	1.64	2.18	2.03	2.13	1.95	1.85	2.08	1.92	1.96	1.98	
<b>1.40 m</b> RCP4.5 High-end (95%)	Water level [m NAP]	3.60	3.54	3.94	4.37	4.20	4.23	4.38	4.05	4.28	3.95	3.86	3.80	
	Water level 100% reliability OSK [2]	3.58	3.53	3.88	4.19	3.93	3.96	4.28	3.96	4.05	3.81	3.68	3.70	
	No closure [3]	5.68	5.46	5.95	6.88	6.43	6.56	6.70	6.29	6.61	6.21	6.08	6.14	
	Difference [m] ([2]-[1])	-0.02	-0.01	-0.06	-0.18	-0.27	-0.27	-0.10	-0.09	-0.23	-0.14	-0.18	-0.10	
	Difference [m] ([3]-[1])	2.08	1.92	2.01	2.51	2.23	2.33	2.32	2.24	2.33	2.26	2.22	2.34	

